

2022-12

# Characterization and simulation of nested groundwater flow systems in basins with contrasting climate and geology

Mussa, Kassim

NM-AIST

---

<https://doi.org/10.58694/20.500.12479/2148>

*Provided with love from The Nelson Mandela African Institution of Science and Technology*

**CHARACTERIZATION AND SIMULATION OF NESTED GROUNDWATER  
FLOW SYSTEMS IN BASINS WITH CONTRASTING CLIMATE  
AND GEOLOGY**

**Kassim Ramadhani Mussa**

**A Thesis Submitted in Fulfillment of the Requirements for the Degree of Doctor of  
Philosophy in Hydrology and Water Resources Engineering of the Nelson Mandela  
African Institution of Science and Technology**

**Arusha, Tanzania**

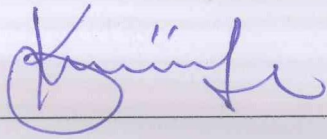
**December, 2022**

## ABSTRACT

The pattern, organization and hierarchy of nested groundwater flow systems, albeit complex, their understanding is very crucial for informed groundwater resources development and management. This study sought to characterize and simulate the impacts of varying climate and anthropogenic influences on the nested groundwater flow systems and the spatio-temporal association of nested groundwater flow systems, utilizing real field test cases of Singida semi-arid fractured aquifer and the Kimbiji coastal, humid sedimentary aquifer in Tanzania. Groundwater flow modelling and simulation of nested groundwater flow systems was carried out using the USGS finite difference modelling code (MODFLOW 6), utilizing ModelMuse version 5 as the Graphical User Interface (GUI). Hydrogeochemical and isotopic signature analyses complemented the modelling approach. The comparison of isotopic composition from borehole, rivers, lakes and rainfall showed that generally, boreholes in the Kimbiji aquifer and some in the Singida aquifer had depleted isotopic values and enriched isotopic values were in samples from open water bodies (e.g., rivers and lakes). The depletion was prominently so in the deep boreholes, indicating a limited influence of evaporation during groundwater recharge. Regional flow fluxes make up 74% of the total inflows into the Kimbiji coastal Neogene aquifer, and only 26% of the inflows are made up of the local flow systems. In the Singida aquifer, regional flow accounts for 56% of the total flux in the lower aquifer and makes 94% contribution to the total amount of groundwater inflow in the Singida aquifer. Only 6% of the groundwater storages comes from local recharge and other sources like lakes. The effect of land cover change dynamics on groundwater recharge has been more prominent in the Kimbiji aquifer, while the effect of climate varying (rainfall and temperature) featured more prominently in the Singida semi-arid aquifer. Dependence of local recharge on heavy rainfalls is one of the key features of the Singida aquifer, while local recharge in the Kimbiji aquifer is quasi-uniform, occurring at more or less similar rate, albeit decreasing with decreasing rainfall amounts and increasing surface temperature, and thus evapotranspiration. Local flow system fluxes were observed to be the main feeders for the upper unconfined aquifers in the two study areas, while regional flow systems are for the deep semi-confined aquifers, with appreciable exchanges of water as revealed by nested groundwater flow simulation. The study findings will contribute to various global, regional and local technical and policy-based efforts towards sustainable groundwater development and management, considering climate variability and non-climatic factors. This includes the contribution to Sustainable Development Goals (SDGs), particularly SDG on access to clean water and sanitation.

## DECLARATION

I, Kassim Ramadhani Mussa, do hereby declare to the Senate of The Nelson Mandela African Institution of Science and Technology that this Thesis titled “*Characterization and Simulation of Nested Groundwater Flow Systems in Basins with Contrasting Climate and Geology*” is my own original work and that it has neither been submitted nor being concurrently submitted for degree award in any other institution.

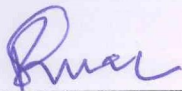


Kassim Ramadhani Mussa

25/01/2023

Date

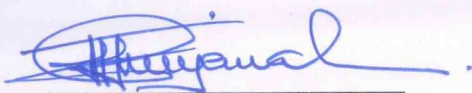
The above declaration is confirmed by:



Prof. Revocatus Lazaro Machunda

25/01/2023

Date



Dr. Ibrahimu Chikira Mjemah

25/01/2023

Date



## **COPYRIGHT**

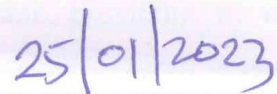
This Thesis is copyright material protected under the Berne Convention, the Copyright Act of 1999 and other international and national enactments, in that behalf, on intellectual property. It must not be reproduced by any means, in full or in part, except for short extracts in fair dealing; for researcher private study, critical scholarly review or discourse with an acknowledgement, without the written permission of the office of Deputy Vice Chancellor for Academics, Research and Innovations, on behalf of both the author and The Nelson Mandela African Institution of Science and Technology.

## CERTIFICATION

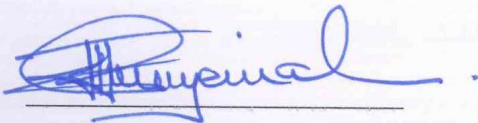
The undersigned certify that they have read and hereby recommend for examination by the Nelson Mandela African Institution of Science and Technology a Thesis entitled “*Characterization and Simulation of Nested Groundwater Flow Systems in Basins with Contrasting Climate and Geology*” in Fulfilment of the Requirements for the Degree of Doctor of Philosophy in Hydrology and Water Resources Engineering at Nelson Mandela African Institution of Science and Technology, Arusha Tanzania.




Prof. Revocatus Lazaro Machunda



Date



Dr. Ibrahimu Chikira Mjemah



Date

## ACKNOWLEDGEMENTS

First and foremost, I thank the Almighty God (Allah) for granting me life and strength to embark on PhD studies. Secondly, I am grateful to the Nelson Mandela African Institution of Science and Technology for accommodating me as a PhD student for all the years. The encouragement from staff (Academic and non-academic) of all walks of life was so catalyzing towards the completion of my PhD work.

I owe a word of gratitude to the Centre of Excellence for Water Infrastructure and Sustainable Energy Futures (Wise Futures) for awarding me a PhD scholarship, providing me with the financial means to cater for tuition fees, accommodation and part of research costs. I also acknowledge the academic secondment to the Indian Institute of Technology-Delhi (IIT Delhi) in India where I learned, networked and got time to develop manuscripts. This program was organized and financed by the World Bank through the Centre of Excellence in Water Infrastructure and Sustainable Energy Futures (WISE-FUTURES).

Moreover, I thank Prof. Kristine Walraevens from the Laboratory for Applied Geology and Hydrogeology, at the Ghent University in Belgium for attaching me to her laboratory through the Global Minds Fellowship Programme. It was under her laboratory and the North South-South Projects that I got to learn a lot about the modified soil moisture balance method, coupled with curve number and other numerous hydrogeological methods. In that line, Marc Van Camp of the same laboratory at Ghent University is equally acknowledged.

I would like to offer my very special thanks to my supervisors, Prof. Revocatus Lazaro Machunda and Dr. Ibrahimu Chikira Mjemah for their unwavering support and belief in me. These two read my numerous revisions and helped make some sense out of the confusion. Supervisors financed the biggest part of my research works where funds from the scholarship were not enough or not available altogether. Through his projects and consultancy works, Dr. Mjemah financed a number of field activities and laboratory analyses in and outside the country.

In line with this, I equally acknowledge the support of Prof. Jan Willem Foppen from IHE Delft, with whom we conceptualized this PhD idea, together with the late Prof. Alfred N.N. Muzuka (May his good soul rest in eternal peace).

I owe a word of appreciation to the management of Sokoine University of Agriculture (my employer) for granting me a paid study leave, and bearing with my relentless request for

extension of study leave. I would as well like to extend my sincere gratitude to my head of department, Dr. Jilisa K. Mwalilino who offered me immense administrative support in the course of my PhD studies.

I am equally indebted to my late wife who could not stop reminding me of my PhD responsibilities even when she was in a hospital bed. My children (Nasrya, Naeemah and Naureen) as well as my father (Mr. Ramadhani Mussa Kika) endured this long process with me, always offering what they could to make sure that I finish the PhD. I am highly indebted to this special group of people.

I am also deeply grateful to my colleagues, Dr. Mateso Said, Dr. Ramadhani Bakari, and Mr. Christopher Warburg for their insightful comments and suggestions. Dr. Said Mateso has been a company through thick and thin, in Tanzania and in India as well.

Prof. Dr. B. R. Chahar of the Civil Engineering Department at the Indian Institute of Technology (IIT) Delhi is acknowledged for hosting me at the Water Resources Simulation Laboratory at IIT Delhi, India. The company of Mr. Adane Kalsido and Ms. Kidist from Ethiopia, Ms. Fatimata Dialo from Burkina Faso, Mr. Noel Bakobye from Ghana is highly appreciated while at IIT Delhi. Lastly, I appreciate the effort of everyone who, knowingly or unknowingly contributed towards achieving this academic milestone.

Last but not least, I owe a word of thanks to my virtual tutor, Mr. Saul Montoya of Hatarilabs. Through him and his Lab I got to learn more about numerical groundwater modelling using state-of-the art techniques and software. Through Mr. Saul Montoya, I learned about Model Muse and numerical groundwater model calibration using python (jupyter lab and pandas).

## **DEDICATION**

This work is wholly dedicated to my late wife, Ms. Hamida Omari Shosi, who sustained a number of spine surgeries in Tanzania and in India at different occasions amidst my tight PhD schedule but she never forgot to remind me about my PhD thesis responsibilities. Despite all the effort, she never survived to witness my success. May the Almighty God grant her eternal peace till we meet again.

## TABLE OF CONTENTS

ABSTRACT .....	i
DECLARATION .....	ii
COPYRIGHT .....	iii
CERTIFICATION.....	iv
ACKNOWLEDGEMENTS .....	v
DEDICATION .....	vii
TABLE OF CONTENTS .....	viii
LIST OF TABLES .....	xii
LIST OF FIGURES.....	xv
LIST OF ABBREVIATIONS AND SYMBOLS.....	xix
CHAPTER ONE .....	1
INTRODUCTION.....	1
1.1 Background of the Problem.....	1
1.2 Statement of the Problem .....	3
1.3 Rationale of the Study .....	4
1.4 Objectives of the Study .....	5
1.4.1 General Objective .....	5
1.4.2 Specific Objectives .....	5
1.5 Research Questions .....	5
1.6 Significance of the Study.....	8
1.7 Delineation of the Study .....	8
CHAPTER TWO.....	10
LITERATURE REVIEW.....	10
2.1 The Evolution and Application of Regional Groundwater Flow Theories .....	10

2.2	Groundwater Flow Modeling and Factors Affecting the Organization and Hierarchy of Groundwater Flow Systems .....	11
2.3	Characterization of Aquifer Types and Groundwater Flow .....	12
2.4	Groundwater Travel times and Residence Time Distributions .....	15
2.5	Land use/cover, Climate Variability and Groundwater Recharge.....	16
2.6	Hydrogeochemical Facies and Signatures for Groundwater Characterization and Evolution Assessment .....	18
2.7	Characterization of the Local Flow System through Water Table Fluctuation.....	20
2.8	Groundwater-Surface Water Interaction and Groundwater Provenance through Stable Isotopic Techniques.....	21
	CHAPTER THREE.....	24
	MATERIALS AND METHODS .....	24
3.1	Description of the Study Areas.....	24
	3.1.1 Climate.....	24
	3.1.2 Geology .....	26
3.2	Fieldwork and Sampling Procedures.....	27
	3.2.1 Water Sampling and Preservation .....	28
	3.2.2 Analysis of Major Ions .....	28
3.3	Characterization of Groundwater Systems in Aquifers based on Hydrogeological, Hydrogeochemical and Isotopic Signatures and Controls.....	30
	3.3.1 Characterization of Hydrogeochemical facies Using Piper (Trilinear) Diagram	30
	3.3.2 Identification of Mechanisms Controlling Groundwater Chemistry .....	30
	3.3.3 Statistical analyses of Hydrogeochemical Parameters .....	32
	3.3.4 Assessing Groundwater Provenance and Evolution Using Stable Isotopes of Water	34
	3.3.5 Characterization of Aquifer Response to Rainfall Events Using the Water Table Fluctuation Method .....	36

3.4	Evaluation of the Combined Effect of Climate Variability and Landcover Dynamics on Spatiotemporal Groundwater Recharge Rates across Regional Aquifers .....	37
3.4.1	Delineation of Potential Groundwater Recharge Zones .....	37
(i)	Slope .....	48
3.4.2	Determining the Factor Relations and Percentage Influence of the Thematic Layers	49
3.4.3	Assessment of Groundwater Recharge in the Kimbiji and Singida Aquifers ..	56
3.5	Groundwater Flow Modelling and Simulation of Nested Groundwater Flow Systems	70
3.5.1	Modelling/Simulation Process.....	70
3.5.2	Kimbiji Aquifer .....	72
3.5.3	Singida Aquifer.....	74
3.5.4	Boundary Conditions, Flow Packages and Solvers .....	77
3.5.5	Model Calibration.....	78
3.5.6	Simulation of Local and Regional Groundwater Flow Systems and Groundwater Balance .....	79
CHAPTER FOUR.....		80
RESULTS AND DISCUSSION .....		80
4.1	To Characterize Groundwater Flow Systems based on Hydrogeological, Hydrogeochemical and Isotopic Signatures and Controls Considering the Difference in Climate and Geology .....	80
4.1.1	Physico-chemical Parameters and Major Ions.....	80
4.1.2	Hydrogeochemical Facies using the Piper (trilinear) Diagram Approach.....	84
4.1.3	Mechanisms Controlling Groundwater Chemistry .....	87
4.1.4	Statistical Analyses of Hydrogeochemical Parameters .....	101
4.1.5	Characterization of Groundwater Evolution and Provenance using Stable Isotopes.....	104
4.1.6	The Response of Watertable to Local Rainfall Events in the Singida and Kimbiji Aquifers .....	116



4.2	Evaluation of the Combined Effect of Climate Variability and Landcover Dynamics on Spatiotemporal Groundwater Recharge Rates across Regional Aquifers .....	121
4.2.1	Delineation of Groundwater Recharge Potential Zones .....	121
4.2.2	Land Cover Change Assessment .....	137
4.2.3	Assessment of the Magnitude and Annual Rate of Land Cover Changes.....	139
4.2.4	Land Cover Classification Accuracy Assessment .....	143
4.2.5	The Weighted Curve Numbers for the Kimbiji and Singida Aquifers .....	143
4.2.6	Potential Evapotranspiration, Rainfall, Runoff, Groundwater Recharge, and Aridity Indices .....	145
4.2.7	Groundwater Recharge Response to Climate and Land Cover Dynamics.....	147
4.3	Simulation of the Effect of the Difference in Climate and Geology on the Magnitude of (Nested) Local and Regional Groundwater Flow Fluxes and Basin Water Balance in Basins with Contrasting Climate and Geology .....	159
4.3.1	Numerical Modelling of Nested Groundwater Flow Systems.....	159
CHAPTER FIVE.....		179
CONCLUSION AND RECOMMENDATIONS .....		179
5.1	Conclusion.....	179
5.2	Recommendations .....	183
REFERENCES.....		185
RESEARCH OUTPUTS .....		210

## LIST OF TABLES

Table 1:	Percentage influence, factor scores and ranks of the main thematic layers for the Kimbiji aquifer .....	50
Table 2:	Percentage influence, factor scores and ranks of the main thematic layers in the Singida aquifer.....	51
Table 3:	Factor classes, class rank and factor weightage for the Kimbiji aquifer .....	53
Table 4:	Factor classes, class rank and factor weightage for the Singida aquifer .....	54
Table 5:	A summary of satellite image data and their attributes for land cover classification .....	60
Table 6:	Characterization of Hydrological Soil Groups .....	63
Table 7:	Antecedent soil moisture classes .....	64
Table 8:	The curve numbers for various land cover classes .....	67
Table 9:	Groundwater exploitation data in the Singida aquifer as of December 2020...	77
Table 10:	Descriptive statistics of hydrogeochemical parameters for the Kimbiji aquifer .....	81
Table 11:	Descriptive statistics of hydrogeochemical parameters for the Singida aquifer .....	82
Table 12:	Gibbs ratios for the Kimbiji aquifer .....	88
Table 13:	Gibbs ratios for the Singida aquifer.....	91
Table 14:	Chloro-Alkali Indices for the Kimbiji aquifer .....	94
Table 15:	Chloro-Alkali Indices for the Singida aquifer .....	94
Table 16:	Hydrogeochemical signatures and ratios for determining geochemical processes in the Kimbiji aquifer .....	96
Table 17:	Hydrogeochemical signatures and ratios for determining geochemical processes in the Singida aquifer.....	97
Table 18:	Hydrogeochemical facies of the Kimbiji aquifer in relation to Residence time of groundwater .....	100

Table 19:	Hydrogeochemical facies of the Singida aquifer in relation to Residence time of groundwater .....	100
Table 20:	Correlation matrix of hydrogeochemical parameters for the Kimbiji aquifer	101
Table 21:	Correlation matrix of hydrogeochemical parameters for the Singida aquifer	102
Table 22:	Principal Components Analysis of the Kimbiji aquifer hydrogeochemical parameters.....	103
Table 23:	Principal Components Analysis of the Singida aquifer hydrogeochemical parameters.....	104
Table 24:	Stable Isotope Results and Deuterium Excess Analysis for the Kimbiji aquifer .....	105
Table 25:	Stable Isotope Results and Deuterium Excess Analysis for the Singida aquifer .....	106
Table 26:	Temporal land cover change matrix for the Kimbiji aquifer.....	138
Table 27:	Temporal land cover change matrix for the Singida aquifer .....	139
Table 28:	The magnitude of change, percentage of change, and the annual rate of change for land cover classes in the Kimbiji aquifer .....	140
Table 29:	The magnitude of change, percentage of change, and the annual rate of change for land cover classes in the Singida aquifer .....	141
Table 30:	Accuracy assessment parameters for land cover classification results.....	143
Table 31:	Land cover related average and weighted curve number for the Kimbiji and Singida aquifers .....	145
Table 32:	Rainfall, PET, and Recharge for 1996/1997, 2004/2005, and 2017/2018 hydrological years for the Kimbiji Aquifer .....	146
Table 33:	Rainfall, PET, and Recharge for 1996/1997, 2004/2005, and 2017/2018 hydrological years for the Singida Aquifer .....	147
Table 34:	The water balance for the upper unconfined layer in the Kimbiji aquifer .....	164
Table 35:	The water balance for the lower semi-confined layer in the Kimbiji aquifer.	165
Table 36:	The water balance for the upper unconfined weathered layer in the Singida aquifer.....	171

Table 37:	The Water balance for the Lower Semi-confined fractured layer in the Singida Aquifer.....	172
-----------	---	-----

## LIST OF FIGURES

Figure 1:	The conceptual framework which guided data collection, research activities, steps and processes used in this study .....	7
Figure 2:	A schematic diagram depicting a topography-controlled water table .....	14
Figure 3:	A schematic diagram depicting a recharge-controlled water table .....	15
Figure 4:	Maps showing the position of the two study areas in relation to the water basins and the country .....	25
Figure 6:	The geology of the Singida aquifer and the lineament system distribution ...	27
Figure 7:	Geological classes in the Kimbiji aquifer .....	38
Figure 8:	Map showing the hydrogeology of the Singida aquifer .....	39
Figure 9:	A map showing the lineament density with lineaments .....	40
Figure 12:	Land cover classes in the Kimbiji aquifer .....	43
Figure 14:	Rainfall distribution in the Singida aquifer .....	44
Figure 16:	Soil classes in the Singida aquifer .....	46
Figure 17:	Soil classes in the Kimbiji aquifer .....	47
Figure 18:	Slope classes in the Singida aquifer .....	48
Figure 19:	Slope classes in the Kimbiji aquifer .....	49
Figure 20:	Schematic diagram of the requisite processes, methods and input data for delineating groundwater potential zones .....	52
Figure 21:	A cross section of the Kimbiji aquifer showing a layered system of the study area (Msindai, 1988) .....	73
Figure 22:	A cross-section of the the Singida aquifer showing a layered systems of the aquifer .....	74
Figure 23:	Piper diagram for Kimbiji aquifer .....	85
Figure 25:	Cationic Gibb's diagram for the Kimbiji aquifer .....	89
Figure 26:	Anionic Gibb's diagram for the Kimbiji aquifer .....	90
Figure 27:	Cationic Gibb's diagram for the Singida aquifer .....	91

Figure 28:	Anionic Gibb's diagram for the Singida aquifer .....	92
Figure 29:	Na/Cl plot for groundwater samples for the Kimbiji aquifer .....	98
Figure 30:	Na/Cl plot for groundwater samples in the Singida aquifer.....	99
Figure 31:	A plot of $\delta^2\text{H}$ versus $\delta^{18}\text{O}$ for the Kimbiji aquifer .....	108
Figure 32:	A plot of $\delta^2\text{H}$ versus $\delta^{18}\text{O}$ for the Singida aquifer.....	109
Figure 33:	A plot of deuterium excess for the Kimbiji aquifer .....	110
Figure 34:	A plot of deuterium excess for the Singida aquifer.....	111
Figure 35:	A plot of deuterium excess versus $\delta^{18}\text{O}$ for the Kimbiji aquifer.....	112
Figure 36:	A plot of deuterium excess versus $\delta^{18}\text{O}$ for the Singida aquifer .....	113
Figure 37:	Daily aquifer response to rainfall in the Kimbiji aquifer .....	116
Figure 38:	Monthly aquifer response to rainfall in the Kimbiji aquifer .....	117
Figure 39:	Daily aquifer response to rainfall in the Singida aquifer .....	118
Figure 40:	Monthly aquifer response to rainfall in the Singida aquifer.....	119
Figure 41:	Groundwater recharge potential of slope classes in the Kimbiji aquifer .....	122
Figure 42:	Groundwater recharge potential of slope classes in the Singida aquifer.....	122
Figure 43:	Groundwater recharge potential of hydrogeological units in the Kimbiji aquifer.....	123
Figure 44:	Groundwater recharge potential of hydrogeological units in the Singida aquifer .....	124
Figure 45:	Groundwater recharge potential of rainfall distribution classes in the Kimbiji aquifer.....	125
Figure 46:	Groundwater recharge potential of rainfall distribution classes in the Singida aquifer.....	126
Figure 47:	Groundwater recharge potential of lineament density classes in the Singida aquifer.....	127
Figure 48:	Groundwater recharge potential of drainage density classes in the Kimbiji aquifer.....	128

Figure 49:	Groundwater recharge potential of drainage density classes in the Singida aquifer.....	129
Figure 50:	Groundwater recharge potential of soil classes in the Kimbiji aquifer .....	130
Figure 51:	Groundwater recharge potential of soil classes in the Singida aquifer .....	130
Figure 52:	Groundwater recharge potential of land cover classes in the Kimbiji aquifer .....	131
Figure 53:	Groundwater recharge potential of land cover classes in the Singida aquifer .....	132
Figure 54:	The groundwater recharge potential map of the Kimbiji Neogene humid aquifer .....	133
Figure 55:	The groundwater recharge potential map of the Singida semi-arid fractured basement aquifer .....	133
Figure 56:	Land cover maps for the Kimbiji and Singida aquifers .....	142
Figure 57:	A 1996/1997 hydrological year graph of rainfall, runoff, PET, net rainfall, and aridity index in the Kimbiji aquifer.....	149
Figure 58:	A 2007/2008 hydrological year graph of rainfall, runoff, PET, net rainfall, and aridity index in the Kimbiji aquifer.....	150
Figure 59:	A 2015/2016 hydrological year graph of rainfall, runoff, PET, net rainfall, and aridity index in the Kimbiji aquifer.....	151
Figure 60:	A 1996/1997 hydrological year graph of rainfall, runoff, PET, net rainfall, and aridity index in the Singida aquifer .....	152
Figure 61:	A 2005/2006 hydrological year graph of rainfall, runoff, PET, net rainfall, and aridity index in the Singida aquifer .....	153
Figure 62:	A 2017/2018 hydrological year graph of rainfall, runoff, PET, net rainfall, and aridity index in the Singida aquifer .....	154
Figure 63:	The graph of Southern Oscillation Index for depicting the influence of El Nino and the Southern oscillation on rainfall.....	155
Figure 64:	A calibration plot for the Kimbiji aquifer .....	160
Figure 65:	A calibration plot for the Singida aquifer.....	161

Figure 66:	A comparison of simulated hydraulic heads and observed hydraulic heads for the Kimbiji aquifer .....	162
Figure 67:	A comparison of simulated hydraulic heads and observed hydraulic heads for the Singida aquifer .....	163
Figure 68:	The layout of the inflows and outflows of the upper unconfined layer in the Kimbiji aquifer .....	164
Figure 69:	The layout of the inflows and outflows of the lower semi-confined layer in the Kimbiji aquifer .....	166
Figure 70:	The map of groundwater heads distribution in the Kimbiji aquifer .....	167
Figure 71:	Groundwater flowlines for the lower semi-confined layer of the Kimbiji aquifer .....	167
Figure 73:	The layout of inflows and outflows of the upper unconfined layer in the Singida aquifer.....	171
Figure 74:	The layout of inflows and outflows of the lower semi-confined layer in the Singida aquifer .....	172
Figure 75:	The map of groundwater heads distribution in the Singida aquifer .....	173
Figure 77:	Groundwater flowline for the lower fractured layer of the Singida aquifer	174



## LIST OF ABBREVIATIONS AND SYMBOLS

‰	Expressed as Permil
2D	Two Dimensional
3D	Three Dimensional
AE	Actual Evapotranspiration
AET	Actual Evapotranspiration
AMC	Antecedent Moisture Condition
APWL	The Accumulated Potential Water Loss
APWL	Accumulated Potential Water Loss
ARC	And The Annual Rate of Change
Ca <sup>2+</sup>	Calcium
CAP	Field Capacity
CI	Class Influence
Cl <sup>-</sup>	Chloride
CN	Curve Number
CNKIMB	Curve Numbers For The Kimbiji Aquifer
CNSING	Curve Numbers For The Singida Aquifer
CO <sub>3</sub> <sup>2-</sup>	Carbonate
COD	The Coefficient of Determination
DEM	Digital Elevation Model
d-excess	Deuterium Excess
DIV	The Discretization By Vertices
DN	Digital Number
DOS	Dark Object Subtraction
EC	Electrical Conductivity
ENSO	El Nino and the Southern Oscillation
EPSG	European Petroleum Survey Group
Eto	Evapotranspiration
FAO	Food and Agriculture Organization
FCC	False Colour Composite
FI	Factor Influence
GIS	Geographical Information System

GMWL	Global Meteoric Water Line
GUI	Graphical User Interface
HCO <sub>3</sub> <sup>-</sup>	Bicarbonate
HDPE	High-Density Polyethylene
IAEA	International Atomic Energy Agency
IDB	Internal Drainage Basin
IMS	Interactive Model Solution Solver
ISA	Ionic Strength Adjustment
ISE	Ion-Selective Electrode
JICA	Japan International Cooperation Agency
K <sup>+</sup>	Potassium
LMWL	Local Meteoric Water Line
LULC	Land Use/Land Cover
MC	The Magnitude of Change
Mg <sup>2+</sup>	Magnesium
mm	millimetre
Na <sup>+</sup>	Sodium
Nf	Fluvial Marine Sand
NO <sub>3</sub> <sup>-</sup>	Nitrate
NORCONSULT	Multidisciplinary Engineering and Design Consultancy, Providing Services to Clients in the Public and Private Sectors Worldwide
NPF	Node Property Flow
Nt	Terrace Deposits
OA-ICOS	Off-Axis Integrated Cavity Output Spectroscope
OLI	Operation Land Imager
OLI-TIRS	Operational Land Imager and Thermal Infrared Sensor
OWA	Ordered Weighted Averaging
PAW	Plant Available Water
PC	Percentage of Change
PCA	Principal Component Analysis
PET	Potential Evapotranspiration

PWP	Permanent Wilting Point
Q1	The First Quartile
QGIS	Quantum Geographical Information System
R	Correlation
r1	Fluvial Deposits
RMSE	Root Mean Square Error
RO	The Runoff
ROIs	Regions of Interest
RTDs	Residence Time Distributions
SCP	Semiautomatic Classification Plugin
SMBM	Soil Moisture Balance Method
SO <sub>4</sub> <sup>2-</sup>	Sulphate
SRTM	Shuttle Radar Topography Mission
sy	Aquifer Specific Yield
TDS	Total Dissolved Solids
TM	Landsat Thematic Mapper
TOA	Top of-Atmospheric
TPDC	Tanzania Petroleum Development Corporation
USDA-NRCS	USDA Natural Resources Conservation Service
USDA-SCS	USDA-Soil Conservation Service
USGS	United States Geological Survey
UTM	Universal Transverse Mercator
VSMOW	Vienna Standard Mean Ocean Water
WOA	Weighted Overlay Analysis
WRB	Wami/Ruvu Basin
WTF	Water Table Fluctuation
WTR	Water Table Ratio
ZB	Zone Budget
δ <sup>18</sup> O and δ <sup>2</sup> H	Stable Isotope's Compositions of Water

## CHAPTER ONE

### INTRODUCTION

#### 1.1 Background of the Problem

Groundwater is an important resource for food security, human health, ecosystems, economic and social prosperity of humankind (Gleeson *et al.*, 2016). However, groundwater storages are rapidly declining at a rate of approximately 545 km<sup>3</sup> per year (Siebert *et al.*, 2010; Konikow, 2013 & Dakhllalla *et al.*, 2016), with inadequate details on how much of that amount is contributed to by regional, sub-regional or local (nested) groundwater flow systems.

In recent years, several studies have been conducted on nested groundwater flow systems and the classification of aquifers into recharge-controlled and topography-controlled, mainly focusing on topographic and hydrogeological factors (Haitjema & Mitchell-Bruker, 2005; Gleeson & Manning, 2008; Gleeson *et al.*, 2011; Liang *et al.*, 2012). Nevertheless, the analysis of topography and hydrogeology only did not provide details on the dynamics of nested groundwater flow systems, including a clear understanding of the distinctive factors and features of the hierarchy, pattern and organization of nested groundwater flow systems.

Therefore, characterizing and simulating nested groundwater flow systems under different anthropogenic and climatic factors is driven by the quest to understand the impacts of natural and human influences on the hierarchy, organization and pattern of groundwater flow systems. That is in addition to assessing the implication of the distortion of nested groundwater flow systems for sustainable groundwater development and availability as reported elsewhere (Wang *et al.*, 2017).

To that effect, new and updated datasets of nested groundwater flow systems are needed periodically to upgrade the understanding of the dynamics and interconnectedness of groundwater flow using field test cases. In addition, the knowledge on how groundwater flow systems are influenced by local and regional climatic and non-climatic factors like land cover changes and regional air masses is equally imperative for sustainable groundwater management.

Moreover, in order to formulate sustainable water resource development and management strategies, decision and policymakers require adequate and correct information on the pattern,

hierarchy and organization of nested groundwater flow systems based on the succinct information on basin water quantity and water budget (Kralik, 2015).

Arguably, previous efforts to examine how groundwater resources are impacted by climatic and anthropogenic factors have mainly been based on examining changes of piezometric levels, primarily using pressure transducers (Polemio, 2016). Nevertheless, with piezometric observations only groundwater pressure at a specific local point is examined, ignoring the contribution of regional and sub-regional groundwater flow systems to basin water budget. It is now increasingly being realized that in addition to piezometric measurements, albeit useful under certain circumstances, better groundwater management strategies can be achieved through a succinct understanding of nested groundwater flow systems too. This can be achieved through regional groundwater flow modeling (Szocs *et al.*, 2015) in combination with hydrogeochemical, geospatial and isotopic approaches. This can foster a detailed investigation of the inadequately explored influence of climate and land cover variabilities on the distortion of the patterns of nested groundwater flow systems. Groundwater flow modeling equally fosters a detailed understanding of the effects of climatic and non-climatic controls (geology, land covers, aquifer geometry etc.) on the organization and spatial distribution of nested groundwater flow systems.

Some of the key factors for the formation of major groundwater flow systems in homogenous and isotropic conditions are topography, geology, climate, basin geometry, and slope (Cardenas, 2007; Welch & Allen, 2012; Liang *et al.*, 2012). Furthermore, groundwater flow system hierarchy is significantly affected by decreasing recharge, which is in turn affected by a decrease in rainfall and changes in certain land cover types (Liang *et al.*, 2012), the latter affecting soil moisture balance in the unsaturated zone and runoff henceforth. While the aforementioned argument does not specify which flow system is mostly affected, it is argued by other researchers that climate variability and change have a limited impact on regional and sub-regional flow systems.

Reportedly, climate variability and change have profound impacts on local flow system due to their relatively rapid and short flow paths (Goderniaux *et al.*, 2013; Huizar-Alvarez, 2016; Havril *et al.*, 2017). This impact is not only with respect to fluxes and water budget, but on water quality and hydrogeochemical signatures (Kurylyk *et al.*, 2015). Purportedly, climate has an influence on groundwater pathways too, as these are affected by the spatial distribution of recharge and discharge zones, which in turn vary with geology and climate (Goderniaux *et al.*,

2013). Arguably, changes in recharge have a bearing on the fragmentation and change in the hierarchy, organization and pattern of groundwater flow systems (Liang *et al.*, 2012; Havril *et al.*, 2017), which ultimately impact the long-term groundwater availability and basin water budget.

The contradiction and contention on the extent to which climate variability and change affect the nested groundwater flow systems have not been widely investigated. However, where that has been explored, only synthetic test cases have been used (Goderniaux *et al.*, 2013). Thus, the dynamics and contribution of nested groundwater flow systems to groundwater sustainability under varying climate, geology, and land cover dynamics are inadequately studied.

Therefore, a clear understanding of nested groundwater flow systems in the basins with contrasting climatic and non-climatic attributes (e.g., geology) is crucial for informed groundwater resource development and management. It equally provides a framework for a better understanding of discharge and recharge regimes and fluxes, locations and appropriate groundwater development and management sites and quantities (Gleeson & Manning, 2008).

Notwithstanding, while systematic investigation of the relationship between topographic and hydrogeological variables on nested groundwater flow systems has partly been carried out (Haitjema & Mitchell-Bruker, 2005; Gleeson & Manning, 2008; Gleeson *et al.*, 2011), a detailed investigation of the connection between climate variability, land cover dynamics and nested groundwater flow systems remains hugely derisory. This includes the understanding of the distinctive factors and features of the hierarchy, pattern and organization of nested groundwater flow systems, and how that is influenced by geological and climatic differences.

Therefore, this study sought to provide scientific proof of, and explanation on the presence of distinguishable nested groundwater flow systems in basins with contrasting climatic and geologic attributes and the extent of the contribution to basin water budget factoring in the difference in climate and geology.

## **1.2 Statement of the Problem**

There is limited understanding on how climate and geology affects the dynamics of nested groundwater flow systems and their distinctive influences on basin water budgets in basins with contrasting climate and geology. This, in turn leads to limited understanding of the hierarchy,

pattern and organization of nested groundwater flow systems. While details of the volumes of groundwater exploitation, recharge rates and water budgets are available (Siebert *et al.*, 2010; Konikow, 2013 & Dakhllalla *et al.*, 2016), individual contributions of each groundwater flow system to basin water budgets have been scanty. The details of the magnitude of individual flow fluxes are globally inadequate and in the study areas (Kimbiji and Singida) are missing altogether.

Conceivably, limited knowledge on the dynamics of nested groundwater flow systems impedes the theoretical development and practical applications of the theory of regional groundwater flow. Consequently, limited application of the groundwater flow theory results in limited understanding of the contribution of nested groundwater flow systems to basin water budget, groundwater availability and sustainability, thus, inadvertently promoting unsustainable groundwater development.

This study therefore sought to characterize and simulate the nested (local and regional) groundwater flow systems, factoring climatic and non-climatic (geology and land use/cover) parameters. The extent of contribution of individual flow systems to basin water budgets and the magnitude of groundwater flow system fluxes were also established in this study.

### **1.3 Rationale of the Study**

This study is imperative for improving the understanding and application of the theory of groundwater flow in groundwater development and management through assessment of the effect of climate variability and land cover dynamics on the variability of the contribution of nested groundwater flow systems in regional aquifers with contrasting climate and geology is imperative.

In addition, the study explored whether the influences of climate and land cover dynamics on nested groundwater flow systems are different in aquifers with contrasting climate and geology using a combination of approaches and techniques, utilizing real field test cases of Singida semi-arid fractured aquifer and the Kimbiji coastal, humid sedimentary aquifer in Tanzania.

Moreover, the use of hydrogeochemical facies and signatures, remote sensing and GIS techniques coupled with numerical groundwater modeling using finite difference modelling code and the state-of-the-art graphical user interface (GUI), ModelMuse helped unravel methodological as well and theoretical issues towards the achievement of the objectives of this study.

The Kimbiji and Singida aquifers are used as test cases to address the research problem based on their contrast in climate and geology. In addition, the two study areas are highly dependent on groundwater for various uses. To that effect, any mismanagement as a result of inadequate knowledge and ill-informed practices will affect the resource itself and society welfare at large.

## **1.4 Objectives of the Study**

### **1.4.1 General Objective**

The general objective of this study is to contribute to improved understanding of the influence of contrasting climate and geology on the hierarchy, pattern and magnitude of nested groundwater flow systems for sustainable groundwater resources development and management.

### **1.4.2 Specific Objectives**

- (i) To characterize local and regional groundwater flow systems based on distinctive hydrogeological, hydrogeochemical and isotopic signatures.
- (ii) To evaluate the combined effect of climate variability and land use/cover dynamics on spatiotemporal groundwater recharge rates.
- (iii) To simulate flux magnitude and contribution to water budget of nested groundwater flow systems using aquifers with contrasting climate and geology as test cases.

## **1.5 Research Questions**

- (i) How characteristic are local and regional groundwater flow systems based on hydrogeological, hydrogeochemical and isotopic signatures and facies in basins with contrasting climate and geology?
- (ii) To what extent do climate variability and land use/cover changes influence groundwater recharge in basins with contrasting climate and geology?
- (iii) What is the extent of variation on the magnitude of fluxes and contribution of nested groundwater flow systems to basin water budget in basins with contrasting climate and geology?



In order to achieve the aforementioned objectives and provide answers to the research questions, several methods, tools and activities were adopted and parameterized as summarized in Fig. 1.

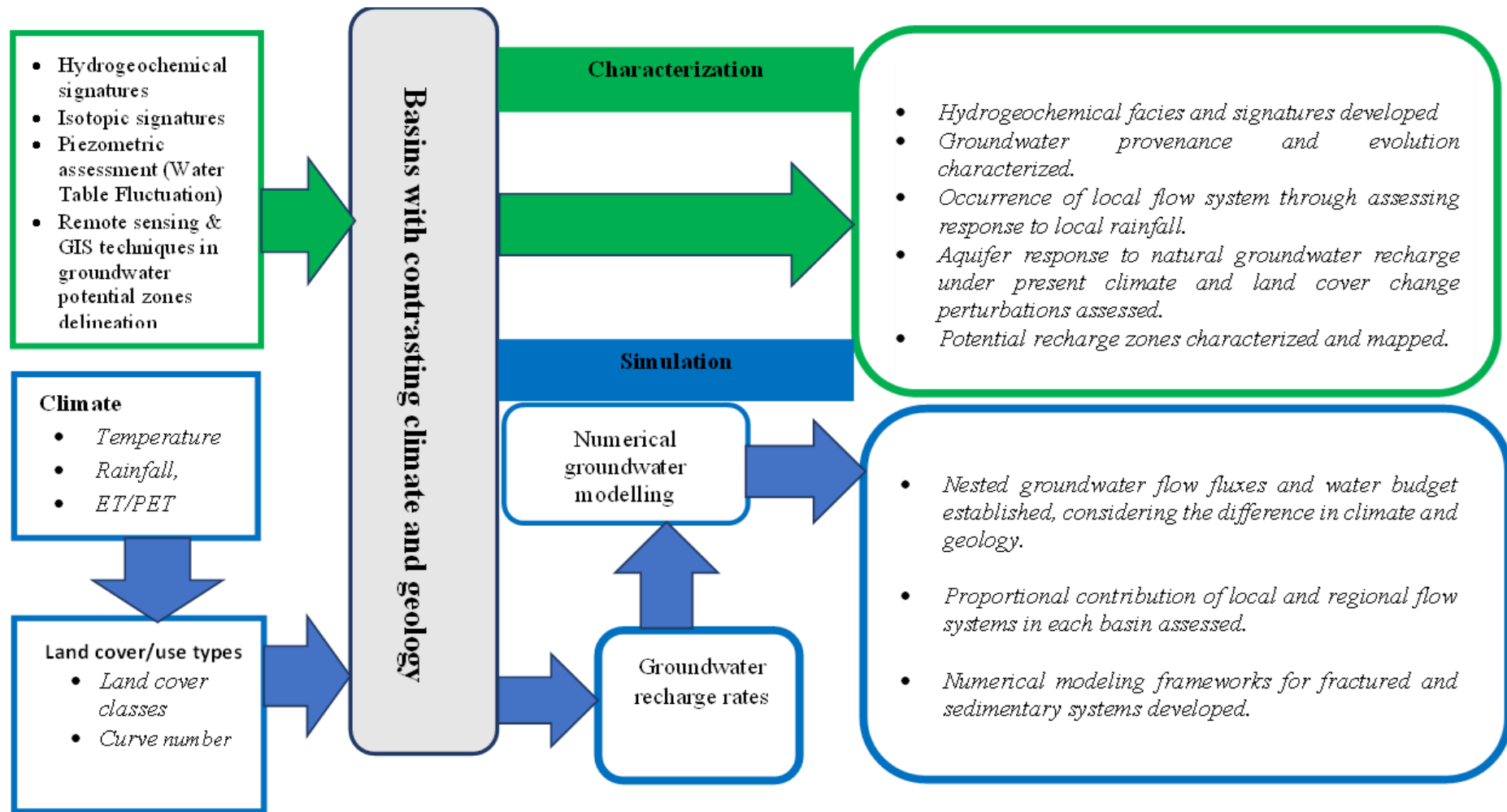


**Figure 1:** The conceptual framework which guided data collection, research activities, steps and processes used in this study

## **1.6 Significance of the Study**

The findings of this study will foster the understanding of the hierarchy, spatial distribution, organization and the behavior of residence time distribution of local and regional groundwater flow systems in the basins similar to the field test cases and beyond. This will contribute to the improvement of the existing theories on regional groundwater flow based on regional aquifers with contrasting climate, geology and anthropogenic pressures. In addition, the study findings will contribute to various global, regional and local technical and policy-based efforts towards sustainable groundwater development and management, considering climate variability and non-climatic factors.

Furthermore, this study produced a multipurpose groundwater flow modeling framework which can be applied for prediction of future groundwater flow conditions, used for studying groundwater flow system dynamics and organizing hydrogeological data, and as a tool to analyze the hypothetical groundwater flow systems.

To the scientific community, this study generated scientific knowledge and evidence on the likely influence of climate variability and land cover dynamics on basin water budgets and contribute to the scanty but growing body of knowledge of numerical regional groundwater flow systems modeling.

## **1.7 Delineation of the Study**

This study sought to improve the understanding of the dynamics of nested groundwater flow systems under climatic and non-climatic factors in regional aquifers with contrasting climate and geology and the implications on groundwater management using the Kimbiji humid and Singida semi-arid aquifers as test cases. The characteristics of local and regional flow systems, groundwater origin and provenance are discussed, utilizing hydrogeochemical and isotopic signatures and facies. Additionally, remote sensing and Geographical Information System (GIS) techniques and numerical groundwater model were used to carry out regional groundwater flow modeling and simulation of the proportional contribution of each flow system and scenarios of groundwater-surface water interactions.

This Dissertation is divided into five chapters. Chapter one consists of the background information, statement of the research problem, general and specific objectives, research questions and the significance of the study. Chapter two presents the literature review where

issues and contentions surrounding regional groundwater flow modeling, and the current state of knowledge regarding nested groundwater flow systems in basins with contrasting climate and geology. Chapter three covers the methodology part of the study, where different approaches, methods and techniques employed in this study are documented and discussed. Chapter four presents the results and discussion on the characterization and simulation of nested groundwater flow systems in the Kimbiji and Singida aquifers. Chapter five presents the conclusion and recommendations. Although thoroughly reviewed in this work, the effect of climate and geology on residence time distribution was not assessed in this work, and therefore remains a knowledge gap to be assessed by other researchers.

Moreover, the modelling part in this study concentrated on steady state part only, leaving the transient part due to excessive time series data inadequacy. Should data collection improve in the future, modelers can safely proceed to transient modelling of nested groundwater flow systems.

## CHAPTER TWO

### LITERATURE REVIEW

#### 2.1 The Evolution and Application of Regional Groundwater Flow Theories

The theory of regional groundwater flow systems was developed by Toth (1962, 1963), utilizing synthetic basins, dubbed the Tothian basins. From there on, the understanding of basin-scale groundwater flow patterns has been based on Toth's findings of a single flow system in a unit basin (Toth, 1962), and nested flow systems in a complex basin (Toth, 1963). Toth (1963) differentiated local, sub-regional and regional groundwater flow systems on the basis of the length of groundwater travel between recharge and discharge locations. In local systems, groundwater recharges and discharges in the same drainage basin, whereas in sub-regional systems, groundwater discharges in a drainage basin down-gradient from that in which it recharged (Toth, 1963). In regional systems, groundwater recharges in the uppermost basin and discharges in the lowermost basin (Toth, 1963).

There was an improvement of the work by Toth (1962), which was carried out by Vandenberg (1980). This was achieved by applying Toth's groundwater flow theory to develop a transient groundwater flow model in a unit basin and studied flow field distortion under a periodically changing water table. Additionally, Zhao *et al.* (2017) drawn-out the work of Toth (1963) by developing a transient solution under a periodically changing water table in a complex basin and examined the transient behavior of nested groundwater flow systems. This was an extended application of Vandenberg (1980) method.

Furthermore, Freeze and Witherspoon (1966) developed a steady state regional flow model using hypothetical layered aquifer systems in the early stages of after the development of Toth's groundwater flow theory. Freeze and Witherspoon (1967) assessed the effect of topography and geologic structures for different permeabilities upon groundwater flow patterns by simulating groundwater flow systems in 2D cross-sections under homogeneous and isotropic conditions.

However, most groundwater basins are located in areas that are made up of dissimilar hydrologic and geologic landscapes, with distinct 3D features, complex topography and geology. This can lead into more complex groundwater flow patterns and hierarchy as reported by Wörman *et al.* (2006) and Wang *et al.* (2016). Groundwater flow modeling using actual field

case studies are therefore needed to empirically validate the findings which are based on synthetic Tothian basins.

## **2.2 Groundwater Flow Modeling and Factors Affecting the Organization and Hierarchy of Groundwater Flow Systems**

Previously, a specified-head top boundary condition has predominantly been used for representing the water table in groundwater flow modeling (Toth, 1963). That procedure assumed that the water table mimics the topography (Liang *et al.*, 2012; Goderniaux *et al.*, 2013; Bresciani *et al.*, 2016). Nevertheless, concerns are looming that the subsequent results do not echo the changes in hydraulic conductivity and basin geometry, and a comparison cannot easily be made (Liang *et al.*, 2012). Furthermore, specifying the hydraulic head along the water table suggests that recharge is an unimpeded result of the model (Sanford, 2002). This makes the approach in general unfit for sustainability studies.

Nevertheless, the water-table configurations in the real situations are more complex than those from the synthetic basins. Therefore, oversimplifications are repetitively being made, which are not yielding representative results. This has been misrepresenting the nested groundwater flow systems in most basins, and the subsequent results may not reflect the field conditions. thus constraining decision making processes (Bresciani *et al.*, 2016). Reportedly, the water table does not always mimic topography, and according to Haitjema and Mitchell-Bruker (2005); Gleeson *et al.* (2011) and Liang *et al.* (2012), in some situations, water table and topography appear poorly related.

Desbarats *et al.* (2002) pointed out that the notion of the relationship between topography and the water table is valid locally but not globally, and sometimes water table and topography mimic each other under undisturbed systems (Haitjema & Mitchell-Bruker, 2005). Conceivably, in order for the water table to rise to the uppermost point in a basin, the ratio of recharge over hydraulic conductivity should be larger than 0.2 (Mitchell-Bruker, 1993; Liang *et al.*, 2012). This is only possible when the low-permeable basin is superimposed by a layer with even greater permeability such as sand. Consequently, the flux upper boundary is thought to be the best approach in groundwater flow systems modeling as it allows for the simulation of complex natural conditions.

In another scientific development, it is argued that the flux upper boundary is desirable for numerical simulation when examining how the flow patterns are affected by changes in

infiltration, hydraulic conductivity and/or basin geometry as reported by Liang *et al.* (2012). Equally important, Liang *et al.* (2012) reported that the combination of recharge and hydraulic conductivity in the development of nested flow systems is the best approach for assessing basin-wide groundwater flow systems. However, there is a premonition in this approach because it is based on isotropic media and limited geometric conditions. Further to that, recharge is also dynamic, influenced by such factors as rainfall dynamics, surface temperature and land cover changes in the recharge sites. This requires an investigation too, particularly predicting the outcome of the organization, the hierarchy of groundwater flow systems and basin water budget under climate and land cover scenarios.

### **2.3 Characterization of Aquifer Types and Groundwater Flow**

Toth (1963) and other subsequent works (e.g., Haitjema & Mitchell-Bruker, 2005; Gleeson *et al.*, 2011), discovered that in regions with recharge-controlled water tables, which are found in dry and high permeability terrains, regional groundwater flow makes up to 60% of the basin groundwater budget. In contrast, regions with topography-controlled water tables, which are purportedly found in humid areas with low permeability terrains, have less than 10% of the groundwater budget coming from regional groundwater flow (Haitjema & Mitchell-Bruker, 2005; Gleeson *et al.*, 2011). Reportedly, local flow systems can penetrate up to 900 m depth, while the subregional systems can go as far as 2400 m depth (Toth, 1963). The regional flow system originating from the highest hill in the basin can penetrate to a depth of over 3000 m. However, the penetration depth of the flow systems may be related to the length of the basin being studied (Freeze & Witherspoon, 1967) and the geology of a place.

Haitjema and Mitchell-Bruker (2005) introduced three simple dimensionless ratios to characterize the groundwater flow regime, which are: (i) the recharge over hydraulic conductivity, ( $R/k$ ); (ii) the distance between hydrological boundaries over the saturated aquifer thickness, ( $L/H$ ); and (iii) the distance between hydrological boundaries over the maximum terrain rise, ( $L/d$ ). It is argued here that, out of these, the recharge over hydraulic conductivity ratio is the most useful. Nevertheless, the other ratios are somehow biased towards topography-controlled basins, which are humid and the interaction between surface and groundwater is noticeable unlike in dry climates characterized by recharge-controlled water table aquifers.

Moreover, recharge-controlled and topography-controlled water tables can be differentiated using a dimensionless criterion, the water table ratio (WTR), where a  $WTR > 1$  depicts a

topography-controlled area and a WTR of  $<1$  depicts a recharge-controlled terrain (Haitjema & Mitchell-Bruker, 2005). Gleeson *et al.* (2011) log-transformed the water table ratio but the interpretation remained the same as  $-\log(\text{WTR})$  indicates recharged-controlled whereas  $+\log(\text{WTR})$  depicts topography-controlled water tables. Since the water-table ratio is derived from six parameters, investigating on what exactly controls the water-table type in regional aquifers with contrasting climatic and non-climatic factors remains open for further research (Gleeson *et al.*, 2011).

Alongside those arguments, Haitjema and Mitchell-Bruker (2005) demonstrated that the nature of the water table depends on recharge, the aquifer transmissivity, the aquifer geometry, and to some degree the topography. This is another area where the proposed study seeks to demonstrate how the difference in groundwater recharge affects the nested groundwater flow systems in both, semi-arid fractured and humid, porous aquifers, and recommend on where, under the prevailing climate and land cover dynamics should aquifer protection and groundwater development be focused.

Notwithstanding, the classification of aquifers into recharge-controlled and topography-controlled proposed by Haitjema and Mitchell-Bruker (2005) brings forward a number of scientifically contentious assumptions as follows: (i) In topography controlled water table terrains, potential recharge is higher than actual recharge while in areas of recharge-controlled water table potential recharge is equal to actual recharge; (ii) Topography-controlled water tables occur in humid areas and recharge-controlled water tables are found in arid/semi-arid areas; (iii) In humid, topography-controlled water table areas, there are unusable aquifers due to very low hydraulic conductivities and usable aquifers are found in dry, recharge controlled water table terrains where hydraulic conductivities are very high. According to Gleeson *et al.* (2011), in some mountainous and dry areas, low water table ratios have been reported. This indicates the presence of a recharge-controlled water table while in some areas with low permeability, high recharge rate and moderate topography resulted in high water table ratio. According to Haitjema and Mitchell-Bruker (2005), this latter scenario is a manifestation of topography-controlled water table basin. This suggests that in some regions, the variables have contrasting influence, thus, the classification and its underlying assumptions remain scientifically contentious, and therefore their application in decision-making can be misleading.

While it is assumed that local climate and land cover dynamics may not matter most in recharge-controlled water table terrains (Haitjema & Mitchell-Bruker, 2005; Gleenson *et al.*, 2011). It is



not clearly shown how the combination of climate and non-climatic factors (e.g., land cover dynamics) are likely to affect the hierarchy, organization and pattern of groundwater flow systems in recharge-controlled and topography-controlled water table basins. The proportional contribution of the nested groundwater flow systems in basins with contrasting climate and geology is conceivably unclear in the literature.

Further, it also remains unclear on what exactly controls the water-table type in aquifers with contrasting climate and non-climatic factors (e.g., geology and land cover types). This question was also put forward by Gleeson *et al.* (2011) as one of the major prevailing research gaps which remain open for further research. This study sought to disentangle such scientific and practical contentions in groundwater development and management.

Diagrammatic representation of topography-controlled water table basin and a recharge-controlled water table basin are presented in Fig. 2 and Fig. 3, respectively. The thickness of the blue lines indicates the importance and magnitude of the flow system. The thicker the line, the more important and the larger is the flow volume.

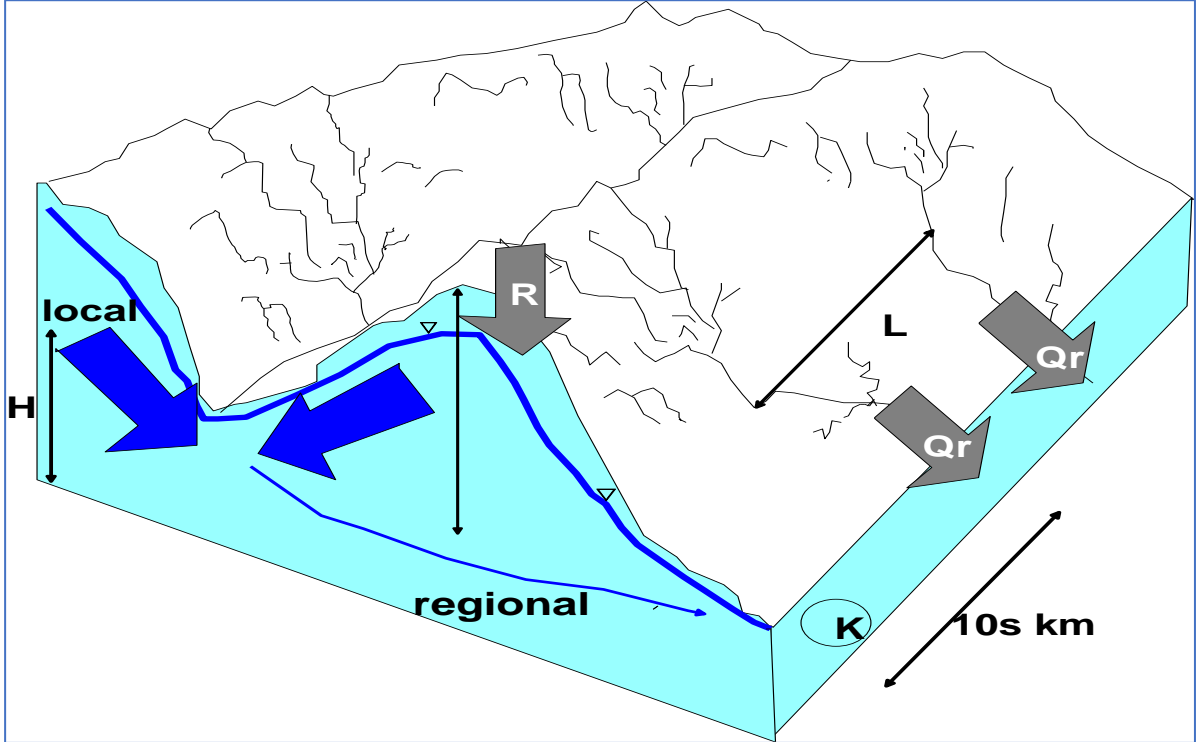


**Figure 2:** A schematic diagram depicting a topography-controlled water table (Modified from Gleeson *et al.*, 2011)



Arguably, models for backward particle tracking are still scarce, and according to Gusyev *et al.* (2014), the constructed transit time distributions at the groundwater discharge points using forward tracking are not equally as many. However, the distinctive behavior of residence time distributions (RTDs) between power law distribution and exponential distribution remains unclear, more so in basins with contrasting climatic and geologic characteristics. Notwithstanding, the knowledge of nested groundwater flow systems and their pathways is paramount for assessing groundwater quality and quantity in a basin.

According to Cardenas (2007), flow and transport under homogenous aquifer conditions follow power-law RTDs. However, it is not clear whether this applies to a topography-controlled water table basins or recharge-controlled water table basins. Furthermore, it still remains scientifically contentious on whether one of the basins could display exponential RTDs, since it is argued that surface water bodies are an expression of the groundwater tables, with the exception of semi-arid areas (Cardenas, 2007). Cardenas (2007) argues further that topography-driven groundwater flow results in power-law RTDs, especially in local and regional flow systems. This, in a way explains that in recharged-controlled water table areas, groundwater flow may not exhibit power-law RTDs, although it contravenes the theory developed by Haitjema and Mitchell-Bruker (2005). Generally, it has been difficult to draw a line between power-law RTDs and other distributions, as reported by McGuire *et al.* (2005). These scientific contentions equally need succinct field testing and therefore call for more detailed assessments of the behavior of RTDs in basins with contrasting climatic and non-climatic attributes in order to contribute to the ongoing discussions on portioning of regional groundwater flow systems based on groundwater travel times and residence time distributions.

## **2.5 Land use/cover, Climate Variability and Groundwater Recharge**

There are considerable stresses on the groundwater systems, both natural (e.g., climate variability and change) and human-induced (land use/cover changes), which have raised concerns about the long-term sustainability of groundwater resources for various uses all over the world regardless of the difference in geological formations or climate of a basin. Land use/cover dynamics and climate variability have knock-on effects on natural groundwater recharge (Crosbie *et al.*, 2012), but the spatial and temporal extents of such effects in basins with contrasting climate and geology are poorly understood and documented (Dowlatabadi & Zomorodian, 2016; Polemio, 2016). This makes it hard to design holistic but succinct groundwater management plans which accommodate the difference in climate and geology.

Arguably, management of groundwater is often carried out with inadequate knowledge of the relationship between groundwater recharge and other climatic and non-climatic factors, resulting in mismanagement of the resource (e.g., overexploitation), double accounting and unsatisfactory estimation of natural groundwater recharge in most basins as had previously been pointed out by other researchers (Sharma, 1986).

The impacts of land use/cover and climate changes on surface water are receiving immense scientific attention (Natkhin *et al.*, 2013), but the attention on groundwater is relatively insufficient. This contention was supported previously by other researchers (Bonan, 1997; Pielke *et al.*, 1998), and recently by Sterling *et al.* (2013), who argued that globally the impacts of land use/land cover changes on atmospheric components of the hydrologic cycle are increasingly recognized. It was hinted further that most hydrologic models mainly focus on river flows and discharge and not on changes in groundwater recharge and storages (Vazquez-Amabile & Angel, 2015).

In Tanzania, several studies have been conducted to assess the impact of climate change and variability, and land use/cover changes on stream flow using different models in the Ngerengere sub-basin (Natkhin *et al.*, 2013), in the Wami River sub-basin (Nobert & Jeremiah, 2012); in the Pangani basin (Notter *et al.*, 2013), in the Wami river sub-basin (Wambura *et al.*, 2015). Moreover, Mbungu and Kashaigili (2017) carried out hydrological modeling in the Little Ruaha River watershed, assessing the impact of climate and land cover changes. Others are Mutayoba *et al.* (2018) in the Mbarali River sub-catchment and Twisa *et al.* (2020) in the Wami river sub-basin.

The corollaries of land cover dynamics on catchment hydrology have equally been conducted in the Little Ruaha river catchment (Chilagane *et al.*, 2020). Some studies, albeit scanty, which aimed at assessing the impact of land cover changes on groundwater recharge in Tanzania have been carried out in the northern part of Tanzania (Lwimbo *et al.*, 2019; Olarinoye *et al.*, 2020). The paucity of studies on the implication of climate variability and land use/cover changes on natural groundwater recharge, considering the difference in climate and geology in responding to such perturbations remains ostensibly clear.

Reportedly, groundwater recharge is positively related to rainfall as pointed out previously (Oke *et al.*, 2011). Factually, decreasing precipitation is said to contribute more to decreasing groundwater table levels (Vazquez-Amabile & Engel, 2015). Nevertheless, this may not be

scientifically true altogether as other factors come into play and the relation between rainfall and natural groundwater recharge may not be linear.

Arguably, the relationship between rainfall and groundwater recharge is becoming more complex (Guzha *et al.*, 2017), which calls for the use of a combination of empirical and conceptual approaches in order to establish a more robust, scientifically plausible trend and status, which take into account more factors other than rainfall alone. Therefore, there is a need to justify the scientific contentions by concerted quantitative evaluation of spatial and temporal variations of groundwater recharge under different geological and climatic conditions.

The literature therefore, divulges inadequate scientific works regarding the impact of spatiotemporal climate variability and land use/cover changes on natural groundwater recharge and groundwater resources in general despite some patches of works. This study therefore employed a comprehensive assessment of the implication of the spatiotemporal climate variability and land cover changes in natural groundwater recharge in basins with contrasting climate and geology. The study used the Singida semi-arid, fractured, consolidated crystalline basement and the Kimbiji, humid, Neogene sedimentary coastal aquifers as test cases.

## **2.6 Hydrogeochemical Facies and Signatures for Groundwater Characterization and Evolution Assessment**

Interest on the use of hydrogeochemical facies and signatures for groundwater classification has increased as evidenced by several previous hydrogeochemical studies in Africa and elsewhere in the world (Koh *et al.*, 2005; Liu *et al.*, 2015; Madhav *et al.*, 2018; Sheikhy-Narany *et al.*, 2014; Srinivas *et al.*, 2017; Tay *et al.*, 2017). In addition to assessing water quality for groundwater monitoring and pollution abatement, hydrogeochemical signatures and facies are useful tools for prospecting the origin of groundwater evolution, groundwater provenance, recharge water and the source of groundwater mineral constituents (Marc *et al.*, 2016; Delana *et al.*, 2018).

Groundwater evolution and chemical constituents are influenced by a multitude of factors. As water moves through the soils and sediments its composition is altered by processes such as weathering, dissolution, leaching, precipitation, and ion exchange. According to Al-Ahmadi (2013), agricultural activities and urbanization also affect the quality of groundwater. Reportedly, chemical composition of groundwater is related to soluble products of rock weathering and decomposition and can reveal changes of those processes with respect to time

and place (Guglielmi *et al.*, 2000; Guglielmi *et al.*, 2002; Mikos *et al.*, 2004; Peng *et al.*, 2013; Vallet *et al.*, 2015).

While it is ostensibly clear that a multitude of factors control groundwater chemistry, it has always been difficult to pinpoint which among physical situation of the aquifer, bedrock mineralogy, anthropogenic activities and the climate of an area are peculiarly vital for determining groundwater evolution and hydrogeochemical processes (Narany *et al.*, 2014). Inadequacy in empirical and scientific evidence forms one of the drivers for the hydrogeochemical investigation of groundwater in the two basins with contrasting climate and geology in Tanzania using hydrogeochemical facies and signatures.

Arguably, groundwater passing through hard consolidated (e.g., Igneous) rocks usually dissolve very little amount of minerals and thus the mineral constituent is expected to be low. On the contrary, sedimentary rocks provide more ions to groundwater because they are relatively more soluble than the hard rocks (Mikos *et al.*, 2004; Peng *et al.*, 2012; Vallet *et al.*, 2015). The processes in the two different geological settings can also be amplified by the respective climate.

Hydrogeochemical signatures are reportedly useful for identifying varying groundwater flows in a basin (Bonzanigo *et al.*, 2001; Cervi *et al.*, 2012; Marc *et al.*, 2016). Such studies therefore, constitute an integral part of modern groundwater investigation techniques. Studies on hydrogeochemical analyses, spatial and temporal variations, and their relationships with the atmospheric and geological environments through which it circulates are thus scientifically imperative. To that effect, hydrogeochemical facies and signatures can be used to inform short term and long-term groundwater management actions and strategies and are therefore powerful tools for gathering hydrogeochemical information and unraveling the nuances of groundwater uses and water resources management challenges (Calmels *et al.*, 2011; Kim *et al.*, 2014; Marc *et al.*, 2016). Hydrogeochemical characterization and assessment of groundwater quality is equally imperative for understanding water types and classifying groundwater uses (Mussa *et al.*, 2019). It is also important in fostering policy formulation for water resources management and groundwater pollution abatement strategies.

The literature provides the following insights. Different groundwater systems result into occurrence of different water types and hydrogeological facies and signatures. Groundwater chemical composition represents hydrogeochemical facies and signatures which can be used to

decipher hydrological processes taking place in a groundwater basin. Nevertheless, one type of water based on hydrogeochemical facies and signatures may be suitable for one purpose but unsuitable for another. However, excessive concentration of dissolved ions in groundwater is undesirable for many uses. It does not favor crop irrigation as it affects plants and agricultural soils physically and chemically through lowering of osmotic pressure in the plant's structural cells. It is not recommended for human and animal consumption either due to associated health risks (Srinivas *et al.*, 2017).

The literature review in this subsection thus garnered valuable information on groundwater evolution, paths, the occurrence, and movement, deducing information on sources of groundwater recharge, discharge and residence time using hydrogeochemical facies and signatures. It further sought to unravel the mechanisms and processes controlling groundwater quality and assess the origin of water using hydrogeochemical signatures to inform short term and long-term sustainable groundwater management actions and strategies bearing in mind the difference in climate and geology.

## **2.7 Characterization of the Local Flow System through Water Table Fluctuation**

Characterization of the response of upper unconfined aquifers to rainfall events using the water table fluctuation method in basins is not a very common endeavor in groundwater studies. Usually, it indirectly happens while estimating groundwater recharge of a shallow aquifers but a succinct mention of the response of a particular aquifer to local rainfall episodes has not been a major focus of most recent studies. To concretize the argument, the following studies (Healy & Cook, 2002; Jassas & Merkel 2014; Saghravani *et al.*, 2015; Huet *et al.*, 2016; Doble & Crosbie, 2017.) utilized the water table fluctuation (WTF) method to assess groundwater recharge in shallow unconfined aquifers with a very little attention on how the difference in geology and climate could affect the response of the aquifers to local rainfall events.

Nonetheless, the method (WTF) has widely been criticized (Jie *et al.*, 2011) for its inadequacy in calculating representative recharge when the aquifers are heterogeneous. Since the two aquifers are heterogeneous, the WTF method was used to assess the aquifer response to local recharge, and thus identify the presence/absence of a local flow system other than estimating groundwater recharge through this method.

A good understanding of groundwater flow systems in a basin is imperative for the choice of drilling technology, cost estimation and collecting water quality information before

groundwater development. In addition, important scientific and policy-related problems need improved and updated data of hydrogeologic parameters and a better understanding of groundwater flow systems at local, regional to continental scales (Gleeson *et al.*, 2014). Besides, according to Haitjema and Mitchell-Bruker (2005) and Gleeson *et al.* (2011), local climate and land cover dynamics are not very important parameters in dry, semi-arid areas where regional and subregional flows are said to be most prominent flow systems, contributing significantly to groundwater storages. However, it was not clearly justified how the combination of climatic and non-climatic parameters are likely to influence the response of aquifers in different geologic environments to local rainfall.

Notwithstanding, it was previously reported by Kurylyk *et al.* (2015) that climate variability and land cover dynamics have instant effects on shallow groundwater systems. Elsewhere, Haitjema and Mitchell-Bruker (2005) hinted that the nature of the water table depends on recharge, the aquifer transmissivity, aquifer geometry, and to some extent the topography. Hitherto, it remains unclear on how the change and variability of recharge affect groundwater flow systems in both, topography-controlled and recharge-controlled water table basins. Moreover, discernments on where, under climate and land cover dynamics should groundwater development be focused on are equally inept. This hovering knowledge forms one of the bases for examining the response of the two aquifers to local rainfall events owing to their difference in climate and geology.

## **2.8 Groundwater-Surface Water Interaction and Groundwater Provenance through Stable Isotopic Techniques**

The use of stable isotopes is conceivably a promising technique in delineating groundwater-surface water interaction, groundwater provenance and assessing sources of groundwater recharge in any basin (Bertrand *et al.*, 2014; Crandall *et al.*, 1999; Kendall *et al.*, 1995). Arguably, isotopic techniques are the most preferred approaches to identify and quantify groundwater recharge, groundwater flow, interconnections between aquifers, and the sources and mechanism of pollution (Aggarwal *et al.*, 2004; Craig, 1961). In that way, the source of recharge (rainfall, riverbed seepage etc.,) can be easily identified (Aggarwal *et al.*, 2004, Mazor, 2004). Nonetheless, Qin *et al.* (2017) and Somaratne *et al.* (2016) recommended complementing stable isotopes data with major cations and anions. In this study, major cations and anions were analyzed to complement stable isotope results.



The global meteoric water line (GMWL) defines the general relation between  $\delta^{2}\text{H}$  and  $\delta^{18}\text{O}$  in the precipitation on a global scale and is described by  $\delta^{2}\text{H} = 8 \times \delta^{18}\text{O} + 10$  (Abid *et al.*, 2012; Oki & Kanae, 2006; Craig, 1961). For regional and local areas, the slope and intercept can differ from the GMWL. So, for local hydrogeological researches, local meteoric water lines (LMWL) can be more appropriate. This has been fully taken into consideration in this study. A comparison of LMWL with GMWL are usually meant to show local deviations from the world average. A direction coefficient (slope) of LMWL with a value greater than 8 indicates multiple moisture circulation, whereas a direction coefficient of less than 8 indicates greater moisture loss through evaporation. The former is an exemplification of depletion while the latter signifies enrichment (Zhang *et al.*, 2021; Craig, 1961). Greater deviations from the meteoric lines are associated with higher evaporation experienced during moisture transfers in air masses and are linked to low humidity conditions, which lead to high kinetic fractionation rate (Oiro *et al.*, 2018).

Accordingly, the higher the humidity, the lower the evaporation rate (Oiro *et al.*, 2018). All the depleted isotope values plotting close to the LMWL indicate limited influence of evaporation in the recharge process, thus implying that groundwater recharge originates from meteoric waters (Rowley *et al.*, 2001). The elevation of recharge area is usually evident from increasingly depleted isotope signatures in groundwater with increasing altitude, which in turn reflects altitudinal effects on precipitation (Hemmings *et al.*, 2015). This systematic variation is also affected by lower temperatures and higher relative humidity at high altitude, wind and their lower influence on condensation and evaporation (Rowley *et al.*, 2001).

Variable infiltration rates due to the difference in the materials making up the vadose zone lead to variability on the deuterium excess (d-excess). This has been reported elsewhere by other researchers (Baskaran *et al.*, 2009; Fynn *et al.*, 2016; Yeh *et al.*, 2009). Arguably, the variable infiltration rates are also a result of variable exposures of the infiltrating water to the effects of evaporation as reported previously (Adomako *et al.*, 2010; Fynn *et al.*, 2016; González-Trinidad *et al.*, 2017).

Conceivably, if d-excess values are high, they connote the influence of both local and regional moisture circulation, indicating highly enriched humidity. Low d-excess values reflect high humidity during formation of vapor mass as it was reported by other researchers (Abiye, 2013; Leketa *et al.*, 2019; Oiro *et al.*, 2018; Yusuf *et al.*, 2018). Arguably, in low humidity regions like Singida, re-evaporation of precipitation from local surface waters could create vapor

masses with isotopic content that plot above the local meteoric water line, as it was reported elsewhere (Abbott *et al.*, 2000; Adomako *et al.*, 2010; Hemmings *et al.*, 2015). It is not uncommon therefore to find groundwater samples plotting above the GMWL in the semi-arid areas due to high humidity during the formation of regional air masses and re-evaporation of precipitation from local surface water bodies like rivers, wetlands and lakes.

## CHAPTER THREE

### MATERIALS AND METHODS

#### 3.1 Description of the Study Areas

##### 3.1.1 Climate

Kimbiqi aquifer is part of the Wami/Ruvu Basin (WRB), one of the nine water basins in Tanzania. With relatively higher long term mean annual evapotranspiration (approximately 1400 mm/year) than mean annual rainfall (1100 mm/year), the Kimbiqi aquifer (Fig. 4B), located in the eastern part of Tanzania towards the Indian Ocean (Fig. 4B and Fig. 4C) is characterized by a humid climate. The Kimbiqi aquifer can only experience slight semi-arid conditions from June to October, and then around January. The air temperatures, both maximum and minimum indicate that the area is generally warm. Mean monthly maximum temperatures can be as high as 32 °C, while the lowest mean monthly minimum temperature is 19 °C. This aquifer really occurs in a warm and humid climate as reported recently (Mussa *et al.*, 2020a).

The Singida aquifer, found in the Internal Drainage Basin (IDB), central Tanzania (See Fig. 4A, and 4C) receives an average rainfall of 500-800 mm annually, and it experiences a unimodal rainfall season, beginning in November until May. The annual evapotranspiration can be as high as 1800 mm per year. Although there are humid months, generally the area is typically semi-arid, with an average aridity index of 0.49 (Mussa *et al.*, 2020b).

Due to a complete absence of rainfall in some months, there can be hyper-arid conditions in the Singida aquifer. The area experiences very high evapotranspiration rates, usually above 100 mm/month throughout the year (Mussa *et al.*, 2020b). Day temperatures range between 25° C to 30° C, while night temperatures may go down to 12° C. The months of June, July, August and September are the driest of all. Generally, the area falls within the driest zone of the Internal Drainage Basin (IDB), and hence the main source of water is groundwater (deep and shallow wells).

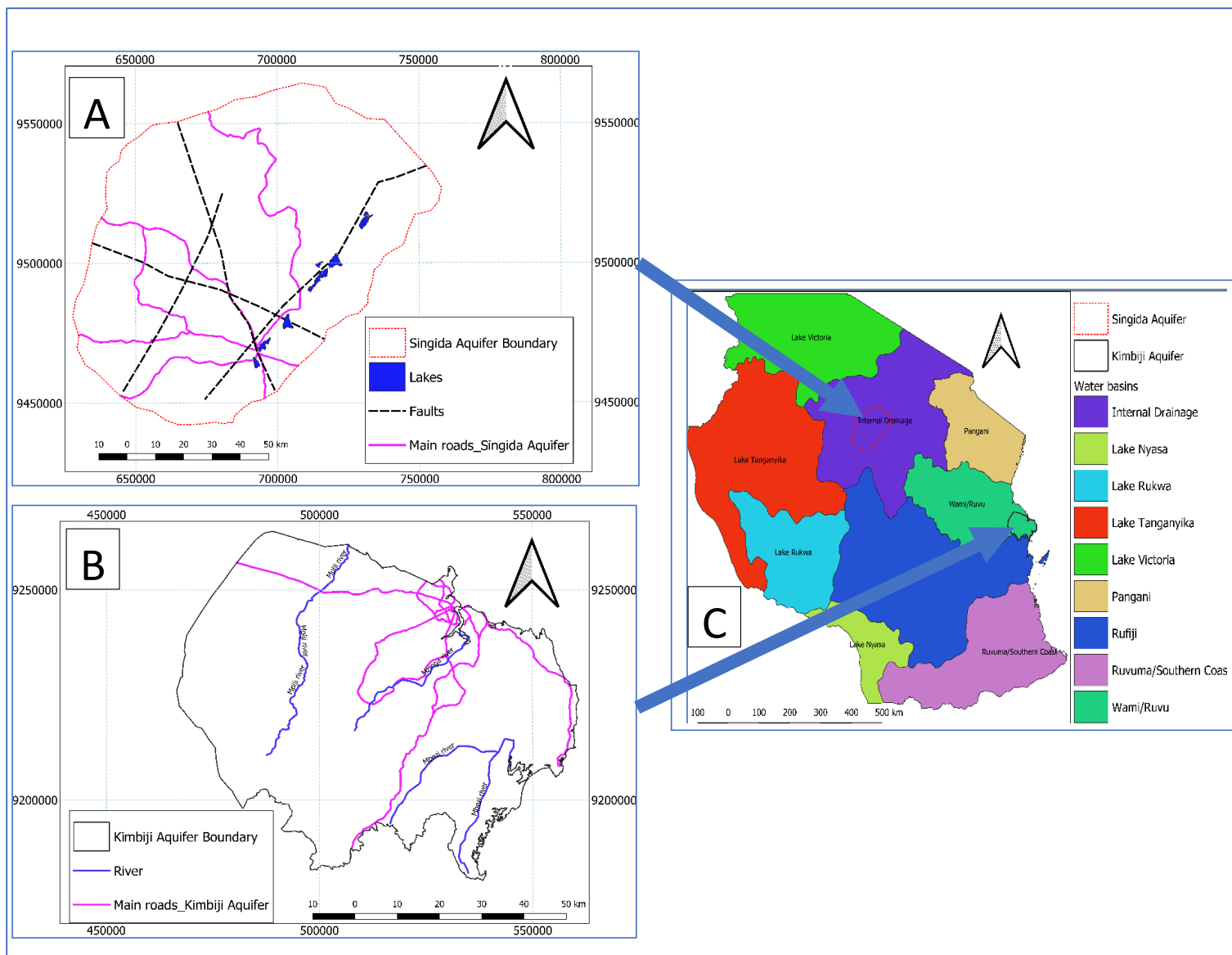


**Figure 4: Maps showing the position of the two study areas in relation to the water basins and the country**

### 3.1.2 Geology

The Kimbiji coastal Neogene aquifer (Fig. 5) is made up of Beach sand dune (b) and fluvial deposits (r1). These are younger (Quaternary) than any other geological units in the Kimbiji aquifer. This study area is also made up of Terrace deposits (Nt) and Fluvial marine sand (Nf). These are of tertiary time scale. Fringes of continental and marine sandstone (C) in the Cretaceous age are also found in the Kimbiji aquifer system. Generally, the geology of the Kimbiji, humid, coastal Neogene aquifer is made up of heterogeneous and layered Neogene (Miocene) sands, overlying an assumed geological basement of Lower Tertiary (Eocene) carbonates. From Dar es Salaam and northwards, the Neogene is overlain by thick Holocene deposits, but to the south, Neogene sands are exposed over an area of approximately 10 000 km<sup>2</sup> (Kent *et al.*, 1971).

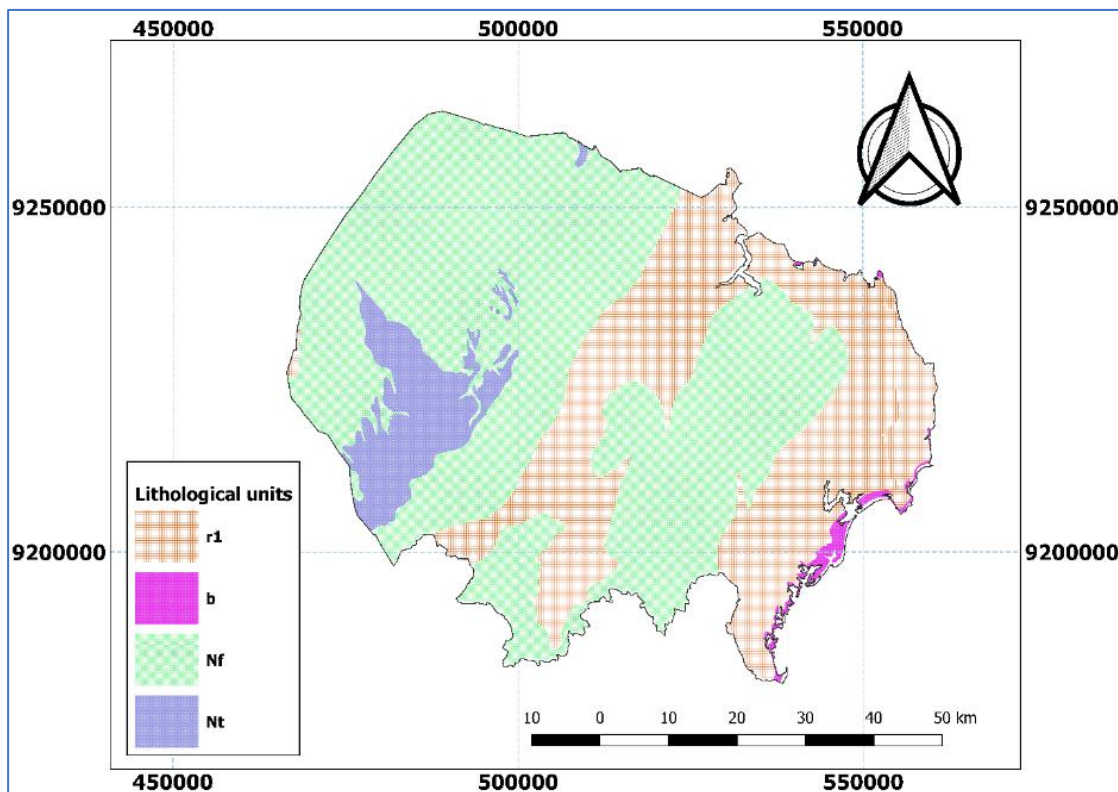


**Figure 5: The Geology of the Kimbiji Aquifer**

Geologically, the Singida aquifer is found within six main geological units, which include some small lakes denoted as Lk (Fig. 6). The main geological units are plutonic rocks consisting of granite and granodiorite, foliated, gneissose or migmatitic. Some massive porphyroblastic, including intimately related regional migmatite. Lithologically, these are of two types: (i) Those with topographic rough texture (gs) and strongly weathered granite with smooth topographic

texture (gs-b) and (ii) There is a Nyanzian system (Z) which occupies the central part of the study area, and extends east west, and north-east, which is made up of banded ironstone; metavolcanics; chlorite schist and pseudo-porphyrity (Fig. 6). Patches of Cenozoic sediments classified into (N), which are mostly alkaline volcanics in the north, north-eastern central - western parts of the study area, characterized by olivine basalt, alkali basalt, phonolite, trachyte, nephelinenite and pyroclastics and (NI), made up of lacustrine; sand, silt, limestone and tuff, which can be observed in the southern, western and north-western parts of the study area. There are also lineaments/faults extending north-south, north-east, and south-west, with some branching to south-east and north-west.

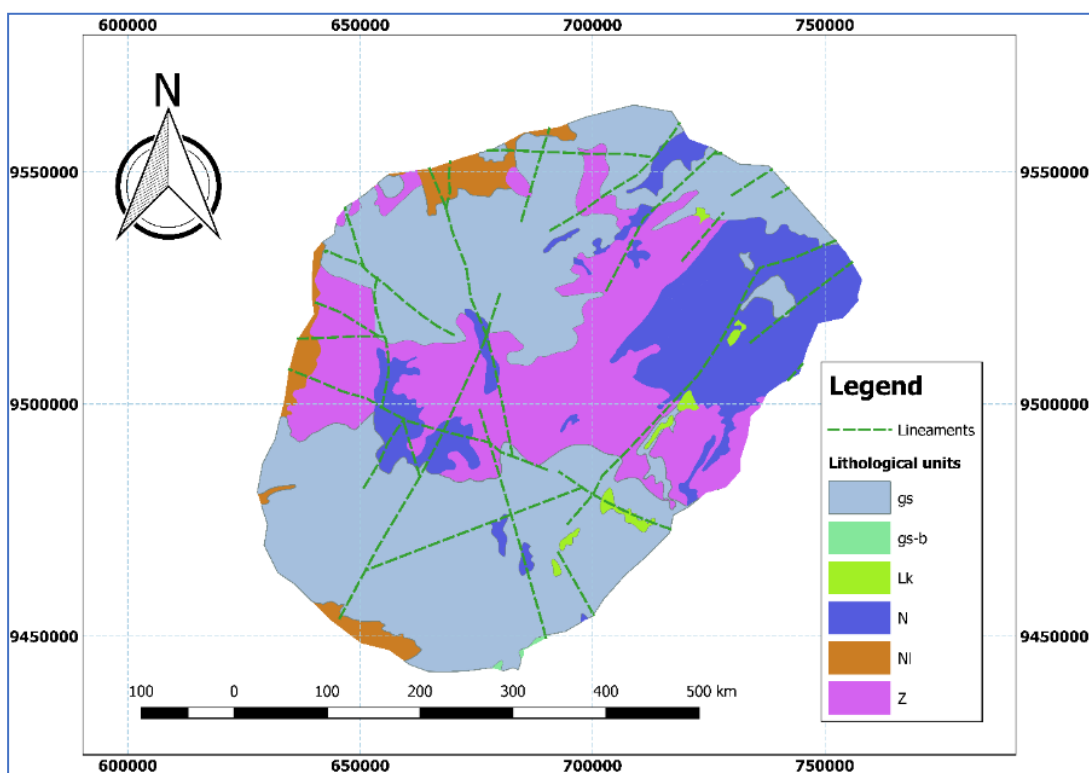


**Figure 6: The geology of the Singida aquifer and the lineament system distribution**

### 3.2 Fieldwork and Sampling Procedures

Fieldwork was carried out in the two aquifers involving water sampling from precipitation, groundwater (deep), groundwater (shallow), groundwater (spring) and surface water (rivers and lakes) for hydrogeochemical analyses to decipher hydrogeochemical facies and signatures in the two aquifers. Physical water quality parameters [i.e., pH, Electrical Conductivity (EC) and Total Dissolved Solids (TDS)] were measured in situ using HANNA HI 9829 Multiparameter Analyser. pH colour-coded buffer solution (NIST-traceable) of  $4.01 \pm 0.02$ ,  $7.00 \pm 0.02$ , and  $10.01 \pm 0.02$  were used to calibrate the meter before sample reading. Direct measurement method

enabled the EC of water samples to be analyzed after calibration with  $180\pm 10$   $\mu\text{S}/\text{cm}$ ,  $1000\pm 10$   $\mu\text{S}/\text{cm}$ ,  $1990\pm 20$   $\mu\text{S}/\text{cm}$ , and  $18,000\pm 20$   $\mu\text{S}/\text{cm}$  Sodium Chloride Standard Solution. The TDS, and pH were equally analyzed by the direct measurement approach.

### **3.2.1 Water Sampling and Preservation**

Standard procedures for water sampling, preservation, transportation, and chemical analyses were conducted as suggested in previous studies (Vogt *et al.*, 2001). Immediately after filtering using  $0.45$   $\mu\text{m}$  syringe filters, water samples for hydrogeochemical investigation were collected in  $0.5$  L air-tight high-density polyethylene (HDPE) bottles thoroughly washed and cleansed before being rinsed thrice by the sample water. Samples were carried and stored at  $4$   $^{\circ}\text{C}$  prior to shipping and analyses at Water Analysis and Testing in Environmental Regions (WATER) laboratory in Iringa, Tanzania.

For major ions (cations and anions), samples were collected from deep and shallow wells, rivers, lakes and springs. Major cations (Sodium, Potassium, Calcium, and Magnesium) and major anions (Chloride, Sulphate, bicarbonate, Nitrate, and Carbonate) were analyzed. It was established that for groundwater signatures and facies, the influence of seasons on the same is infinitesimally small (Kammoun *et al.*, 2018b). Arguably, seasons can only affect ion concentrations but not the water type and the groundwater hydrogeochemical signatures and facies. To that effect, the major focus was put on hydrogeochemical facies and signatures and not the concentration of ions for water quality assessment.

### **3.2.2 Analysis of Major Ions**

Chloride was measured using Ion-Selective Electrode (ISE) Method. An HQ440D Laboratory Chloride ( $\text{Cl}^-$ ) Ion Meter was used to assess Chloride levels in all test water samples. In either low or high range Chloride measurements, the Chloride Ionic Strength Adjustment (ISA) Buffer was added to samples and standards for minimization of associated errors/interferences. Nitrate analyses were accomplished using Cadmium Reduction Method. Hach DR1900 Portable Spectrophotometer was used to assess Nitrate concentration using NitraVer 5 Nitrate Reagent Powder Pillow. NitraVer 5 Reagent contains Cadmium metal that reduces nitrates present in the sample to nitrite. The nitrite ion reacts in an acidic medium with sulfanilic acid to form an intermediate diazonium salt which couples with gentisic acid to form an amber-coloured product. Sulfate analysis followed SulfaVer 4 Method. Hach DR1900 Portable

Spectrophotometer served the analytical activity with SulfaVer 4 Sulfate Reagent Powder Pillows. The method employs the reaction of Sulfate ions in the sample with barium in the SulfaVer 4 Sulfate Reagent to form insoluble barium sulfate. The amount of turbidity formed is proportional to the sulfate concentration. The SulfaVer 4 also contains a stabilizing agent to hold the precipitate in suspension.

Calcium analyses involved Flame Emission Photometry using a JENWAY PFP7 Flame Photometer Instrument. Calcium was measured using the calcium hydroxide band emission at 622 nm and usually gives an Orange-coloured flame. Potassium analyses involved Flame Emission Photometry using a JENWAY PFP7 Flame Photometer Instrument. Potassium was measured using an emission band at 766 nm and gave a Violet-coloured flame. The instrument principle of operation is similar to that of Calcium assessment. As for Sodium, the measurement employed Flame Emission Photometry using a JENWAY PFP7 Flame Photometer Instrument. Sodium was measured by using an emission band at 589 nm and gave a yellow-coloured flame. Magnesium analyses were based on the Calculation Method. Magnesium was estimated as the difference between Total hardness (analyzed using Titrette® Bottle-top Burette, a class A robust digital burette, 0.01N EDTA Standard solution with Eriochrome Black-T Indicator, and Ammonia Buffer of pH 10.0±0.1), and Calcium. Equation 1 was used to deduce the amount of Magnesium in a water sample.

$$\text{Magnesium (mg/L)} = [\text{Total hardness (mg/L)} - \text{Calcium hardness (as CaCO}_3\text{ mg/L)}] \times 0.243. (1)$$

In order for the laboratory results to be reliable, they were checked by Ionic Balance Error (%IBE) as shown in Equation 2, where concentrations are in milliequivalent per litre (meq/L) and was found to be <10%. This suggests that the analyses are scientifically acceptable (Kaka *et al.*, 2011).



$$\%IBE = \left[ \frac{\sum \text{Cations} - \sum \text{Anions}}{\sum \text{Cations} + \sum \text{Anions}} \right] \times 100 \quad (2)$$

### 3.3 Characterization of Groundwater Systems in Aquifers based on Hydrogeological, Hydrogeochemical and Isotopic Signatures and Controls

#### 3.3.1 Characterization of Hydrogeochemical facies Using Piper (Trilinear) Diagram

The geochemical evolution of groundwater in the two aquifers was explained by plotting the concentrations of major cations and anions in the piper trilinear diagram, as suggested by Piper (1944). The nature and distribution of hydrogeochemical facies were determined by providing insights into how groundwater chemical composition changes within the two aquifers. The Trilinear (piper) diagram was also used to graphically demonstrate the relationships between the most important dissolved chemical constituents in a set of groundwater samples. A total of 15 and 9 samples were collected from the Kimbiji and Singida aquifer respectively, with a representative distribution in each study area.

#### 3.3.2 Identification of Mechanisms Controlling Groundwater Chemistry

Gibb's ratios and diagrams were used to identify factors and processes controlling groundwater chemistry, which can be related to the physical situation of the aquifer, bedrock mineralogy and climatic conditions. Gibbs (1970) suggested two indices: (a) TDS versus  $\text{Na}^+ / (\text{Na}^+ + \text{Ca}^{2+})$  for cations and (b) TDS versus  $\text{Cl}^- / (\text{Cl}^- + \text{HCO}_3^-)$  for anions to illustrate the natural mechanisms controlling groundwater chemistry. The mechanisms include rainfall dominance, rock weathering dominance, and evaporation processes. Gibb's indices were calculated using Equations 3 and 4.

$$\text{Gibb's ratio I (Cations)} = \frac{[\text{Na}^+]}{[\text{Na}^+ + \text{Ca}^{2+}]} \quad (3)$$

$$\text{Gibb's ratio II (Anions)} = \frac{[\text{Cl}^-]}{[\text{Cl}^- + \text{HCO}_3^-]} \quad (4)$$

##### (i) Assessment of Groundwater Residence Time

Determination of groundwater residence time in the Singida and Kimbiji aquifers was carried out using the hydrogeochemical facies proposed by Schoeller (1967). The facies explain the

distribution and genesis of principal groundwater types along the water flow paths in the aquifers. These facies also provided important information on the progressive ion enrichment during the stay of groundwater on the basis of residence and transit times. They equally provided information on the rock-water interaction. The facies were arranged by taking the ionic percentages in relative decreasing order of their abundances.

**(ii) The Chloro-Alkaline Indices for Assessing Cation Exchange in the Groundwater System**

The Chloro-Alkaline indices (CAIs) were used to study the cation exchange between the groundwater and its host environment during residence or travel (Schoeller, 1965; 1977; Marghade *et al.*, 2012; Li *et al.*, 2013). The CAIs were also used to understand the changes in the chemical composition of groundwater along its flow path.

Schoeller (1965, 1977) proposed two CAIs, (CAI<sub>1</sub> and CAI<sub>2</sub>). These were used to interpret ion exchange between groundwater and its host environment in the two basins. A rule of thumb is that, a positive CAI indicates the exchange of Na<sup>+</sup> and K<sup>+</sup> from the water with Mg<sup>2+</sup> and Ca<sup>2+</sup> of the rocks, whereas a negative CAI connotes an exchange of Mg<sup>2+</sup> and Ca<sup>2+</sup> from the water with the Na<sup>+</sup> and K<sup>+</sup> of the rocks. The following equations (Equations 5 and 6) were used to calculate the CAIs with concentrations expressed in meq/L.

$$CAI_1 = \frac{[Cl^- - (Na^+ + K^+)]}{[Cl^-]} \tag{5}$$

$$CAI_2 = \frac{[Cl^- - (Na^+ + K^+)]}{[SO_4^{2-} + HCO_3^- + CO_3^{2-} + NO_3^-]} \tag{6}$$

**(iii) Assessment of Geochemical Processes Using Hydrogeochemical Signatures**

The following hydrogeochemical signatures were used to assess the origin of groundwater in the two aquifers as shown in equation 7 through 12.

$$HCO_3^- : Cl^- \left\{ \begin{array}{l} > 1.0: \text{recharge upper water flow course of carbonate rocks} \\ < 1.0: \text{Lower water flow course of carbonate rocks} \\ < 0.2: \text{Saline water and brines} \end{array} \right\} \tag{7}$$

$$\text{Na}^+ : \text{Cl}^- \left\{ \begin{array}{l} = \mathbf{0.876}: \text{Seawater} \\ < \mathbf{0.876}: \text{Replacement of Na by Ca or Mg} \\ > \mathbf{0.7}: \text{Loss of Na through precipitation of evaporate rocks} \\ > \mathbf{1.0}: \text{Water flow through crystalline or volcanic rocks} \end{array} \right\} \quad (8)$$

$$\text{Mg}^{2+} : \text{Ca}^{2+} \left\{ \begin{array}{l} = \mathbf{0.5 - 0.7}: \text{Calcium carbonate rocks} \\ = \mathbf{0.71 - 0.9}: \text{CaMg(CO}_3\text{)}_2 \text{ rocks} \\ > \mathbf{0.9}: \text{Mg - rich rocks or seawater mixture} \\ < \mathbf{0.5}: \text{Ca}^{2+} \text{ + rich water} \end{array} \right\} \quad (9)$$

$$\text{Na}^+ : \text{K}^+ \left\{ \begin{array}{l} < \mathbf{15}: \text{Na depleted water} \\ \mathbf{15 - 25}: \text{Natural recharge area} \\ \mathbf{50 - 70}: \text{Lower water flow course} \\ > \mathbf{70}: \text{Volcanic rocks} \end{array} \right\} \quad (10)$$

$$\text{Mg}^{2+} + \text{Ca}^{2+} : \text{Na}^+ + \text{K}^+ \left\{ \begin{array}{l} > \mathbf{1.0}: * \text{ Upper water flow course} \\ * \text{ Precipitation of NaCl from brine} \\ * \text{ Base ion exchange} \\ < \mathbf{1.0}: * \text{ Lower water flow course} \\ * \text{ Reverse ion exchange} \end{array} \right\} \quad (11)$$

$$\text{Ca}^{2+} : \text{SO}_4^{2-} + \text{HCO}_3^- \left\{ \begin{array}{l} > \mathbf{1.0}: \text{Ca - Cl brines} \\ < \mathbf{1.0}: \text{Normal hydrological cycle} \end{array} \right\} \quad (12)$$

### 3.3.3 Statistical analyses of Hydrogeochemical Parameters

#### (i) Correlation and Principal Component Analyses

Using correlation and multivariate statistical analysis (e.g., PCA) helped to identify hydrogeochemical processes affecting the major ion chemistry of the two study areas as it was applied in other studies (Wu *et al.*, 2014, 2015). Correlation and principal component analyses were carried out to disclose the relationship between each pair of the physicochemical parameters. In this study, correlation and principal component analyses and other statistical parameters were carried out using R and Excel software.

The linear correlations between hydrogeochemical parameters were assessed by correlation coefficients ranging between  $-1$  and  $1$ . Arguably, large coefficients reveal the significance of the relationship between two parameters. According to previous researchers (Hamzaoui-Azaza *et al.*, 2009), a positive coefficient articulates similarity and agreement between the correlated

parameters, and a negative coefficient exhibits that variable are developing in opposite directions. Correlation analysis for pH, EC, TDS and major ions was performed to describe the relationship between hydrogeochemical parameters in the two aquifers. Correlation analysis was also useful in understanding the chemical reactions occurring in groundwater systems (Wu *et al.*, 2014). A correlation coefficient of  $r \geq 0.5$  is considered a significant threshold.

Principal component analysis of 11 and 12 variables for Kimbiji and Singida aquifers respectively was performed. This statistical method has been used frequently in hydrogeochemical and water quality studies (Helena *et al.*, 2000, Adams *et al.*, 2001, Stamatis *et al.*, 2011). The variables for executing PCA were pH, TDS, EC,  $\text{Na}^+$ ,  $\text{K}^+$ ,  $\text{Mg}^{+2}$ ,  $\text{Ca}^{+2}$ ,  $\text{HCO}_3^-$ ,  $\text{CO}_3^{2-}$ ,  $\text{Cl}^-$ ,  $\text{SO}_4^{-2}$ , and  $\text{NO}_3^-$ . The PCA method allows a large dataset of variables, and physical and chemical parameters in water samples to be compressed into a smaller number of uncorrelated orthogonal factors by interpreting the correlation matrix (Jackson, 1991; Meglen 1992; Cloutier *et al.*, 2008). The varimax rotation was adopted to augment the contribution of higher significant variables by keeping only the important information and decreasing the variables with smaller contributions. The PCA also produced eigenvectors of a variance-covariance and correlation matrix from a raw dataset (I observations and J variables) (Davis 1973, 1986; Hamzaoui-Azaza *et al.*, 2009).

Principal component analysis was specifically carried out for a better understanding of the origin and evolution of groundwater chemistry as it has been applied in previous studies (Abou Zakhem *et al.*, 2017; Sheikhy *et al.*, 2014). The Kaiser Criterion varimax rotation was applied and helped in dropping the PCs with eigenvalues less than 1. This resulted into a simpler structure of components as discoursed previously by Al-Tamir (2008). The eigenvalue contains the information accounted for by an average single item in PCA. The PCA method decomposes the original matrix X with I observations of J variables into factor scores and factor loading matrices, as shown in Equation 13.

$$X = TP' + E \tag{13}$$

Where, the variables of the matrix X are standardized; T (I, J) corresponds to the matrix of J principal components; P' is the transpose of the original data; and E is the residual matrix.

## (ii) Assessment of Data Dispersion

Quartile analyses were carried out to determine outliers in the hydrogeochemical data. The interquartile range (IQR), which is usually the difference between the third quartile ( $Q_3$ ) and the first quartile ( $Q_1$ ) was used to find out the outlying data points. The rule of thumb was that, the observations which fall below  $Q_1 - 1.5(IQR)$  or above  $Q_3 + 1.5(IQR)$  were regarded as outliers. Further to that, descriptive statistics such as mean, median, maximum and minimum values of the physico-chemical parameters and major ions were calculated to aid in the interpretation of data dispersion from the central tendency.

### 3.3.4 Assessing Groundwater Provenance and Evolution Using Stable Isotopes of Water

Stable Isotopes water samples were collected and stored in 100 mL air-tight High-Density Polyethylene (HDPE) bottles. The sampling procedure ensured no air bubbles were allowed to minimize the chances of evaporation of collected samples before analysis which could falsify the results and any ensuing actionable and policy recommendations thereof. Furthermore, the sampling bottles were stored away from light in accordance with the International Atomic Energy Agency (IAEA, 1983) guidelines prior to their shipping and analyses. Samples were sent to the National Institute of Oceanography Laboratory in Karachi, Pakistan for analysis. Standard procedures for analyses of stable isotopes of water were followed as documented by Clark and Fritz (1997), Mook and Fries (2001), Aggarwal *et al.* (2004) and Otte *et al.* (2017). Determination of the stable isotope's compositions of water ( $\delta^{18}O$  and  $\delta^2H$ ) were carried out using an off-axis integrated cavity output spectroscope (OA-ICOS); model DLT-100, laser isotope analyzer (Los Gatos Research).

All the results are reported in  $\delta$  notation relative to Vienna Standard Mean Ocean Water (VSMOW). The  $\delta O$  and  $\delta D$  results are compared with the Global and Local Meteoric Water Lines which were established using isotope data in precipitation from different parts of the world, including Tanzania. The stable isotope abundances are given in  $\delta$  notations (expressed as permil, ‰) and based on Vienna Standard Mean Ocean Water (VSMOW) standard procedures as shown in equation 14 (Gonfiantini, 1978; Clark & Fritz, 2000). In each case, samples were measured in duplicates to offer the needed analytical measurement precision of  $\pm 0.1\%$  for  $\delta^{18}O$  and  $\pm 1\%$  for  $\delta^2H$ .

$$\delta_{Sample(\text{‰})} = \left[ \frac{R_{Sample} - R_{vsmow}}{R_{vsmow}} \right] \times 1000 \quad (14)$$

Where;  $R_{sample}$  and  $R_{vsmow}$  are the isotopic ratios of the sample and Vienna Standard Mean Ocean Water (VSMOW), respectively.

A total of 30 samples were collected in the two study areas for analysis of stable isotopes of water. This is in addition to the hydrogeochemical characterization of groundwater using hydrogeochemical signatures. Ten samples (1 rainwater, 3 samples from lakes and 6 groundwater samples) were collected for analysis in the Singida aquifer, while 20 samples (15 groundwater samples, 1 rainwater sample and 4 river samples) were collected from the Kimbiji aquifer. The choice and number of sampling sites were constrained by both, availability and accessibility to wells, lakes and rivers in each of the study areas. The representation of the major well fields in each study area played a key role in determining where to sample. A positive and negative value connotes enrichment and depletion in the heavy isotope respectively, relative to the standard.

#### **(i) Deuterium Excess and its Application for Deciphering Hydroclimatic Processes**

Deuterium excess (d-excess) was used to describe the influence of evaporation and precipitation so as to strengthen the use of stable isotopes to study the origin and geochemical evolution of groundwater. This added up to the deviation from a slope of 8 on a plot of Deuterium versus  $\delta^{18}\text{O}$ , which usually indicates mixing between different water groups.

Moreover, deuterium excess was used to indicate the deviation of local samples from the GMWL as well as an indication of climate sensitivity at the source of humidity and along the trajectory of air masses into the atmosphere. Therefore, d-excess was used to reflect the prevailing conditions during the evolution and interaction or mixing of air masses enroute to the precipitation site.

Low d-excess value ( $<8$ ) indicates evaporated rainfall whereas high d-excess value point towards recycled moisture. If the d-excess values ranged between 8 and 10, it is expected that it may be due to primary precipitation. Deuterium excess (d-excess) was calculated using equation 15, and the ensuing interpretation was undertaken in order to ascertain the possible source of precipitation of the two study areas which basically lead to either local or regional recharge to the aquifers.

$$\text{d-excess (‰)} = \delta^2\text{H} - 8\delta^{18}\text{O} \quad (15)$$

### 3.3.5 Characterization of Aquifer Response to Rainfall Events Using the Water Table Fluctuation Method

An attempt to characterize the groundwater flow systems in the study areas was equally facilitated by using the water table fluctuation (WTF) method. The WTF method was used to assess groundwater response to rainfall events. The method (WTF) has widely been criticized (Labrecque *et al.*, 2019) for its inadequacy in calculating representative recharge when the aquifers are heterogeneous. Therefore, given that the span of the two study areas (Kimbiji and Singida) make them heterogeneous, the WTF method was only used to assess the aquifer response to local rainfall, and thus depict the presence/absence of a local flow system other than estimating groundwater recharge through this method. The specific purpose was to add up to the bigger research theme on characterization of the nested (local and regional) flow systems in aquifers with contrasting climate and geology.

The following Equation (Equation 16) was used to estimate the aquifer response ( $A_r$ ) to rainfall events through assessing the change in water table elevation ( $\Delta h$ ) with time ( $\Delta t$ ). The principle is modified from the general equation used in the WTF method for assessing groundwater recharge where the product quotient of change in water table elevation with change in time is multiplied by the aquifer specific yield ( $s_y$ ).

$$A_r = \frac{\Delta h}{\Delta t} \quad (16)$$

A groundwater data logger (diver) was installed in the observation borehole at Maji Yard located in the vicinity of the IDB head offices for the Singida aquifer. For the Kimbiji aquifer, divers installed in 2011 at the observation borehole at Gymkhana club in Dar es Salaam provided data to quantify the response of the costal aquifer to the rainfall events.

The 20 m range AA258 was installed in Singida and data were downloaded with a date range from January 2019 to December 2020. Moreover, data from a diver h0461 of 10 m range installed at the Gymkhana club monitoring borehole were obtained for characterizing aquifer response to rainfall episodes. The data had a date range from July 2011 to June 2012. All the datasets were arranged in a hydrological year format to capture the periods of maximum soil

moisture deficit before the rainfall season begins where water would be needed to compensate for the soil moisture deficit first before any runoff and consequently water table rise could be realized. Using water level fluctuation data measured in cmH<sub>2</sub>O groundwater hydrographs were constructed for each monitoring borehole and were used to characterize the aquifer responses to local rainfall episodes, and thus depict local flow systems as carried out previously (Healy & Cook, 2002).

### **3.4 Evaluation of the Combined Effect of Climate Variability and Landcover Dynamics on Spatiotemporal Groundwater Recharge Rates across Regional Aquifers**

#### **3.4.1 Delineation of Potential Groundwater Recharge Zones**

##### **(i) Hydrogeology/Lithology**

The Kimbiji aquifer is made up of Beach sand dune (b) and fluvial deposits (r1). These are younger (Quaternary) than any other geological units in the Kimbiji aquifer. This study area is also made up of Terrace deposits (Nt) and Fluvial marine sand (Nf). These are of tertiary time scale. Fringes of continental and marine sandstone (C) in the Cretaceous age are also found in the Kimbiji aquifer system (Fig. 7). Generally, the geology of the Kimbiji humid, coastal Neogene aquifer is made up of heterogeneous and layered Neogene (Miocene) sands, overlying an assumed geological basement of Lower Tertiary (Eocene) carbonates.

From Dar es Salaam northwards, the Neogene is overlain by thick Holocene deposits, but to the south, Neogene sands are exposed over an area of approximately 10 000 km<sup>2</sup> (Kent *et al.*, 1971). Regarding recharge potential, the fluvial deposits (r1), have the highest potential followed by fluvial marine sand (Nf). The Terrace deposits (Nt) and Beach sand dune (b) are third and fourth respectively, in terms of groundwater recharge potential in the Kimbiji aquifer (Fig. 7).



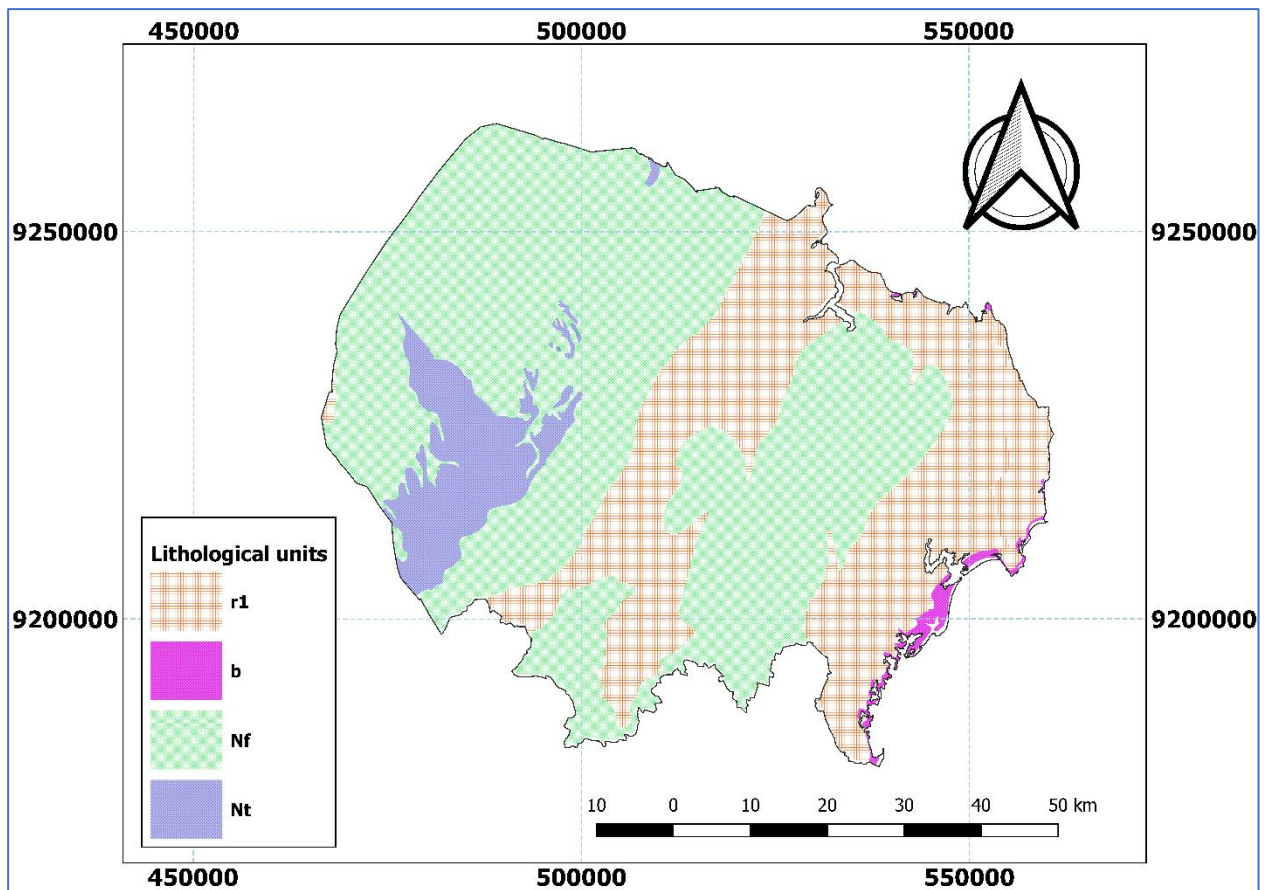


**Figure 7: Geological classes in the Kimbiji aquifer**

The Singida aquifer is hugely made of four main hydrogeological classes which are important for determining groundwater recharge potential (Fig. 8). These are the Precambrian craton (B-L/M1), which are the shields in which the basement rock has cropped out at the surface and platforms. The basement is overlaid by sediments and sedimentary rock. The Precambrian craton in the study area is composed of ancient crystalline basement rock, which in some areas are covered by younger sedimentary rocks (Hamilton, 1998; Stanley, 1999; Grotzinger & Jordan, 2010). The Kimberlites (B-L/M2), which are rock fragments (xenoliths) carried up from the mantle by magmas containing peridotite and delivered to the surface as inclusions in subvolcanic pipes called kimberlites (Hamilton, 1998; Grotzinger & Jordan, 2010; Petit, 2010). These inclusions have densities consistent with craton composition and are composed of mantle material residual from high degrees of partial melt. Peridotite is strongly influenced by the inclusion of moisture. Generally, there are two main hydrogeological features which determine the potential of the area for groundwater recharge, the Precambrian craton (B-L/M1) and the tertiary to quaternary unconsolidated materials (U-L/H). The latter (U-L/H) have very high potential while the former is very poor at influencing groundwater recharge through primary porosity and permeability (Fig. 8). There is also a small patch of tertiary to quaternary volcanic

rocks (I-L/M) on the eastern side of the study area. The potential of tertiary to quaternary volcanic rocks in influencing groundwater recharge is considerably good.

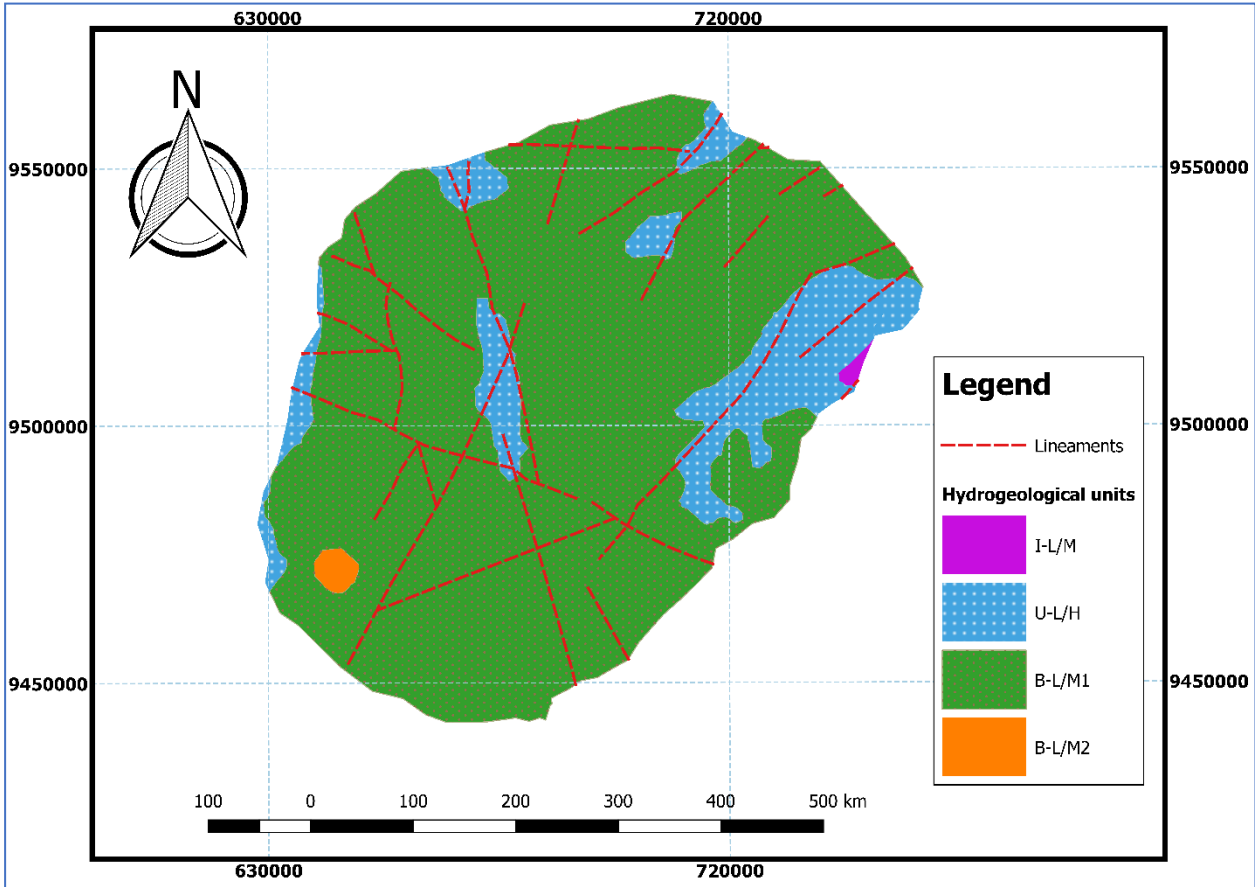


**Figure 8: Map showing the hydrogeology of the Singida aquifer**

**(ii) Lineaments and Lineament Density**

The Lineaments form what is called secondary porosity in crystalline basement aquifers. Thus, groundwater occurrence, flow and the recharge in the Singida aquifer is mainly by this type of porosity, and as shown in the Fig. 9, the area is highly fractured. The open fractures are excellent features for artificial recharge too. Lineament density varies between 0 to 10 km/km<sup>2</sup> (Fig. 7). The lineaments are not important features in the Kimbiji aquifer; thus, the lineament density map was not part of the groundwater recharge potential package for the Kimbiji aquifer.

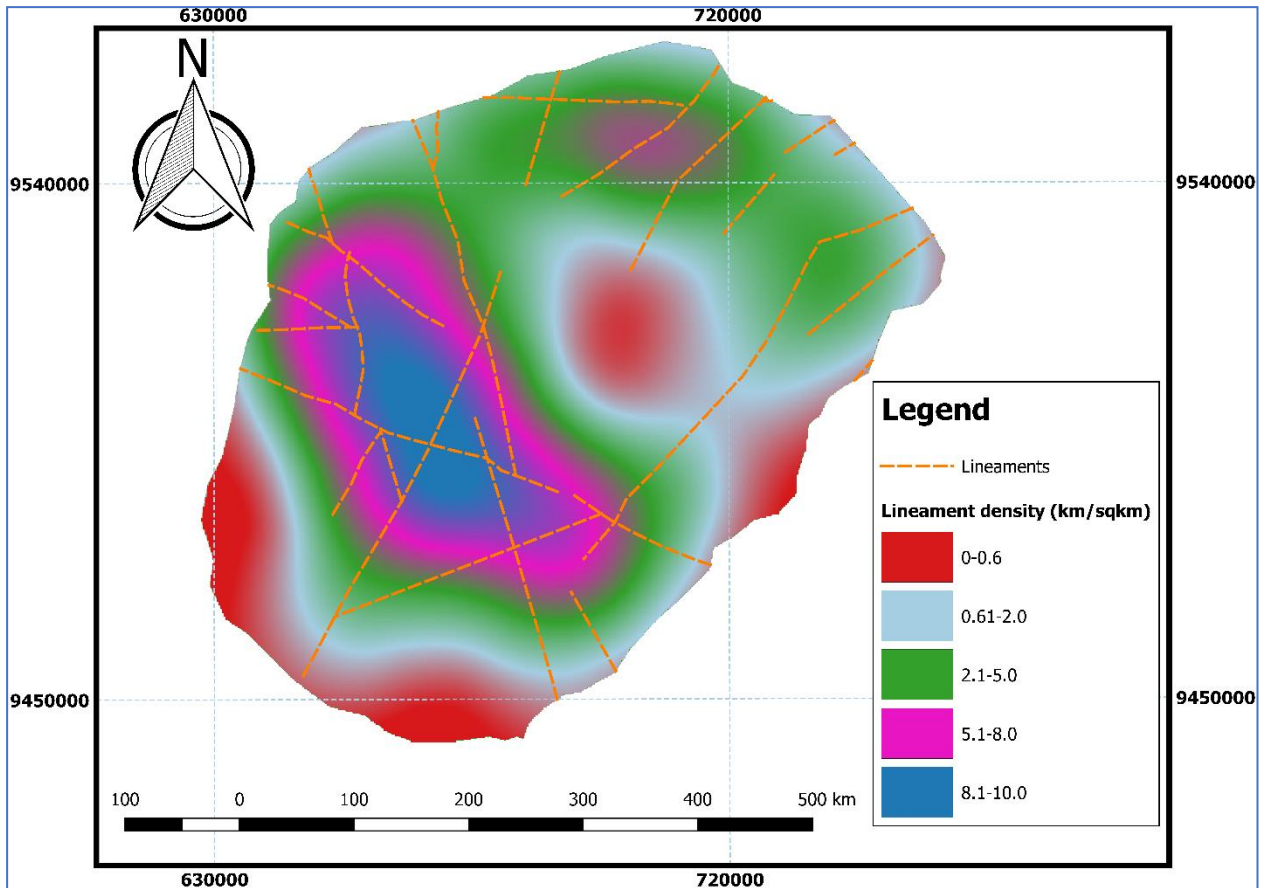


**Figure 9: A map showing the lineament density with lineaments**

The rule of thumb is, the higher the lineament density, the more likely is recharge to occur. Therefore, the lineament density of 0–0.6 km/km<sup>2</sup> is very poor in terms of groundwater recharge potential while the potential of 8–10 km/km<sup>2</sup> is very high. Lineament density is the result of the length of lineaments in a square kilometer area. It was established using equation 17 as suggested by other researchers (Das *et al.*, 2017).

$$L_d = \frac{\sum_{i=1}^n (L_i)}{A} \quad (17)$$

where,  $L_d$  is lineament density (km/km<sup>2</sup>),  $L_i$  is the total length of all lineaments (km) and  $A$  is the area of the grid (km<sup>2</sup>).

### (iii) Drainage and Drainage Density

Drainage density was derived from the stream network of the two study areas (Fig.10 & Fig. 11). Such geological structures gave an idea of how drained the study areas are, which is also an indication of the likelihood of the occurrence of surface runoff as a result of more drainage channels. Drainage density was calculated using Equation 18.

$$D_d = \frac{\sum_{i=1}^n (D_i)}{A} \quad (18)$$

where,  $D_d$  is drainage density ( $\text{km}/\text{km}^2$ ),  $D_i$  is the total length of streams ( $\text{km}$ ) and  $A$  is an area of a grid ( $\text{km}^2$ ).

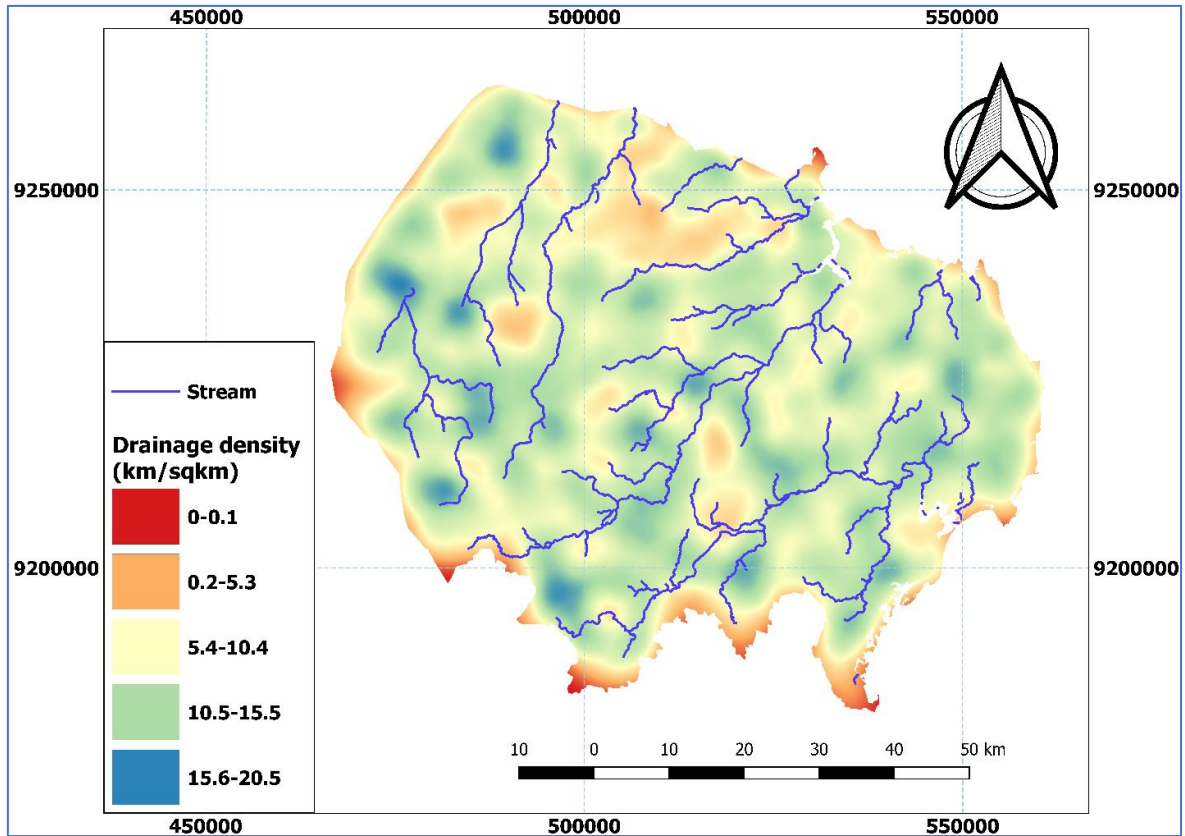


**Figure 10: Drainage density classes in the Kimbiji aquifer**

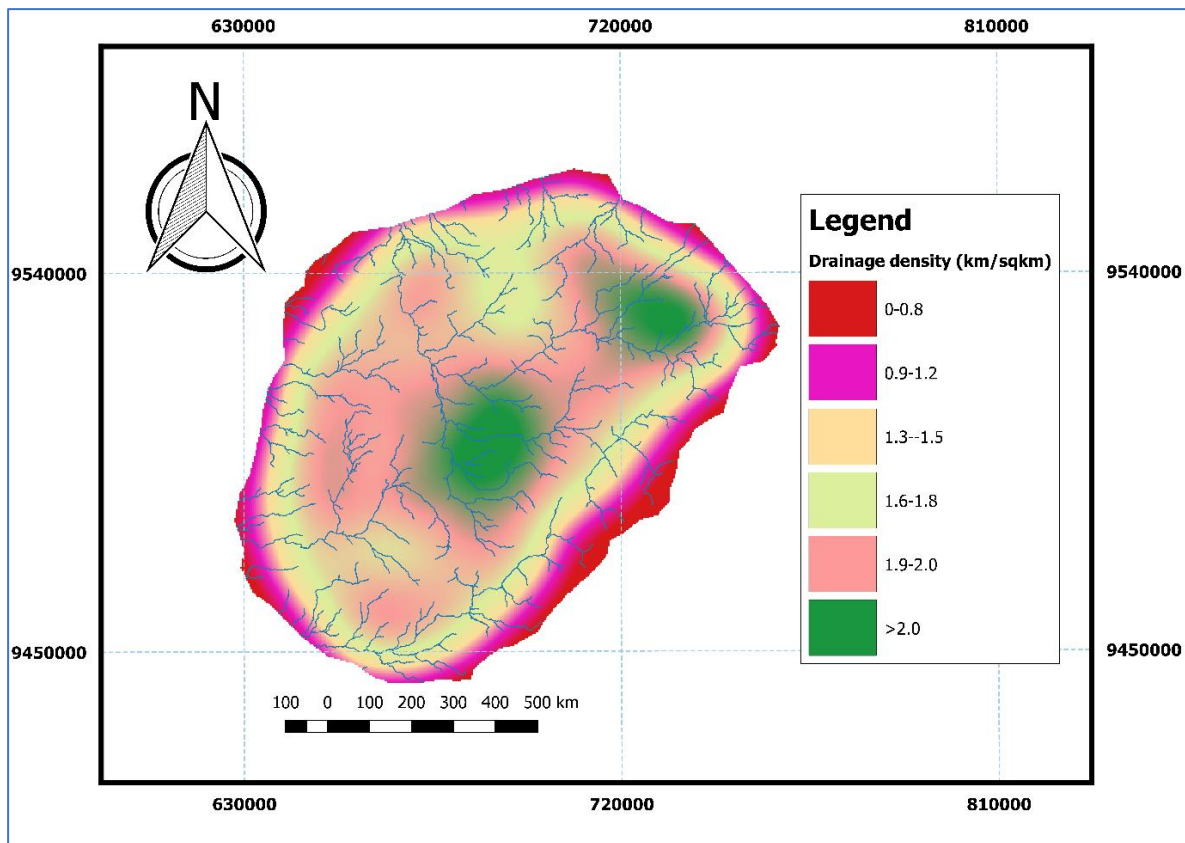


**Figure 11: A map showing the drainage density of the Singida aquifer**

**(iv) Land Cover**

In terms of land uses/covers as inputs for delineating groundwater potential zones, the study areas were classified into 8 distinct classes namely, water bodies, wetlands, built-up area, forest, grassland, bushes, woodland and cultivated area. Cultivated, grassland and bushland are the most dominant land covers while built-up area, wetland and water bodies (mainly lakes) occupy a small portion of the study areas. Land use land cover (LULC) classification followed a detailed understanding of the spatial extents and geographical delineations of the two study areas as detailed in the following sections. All the data were exported into QGIS and reprojected to the Universal Transverse Mercator Projection WGS 84/UTM Zone 37S, (EPSG: 32737) for Kimbiji aquifer and WGS 84/UTM Zone 36S, (EPSG: 32736) for Singida aquifer (Fig. 12 & Fig. 13). A detailed LULC classification is documented under groundwater recharge estimation section.



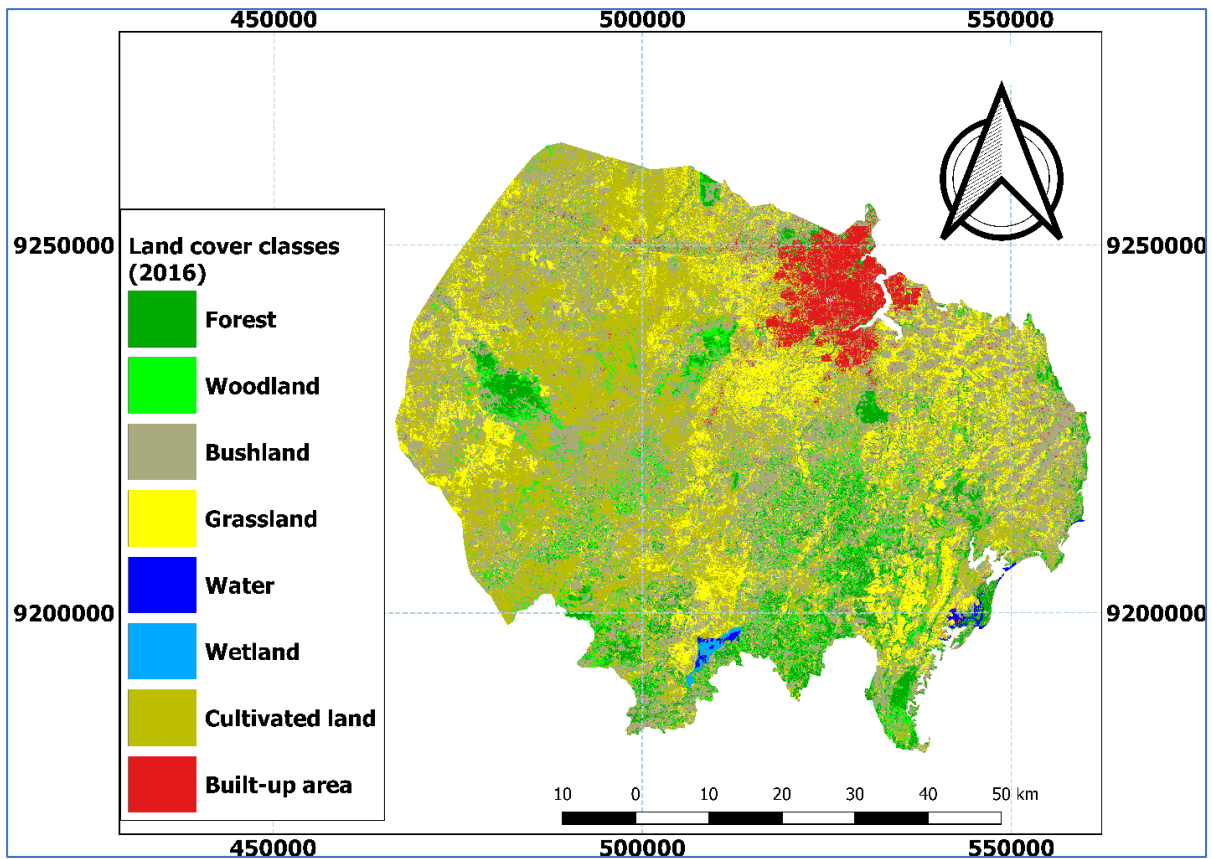


Figure 12: Land cover classes in the Kimbiji aquifer

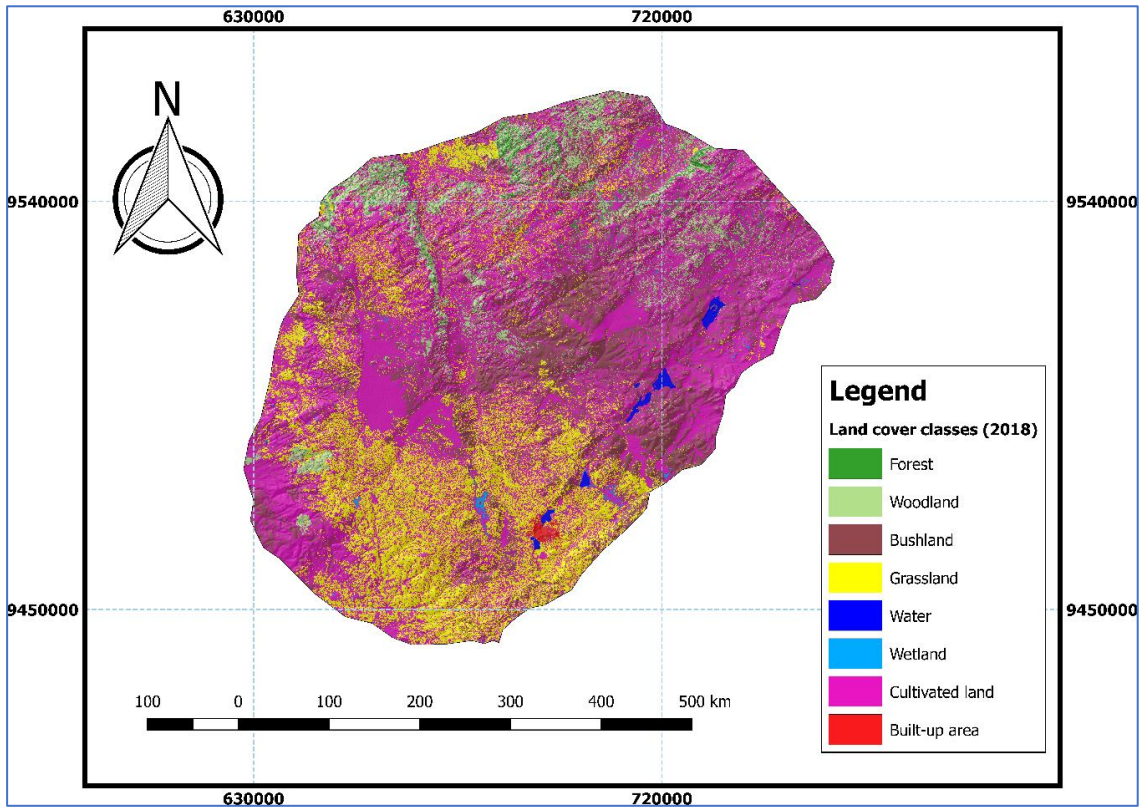
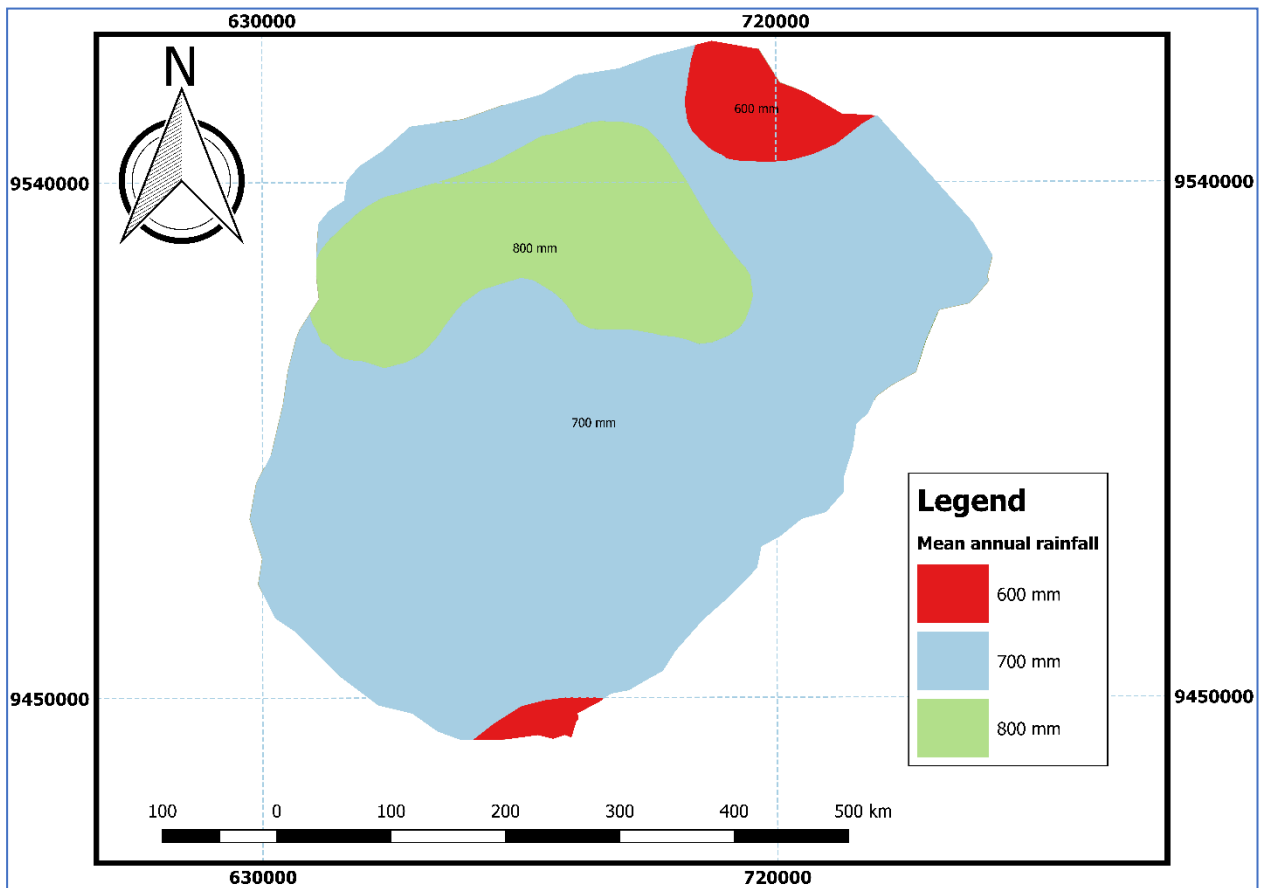


Figure 13: Land use/cover map of the Singida aquifer

**(v) Rainfall Distribution**

The Singida aquifer is divided into three distinctive rainfall zones (Fig. 14) while the Kimbiji aquifer has two rainfall zones (Fig. 15). The first zone in the Singida aquifer that covers the largest part of the study area receives a maximum of 700 mm per year. The second zone which is a small patch in the south and north (red colored) receives a maximum of 600 mm per year and is the driest zone in the study area. The third zone, which is relatively small, located in the north western, extending towards the central part of the study area receives a maximum of 800 mm per year. The Kimbiji aquifer has a zone which receives a maximum of 1100 mm per year, and this is the largest of the two zone, and the other zone receives a maximum of 900 mm per year. With respect to rainfall, the rule of thumb is, the more the rainfall received, the higher the likelihood of groundwater recharge provided that other favorable conditions exist.



**Figure 14: Rainfall distribution in the Singida aquifer**

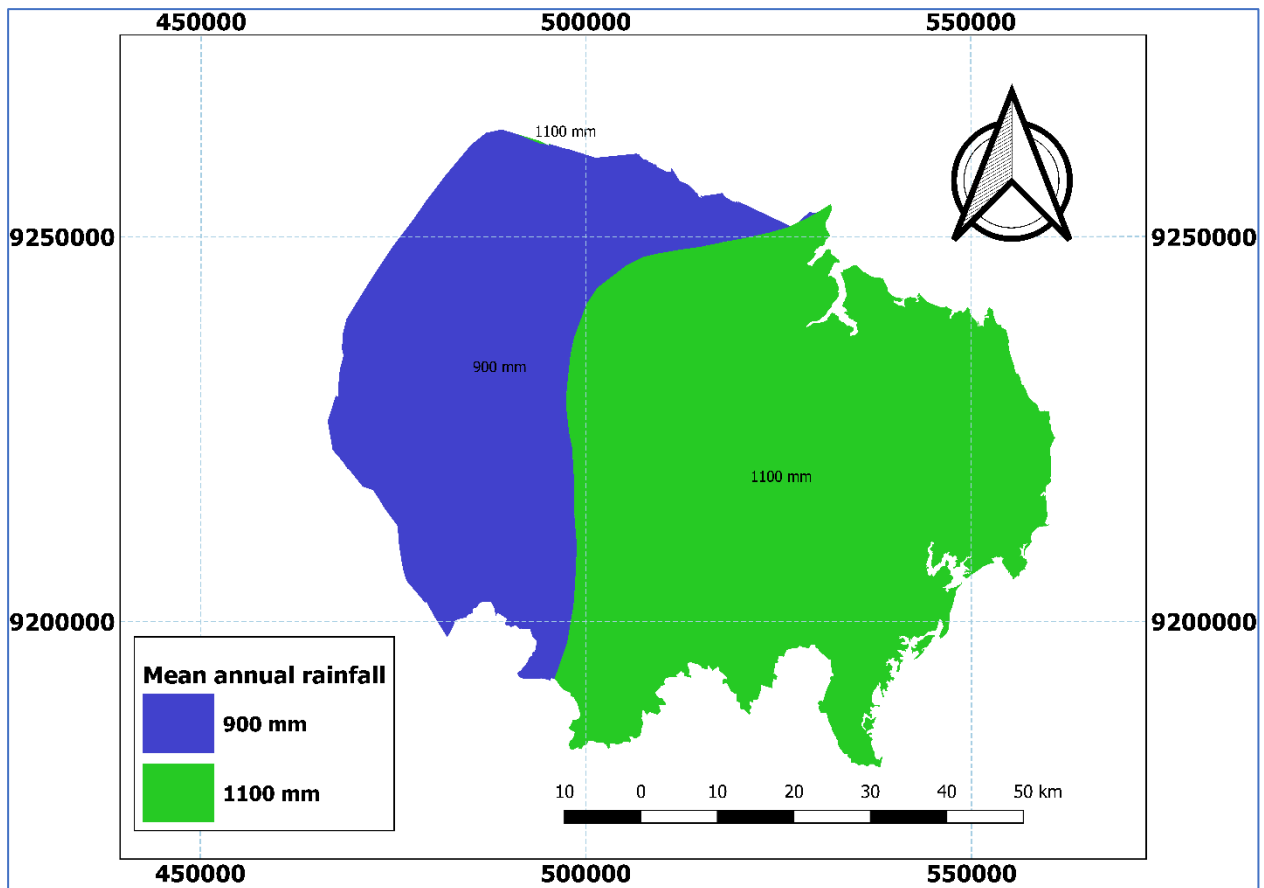


**Figure 15: Rainfall distribution in the Kimbiji aquifer**

**(vi) Soil**

In the Singida aquifer, there are six soil types (Fig. 16). The first type is ferric Acrisols (Af3-1/2a). Acrisols are defined by the presence of a subsurface layer of accumulated kaolinitic clays. It is also made up of sedimentary materials and is found in landscapes that have an undulating topography. This covers the biggest part of the study area (Fig. 16). There are also calcic cambisols (Bk29-2ab), which are characterized by an increasing clay content with depth. Moreover, the study area is also covered by eutric fluvisols (Je52-2/3a) in the north, north western and western parts of the study area. This is regarded as the most suitable soil for water infiltration, and potential groundwater recharge thereof. These are formed from unconsolidated water-borne materials and are of recent alluvial deposits with good properties for water infiltration. Lithosols (I-L-R-bc), consisting of thin soil made up of mainly partially weathered rock fragments, also make up the soil types in the study area. They are shallow soils consisting of imperfectly weathered rock fragments. The potential for groundwater recharge is fairly low. Dystric nitosols (Nd38-2bc) and eutric nitosols (Ne38-2ab) which are deep, red, well-drained soils with a clay content of more than 30% and a blocky structure are also found in the study



area. In addition to being inherently the most fertile soils of the tropical soils due to their high nutrient content, their characteristic depth gives them a permeable structure and thus a very good groundwater recharge potential. The distribution of soil classes in the Singida aquifer is presented in Fig. 16.

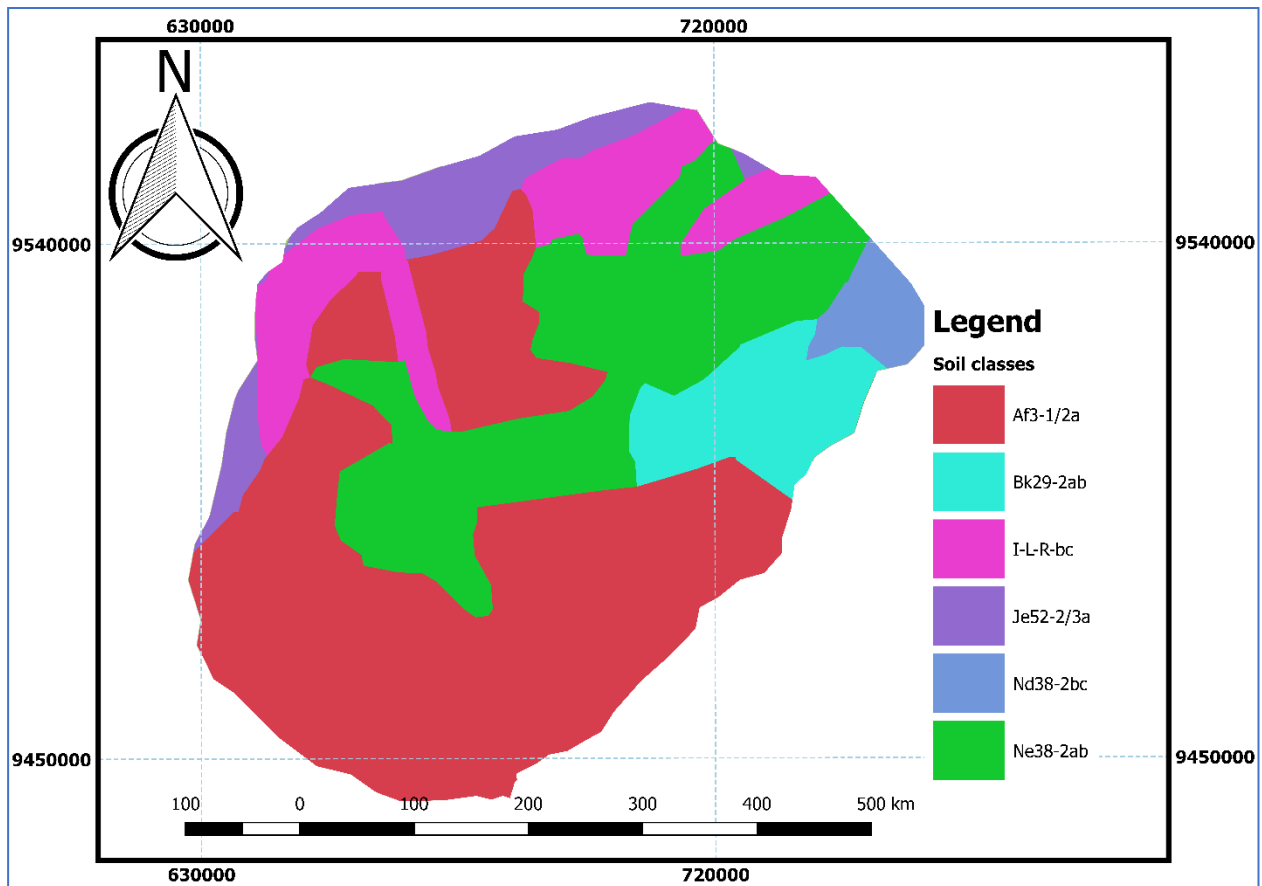


**Figure 16: Soil classes in the Singida aquifer**

In the Kimbiji aquifer there are Orthic Acrisols (Ao67-2bc), which have a clay-rich subsoil and is associated with humid, tropical climates (Fig. 17). The runoff potential of these soils is moderately high, and thus their recharge potential is moderately low. This is because, the Acrisols have a layer of accumulated kaolinitic clays where less than half of the ions available to plants are calcium, magnesium, sodium, or potassium and also by the lack of an extensively leached layer below the surface horizon (uppermost layer). The Ferric Luvisols (Lf78-1/2ab) are widespread in temperate climates and are generally fertile. Owing to their fertility, they are used for agriculture, and the spatial coverage in the study area is relatively larger than the Arenosols. This makes their groundwater recharge potential very good.

As it is for other Arenosols, Cambic Arenosols (Qc30-1/2a) are sandy-textured soils that lack any significant soil profile development. They exhibit only a partially formed surface horizon

(uppermost layer) that is low in humus. Given their excessive permeability and low nutrient content, agricultural use of these soils requires careful management. The recharge potential of Cambic Arenosols is comparable to that of Ferralic Arenosols, which is very high. However, the Cambisols have a relatively higher spatial coverage than the Arenosols.

The Ferralic Arenosols (Qf35-1b, Qf31-1ab) are characteristically red or yellowish sandy soils, which mainly occur in the humid areas. Ferralic Arenosols are generally poor soils with the clay content below 10%. Therefore, being sandy, with limited clay content, their runoff potential is relatively low. Despite their low runoff potential, and thus high recharge potential, their spatial extent is very limited because they occupy very minute fringes of this case study as shown in Fig. 17. Eutric Planosols (We8-1/2a) usually have a base saturation of less than 50 percent in at least a part of the slowly permeable horizon within 125 cm of the surface. Owing to their topographical position and the presence of a B horizon of fine and impermeable texture, these soils are often flooded during the rainy season. They have a low recharge potential for that matter.

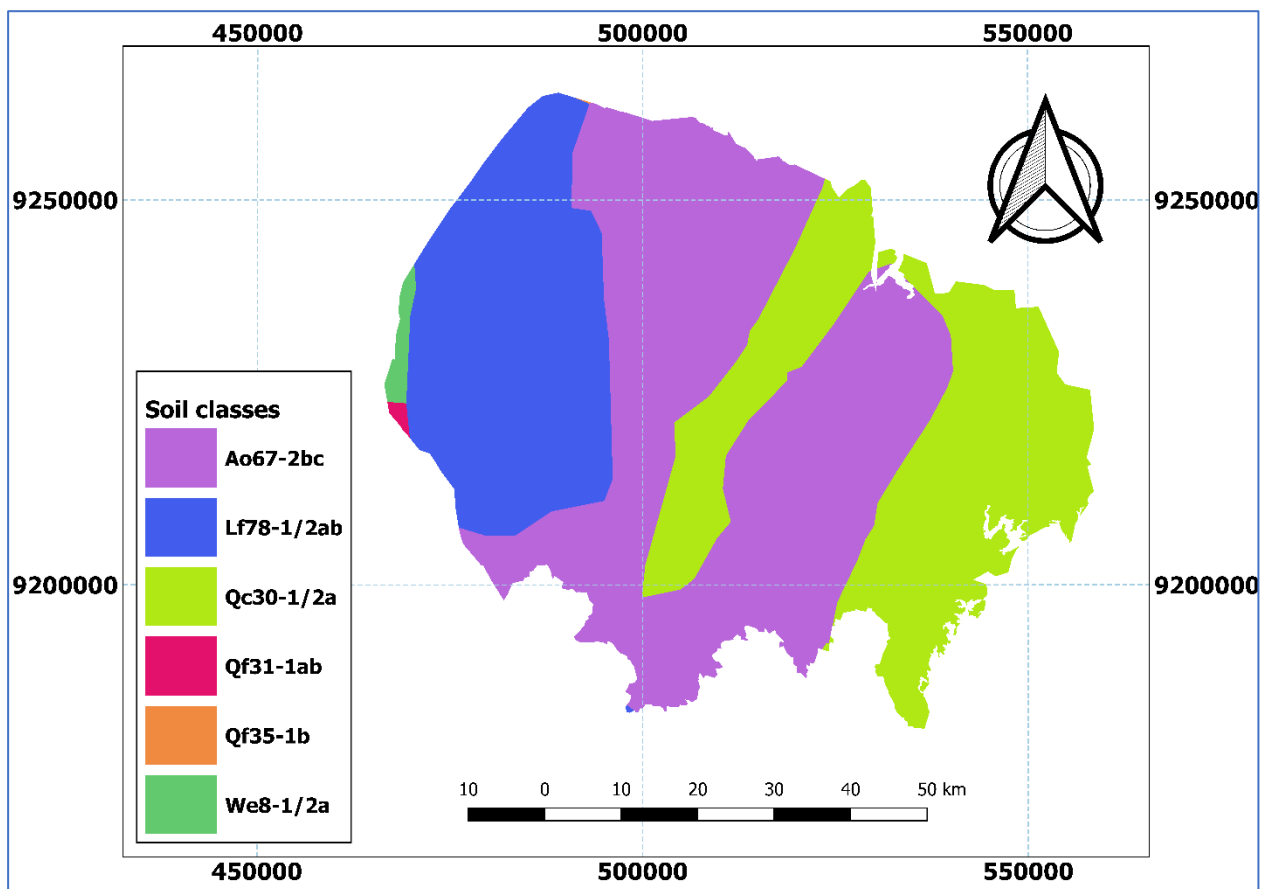


**Figure 17: Soil classes in the Kimbiji aquifer**

**(i) Slope**

The two study areas were divided into 3 slope classes. These are flat to gentle slope areas, moderate slope and steep slope as shown in Fig. 18 and Fig. 19 for Singida and Kimbiji aquifers, respectively. Generally, the largest portion of the two study areas is flat to moderately sloppy, which favors groundwater recharge.

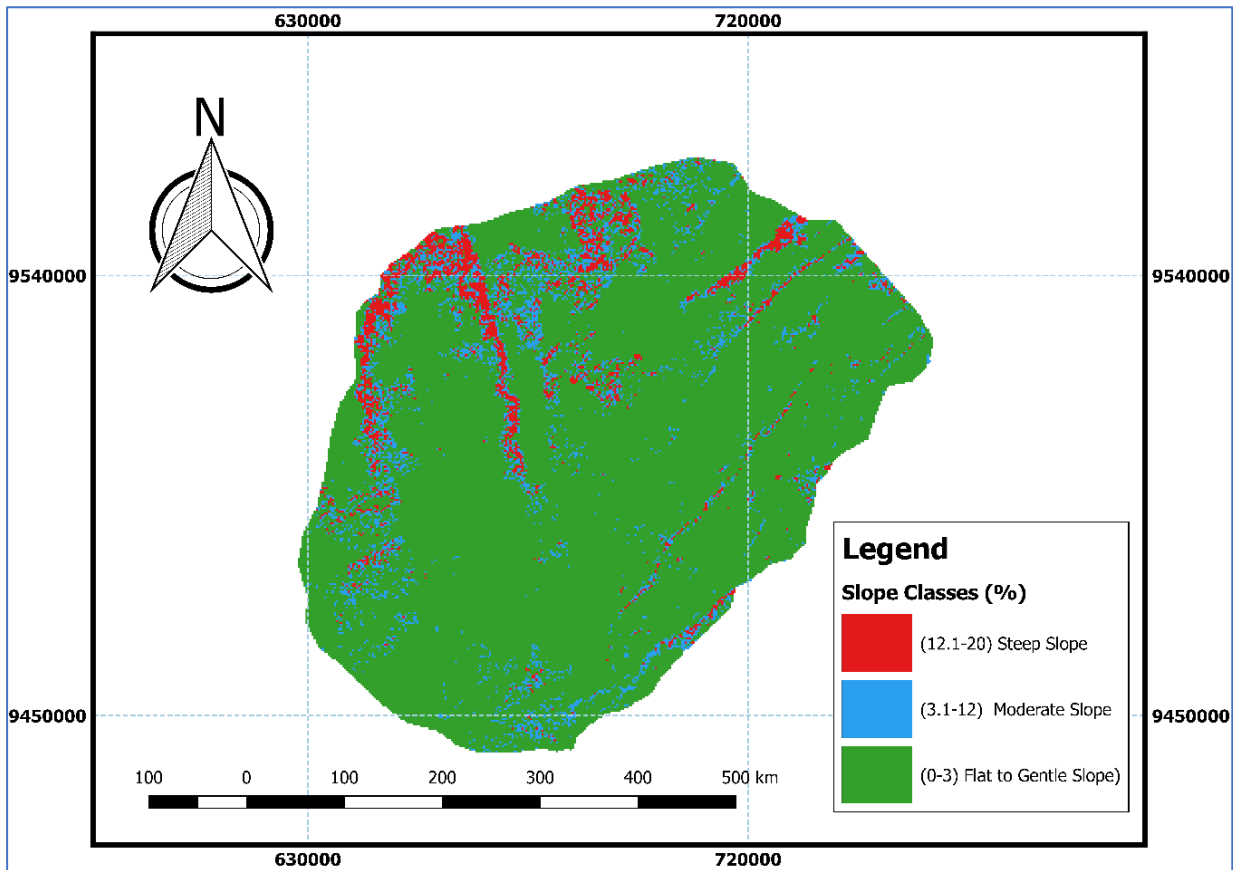


**Figure 18: Slope classes in the Singida aquifer**

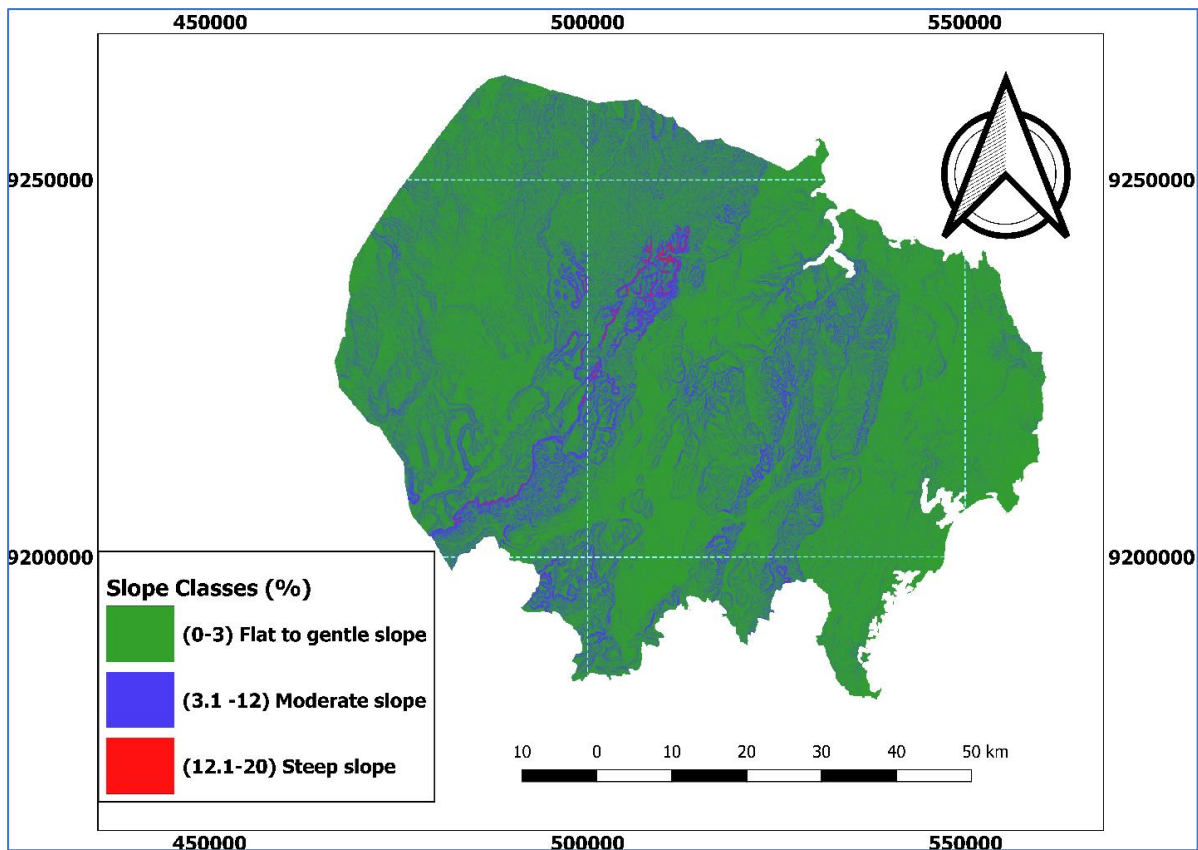


**Figure 19: Slope classes in the Kimbiji aquifer**

### **3.4.2 Determining the Factor Relations and Percentage Influence of the Thematic Layers**

The percentage influence score was derived from the interrelationship among all the factors shown in Table 1 and Table 2. A score of 1 and 0.5 were assigned for major influence and minor influence, respectively for all the parameters. Therefore, the total weight of each factor results from the sum of the measure of influence for each parameter. The higher the weight of the parameter the higher the influence on groundwater recharge potential and low influence connotes low groundwater recharge potential, as discussed in previous studies (Das *et al.*, 2017).

**Table 1: Percentage influence, factor scores and ranks of the main thematic layers for the Kimbiji aquifer**

Thematic layer	Major Influence ( $I_{major}$ )	Minor Influence ( $I_{minor}$ )	Factor Score (FS) = ( $I_{major} + I_{minor}$ )	Factor Influence (FI) = $\frac{(FS)}{\sum(FS)} \times 100$
Geology	Drainage density, Soil, rainfall, land cover, slope		5.0	23
Rainfall	Geology, drainage density, land cover, soil	Slope	4.5	20
Soil	Geology, rainfall, land cover, drainage density		4.0	18
Land use/cover	Drainage density, soil, rainfall	Slope	3.5	16
Drainage density	Geology, soil	Land cover, rainfall	3.0	14
Slope	Drainage density	Land cover, geology	2.0	9
			$\sum(FS)$ = 22	100

**Table 2: Percentage influence, factor scores and ranks of the main thematic layers in the Singida aquifer**

<b>Thematic layer</b>	<b>Major Influence (<math>I_{major}</math>)</b>	<b>Minor Influence (<math>I_{minor}</math>)</b>	<b>Factor Score (FS) = <math>(I_{major} + I_{minor})</math></b>	<b>Factor Influence (FI) = <math>\frac{(FS)}{\sum(FS)} \times 100</math></b>
Lineament density	Hydrogeology, soil, drainage density, land use/cover, slope		5.0	21
Geology/Lithology	Drainage, soil, lineaments,	Slope, drainage density	4.0	17
Land use/cover	Drainage density, Soil, hydrogeology	Lineament density,	3.5	15
Soil	Drainage density, land use/cover, hydrogeology,	Lineament density	3.5	15
Rainfall	Drainage density, land use/cover, hydrogeology		3.0	13
Slope	Drainage density, hydrogeology		2.5	11
Drainage density	Land use/cover, hydrogeology		2.0	8
			$\sum(FS)$ = 23.5	100

The proposed factor scores and factor influence for all the parameters were calculated by using Equation 19 and Equation 20, respectively, while class influence of each factor was calculated using Equation 21 and Equation 22.

$$FS = (I_{major} + I_{minor}) \quad (19)$$

$$FI = \frac{FS}{\sum(FS)} \times 100 \quad (20)$$

The ranking was given for each individual parameter of each thematic map and weights were assigned according to the multi influencing factor of that particular feature on the hydrogeological environment of the study areas. Figure 20 summarizes the inputs, materials, methods, approaches and processes as contained in Table 3 and Table 4.

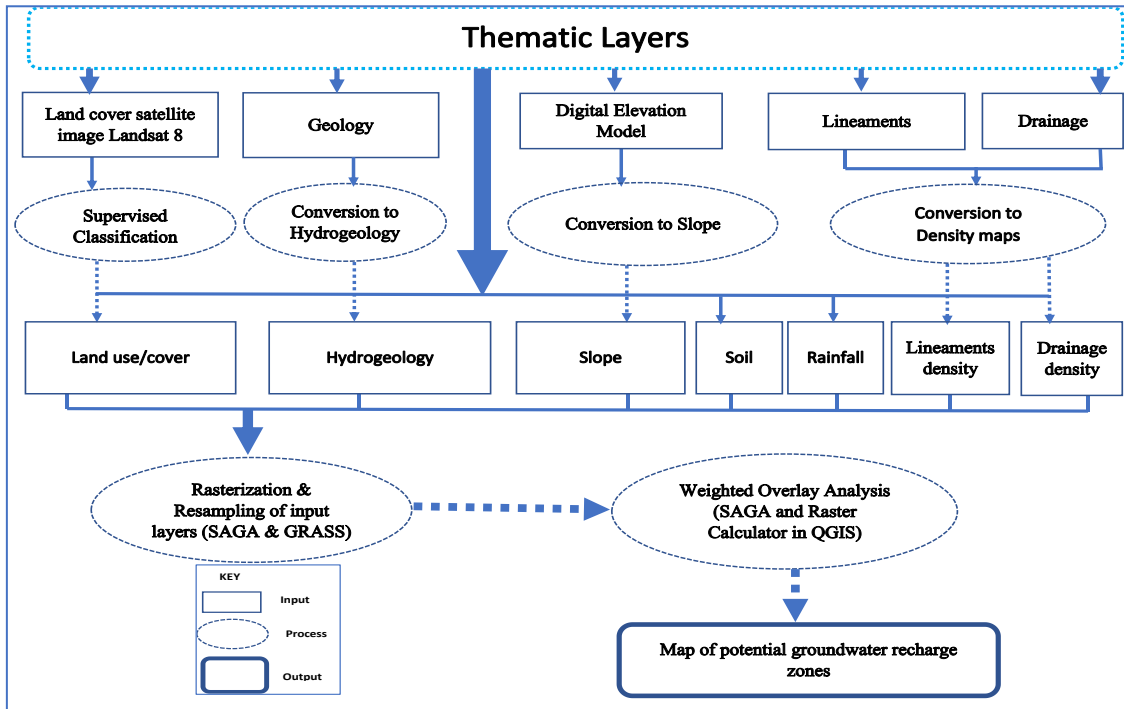


**Figure 20: Schematic diagram of the requisite processes, methods and input data for delineating groundwater potential zones**

Given a total number of classes (N) of a thematic factor, the influence of the first class ( $CI_1$ ) to groundwater recharge is the same as the factor influence (FI) as shown in Equation 21.

$$CI_1 = FI \quad (21)$$

The influence of the second class ( $CI_2$ ) in a thematic factor is equal to the Influence of the first class ( $CI_1$ ) minus the ratio between the factor influence (FI) and the total number of classes (N) in that particular thematic factor. Therefore, for calculating CI for all classes with  $n \geq 2$ , Equation 22 applies.

$$CI_n = CI_{n-1} - \frac{(FI)}{N} \quad (22)$$

**Table 3: Factor classes, class rank and factor weightage for the Kimbiji aquifer**

Factor Parameter	Class	Class Rank (Equation 3 and Equation 4)	Reclassified Ranks (Scale 1–5)	Factor Weightage (%)
Geology	r1 (Fluvial deposits)	23	5	23
	Nf (Fluvial marine sand)	17	4	
	Nt (Terrace deposits)	12	3	
Rainfall	b (Beach sand dune)	6	1	20
	1100 mm	20	5	
	900 mm	10	3	
Soil	Qc30-1/2a (Cambic Arenosols)	18	5	18
	Ao67-2bc (Orthic Acrisols)	15	4	
	Lf78-1/2ab (Ferric Luvisols)	12	3	
	Qf35-1b (Ferralic Arenosols)	9	2.5	
	(Qf31-1ab (Ferralic Arenosols)	6	2	
	We8-1/2a (Eutric Planosols)	3	1	
Land cover	Grassland	16	5	16
	Cultivated land	14	4	
	Wetland	11	3	
	Forest	8	3	
	Bare land	6	2	
Slope	Built-up area	3	1	14
	0-3	14	5	
	3.1-12	9	3	
	12.1-20	5	2	
	0–0.1	9	5	
Drainage density	0.2-5.3	7	4	9
	5.4-10.4	5	3	
	10.5-15.5	4	2	
	15.6-20.5	2	1	



**Table 4: Factor classes, class rank and factor weightage for the Singida aquifer**

Factor Parameter	Class	Class Rank (Equation 3 and Equation 4)	Reclassified Ranks (Scale 1–5)	Factor Weightage (%)
Lineament density	8.1–10.0	21	5	21
	5.1–8.0	16	4	
	2.1–5.0	11	3	
	0.6–2.0	6	1	
Hydrogeology	Tertiary quaternary unconsolidated	17	5	17
	Tertiary quaternary volcanic aquifer	13	4	
	Kimberlites	9	3	
	Precambrian Craton	5	1	
Land cover	Grassland	15	5	15
	Cultivated land	12.5	4	
	Water body	10	3	
	Forest	7.5	3	
	Bare land	5.0	2	
	Built-up area	2.5	1	
	Je52-2/3a (Eutric Fluvisols)	15	5	
	Af3-1/2a (Ferric Acrisols)	12.5	4	
Soil	Nd38-2bc (Dystric Nitosols)	10	3	15
	Ne38-2ab (Eutric Nitosols)	7.5	3	
	Bk29-2ab (Calcic Cambisols)	5.0	2	
	I-L-R-bc (Lithosols)	2.5	1	
	800 mm	13	5	
Rainfall	700 mm	9	4	13
	600 mm	5	2	
	0–3.0	11	5	
Slope	3.1–12.0	7	3	11
	12.1–20	3	1	
	0–0.80	8	5	
Drainage density	0.81–1.2	6.4	4	8
	1.21–1.5	4.8	3	
	1.51–1.8	3.2	2	
	1.81–2.0	1.6	1	

**(i) Rasterization, Resampling and Reclassification**

Vector input layers were rasterized and resampled using QGIS wrap projection algorithm/function to resize the grid cells and reproject the input thematic layers. Thereafter, reclassification using GRASS reclass algorithms was carried out to put all the factor classes in a consistent and a normalized scale. Reclassification to a scale of 1 to 5 was made to harmonize the results obtained through Equations (21) and (22). This was the final input which was then subjected to Weighted Overlay Analysis (WOA).

**(ii) Weighted Overlay Analysis**

Weighted overlay analysis is a method of modeling suitability which aimed at creating a composite map by combining the geometry and attributes of all 6 and 7 input thematic layers in the Kimbiji and Singida aquifers, respectively as discussed by other researchers (Saraf & Choudhary, 1998). The logic behind weighted overlay analysis is to get a combined scenario map that represents the overall groundwater recharge potential possibility of a given area in the context of the chosen and weighted input parameters and their corresponding factor classes. Unlike the weighted overlay approach using the spatial analyst tool in ArcGIS software, the ordered weighted averaging (OWA) in QGIS software, which is the equivalent of the ArcGIS is somehow limited.

Therefore, weighted overlay analysis in this study was a two-pronged process. Thematic maps were added together in a weighted combination with their factor weightage as percentage (Table 3 & 4). This step involved multiplying each layer's weight by each cell's ranked value, and, as a result, a weighted cell value was produced. This was carried out using the algorithm in a SAGA GIS. Thereafter, the weighted cell values were totaled for each overlaying cell and then written to an output layer using the raster calculator function in QGIS software. The raster calculator operation in QGIS superimposes multiple raster layers, representing different hydrogeological, topographic and hydroclimatic themes together with their resampled grid cells and their ranked classes. Thus, the two processes were used to integrate the thematic layers of soil, hydrogeology, lineament density, slope, land cover, rainfall distribution, and drainage density of the study areas to produce a final weighted overlay analysis output. This step resulted in the groundwater potential recharge zone maps. The resulting maps consisted of zones of groundwater potential, which were put into a scale of very good (5), good (4), intermediate (3), poor (2) and very poor (1). This categorization of potential recharge zones in the study areas

was used to depict the potential of the study areas with regard to groundwater recharge, both from rainfall as well as for artificial recharge techniques.

### 3.4.3 Assessment of Groundwater Recharge in the Kimbiji and Singida Aquifers

#### (i) Description of the Modified Soil Moisture Balance Method Coupled with Curve Number

Natural groundwater recharge estimation in this study was carried out using the Modified Soil Moisture Balance Method (MSMB), which was originally developed in the 1940s by Thornthwaite (1948), and later revised by Thornthwaite and Mather (1957). The MSMB method capitalizes on the concept of the water balance in the unsaturated zone, keeping track of the accumulated potential water loss (APWL) and the amount of water stored in the soil ( $S_B$ ) (Mishra *et al.*, 2004; Vinithra & Yeshodha, 2016; Satheeshkumar *et al.*, 2017; Nugroho *et al.*, 2019). As soil moisture diminishes water in the soil becomes more and more tightly bound to the soil particles, and it is therefore difficult to be removed.

Different parameters of the soil moisture budget were computed using the Thornthwaite Water Balance software as applied elsewhere (McCabe & Markstrom, 2007), utilizing the PET (calculated from daily maximum and minimum temperature) and rainfall obtained from the gauging stations. The water balance referred to in this method is basically the balance between the incoming water from precipitation and the outflow of water by evapotranspiration (Bakundukize *et al.*, 2011; Uwizeyimana *et al.*, 2019). Calculations to determine  $S_B$  and APWL were performed for each day using daily precipitation ( $P$ ) and potential evapotranspiration (PET) data. The accumulated potential water loss (APWL) represents the accumulated rainfall deficits and increases with the increasing differences between PET and precipitation (minus runoff). Principally, natural groundwater recharge is only possible when precipitation minus runoff is larger than the PET, and it usually happens during the rainy season. This scenario is represented by Equation 23.

$$(P - R_o) - PET > 0 \quad (23)$$

Nevertheless, this scenario does not ensure a spontaneous recharge as the amount of water that is left after subtracting the PET from the rainfall minus runoff will first be held by the soil. At a certain point, the amount of water held by the soil ( $S_B$ ) will exceed its maximum threshold

called the field capacity (CAP). The surplus of water after reaching the field capacity recharges the aquifer. At this point, the actual evapotranspiration (AET) is equal to the PET. This scenario is represented by Equation 24.

$$(P - R_o) - PET > CAP - S_{B(n-1)} \quad (24)$$

During the dry season, PET is normally higher than the amount of precipitation minus runoff. In this case, there is no enough water available to reach or even surpass the PET. Thus, the actual evapotranspiration will be infinitesimally smaller than the PET. This situation is represented in Equation 25.

$$(P - R_o) - PET < CAP - S_{B(n-1)} \quad (25)$$

Understanding the concept of field capacity is very instrumental in the soil moisture balance method. It denotes an upper limit of moisture content a soil can hold against the pull of gravity. Soil water holding capacity is affected by soil type as well as vegetation type (rooting depth), and it is usually the product of water content at field capacity and average rooting depth. According to McKenna and Sala (2018) and Rezaei-Sadr and Sharifi (2018), in a conceptual sense, groundwater recharge can commence when the moisture content exceeds field capacity. It is therefore ostensible that no rainfall-based (natural) recharge will happen in the dry season because the soil water content decreases logarithmically and reaches its minimum at the permanent wilting point (PWP) during the dry season. According to Raes *et al.* (2016), PWP is the soil water content at which plants can no longer extract water and will wilt permanently. The difference between the water at field capacity and the water at the permanent wilting point, multiplied by the rooting depth, is referred to as the plant available water (PAW) (Raes *et al.*, 2016). The PAW was therefore estimated as shown in Equation 26.

$$PAW = (CAP - W_{pwp}) D_r \quad (26)$$

Where  $D_r$  is the rooting depth

A deeper rooting zone means that there is a larger volume of water stored in the soil zone and, therefore, a reduced amount of water going to the groundwater reservoir as recharge. Arguably, in an area with thin soils, low values of PAW (<200 mm) should be used, while in areas with deep soils, medium to high values of PAW (>200 mm) should be used (Bakundukize *et al.*, 2011). To that effect, a PAW of 250 for the Kimbiji aquifer was used due to their relatively

deep soils while a PAW of 100 was used for the Singida aquifer. This was guided by the type of soils, vegetation and amount of annual rainfall received in each study area which is reflected in the plant available water.

## **(ii) Runoff Estimation**

Runoff is invariably one of the most important parameters for natural groundwater recharge estimation using the soil moisture balance method. The generation of runoff in a landscape is controlled by the interaction of precipitation with the topography, land use and soil properties of the land surface as provided for by Patil *et al.* (2008). The SMBM converts rainfall to surface runoff using curve number which is derived from basin characteristics and 5-day antecedent rainfall. This method was previously criticized by other researchers (Huang *et al.*, 2006; Terzoudi *et al.*, 2007), citing that the amount of generated runoff does not take into account the rainfall intensity nor the slope factor. To date, the method is widely accepted and used by scientists in different domains for estimation of runoff (Bakundukize *et al.*, 2011; Bakundukize, 2012; Satheeshkumar *et al.*, 2017; Uwizeyimana *et al.*, 2019) after working on some or all of the cited shortcomings.

This study has equally minimized the shortfalls of the method, including offsetting the two aforementioned shortcomings by considering the two factors in the modified soil moisture balance method. Surface runoff, which is the fraction of precipitation that flows on impervious surfaces or over the land surface was subtracted from the precipitation to compute the residual amount of precipitation which participates into the further steps of the soil moisture balance process.

Generally, the runoff results from the interaction of precipitation with the topography, land use and soil properties of the land surface under study as opined by Patil *et al.* (2008). In the process of estimating surface runoff, curve number is such an important parameter. However, the determination of a curve number for the two study areas, there are a number of factors to be considered which are key and greatly contribute to the derivation of the curve number of any landscape. These are the hydrologic conditions of a basin, hydrological soil groups found in the basin, antecedent soil moisture conditions and land cover types. Each of these factors are described in detail:

**(a) Land Cover Classification and Assessment**

Land use land cover (LULC) classification followed a detailed understanding of the spatial extents and geographical delineations of the study areas.

Thereafter, clear and cloudless satellite images were downloaded from the United States Geological Survey (USGS) earth explorer site (<https://earthexplorer.usgs.gov> and Global Visualization site; <https://glovis.usgs.gov>), covering path 166 and row 65 for Kimbiji aquifer and path 169 and row 63 for the Singida aquifer as summarized in Table 5.

In order to carry out LULC classification using the semiautomatic classification in QGIS the knowledge of specific areas of the image and what underlying values belong to which class was critically important. Satellite images from Landsat Thematic Mapper (TM) which included the following years (1997, 2005 & 2008) and Landsat 8 (OLI-TIRS) for 2016 and 2018 were downloaded. The selected images were captured in the range of 1997, 2005 and 2018 for the Singida study area and 1997, 2008 and 2016 for the Kimbiji study area, and they were subjected to digital image processing as detailed in the preceding subsections.

**Table 5: A summary of satellite image data and their attributes for land cover classification**

<b>Kimbiji</b>					<b>Singida</b>					
<b>Year</b>	<b>Sensor ID</b>	<b>Path/Row</b>	<b>Acquisition date</b>	<b>Cloud cover (%)</b>	<b>Year</b>	<b>Spacecraft ID</b>	<b>Sensor ID</b>	<b>Path/Row</b>	<b>Acquisition date</b>	<b>Cloud cover (%)</b>
1995	TM (SAM)	166/65	25/06/1995	10	1997	Landsat 5	TM (SAM)	169/63	6/8/1997	1
2008	TM (BUMPER)	166/65	28/06/2008	10	2005	Landsat 5	TM (SAM)	169/63	17/02/2005	1
2016	OLI TIRS	166/65	8/10/2016	10	2018	Landsat 8	OLI-TIRS	169/63	17/09/2018	4

The preprocessing started by carrying out image mosaicking and satellite band rendering. This was followed by converting a digital number (DN) values irradiance to top of-atmospheric (TOA) reflectance. Atmospheric correction was performed by dark object subtraction (DOS), which is an empirical atmospheric adjustment technique for satellite imaging. The technique assumes that the reflectance of dark objects includes an important component of atmospheric scattering which obscures some important features for LULC classification. Thereafter, the image was set into a false colour composite (FCC), ready for classification.

Land use/cover classification entailed categorizing pixels in the satellite image into classes based on the ground cover. This was done by comparing the reflection values of different spectral bands in different areas. Since this was a supervised classification, sample classes were determined, using which the classification was based. In that regard, training inputs were established, namely the regions of interest (ROIs), which were afterwards visualized in a spectral signatures plot by highlighting the ROIs and clicking on. This was a very handy technique to assess the quality of the classification. The rule of thumb is, classes in which ROIs have very similar values are preferred as this increases the precision of the classification.

To prepare the LULC map from satellite imageries, a classification scheme which defined the LULC classes was considered. The choice of the number of LULC classes was based on the requirements of this study, which would serve a purpose for estimating curve numbers and recharge thereof. Seven major LULC classes were chosen for mapping in each of the two study areas. After the preparation of the classification scheme, the maximum likelihood classification technique in the Semiautomatic Classification Plugin (SCP) in QGIS was adopted for LULC mapping for all the six images, three for each study area.

Nevertheless, before the selection of training samples, an empirical assessment of the satellite images, google earth images and toposheets of the study areas was carried out. For most of the classes, a minimum number of 10 training samples as recommended by other studies (Arora & Mathur, 2001; Saha *et al.*, 2005) was chosen. Using hand-held GPS, 50 ground-truthing points for the ground features were taken from each study areas during field survey for assessing the classification accuracy. The accuracy assessment was further achieved using the confusion matrix method as reported in previous studies (Congalton & Green, 2008). Kappa coefficients were calculated as classification accuracy indicators.



The choice of the number of LULC classes was based on the requirements of and purpose of this study. The major focus was choosing images which would serve a purpose for estimating curve numbers and recharge thereafter. This was also emphasized in the choice of LULC classes. Eight major LULC classes were chosen for mapping in each of the two study areas.

The magnitude of change (MC), (Equation 27), the percentage of change (PC), (Equation 28), and the annual rate of change (ARC) (Equation 29) for each LULC class in the two study areas for three different time spans were calculated as shown in the respective Equations.

$$MC(km^2) = A_i - A_f \quad (27)$$

$$PC(\%) = \frac{A_i - A_f}{A_i} \times 100 \quad (28)$$

$$ARC(km^2 \cdot year^{-1}) = \frac{A_i - A_f}{n} \quad (29)$$

Where;  $A_i$  is the class area ( $km^2$ ) at the initial time,  $A_f$  is the class area ( $km^2$ ) at the final time, and  $n$  is the number of years of the respective time period where land cover change analysis has been carried out.

#### **(b) Hydrological Soil Groups**

Soil properties significantly influence the amount of runoff in an area. The influence of both the soil's surface condition (infiltration rate) and its horizon (transmission rate) are key in determining the potential of any soil to groundwater recharge. The two properties which indicate a soil's runoff potential form the qualitative basis of the classification of all soils into four hydrologic soil groups as summarized in Table 6.

**Table 6: Characterization of Hydrological Soil Groups**

<b>Hydrologic Soil Group</b>	<b>Description</b>	<b>Final infiltration rate</b>
<b>Group A</b>	Soils having high infiltration rates even when thoroughly wetted. A high rate of water transmission. These are typical of deep, well to excessively drained sands or gravels.	8-12 mm/hour.
<b>Group B</b>	Soils having moderate infiltration rates when thoroughly wetted and a moderate rate of water transmission. Examples are moderately deep to deep, moderately well to well drained soils with moderately fine to moderately coarse textures.	4-8 mm/hour
<b>Group C</b>	Made up of soils having low infiltration rates when thoroughly wetted and a low rate of water transmission. This group is made up of soils with a layer that impedes the downward movement of water or soils of moderately fine to fine texture.	1 – 4 mm/hour
<b>Group D</b>	<p>This group is composed of soils having very low infiltration rates when thoroughly wetted as well as a very low rate of water transmission. These are typical of clay soils, which have a high swelling potential.</p> <p>The group is also made up of soils with a permanently high-water table and soils with a clay pan or clay layer at or near the surface, or shallow soils over nearly impervious material.</p>	Less than 1 mm/hour

### (c) Antecedent Moisture Condition

The soil moisture condition in a basin before runoff occurs is another important factor influencing the final CN value, and subsequent groundwater recharge. Runoff is affected by the soil moisture before a rainfall event. This is known as antecedent moisture condition (AMC). In the modified soil moisture balance method with Curve number, the AMC is categorized into three classes (Table 2). The classes are based on the 5-day antecedent rainfall, which is the accumulated total rainfall preceding the runoff under consideration. The AMC is an indicator of the wetness and availability of moisture content of soil storage prior to a storm rainfall event (Gitika & Ranjan, 2014; Ahmad *et al.*, 2015).

The CN method distinguishes the dormant and the growing season in order to highlight the differences in actual evapotranspiration between the two seasons. The values of CN used in this study as proposed previously by USDA-SCS (1972) are valid for an average relationship where initial abstraction,  $I_a = 0.2S$ , and for average antecedent soil moisture condition (AMC II),  $S$  being the potential maximum retention. Moreover, the curve number, as determined in this study was termed CN II which is derived from AMC II (average soil moisture condition). The other moisture conditions are AMC I (dry) and AMC III (moist) which were not used in this study. The application of the three AMC classes is hugely determined by the rainfall intensity of the previous 5 days, known as 5-day antecedent rainfall and season. The Antecedent soil moisture classes as summarized in Table 7.

**Table 7: Antecedent soil moisture classes**

AMC Group	Soil Characteristics	5-day antecedent rainfall (mm/5 days)	
		Dormant Season	Growing Season
I	The soils in the drainage basin are practically dry (i.e., the soil moisture content is at wilting point).	< 13	< 36
II	Average condition.	13 – 28	36 – 53
III	The soils in the drainage basins are practically saturated from antecedent rainfalls (i.e., the soil moisture content is at field capacity).	> 28	> 53

To determine the appropriate CN value, a table relating the value of CN to land use / cover type, land cover treatment and/or practice, hydrological condition, and hydrological soil group was used in this study (Table 3). With the aid of those tables, coupled with succinct field campaigns and ground truthing, the curve numbers for the two study areas were determined. Calculation of the weighted average CN, taking into account the areas they occupy, utilizing the data given in Table 3 was carried out using Equation 30.

$$CN = \frac{\sum CN_i A_i}{A} \quad (30)$$

Where  $CN_i$ ; – curves number in per unit,  $A_i$  - Area ( $km^2$ ) and  $A$ - the total area of the study area. The data in Table 3 facilitated the estimation of the mean weighted curve number.

### (iii) Estimation of Weighted Curve Numbers for Kimbiji and Singida Aquifers

The two equations (31) and (32) were used to calculate weighted curve numbers for the Kimbiji aquifer ( $CN_{KIMB}$ ) and the Singida aquifer ( $CN_{SING}$ ), respectively. The letters CN and A stand for curve number and area, respectively. The subscripts abbreviate the respective land covers, where  $f$  is forest,  $w$  is woodland,  $bs$  denotes bushland and  $gs$  stands for grassland. Further,  $wa$  represents water,  $we$  is for wetland,  $cl$  connotes cultivated land and  $ba$  is for built-up area.

$$CN_{KIMB} = \frac{(CN_f \cdot xA_f) + (CN_w \cdot xA_w) + (CN_{bs} \cdot xA_{bs}) + (CN_{gs} \cdot xA_{gs}) + (CN_{wa} \cdot xA_{wa}) + (CN_{we} \cdot xA_{we}) + (CN_{cl} \cdot xA_{cl}) + (CN_{ba} \cdot xA_{ba})}{A_{KIMB}} \quad (31)$$

$$CN_{SING} = \frac{(CN_f \cdot xA_f) + (CN_w \cdot xA_w) + (CN_{bs} \cdot xA_{bs}) + (CN_{gs} \cdot xA_{gs}) + (CN_{wa} \cdot xA_{wa}) + (CN_{we} \cdot xA_{we}) + (CN_{cl} \cdot xA_{cl}) + (CN_{ba} \cdot xA_{ba})}{A_{SING}} \quad (32)$$

Equation 33 underpins the prediction of runoff from the amount of rainfall, using a shape factor (S), called the potential maximum retention. The shape factor combines the effects of soil, vegetation, land use and antecedent soil moisture (i.e., soil moisture prior to a rainfall event). The rule of thumb is, at the start of the rainfall event, water will be intercepted by land covers/crops, stored in small depressions, and infiltrated in the soil as initial abstraction ( $I_a$ ). After runoff has been generated, some of the additional precipitation will infiltrate forming the actual retention (F). With increasing precipitation, the actual retention eventually reaches a maximum value which is the potential maximum retention (S) as depicted in Equation 34.

$$R_o = \frac{(P - I_a)^2}{(P - I_a) + S} \text{ for } P > I_a \quad (33)$$

However, if  $P < I_a$ , then it follows that  $R_o = 0$ , Where  $R_o$  is the runoff (mm),  $P$  is the precipitation (mm),  $I_a$  is the initial abstraction (mm), and  $S$  is the potential maximum retention (mm), and  $I_a = 0.2S$ .

$$\text{Therefore, } R_o = \frac{(P - 0.2S)^2}{P + 0.8S} \quad (34)$$

If the parameter  $S$  is known,  $CN$  can be calculated from Equation 35.

$$CN = \frac{25400}{254 + S} \quad (35)$$

Where,  $CN$  is a dimensionless parameter known as Curve number, whose value ranges from 0 to 100.

Curve number designates the runoff response characteristics of an area which depend on the land use type, land treatment, hydrological condition, hydrological soil group and antecedent soil moisture of the area. Other studies (USDA-NRCS, 1986) described the hydrologic condition as the effects of cover type and treatment on infiltration and runoff and is generally estimated from density of plant and residue cover on sample areas. Good hydrologic condition indicates that the soil usually has a low runoff potential for that specific hydrologic soil group, cover type, and treatment. The curve numbers for various land cover classes are summarized in Table 8.

Antecedent moisture is considered to be low when there has been little preceding rainfall and high when there has been considerable preceding rainfall prior to the modelled rainfall event. For modeling purposes, in this study the AMC II, which is essentially an average moisture condition was considered. It is practically straightforward to estimate the parameter  $S$  using Equation 36 when the  $CN$  is known.

$$S = \frac{25400}{CN} - 254 \quad (36)$$

Therefore, runoff was estimated using Equation 37, which is embedded in the recharge calculation tool using the modified soil moisture balance method which is coupled with curve number.

$$R_o = \frac{\left[ P - 0.2 \left( \frac{25400}{CN} - 254 \right) \right]^2}{\left[ P + 0.8 \left( \frac{25400}{CN} - 254 \right) \right]} \quad (37)$$

Table 8: Description of curve numbers for various land cover classes as adopted from previous studies (Nag, 2005; Chowdhury *et al.*, 2008; Samson & Elangovan, 2015).

**Table 8: The curve numbers for various land cover classes**

Land use/Cover type	Hydrologic condition	Curve numbers for hydrologic soil group			
		A	B	C	D
Woodlands and Forests	Poor	45	66	77	83
	Fair	36	60	73	79
	Good	30	55	70	77
Grassland for humid to subhumid areas	Poor	68	79	86	89
	Fair	49	69	79	84
	Good	39	61	74	80
Grassland for semi-arid areas	Poor	—	80	87	93
	Fair	—	71	81	89
	Good	—	62	74	85
Dryland shrubs/bushes	Poor	63	77	85	88
	Fair	55	72	81	86
	Good	49	68	79	84
Impervious areas (Built-up areas)	Paved parking lots, roofs, driveways, Streets, and roads	98	98	98	98
Cultivated area (Row Crops) e.g., corn, sugar beets, soybeans	Good	64	75	82	85
Small Grain e.g., wheat, barley, flax	Good	60	72	80	84
Wetlands	For swamps and wetlands with open water year-round such that at least 1/3 of the wetland is water, regardless of the soil type.	85	85	85	85
	Irrespective of soil type, this applies to wetlands with no open water and the calculations are for a 25-year frequency or shorter,	78	78	78	78
Water (Rivers, Reservoirs and Lakes)	Rivers and reservoirs	97	97	97	97
	Lakes	100	100	100	100

#### (iv) Potential Evapotranspiration

Potential evapotranspiration was calculated using the Penman-Monteith (PM) method and the Hargreaves-Samani (HS). The combination of the two methods was chosen to assess the significance of the claims on PET overestimation and underestimation (Bakundukize *et al.*, 2011; Lwimbo *et al.*, 2019). According to Oudin *et al.* (2005) and Kingston *et al.* (2009), the two temperature-based PET methods (i.e., PM and HS) are as reliable as physically based methods. Therefore, PET calculated using the Penman-Monteith (PM) method was compared with PET which was calculated using Hargreaves-Samani (HS) method.

The Penman-Monteith uses equation 38 which is embedded in the reference evapotranspiration (ET<sub>o</sub>) program developed by the United Nation's Food and Agricultural Organization (FAO). This program has proven to be the best method to estimate potential evapotranspiration in data scarce environments like Tanzania (Mjemah *et al.*, 2011). The method does not require a wide variety of weather data, which are basically not always available in many parts of the world (Bakundukize *et al.*, 2011). The ET<sub>o</sub> program requires meteorological data inputs, mainly daily maximum, and minimum temperature as well as the climatic station characteristics like geographical coordinates (latitude and longitudes) of the station, elevation, topographic attributes, and station descriptions, including the country where the station is found. Of equal importance are the characteristics of wind systems in the study area. After providing all the aforementioned inputs into the ET<sub>o</sub> program, the other variables shown in Equation (38) are numerically estimated. As  $\gamma$  varies only slightly over normal temperature ranges, a single value of 2.45 MJ kg<sup>-1</sup> is taken in the simplification of the FAO Penman-Monteith equation. This is the latent heat for an air temperature of about 20° C.

$$PET_{PM} = \frac{0.48\Delta(R_n - G) + \gamma \frac{900}{T + 273} U_2 (e_s - e_a)}{\Delta + \gamma(1 + 0.34U_2)} \quad (38)$$

Where,  $PET_{PM}$  the evapotranspiration (mm day<sup>-1</sup>) calculated using the Penman-Monteith equation,  $R_n$  net radiation at the crop surface (MJ m<sup>-2</sup> day<sup>-1</sup>),  $G$  soil heat flux density (MJ m<sup>-2</sup> day<sup>-1</sup>),  $T$  mean daily air temperature at 2 m height (°C),  $U_2$  wind speed at 2 m height (m s<sup>-1</sup>),  $e_s$  saturation vapour pressure (kPa),  $e_a$  actual vapour pressure (kPa),  $e_s - e_a$  saturation vapour pressure deficit (kPa),  $\Delta$  slope vapour pressure curve (kPa °C<sup>-1</sup>),  $\gamma$  psychrometric constant (kPa °C<sup>-1</sup>).

The other method was the temperature-based Hargreaves-Samani (HS) approach. Numerically, the PET using Hargreaves-Samani approach was calculated as shown in Equation 39, and its requisite requirements are described thereafter. According to Martínez-Cob and Tejero-Juste (2004), no local correction is required for windy locations for the Hargreaves-Samani equation. Moreover, it was recommended using an empirical coefficient equal to 0.0020 for non-windy locations like the Kimbiji aquifer instead of the original value (0.0023) proposed by Hargreaves and Samani (1985), which in this study was applied in the Singida semi-arid aquifer. Equation 17 represents the HS method of the temperature-dependent PET method used in this study.

$$PET_{HS} = k_{RS} \cdot R_a (T_{max} - T_{min})^{HE} \left( \frac{T_{max} + T_{min}}{2} + HE \right) \quad (39)$$

Where,  $PET_{HS}$  is daily PET in mm/day calculated using the Hargreaves-Samani method;  $R_a$  is extraterrestrial radiation in mm/day;  $T_{max}$  and  $T_{min}$  are daily maximum and minimum air temperature in °C, respectively;  $K_{RS}$  is the empirical radiation adjustment coefficient (0.0020) for the Kimbiji and (0.0023) for the Singida aquifer;  $HE$  is empirical Hargreaves exponent, and the value is set to 0.5 in the two study areas; and  $HT$  is empirical temperature coefficient, and the value is set to 17.8.

The daily rainfall and PET data were arranged into hydrologic years, starting at the beginning of the short rainy season, and terminating at the dry season after the long rainy season (October to November) for the bimodal Kimbiji aquifer and November to October for unimodal Singida aquifer. Organizing data in a hydrological year has the advantage of facilitating the computation of the change in soil moisture storage at the beginning of the hydrologic year, because the soil moisture storage at the end of the dry season is normally considered to be completely depleted. Additionally, the concept of hydrologic year reflects the natural climatic reality in the sense that it commences with the start of the period of soil moisture replenishment, goes through the period of maximum groundwater recharge, if any, and culminates with the season of maximum soil moisture utilization (Bakundukize *et al.*, 2011; Mjemah *et al.*, 2011).

Moreover, Aridity index (AI), which is the ratio of rainfall and potential evapotranspiration was also used to characterize the study areas. According to previous studies (Mussa *et al.*, 2020), when  $AI < 0.05$ , that indicates hyper-aridity. The area is in arid conditions if  $0.05 < AI < 0.2$ . Moreover,  $0.2AI < 0.5$  signals semi-arid conditions. Dry sub-humid and humid conditions are



represented by  $0.5 < AI < 0.65$  and  $0.65 < AI < 0.75$ , respectively. Hyper-Humidity occurs when  $AI > 0.75$ .

### **3.5 Groundwater Flow Modelling and Simulation of Nested Groundwater Flow Systems**

#### **3.5.1 Modelling/Simulation Process**

##### **(i) Developing a Conceptual Model**

This was descriptive representation of a groundwater system that incorporates an interpretation of the geological and hydrological conditions, including information about the water budgets and groundwater exploitation. Conceptual modeling equally involved description of the known physical features and the groundwater flow processes within the study area. Additionally, constructing a conceptual model enabled defining the geological and hydrogeological framework of the study areas, including number of layers, the thickness of each layer, lithology, and structure of the aquifers and confining units. Detailed hydrostratigraphic units of various basins were described based on the available lithology logs, geophysical survey and geological data and maps.

The model domain was extended until a hydrogeological boundary (no flow boundary and/or constant head) was encountered. In addition, another factor considered in the selection of the model domain was determining when the limits of the model domain were sufficiently remote to reduce the impact of the assumed boundary conditions on the model outcomes. **Numerical Model Setup**

Two dimensional (2D) models of the test study cases were constructed using finite difference numerical groundwater modeling CODE (MODFLOW) (Harbaugh, 2005). ModelMuse, a Graphical User Interface (GUI) was used for processing MODFLOW. Out of the numerous groundwater flow governing Equations, Equation 40 and 41 were solved by the model, representing 2D steady-state groundwater flow system in confined anisotropic conditions without a source or sink and 2D steady state, groundwater flow system in unconfined anisotropic conditions with and without a source or sink, respectively.

$$\frac{\partial}{\partial x} \left( hK_x \frac{\partial h}{\partial x} \right) + \frac{\partial}{\partial y} \left( hK_y \frac{\partial h}{\partial y} \right) = \pm R \quad (40)$$

$$\frac{\partial}{\partial x} \left( T_x \frac{\partial h}{\partial x} \right) + \frac{\partial}{\partial y} \left( T_y \frac{\partial h}{\partial y} \right) = \pm R \quad (41)$$

Where  $x$  and  $y$  are the Cartesian coordinates in  $x$  and  $y$  directions respectively ( $L$ ),  $K_x$  and  $K_y$  are the hydraulic conductivity components,  $T$  represents aquifer Transmissivity and  $h$  represents the hydraulic head with the unit of ( $L$ ).

Steady-state groundwater flow model was developed to simulate the status quo /natural conditions. This assumed that the groundwater system is at steady state, and thus hydraulic heads at any given point in the aquifer do not change through time.

## (ii) Model Discretization

The discretization by vertices (DIV) method in Modflow 6 was used for discretizing the model domain for the two study areas. The model areas were converted into a domain consisting of an array of nodes and associated finite difference blocks/cells based on two layers in each case study with variable aquifer thickness and hydraulic conductivities. Regular model grid of specified rows and columns with 500 m length and 500 m width were used. Nevertheless, where necessary, very fine discretization was applied in some features like boreholes, lakes, and rivers using the quadtree refinement feature in Modflow 6.

The appropriate level of spatial discretization was selected to cater for the balance between the desired level of accuracy, the hydrologic boundary conditions, domain heterogeneity and the resolution of the available data on one hand, and the model run time and memory requirements on the other hand. Fine discretization was used whenever required to ensure adequate representation of the feature such as rivers, pumping wells, lakes and other features of importance. In addition, when the model domain seemed to have a complex geometry that could only be represented with a fine grid, fine discretization was opted. The surface elevation was derived from Aster GDEM (<https://earthexplorer.usgs.gov>) with a 30 m resolution, was resampled to the groundwater model grid size of 500 m to fit within the groundwater model grid size.

### **(iii) Setting Boundary Conditions**

Steady state problems require at least one boundary node with a known head in order to give the model a reference elevation from which to calculate heads. In transient solutions the initial conditions provide the reference elevation for the head solution, also taking into account the groundwater balances, as they are a key function for the transient simulations and calibration. The head distribution everywhere in the system at the beginning of the simulation formed the boundary conditions for the steady-state models. Other types of boundary conditions included constant head (the ocean), No flow boundaries (impervious rocks), the general head boundary (for regional flow simulation), specified flux boundaries (recharge and wells), and head-dependent flux boundaries (rivers and lakes).

### **3.5.2 Kimbiji Aquifer**

#### **(i) Hydrogeology of the Kimbiji Aquifer**

Hydrogeologically, the Kimbiji is covered by an unconfined aquifer in the upper parts and a confined aquifer in the lower parts (Fig. 21), with strong artesian flow characteristics of more than  $3 \text{ L s}^{-1}$  (Ruden, 2007; Bakari *et al.*, 2012). Reportedly, groundwater flows from west to east, driven by artesian pressure arising from the western hinterland (Bakari *et al.*, 2012). Based on a drilling report of six deep wells in the study area (NORCONSULT, 2008), alluvium and granular materials comprise the upper, unconfined freshwater aquifer, consisting of fine to medium sand that contains varying amounts of silt and clay. The unconfined aquifer is shallow in its southwestern part, with an average thickness of 10 m, but around 50 m deep in the eastern part of the study area. The depth of the water table in the unconfined aquifer ranges from at/or near the land surface in low-lying areas close to the ocean to tens of meters below the surface in areas of higher elevation like Pugu, Chanika and Kisarawe. The upper aquifer is of special significance for the present water supply because most of the groundwater used in the study area is withdrawn from this zone (JICA, 2005). The lower confined aquifer is comprised mainly of medium to coarse sands, and sometimes gravels and pebbles occur, interbedded with clayey-rich material. There is no obvious lithological boundary between the two aquifer units, apart from the numerous and nearly cyclic sand and marl beds. Consequently, a gradual transition from upper unconfined to lower confined conditions is expected.

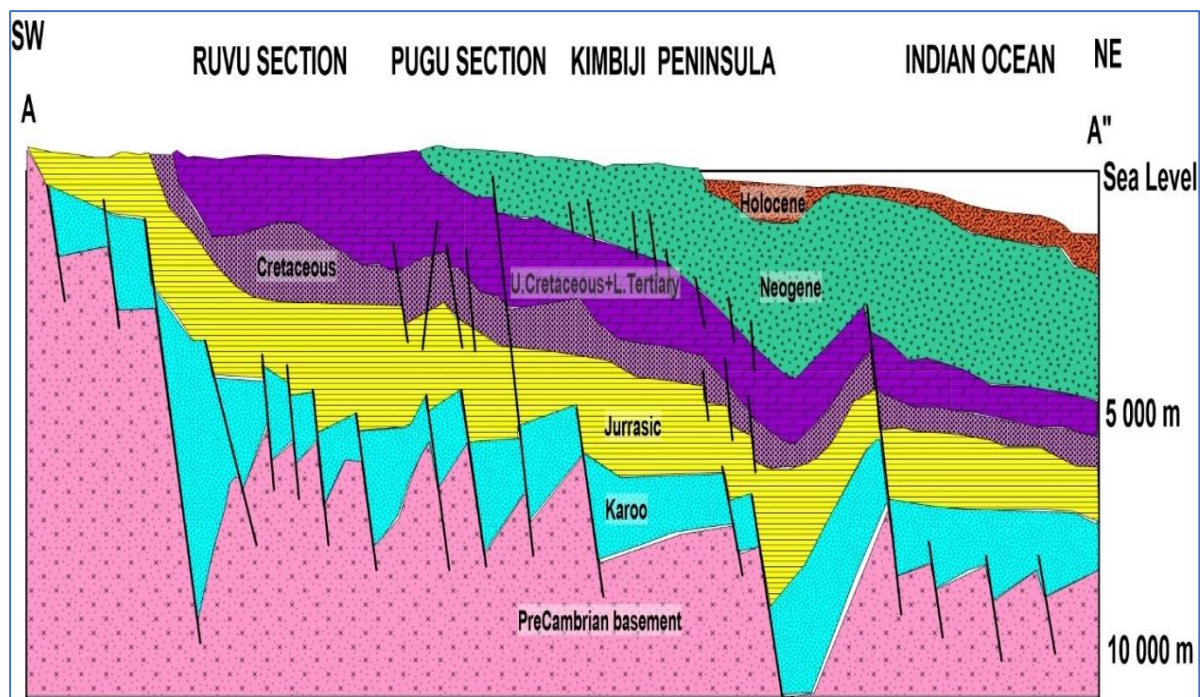


**Figure 21:** A cross section of the Kimbiji aquifer showing a layered system of the study area (Adapted from Msindai, 1988)

The average saturated thickness of the aquifer system is around 1000 m, and the overall flow direction is from west to east, driven by artesian pressure arising from the western hinterland (TPDC, 2007, Bakari *et al.*, 2011). The hydraulic parameters for the Kimbiji aquifer were reported by Mjemah *et al.* (2009; 2012). The upper, unconfined aquifer has average transmissivity and hydraulic conductivity of  $34 \text{ m}^2\text{d}^{-1}$  and  $1.58 \text{ md}^{-1}$  respectively. The lower, semi-confined aquifer has an average value of  $63 \text{ m}^2\text{d}^{-1}$  for transmissivity and  $2.14 \text{ md}^{-1}$  for hydraulic conductivity respectively. Reportedly, an average elastic early-time storativity for the unconfined is 0.01, while the lower aquifer has an average storativity of  $3 \times 10^{-4}$ . These hydraulic parameters reasonably represent the geological formation of the aquifers, as deduced from borehole descriptions reported in Mjemah *et al.* (2009; 2012).

## (ii) Groundwater Recharge and Exploitation in the Kimbiji Aquifer

The 2015/2016 recharge estimation indicated that the aquifer receives 128.7 mm/year, which is equivalent to 0.129 m/year over the entire study area. According to Mussa *et al.* (2019), study in this study area, groundwater exploitation in the Kimbiji aquifer is estimated at  $15.17 \times 10^6 \text{ m}^3/\text{year}$  from the groundwater system in this study area. This is equivalent to  $4.81 \times 10^{-4} \text{ L/s}$  and almost  $0.5 \text{ m}^3/\text{s}$  that is being exploited from the Kimbiji aquifer per day.

### 3.5.3 Singida Aquifer

#### (i) Hydrogeology of the Singida Aquifer

Hydrogeologically, groundwater occurs in weathered shallow layers and in fissures and fractures of basement rocks in the Singida aquifer. Groundwater occurring in weathered shallow layers have low capacity due to small, saturated aquifer thickness and low permeability too. Moreover, a hard pan layer has covered most parts, which considerably decreases infiltration rate, thereby preventing the formation of aquifers in some parts of the Singida semi-arid aquifer. Groundwater occurring in fissures and fractures of basement rocks characterize long, narrow and isolated reservoirs, which are basically filled up with gravel, sand and other particles with good permeability. In some places of the Singida aquifer, fractures act as expanded water conduits across long distances, extending from north east to South-west. The orientation of the fractures mostly defines the groundwater flow direction in the Singida aquifer.

Reportedly, most crystalline basement aquifers are made up of three zones, which are an upper weathered zone, a middle-fractured zone, and a lower and often less fractured zone which makes the aquifer basement (Krásný & Sharp, 2003). The Singida aquifer has the aforesaid structure as shown in Fig. 22.

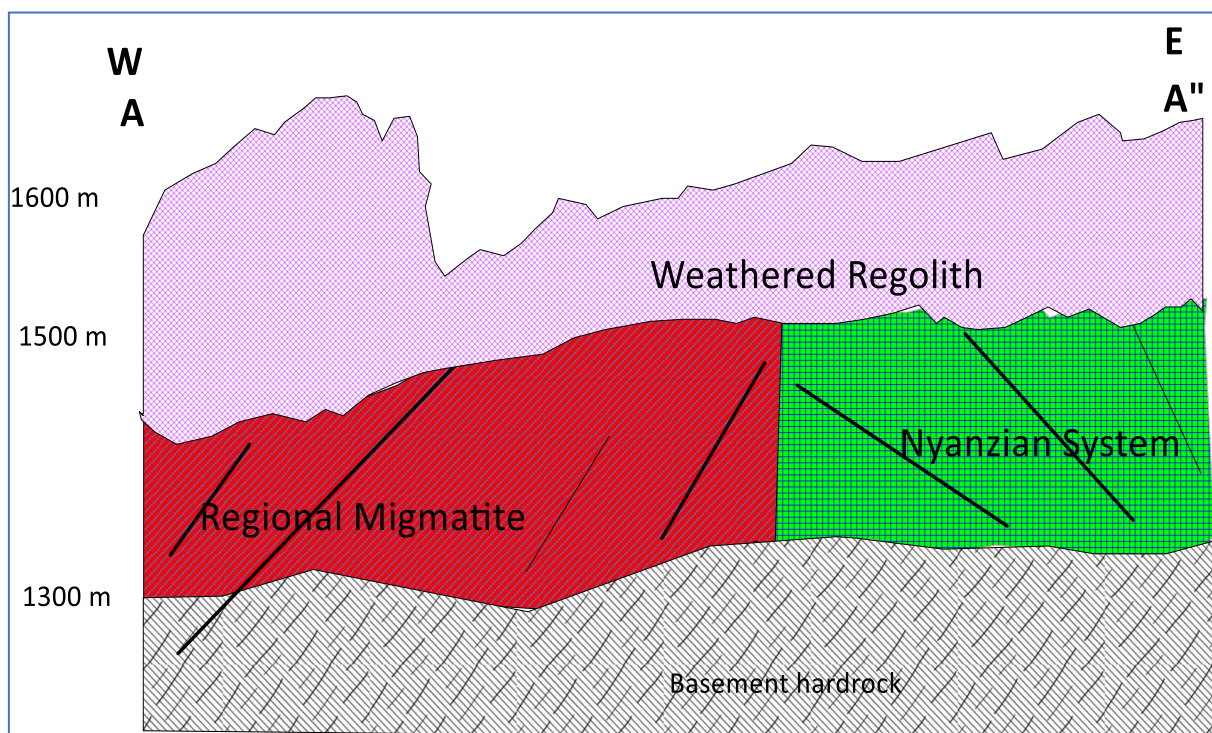


**Figure 22:** A cross-section of the Singida aquifer showing a layered system of the study area (Author's construction from filed data)

Groundwater occurring in joints and cracks of basement rocks in the study area are mostly in confined conditions due to hardpan layer (pressure reaches up to 100 meters). Surrounding lands cannot contribute to recharge these aquifers, and they are mostly recharged in hilly distant areas, as opined by Mussa *et al.* (2020); Haitjema and Mitchell-Bruker (2005) and Gleeson *et al.* (2011). There Singida semi- arid fractured basement aquifer is made of complex water sources and this is reflected in the acquired water quality data as it was discussed in other section of this dissertation.

## **(ii) Groundwater Recharge and Exploitation in the Singida Aquifer**

Hydraulic parameters and the most promising potential groundwater areas have been identified through the interpretation of the existing lineaments, local geology and geomorphology, topography, hydrology and also through studying the characteristics of drilled boreholes in the study area, and vertical electrical sounding reports. The Singida aquifer system falls in the continuum between porous media and conduit systems due to the fact that both local and regional recharges occur. According to Toth (1963), the likelihood of finding superimposed flow systems in hard rock aquifers is very high because regional flow system occurs within the major interconnected fracture systems. In some areas, fractures are exposed to the surface, and these create a preferential flow, which bypasses the path to the conventional water table. Due to the high porosity of the regolith zone, it acts as a water reservoir which feeds water down into the fractured bedrock.

The unconsolidated weathered zone is made up of the porous media, while the consolidated fractured bedrock is made of fractured conduits in which water flows and is stored in the aquifer matrix between the conduits. This has been described previously by other researchers in similar geological and climatic environments (Deyassa *et al.*, 2014; Guihéneuf *et al.*, 2014; Ren *et al.*, 2018; Ofterdinger *et al.*, 2019). Groundwater flow in most hard-rock aquifers, including the Singida semi-arid fractured aquifer is very complex. In most cases, groundwater flow is governed by the hydraulic potential gradient as well as the hydraulic conductivities in the regolith and the underlying fractured bedrock.

Additionally, groundwater flow in crystalline rocks depends on fracture aperture, porosity, and the connectivity of the fractures (Ren *et al.*, 2018). However, due to the complexity of groundwater flow systems in hard-rock aquifers, in some areas of the Singida aquifer, groundwater flow is essentially shallow, mainly focused in the weathered and fractured zone, and limited to only 50 m below ground level.

As discussed elsewhere previously, most fractured basement aquifers are semi-confined, with a phreatic aquifer lying on top of the fractured basement aquifer (Deyassa *et al.*, 2014). Usually, the two systems are intimately interconnected and can hardly be separated. Since evapotranspiration is much higher than rainfall in the Singida aquifer as it is for other semi-arid to arid areas, groundwater recharge is at times episodic, influenced by such climatic extremes as ENSO. However, local land features and topography e.g., the presence of inselbergs in the Singida aquifer influences local recharge, although it is not uniformly distributed.

The rate of fracturing also facilitates groundwater recharge, both from rainfall and regional flows. Owing to its climate and geology, the latter contributes significantly to the groundwater flow and storages in the Singida aquifer. It remains hugely unclear whether well yields are firmly correlated with the existing lineaments in the Singida aquifer due to the interconnectedness of the two aquifer systems in the area (Guihéneuf *et al.*, 2014).

Wells located in flat areas show higher yields but with their water being a bit saltier than wells in the hill tops and slopes whose water is a bit fresh, with low yields. Unwittingly, the influence of topography on borehole yield in the Singida aquifer is not surprising as the correlation was previously established by other studies (Coltorti *et al.*, 2007; Neves *et al.*, 2005; Ofterdinger *et al.*, 2019). The wells fields located in Irao, Mwankoko and Utemini which are in the flat areas, and wells located in Sepuka, Kititimo and Puma represent the high yield, salty and the low yield, fresh groundwater systems respectively.

A total of 508.3 m<sup>3</sup>/h is exploited from the Singida aquifer (Table 9). That is equivalent to 4.45 x 10<sup>6</sup> m<sup>3</sup> per year. Therefore, almost 0.15 m<sup>3</sup> is extracted from the Singida aquifer per second. This amount of water is almost 1/5 of what is exploited from the Kimbiji aquifer. The recharge estimation indicated that in the 2017/2018 hydrological year, the aquifer received 45.9 mm/year, which is equivalent to 0.046 m/year.



**Table 9: Groundwater exploitation data in the Singida aquifer as of December 2020**

<b>Borehole Number</b>	<b>Wellfield/location</b>	<b>Time (Hours/Mins)</b>	<b>Time (Hours)</b>	<b>Yield (m<sup>3</sup>)</b>	<b>Yield (m<sup>3</sup>/hour)</b>
1292/2010	Mwankoko	20	20.00	1431	71.6
884/2011	Mwankoko	20	20.00	1951	97.6
399/2012	Irao	19:44	19.73	1973	100.0
400/2012	Irao	20:09	10.15	1339	131.9
438/09	Utemini	17	17.00	890	52.4
325/06	Utemini	18	18.00	313	17.4
97/02	Kititmo	19	19.00	186	9.8
141/06	Njuki	1:33	1.55	43	27.7
<b>Total</b>					<b>508.3</b>

For modeling purposes, the quantity of groundwater exploited was converted into meters per second, and it was realized that 0.14 m<sup>3</sup> goes out of the Singida aquifer per second. To account for other unaccounted for exploitations and losses, this was approximated to 0.15 m<sup>3</sup>/s. This is just a fifth of what is exploited from the Kimbiji aquifer. That owes to the surge in population in the Dar es Salaam city and its suburbs. The hydraulic conductivity obtained from pumping tests conducted in the year 2018 revealed that, the hydraulic conductivity of the lower fractured basement aquifer is  $8 \times 10^{-10}$  m/s, with fractures having  $1 \times 10^{-8}$  m/s. The upper weathered zone has hydraulic conductivity of approximately  $1 \times 10^{-5}$  m/s.

### 3.5.4 Boundary Conditions, Flow Packages and Solvers

For the Kimbiji aquifer, the boundary conditions involved constant head (the ocean to the east of the study area), while recharge and exploitation wells represented specified flux boundary conditions. There is no constant head boundary condition in the Singida aquifer. The head dependent fluxes for the Kimbiji aquifer were rivers and the general head boundaries. For the Singida aquifer, the head dependent flux boundaries comprised of lakes, and the general head boundaries. To the North and South, there were no-flow boundaries, mostly for the upper aquifer in the Kimbiji aquifer while the western side of this study area is where the regional flow component is coming from. The Singida aquifer, despite the flow being North South as determined during field work, there are fractures which at times and places alter that predetermined flow direction. Generally, there are no flow boundaries in the East and West of this study area. For the two aquifers, the Node Property Flow (NPF) package was used in tandem with the Interactive Model Solution (IMS) solver. The IMS was used with 100 outer and inner iterations for both study areas.



### 3.5.5 Model Calibration

The generation of simulated heads started with the conversion of observed heads into a shapefile using QGIS software. Thereafter, the shapefile of observed heads was imported into a respective groundwater flow model in order to create a nam file in Modflow, which includes the observed heads. Simulated heads were visualized using python through anaconda prompt by creating jupyter notebooks.

Thereafter, as it has been the case with other previous studies (Mayer *et al.*, 2007), a trial-and-error calibration technique was used in this study. This approach involved modifying aquifer parameters until the results of the simulated heads matched the measured/observed heads. The models were calibrated under steady state conditions and model computed hydraulic heads were compared with the observed hydraulic heads collected during field works and from existing databases until an acceptable agreement between the two sets of data was reached. A calibration target of  $\pm 5$  was set as an acceptable threshold for the two models and calibration was carried out using python. To quantitatively assess calibration accuracy and the ability of the models to reproduce the observations and model reliability, the Root Mean Square Error (RMSE) was calculated using Equation 42. The optimal value of RMSE is 0

$$RMSE = \sqrt{\frac{\sum_{i=1}^N (P_i - O_i)^2}{N}} \quad (42)$$

Where,  $O_i$  and  $P_i$  are the observed and predicted data respectively.  $N$  is the number of the observed measured pairs.

In addition, the coefficient of determination (COD) was used to explain how much of the variation in simulated heads is explained by the variation of the observed heads in the two aquifers. This parameter equally explains the validity and reliability of the model results (Islam *et al.*, 2017; Poeter *et al.*, 2005). Correlation (R) and standard error (SE) were also used to gauge the performance of the models. Model calibration was carried out using 31 hydraulic head data for the Kimbiji aquifer and about 39 hydraulic head data in the Singida aquifer. The flow models were calibrated by adjusting some parameters, particularly the recharge and river stage for the Kimbiji aquifer and the lake stage for the Singida aquifer, until the best fit was obtained between the observed heads and simulated heads.

### **3.5.6 Simulation of Local and Regional Groundwater Flow Systems and Groundwater Balance**

Groundwater modelling and nested groundwater flow system simulation in this study dwelled only on the steady-state approach. Time series data scarcity in the two study areas hindered the construction of the transient model. Therefore, two steady-state groundwater models (Kimbiji and Singida) were used to predict the water balance for 2017/2018 for the Singida aquifer and 2015/2016 for the Kimbiji aquifer. Zone budget simulation was applied to simulate the contribution of each flow system and the exchange between aquifer layers and sinks, and sources.

## CHAPTER FOUR

### RESULTS AND DISCUSSION

#### 4.1 To Characterize Groundwater Flow Systems based on Hydrogeological, Hydrogeochemical and Isotopic Signatures and Controls Considering the Difference in Climate and Geology

##### 4.1.1 Physico-chemical Parameters and Major Ions

The EC in the groundwater samples from Kimbiji aquifer ranges from 211  $\mu\text{S}/\text{cm}$  (S21) to 8584  $\mu\text{S}/\text{cm}$  (S19), while TDS ranges from 105 mg/L (S21) to 4290 mg/L (S19) as shown in Table 10. The huge difference between the average and median values is an indication that there are extreme values of EC in the Kimbiji aquifer. This is also explained by the higher extreme boundary values (which is 3546  $\mu\text{S}/\text{cm}$ ). This actually means any value above 3546  $\mu\text{S}/\text{cm}$  is an outlier. The TDS also suffers from extreme values. This is because there is a linear relationship between TDS and EC as explained by previous studies (Emenike *et al.*, 2018; Rusydi, 2018). On the other hand,  $\text{HCO}_3^-$  in the Kimbiji aquifer also suffers from extremes albeit to a lesser degree as compared to EC and TDS (Table 10). In the Kimbiji aquifer,  $\text{K}^+$ ,  $\text{Ca}^{2+}$ ,  $\text{Mg}^{2+}$ ,  $\text{Cl}^-$  and  $\text{NO}_3^-$  are affected by outliers while the rest of the parameters are not.

The EC values from the Singida aquifer range between 216 to 4910  $\mu\text{S}/\text{cm}$ , indicating a range of varying groundwater quality and mineralization. As it was for the Kimbiji aquifer, EC and TDS in the Singida aquifer also have outliers as can be seen from Table 4. However, the degree of variation between the mean and the median is not huge. Nevertheless,  $\text{Na}^+$ ,  $\text{Cl}^-$  and  $\text{NO}_3^-$  are affected by outliers, with higher maximum values than the higher extreme boundary. The other parameters in the Singida aquifer are not affected by outliers as it can be seen from Table 11.

The pH of the groundwater samples from the Kimbiji aquifer ranges between 5.4, Acidic and 7.7, almost neutral as presented in Table 10. For the Singida Aquifer, the pH values ranged from 6.0 to 8.7 as presented in Table 11. Since it has been established that the permissible pH value for public supplies may range between 6.5 to 8.5 (Emenike *et al.*, 2018), the water quality from pH point of view is deemed excellent in all the samples except for S17 and S18 in the Kimbiji aquifer whose pH values were 5.8 and 5.4 respectively. The exception for the Singida aquifer is for samples S57 and S61, whose pH values are 6.3 and 6.0, respectively.

**Table 10: Descriptive statistics of hydrogeochemical parameters for the Kimbiji aquifer**

<b>Parameter</b>	<b>Max</b>	<b>Min</b>	<b>Mean</b>	<b>Median</b>	<b>Q1</b>	<b>Q2</b>	<b>Q3</b>	<b>IQR</b>	<b>Lower Extreme boundary</b>	<b>Higher extreme boundary</b>
<b>pH</b>	7.7	5.4	6.6	6.7	6.3	6.8	6.9	0.6	5.4	7.8
<b>EC</b>	8584.0	136.0	1470.5	700	433.5	738	1678.5	1245	-1434	3546
<b>TDS</b>	4290.0	68.0	727.9	350	216	369	839.5	623.5	-719.25	1774.75
<b>Na<sup>+</sup></b>	344.0	15.8	120.2	81.2	45.4	81.2	203.7	158.3	-192.05	441.15
<b>K<sup>+</sup></b>	23.8	1.5	7.5	6.2	3.85	6.2	10.65	6.8	-6.35	20.85
<b>Ca<sup>2+</sup></b>	876.0	2.2	124.6	43.3	7.4	53.3	129.5	122.1	-175.75	312.65
<b>Mg<sup>2+</sup></b>	335.3	0.8	37.3	10.6	2.85	13.5	38.35	35.5	-50.4	91.6
<b>Cl<sup>-</sup></b>	1700.0	7.0	236.7	61.2	24.45	75	282	257.55	-361.875	668.325
<b>SO<sub>4</sub><sup>2-</sup></b>	82.0	0.0	31.5	30	6	31	57	51	-70.5	133.5
<b>NO<sub>3</sub><sup>-</sup></b>	298.0	1.1	60.4	27	8.7	31.3	95.65	86.95	-121.725	226.075
<b>HCO<sub>3</sub><sup>-</sup></b>	456.0	22.2	153.8	125.4	59.05	146	221.2	162.15	-184.175	464.425

**Table 11: Descriptive statistics of hydrogeochemical parameters for the Singida aquifer**

<b>Parameter</b>	<b>Maximum</b>	<b>Minimum</b>	<b>Mean</b>	<b>Median</b>	<b>Q1</b>	<b>Q2</b>	<b>Q3</b>	<b>IQR</b>	<b>Lower Extreme Boundary</b>	<b>Higher extreme Boundary</b>
<b>pH</b>	8.7	6.0	7.3	7.2	6.8	7.2	8.0	1.3	4.8	9.9
<b>EC</b>	4910.0	216.0	1561.4	1471.5	781.0	1471.5	1570.0	789.0	-402.5	2753.5
<b>TDS</b>	2456.0	108.0	823.0	756.0	468.0	756.0	808.0	340.0	-42.0	1318.0
<b>Na<sup>+</sup></b>	783.0	16.1	242.9	157.0	76.7	157.0	234.5	157.8	-160.0	471.2
<b>K<sup>+</sup></b>	16.8	5.6	9.4	8.1	6.2	8.1	10.2	4.0	0.2	16.2
<b>Ca<sup>2+</sup></b>	92.3	4.7	41.3	35.1	15.0	35.1	60.9	45.9	-53.9	129.8
<b>Mg<sup>2+</sup></b>	13.0	0.5	6.1	4.4	3.0	4.4	10.7	7.7	-8.6	22.3
<b>Cl<sup>-</sup></b>	690.0	8.4	196.6	145.0	36.9	145.0	211.0	174.1	-224.3	472.2
<b>SO<sub>4</sub><sup>2-</sup></b>	92.0	3.0	50.4	72.0	13.0	72.0	82.0	69.0	-90.5	185.5
<b>NO<sub>3</sub><sup>-</sup></b>	110.0	22.6	44.9	36.0	24.1	36.0	46.3	22.2	-9.2	79.6
<b>HCO<sub>3</sub><sup>-</sup></b>	301.0	13.1	146.3	162.6	99.0	162.6	208.1	109.1	-64.7	371.8
<b>CO<sub>3</sub><sup>2-</sup></b>	11.1	0.0	3.1	0.0	0.0	0.0	6.1	6.1	-9.2	15.3

Groundwater in the Kimbiji aquifer falls in the first 3 types (Type I to III) as the maximum recorded EC was not above 10 000  $\mu\text{S}/\text{cm}$ . Group I samples, based on EC are S1, S2, S4, S8, S10, S12, S14, and S21. These have  $\text{EC} < 700 \mu\text{S}/\text{cm}$ . The water in this group is non-saline. The second type (Type II) has EC values between 700 and 2000  $\mu\text{S}/\text{cm}$ . This constitutes S6, S11, S13, S17, and S18. The water in this group is slightly saline. The third type is characterized by moderate salinity because the EC is higher than 2000 and less than 10 000  $\mu\text{S}/\text{cm}$ . The samples in the Kimbiji aquifer falling in this type are S16 and S19.

From TDS point of view, the Kimbiji groundwater falls in two types, type I and II. Only two samples S16 and S19 fall in the second type (brackish) whose EC concentrations are 1838 and 4290 mg/L respectively. The other 13 samples are type I (freshwater) with  $\text{TDS} < 1000 \text{ mg}/\text{L}$ . Samples S57 and S60 fall in the third type, which is characterized by moderate salinity with EC values ranging between 2000 and less than 10 000  $\mu\text{S}/\text{cm}$ . The samples have 4910 and 2400  $\mu\text{S}/\text{cm}$ . Type II water constitutes of S52, S53, S54, S56 and S58, whose EC ( $\mu\text{S}/\text{cm}$ ) concentrations are 936, 1511, 1555, 1615 and 1432 respectively. The other samples (S57 and S61) are in type I water, (non-saline water) whose EC values are 216 and 316  $\mu\text{S}/\text{cm}$ , respectively.

The water in the Singida aquifer also falls in two grounds of TDS classification. Type I and II, and only two samples S59 and S60 fall in the second group with TDS values (mg/L) of 2456 and 1160 respectively. The other samples (S52, S53, S54, S56, S58, S61) fall in the first group (Type I), which is fresh water. According to previous studies (Rhoades *et al.*, 1992; Todd & Mays, 2005; Rusydi, 2018), water classification based on EC is divided into 6 types, namely, type I, which is non-saline ( $\text{EC} < 700 \mu\text{S}/\text{cm}$ ); type II is slightly saline (700 and 2,000  $\mu\text{S}/\text{cm}$ ); type III is moderately saline, if EC is higher than 2000 and less than 10 000  $\mu\text{S}/\text{cm}$ ; type IV is highly saline with EC value from 10 000 till 25 000  $\mu\text{S}/\text{cm}$ ; type V is very highly saline, if EC value between 25 000 and 45 000  $\mu\text{S}/\text{cm}$ ; and type VI is brine water with EC more than 45 000  $\mu\text{S}/\text{cm}$ .

Moreover, according to other researchers (Rusydi, 2018), TDS is classified into four types. Type I is freshwater with  $\text{TDS} < 1000 \text{ mg}/\text{L}$ ; type II is brackish water with TDS between 1000 and 10 000 mg/L; type III is saline water with TDS from 10 000 till 100 000 mg/L; and type IV is brine water with  $\text{TDS} > 100 000 \text{ mg}/\text{L}$ . In all the areas where the values of TDS are below 1000 mg/L, with the dominance of Sodium and bicarbonate ions over Ca and Cl ions, the water falls in the precipitation domain, indicating a meteoric origin. The two aquifers have principally exhibited this characteristic. Further to that, samples with TDS approaching 1000 mg/L are of geogenic origin. These groundwater locations explain the importance of rock-water interaction as the principal mechanism that controls groundwater quality. This behavior has been exhibited by both, the

Singida and Kimbiji aquifers. On the other hand, samples with TDS above 1000 mg/L confirm that evaporation is the major mechanism controlling groundwater quality. This is possibly so in shallow wells of sandy aquifer materials as it is generally known for the coastal aquifers like Kimbiji, where it was observed also that there are mixed old and young water. This explains the presence of local, sub-regional and regional flows systems which influence groundwater recharge in the aquifer. Moreover, anthropogenic influence on the groundwater system has been observed.

As for Singida aquifer, anthropogenic activities influence groundwater quality. Nonetheless, a mixture of qualitatively young and old water, with high residence time, which is highly mineralized as depicted by EC and TDS has been observed. Generally, the groundwater in the Singida aquifer is highly rich in Sodium ions. This is due to base ion exchange, where there is an exchange between  $\text{Na}^+$  and  $\text{K}^+$  of the aquifer material with  $\text{Ca}^{2+}$  and  $\text{Mg}^{2+}$  from the groundwater. This signifies that more sodium is released into the groundwater from the hosting environment.

Further to that, for samples with TDS between 100 - 1000 mg/L there is a dominance of Sodium and bicarbonate ions over  $\text{Ca}^{2+}$  and  $\text{Cl}^-$  ions, the water falls in the precipitation domain, indicating a meteoric origin. Generally, mineral dissolution through water-rock interactions, anthropogenic activities such as agriculture and waste management, and ion exchanges have been found to be the major sources of hydrogeochemical variations in the two study areas. The processes have been reported elsewhere by other researchers (Emenike *et al.*, 2018).

#### **4.1.2 Hydrogeochemical Facies using the Piper (trilinear) Diagram Approach**

In the Kimbiji aquifer, the trilinear approach grouped the water samples into mixed type, Na-Cl type- Ca-Cl type, Ca- $\text{HCO}_3$  type and Na- $\text{HCO}_3$  type. Samples S11, S16, S17, and S18 from Mkuranga Mizani, Pugu Kajiungeni, Kazimzumbwi Kisarawe and Pugu Kinyamwezi are dominated by  $\text{Cl}^-$  as the major anion. This tells that there is a huge likelihood that human activities are already influencing groundwater quality in this part of the Kimbiji aquifer. Moreover, this also signifies a possibility of long transit times of groundwater, thereby hinting on a possibility of regional/sub-regional recharge (Fig. 23).

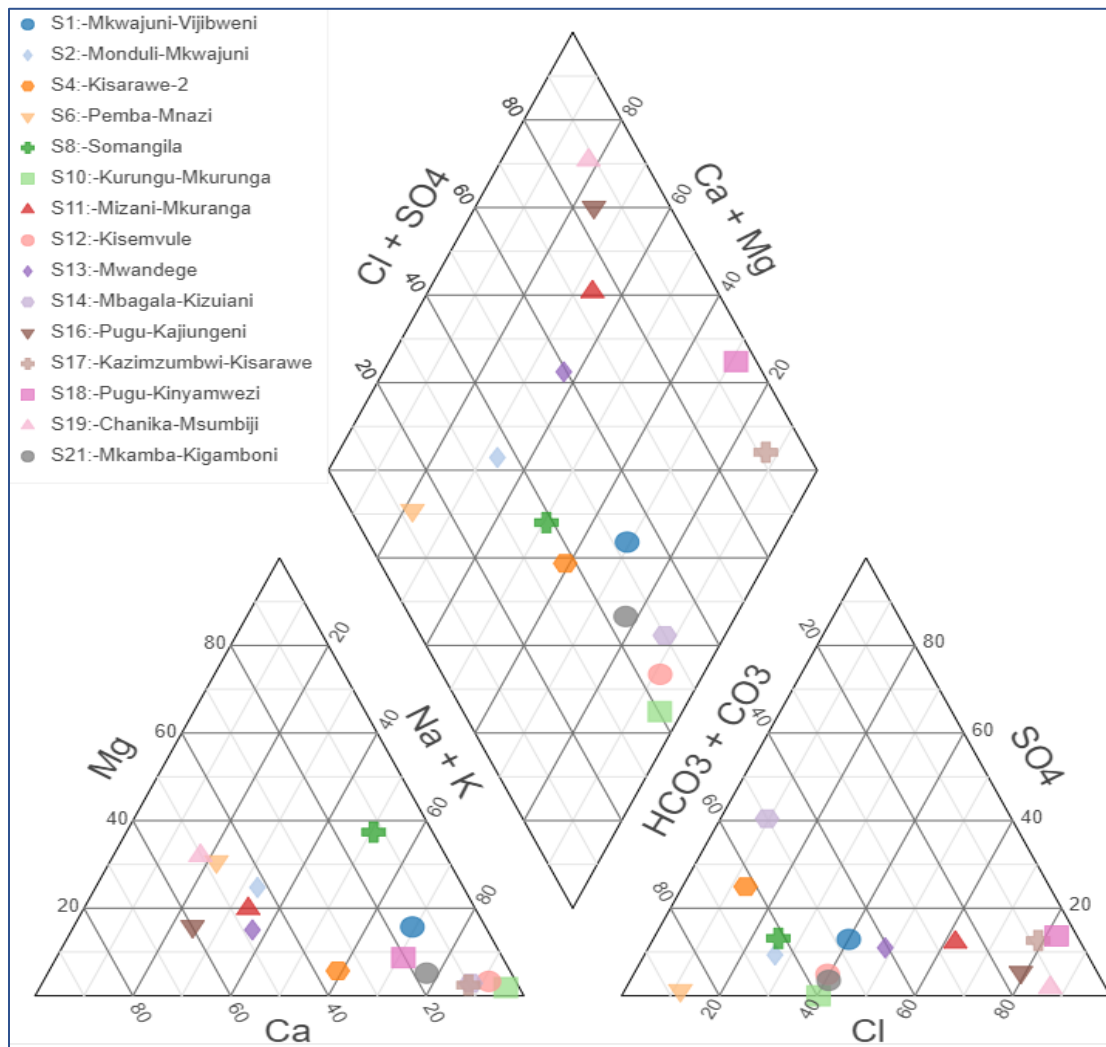


**Figure 23: Piper diagram for Kimbiji aquifer**

To that effect, major cations for the Kimbiji aquifer are  $\text{Ca}^{2+}$  and  $\text{Na}^+$  and the dominant water types are Ca-Cl for S11 and S16 and Na-Cl for S17 and S18. Samples S1, S10, S12, S13 and S21 exhibit a mixture of  $\text{Cl}^-$  and  $\text{HCO}_3^-$ . The mixed water types are Na-Cl- $\text{HCO}_3$ . For samples S2, S4, S6, S8, S11, S14, S19 exhibit bicarbonate as the major anion while  $\text{Ca}^{2+}$  is the major ion for S2, and S11,  $\text{Na}^+$  being the major cation for S8, S14, a mixture of Ca-Mg dominates S6, S19, and S4 is dominated by Ca-Na mixture. The water types are therefore of four hydrogeochemical facies. The Ca- $\text{HCO}_3$  (S2, S11), Na- $\text{HCO}_3$  (S8, S14), Ca-Mg- $\text{HCO}_3$  (S6, S19) and Ca-Na- $\text{HCO}_3$  for S4. In addition to the hydrogeochemical facies, this study has also identified ionic sequences, which are  $\text{Na}^+ > \text{Ca}^{2+} > \text{Mg}^{2+} > \text{K}^+ : \text{HCO}_3^- + \text{CO}_3^{2-} > \text{Cl}^- > \text{SO}_4^{2-}$  for S1, S2, S4, S21;  $\text{Ca}^{2+} > \text{Na}^+ > \text{Mg}^{2+} > \text{K}^+ : \text{HCO}_3^- + \text{CO}_3^{2-} > \text{Cl}^- > \text{SO}_4^{2-}$  for S6, S13;  $\text{Na}^+ > \text{Mg}^{2+} > \text{Ca}^{2+} > \text{K}^+ : \text{HCO}_3^- + \text{CO}_3^{2-} > \text{Cl}^- > \text{SO}_4^{2-}$  for S8;  $\text{Na}^+ > \text{K}^+ > \text{Ca}^{2+} > \text{Mg}^{2+} : \text{HCO}_3^- + \text{CO}_3^{2-} > \text{Cl}^- > \text{SO}_4^{2-}$  for S10, S12;  $\text{Ca}^{2+} > \text{Na}^+ > \text{Mg}^{2+} > \text{K}^+ : \text{Cl}^- > \text{HCO}_3^- + \text{CO}_3^{2-} > \text{SO}_4^{2-}$  for S11, S16, S19;  $\text{Na}^+ > \text{Ca}^{2+} > \text{K}^+ > \text{Mg}^{2+} : \text{HCO}_3^- + \text{CO}_3^{2-} > \text{SO}_4^{2-} > \text{Cl}^-$  for S14; and  $\text{Na}^+ > \text{Ca}^{2+} > \text{K}^+ > \text{Mg}^{2+} : \text{Cl}^- > \text{SO}_4^{2-} > \text{HCO}_3^- + \text{CO}_3^{2-}$  for S17, S18.



Trilinear diagram has proved instrumental in delineating the hydrogeochemical facies by graphically demonstrating the relationships between the most important dissolved constituents in a set of groundwater samples. The geochemical evolution of groundwater in the Kimbiji aquifer was divulged and understood by plotting the concentrations of major cations and anions in the piper trilinear diagram (Piper, 1944, 1953). The nature and distribution of hydrogeochemical facies was determined by providing insights into how groundwater quality changes within the Kimbiji aquifer system.

For the Singida aquifer, the piper diagram (Fig. 24) shows that sodium is the major cation for all samples while chloride is the major anion for S53, S59, S60, S61, and bicarbonate is the major anion for Samples S52, S54, S56, S57, and S58. To that effect, the water type in the former groups is Na-Cl while the latter group exhibits Na-HCO<sub>3</sub> water type. The major ions sequence is Na<sup>+</sup>>Ca<sup>2+</sup>>Mg<sup>2+</sup>: HCO<sub>3</sub><sup>-</sup> + CO<sub>3</sub><sup>2-</sup>> Cl<sup>-</sup> >SO<sub>4</sub><sup>2-</sup> for S52, S54, S56, S57. The sequence is Na<sup>+</sup>>Ca<sup>2+</sup>>Mg<sup>2+</sup>: HCO<sub>3</sub><sup>-</sup> + CO<sub>3</sub><sup>2-</sup> > SO<sub>4</sub><sup>2-</sup> > Cl<sup>-</sup> for S58 and it is Na<sup>+</sup>>Ca<sup>2+</sup>>Mg<sup>2+</sup>: Cl<sup>-</sup> > HCO<sub>3</sub><sup>-</sup> + CO<sub>3</sub><sup>2-</sup> > SO<sub>4</sub><sup>2-</sup> for S53, S59, S60, and S61. However, there is an observed similarity between the groundwater samples S54 (Mwankoko borehole) and the three surface water bodies (lakes). Samples S53, S54, S59 and S60 are all Na-Cl water type. In all these samples, Na<sup>+</sup> is the major cation while Cl<sup>-</sup> is the major anion. This is possibly an ostensible indication that there is likelihood of interaction between groundwater and surface water in the Singida aquifer.

Moreover, the similarity of hydrogeochemical signatures between a distant surface water body, S60 (Lake Inkhanoda) and the S54 (Mwankoko borehole) is an indication that the Singida aquifer is fed by sub-regional to regional groundwater flow systems. Generally, there are two hydrogeochemical facies in the Singida semi-arid fractured aquifer. The first group shows that alkalis and strong acids predominate (S53, S56, S59, S60). The sample S54 hovers around the balance between carbonate and chloride anions. The other group (carbonate hardness exceeds 50%) is made up of S52, S57, S58, and S60).

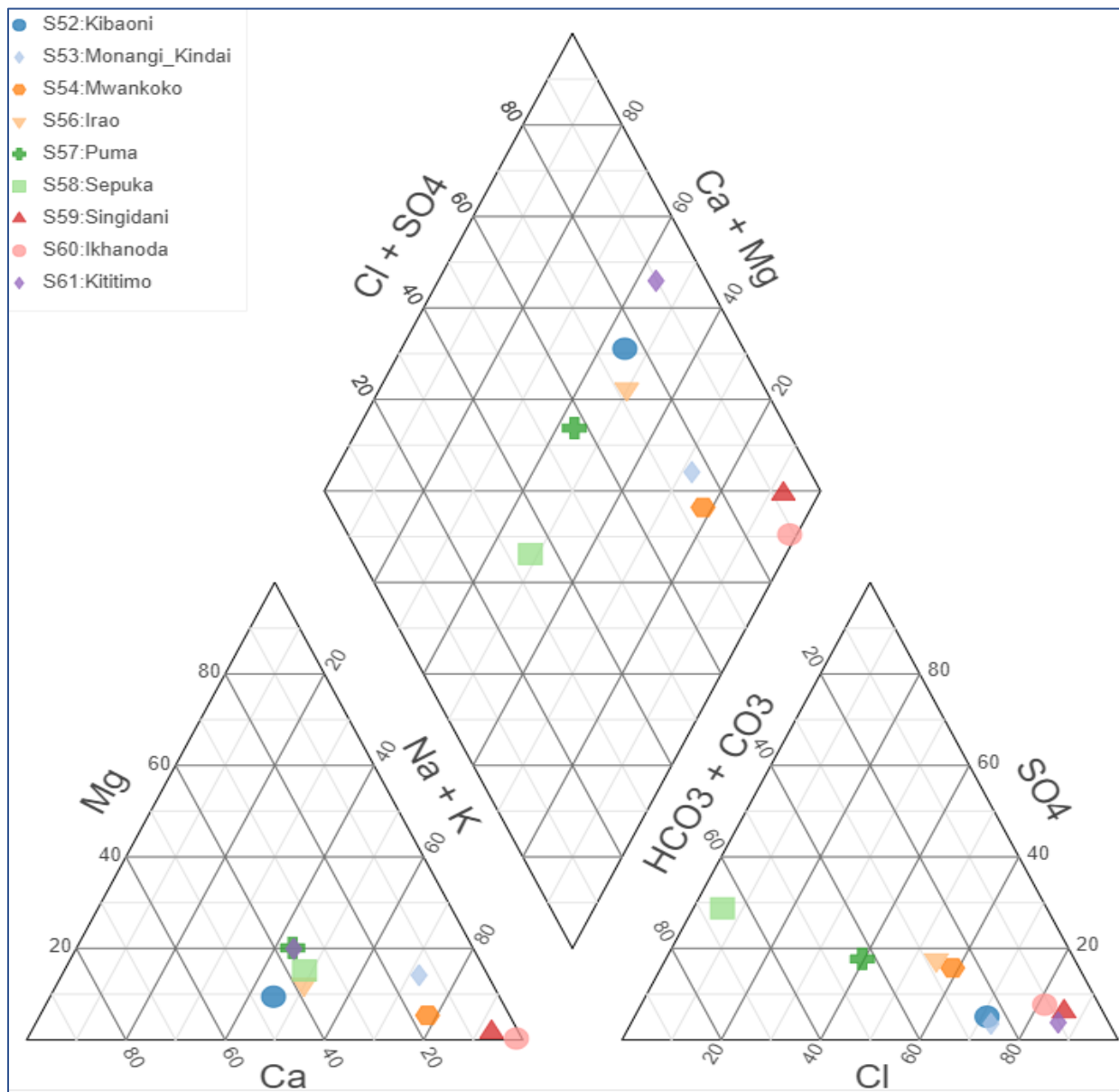


**Figure 24: Piper diagram for Singida aquifer**

### 4.1.3 Mechanisms Controlling Groundwater Chemistry

Identification of the mechanisms controlling groundwater chemistry and quality (i.e., Precipitation, Rock-water interaction, and Evaporation) using Gibb's approach was carried out. Table 12 shows the Gibbs ratios which were used to identify the dominant mechanisms controlling groundwater evolution and quality in the Kimbiji aquifer. The Gibbs ratios are also represented in Gibb's diagrams (Fig. 25 & Fig. 26). In samples with TDS below 100 mg/L (Table 12), the water in all samples is of geogenic origin, mainly being controlled by rock-water interaction mechanism. This is a manifestation of dissolution with rock forming minerals as reported previously (Marandi & Shand, 2018). Such type of water where TDS is less than 100 mg/L is regarded as fresh water. The ratio of cations ( $\text{Na}^+/\text{Na}^+ + \text{Ca}^{2+}$ ) varies from 0.5 to 0.9 while that of anions varies from 0.06 to 0.17

(Table 12). This is an indication that the water is devoid of chloride ions but very rich in bicarbonate ions which further signifies the freshness of the water in this study area.

For samples that are rich in Sodium ions, there is a greater possibility of exchange between  $\text{Na}^+$  of the aquifer material with  $\text{Ca}^{2+}$  and  $\text{Mg}^{2+}$  from the groundwater. In this mechanism, more sodium is released into the groundwater from the aquifer hosting environment while  $\text{Ca}^{2+}$  and  $\text{Mg}^{2+}$  are being deposited into the aquifer materials. Moreover, for samples with TDS between 100 - 1000 mg/L there is a dominance of Sodium and bicarbonate ions over  $\text{Ca}^{2+}$  and  $\text{Cl}^-$  ions. This type of water falls in the rock-water interaction domain, indicating a geogenic origin.

**Table 12: Gibbs ratios for the Kimbiji aquifer**

Sample Number	Place Name	TDS	$\text{Na}^+/\text{Na}^++\text{Ca}^{2+}$	$\text{Cl}^-/\text{Cl}^-+\text{HCO}_3$
S1	Mkwajuni-Vijibweni-Kigamboni	276	0.81	0.46
S2	Monduli-Mkwajuni-Kigamboni	350	0.43	0.29
S4	Kisarawe 2, Mwasonga-Kigamboni	308	0.62	0.17
S6	Pemba Mnazi-Kigamboni	404	0.30	0.11
S8	Somangila-Kigamboni	68	0.80	0.29
S10	Kurungu-Mkurunga	333	0.97	0.40
S11	Mizani-Mkurunga	966	0.41	0.71
S12	Kisemvule-Mkurunga	95	0.94	0.41
S13	Mwandegge-Mkurunga	369	0.42	0.54
S14	Mbagala Kizuiani	156	0.90	0.16
S16	Pugu Kajiungeni	1838	0.28	0.83
S17	Kazimzumbwi-Kisarawe	713	0.89	0.90
S18	Pugu-Kinyamwezi	648	0.77	0.95
S19	Chanika-Msumbiji	4290	0.26	0.88
S21	Mkamba-Kigamboni	105	0.81	0.42

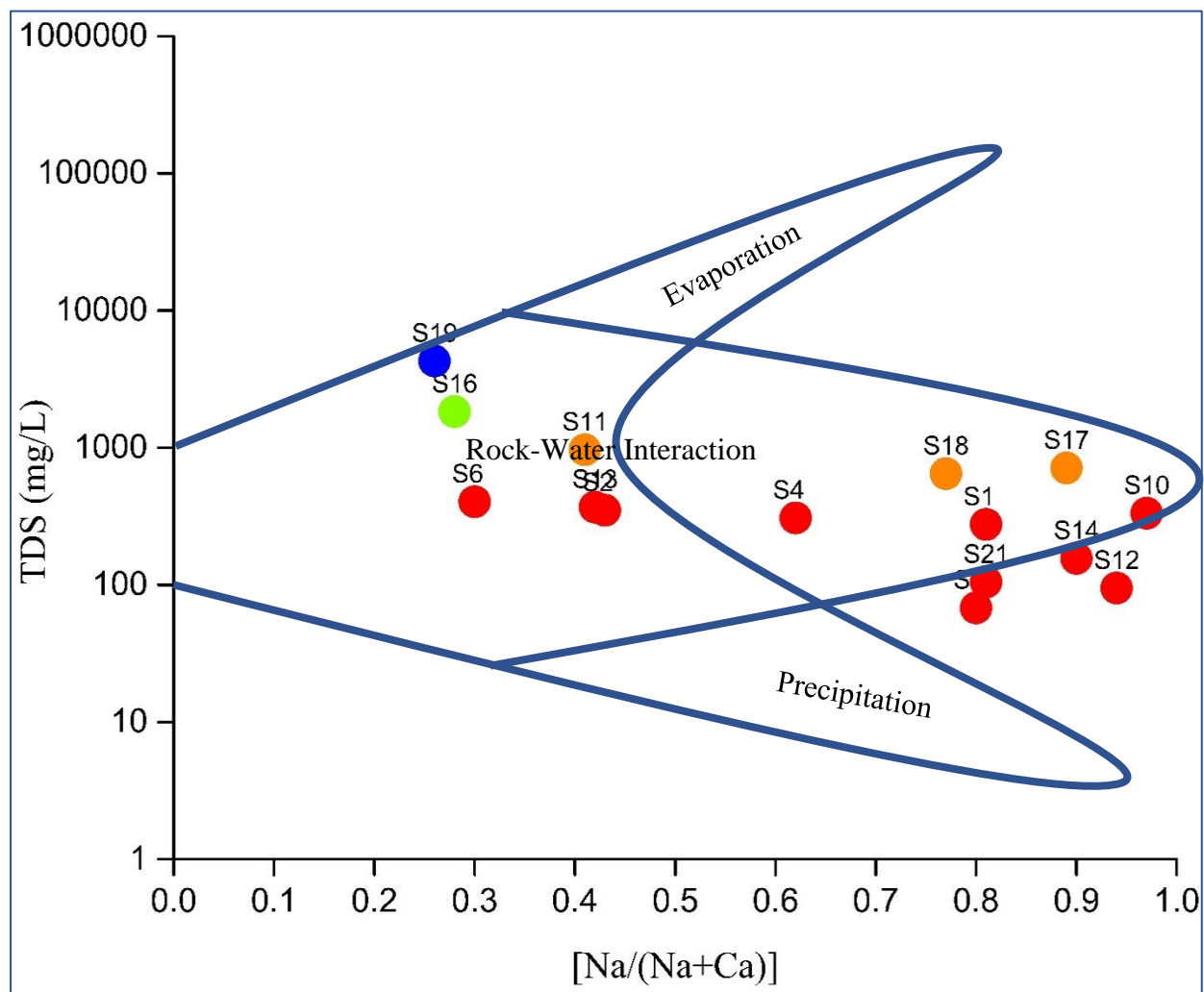


**Figure 25: Cationic Gibb's diagram for the Kimbiji aquifer**

The mechanisms controlling groundwater geochemistry have been revealed by assessing the reaction between groundwater and aquifer minerals. This has a significant role in water quality which is useful to understand the origin and provenance of groundwater (Gibbs, 1970; Subramani *et al.*, 2009; Vasanthavigar *et al.*, 2012). The Gibbs ratio 1 values range from 0.26 to 0.94 and Gibbs ratio 2 values range from 0.11 to 0.95. The majority of the samples irrespective of the formation are falling in the rock-water interaction zone. This is due to the chemical weathering with the dissolution of rock forming minerals. The Gibbs diagrams (Fig. 23 & Fig. 24) revealed that the hydrochemistry of groundwater in the Kimbiji aquifer falls mainly in the rock weathering region and this is due to dissolution with rock forming minerals. However, sample 19 (S19), drawn from a shallow borehole is in transition to the evaporation domain. Being in the shallow aquifer of sedimentary formation, it is very much likely affected by evaporation.

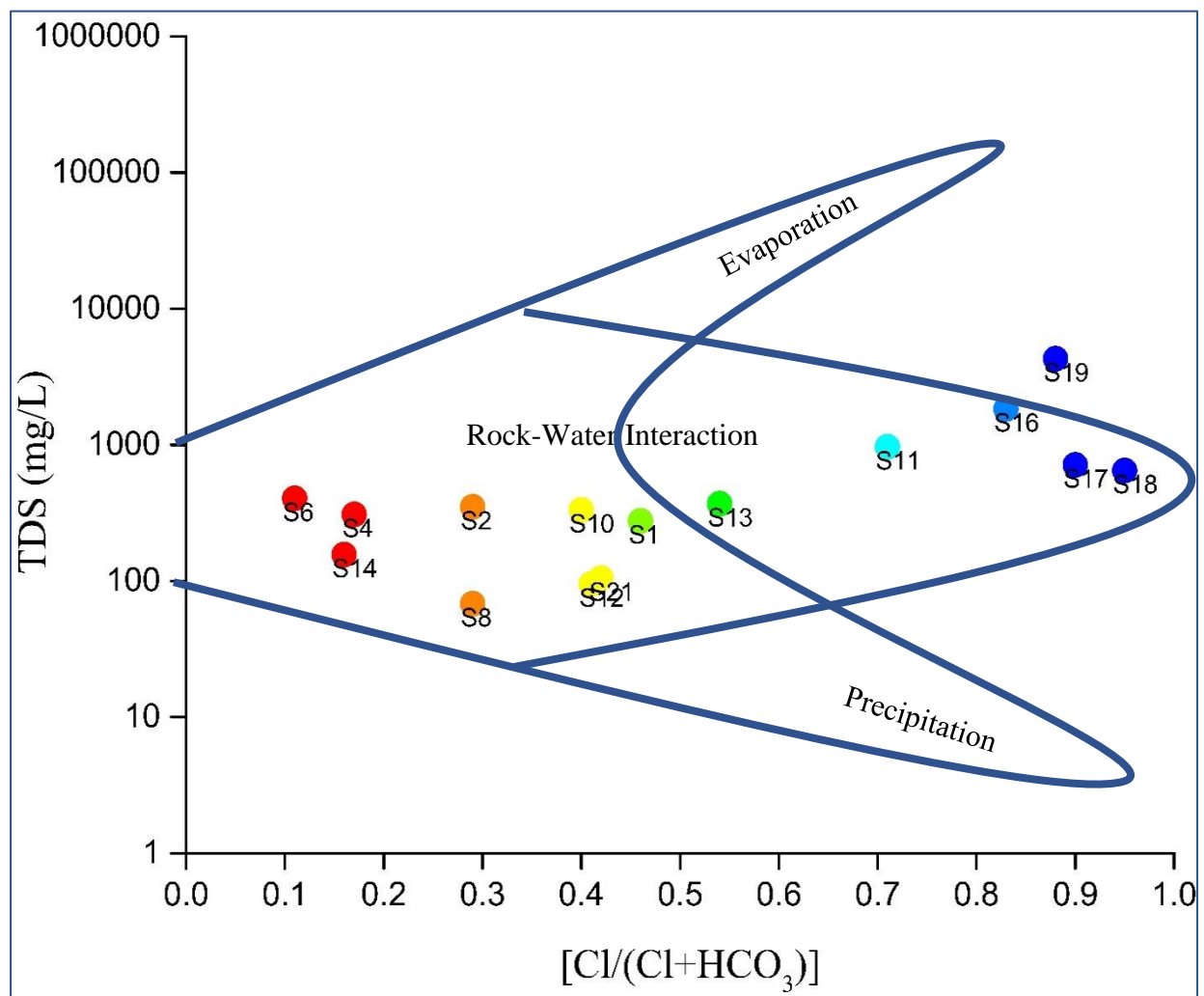


**Figure 26: Anionic Gibb's diagram for the Kimbiji aquifer**

The cationic Gibb's ratios for the Singida aquifer ( $\text{Na}^+/\text{Na}^++\text{Ca}^{2+}$ ) range from 0.55 (S61) to 0.99 (0.99) (Table 13). The anionic Gibb's ratio ( $\text{Cl}^-/\text{Cl}^-+\text{HCO}_3^-$ ) lies between 0.03 (S58) and 0.81 (S59). Gibb's diagrams (Fig. 27 & Fig. 28) indicate that the main mechanism that controls groundwater chemistry in the Singida aquifer is rock-water interaction. This is due to the fact that the depth of boreholes in this particular aquifer are around 100 m and above. In addition, most groundwater is found within the semi-confined aquifer where evaporation cannot easily affect the water. The cationic Gibb's ratio has depicted lake water samples (S59, S60) being on transit to the evaporation domain (Fig. 27). This is because, coming from the open water bodies, they are affected by evaporation.

**Table 13: Gibbs ratios for the Singida aquifer**

Sample Number	Place Name	TDS	Na <sup>+</sup> /Na <sup>+</sup> +Ca <sup>2+</sup>	Cl <sup>-</sup> /Cl <sup>-</sup> +HCO <sub>3</sub>
S52	Majengo	468	0.56	0.50
S53	Kindai	756	0.87	0.50
S54	Mwankoko	777	0.86	0.50
S56	Irao	808	0.63	0.39
S57	Puma	108	0.59	0.24
S58	Sepuka	716	0.63	0.03
S59	Singidani	2456	0.96	0.81
S60	Ikhanoda	1160	0.99	0.77
S61	Kititimo	158	0.55	0.74

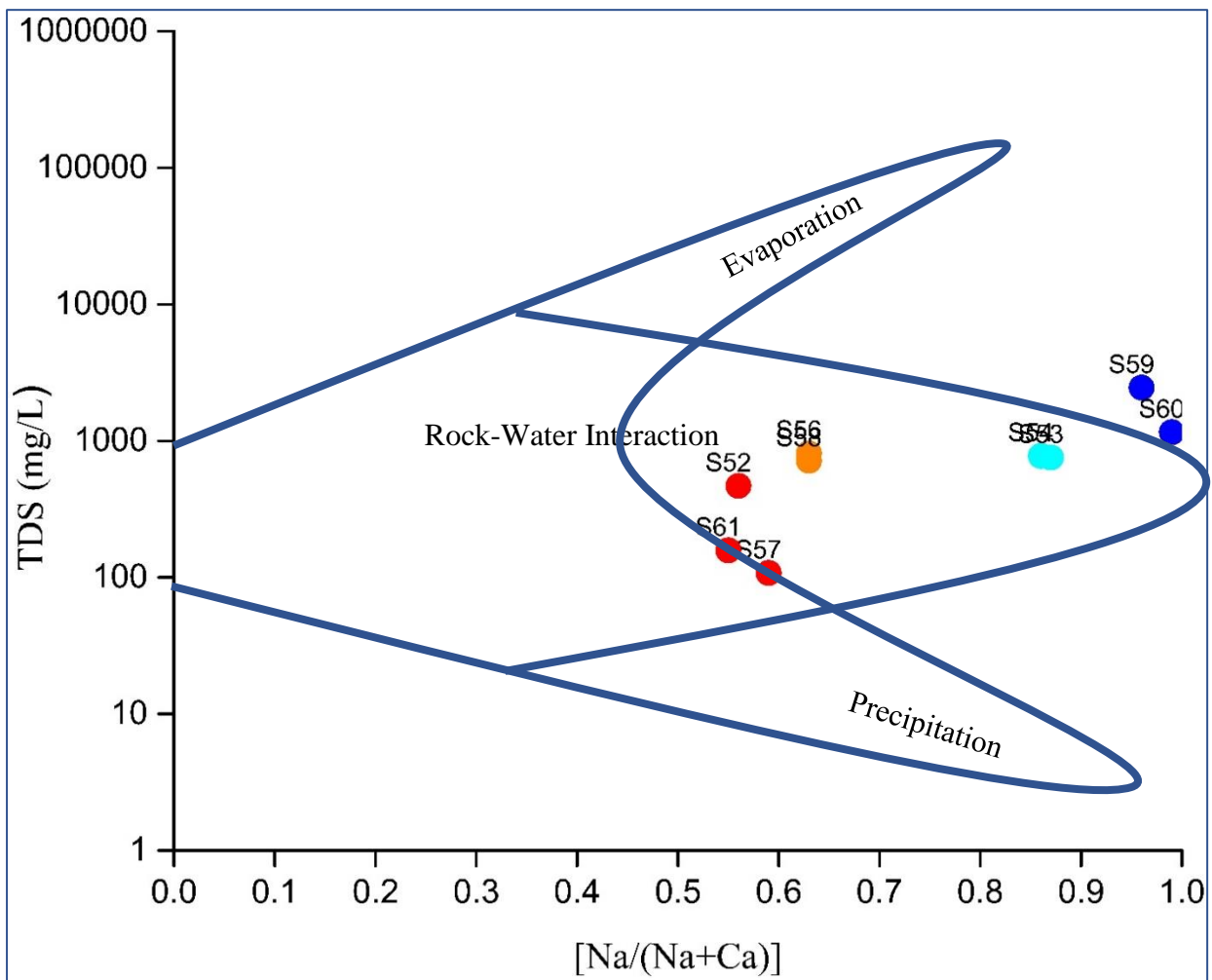


**Figure 27: Cationic Gibb's diagram for the Singida aquifer**

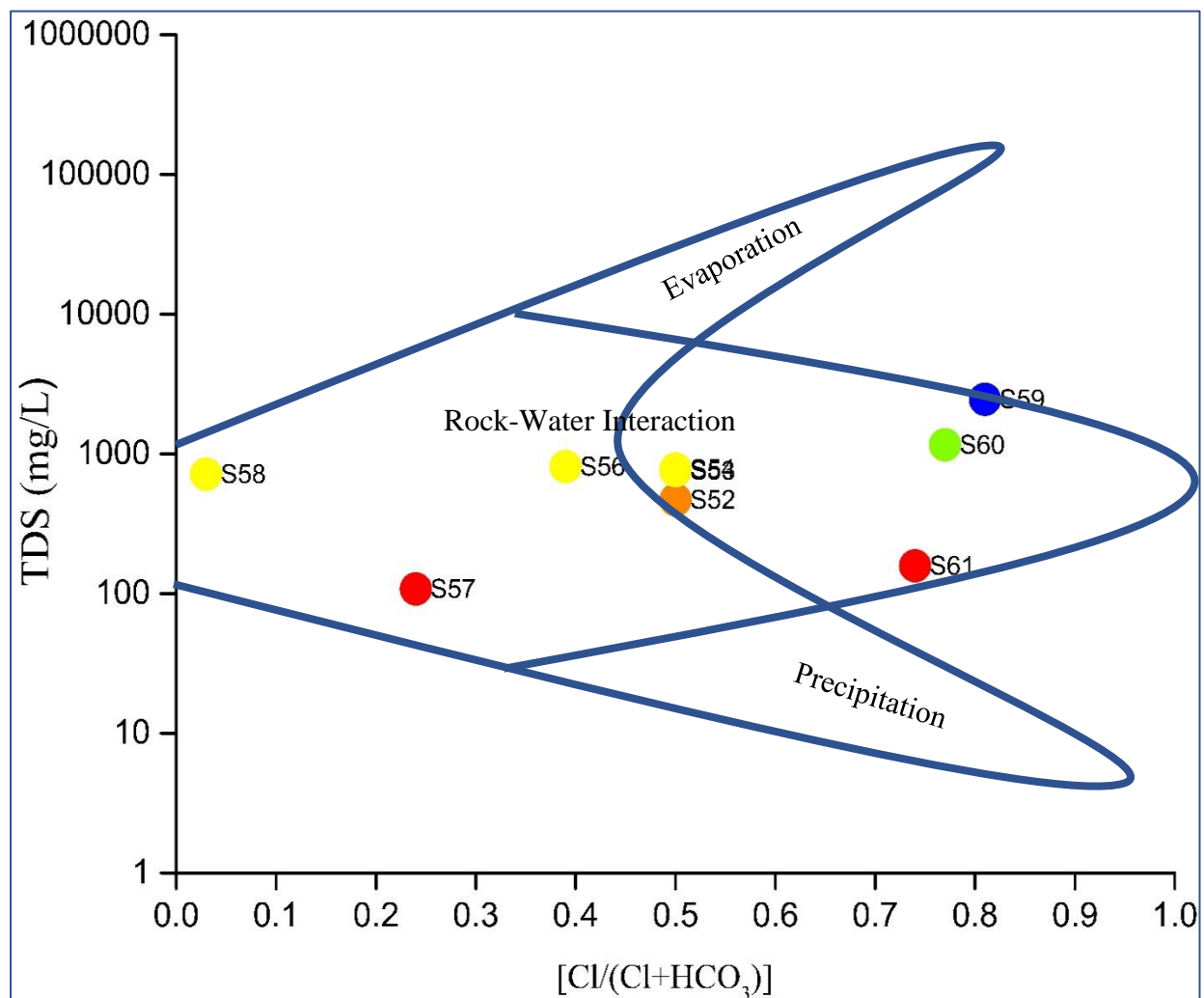


**Figure 28: Anionic Gibb's diagram for the Singida aquifer**

All the samples with the  $\text{Ca}^{2+}$  and  $\text{HCO}_3^-$  over  $\text{Na}^+$  and  $\text{Cl}^-$  indicate a meteoric origin as they fall in the precipitation domain. In this situation, rock-water interaction is responsible as the main source of dissolved ions in groundwater. However, a progressive abundance of  $\text{Na}^+$  in some areas of the Kimbiji aquifer (Pugu and Chanika areas), and the areas close to the ocean has been observed, and it goes hand in hand with increasing TDS. An increase in  $\text{Na}^+$  and  $\text{Cl}^-$  in water raises the levels of TDS, as observed in several samples (i.e., S16, S19). Generally, samples with TDS approaching 1000 mg/L are of geogenic origin. These groundwater samples explain the importance of rock-water interaction as the principal mechanism that controls groundwater quality, while samples with TDS above 1000 mg/L exhibit evaporation as the major mechanism controlling groundwater quality. This is possibly so in shallow wells of sandy aquifer materials as it is generally known for the coastal aquifer like Kimbiji. However, evaporation is not a common mechanism which controls groundwater chemistry in the Kimbiji aquifer.

Sodium has been observed to be the major cation in all samples in the Singida aquifer, while there are varying cationic dominance for the Kimbiji aquifer. Sodium dominates the upper section of the

Kimbiqi aquifer, while the middle and the lower part of the aquifer is dominated by  $\text{Ca}^{2+}$  and  $\text{Mg}^{2+}$ . In the Singida aquifer,  $\text{SO}_4^{2-}$  is not a common anion in groundwater, while  $\text{Cl}^-$  and  $\text{HCO}_3^-$  are the most common anions. In the Kimbiqi aquifer, there has been an exchange between Sodium and Calcium as the major cationic constituents of groundwater, with  $\text{HCO}_3^-$  being the most dominant anion, except for S11, S16, S17, S18 and S19 where  $\text{Cl}^-$  has been dominant.

Groundwater in the two study areas can be classified into two types, the  $\text{HCO}_3^-$  type and the  $\text{Cl}^-$  type. The bicarbonate type indicates intensive groundwater flushing due to good drainage conditions, while the Chloride type indicates inadequate water flushing as a result of quasi stagnant conditions as opined by other researchers (Chebotarev, 1955). The Sulphate type, which indicates the intermediate conditions ranging between the bicarbonate type and the chloride type is not a common type in the two study areas. However, with progressive anthropogenic interferences, no sooner the sulphate will be one of the common water types in either of the study areas. This is because, the bicarbonate and chloride ions are gradually being replaced with sulfate type water due to expanding anthropogenic influences. This scenario has also been reported by other previous studies elsewhere (Gao *et al.*, 2020). Nitrate pollution as a result of anthropogenic activities is also attributed to groundwater quality degradation in this study, as it has been reported by other researchers (Gao *et al.*, 2020).

**(i) Understanding the Changes in the Chemical Composition of Groundwater along the Flow Paths using Chloro-Alkaline Indices**

The Chloro-Alkaline Indices (CAIs) were used to understand the changes in the chemical composition of groundwater along its flow path in the Kimbiqi aquifer (Table 14). Moreover, the CAIs were used to interpret ion exchange between groundwater and its host environment. A positive CAI (S11, S13, S16, S19) indicates the exchange of  $\text{Na}^+$  and  $\text{K}^+$  from the water with  $\text{Mg}^{2+}$  and  $\text{Ca}^{2+}$  of the rocks, and it is negative (S1, S2, S6, S8, S10, S12, S14, S17, S18, S21,) when there is an exchange of  $\text{Mg}^{2+}$  and  $\text{Ca}^{2+}$  of the water with the  $\text{Na}^+$  and  $\text{K}^+$  of the rocks.

It has therefore been observed that in the largest part of the Kimbiqi aquifer, there is a progressive exchange of  $\text{Ca}^{2+}$  and  $\text{Mg}^{2+}$  in groundwater with  $\text{Na}^+$  and  $\text{K}^+$  from the aquifer materials. This is possibly one of the major reasons as to why most samples are  $\text{Na}^+$  rich in the Kimbiqi aquifer. It was therefore revealed that apart from anthropogenic activities, aquifer materials release Na and K in groundwater. Therefore, there is a possibility that groundwater residence time is large, and water could be recharged from a distant sub-basin from which it is discharged, signifying the presence of sub-regional to regional flow systems. Such scenario has been reported previously (Marc *et al.*, 2016).



The CAIs were also used to understand changes in the chemical composition of groundwater along its flow path in the Singida aquifer. With all the indices being negative (Table 15) in the Singida aquifer, this explains an exchange of  $\text{Ca}^{2+}$  or  $\text{Mg}^{2+}$  in groundwater with  $\text{Na}^+$  or  $\text{K}^+$  in aquifer materials taking place. Literally,  $\text{Ca}^{2+}$  and/or  $\text{Mg}^{2+}$  are constantly being removed from the groundwater and  $\text{Na}^+$  and/or  $\text{K}^+$  are released into the groundwater in the Singida aquifer. This corresponds well with what has been observed in the piper diagram, and thus confirms the dominance of Sodium as the major cation in the Singida aquifer.

**Table 14: Chloro-Alkali Indices for the Kimbiji aquifer**

Sample Number	Place Name	CAI-I	CAI-II
S1	Mkwajuni-Vijibweni-Kigamboni	-1.1	-0.7
S2	Monduli-Mkwajuni-Kigamboni	-1.0	-0.2
S4	Kisarawe 2, Mwasonga-Kigamboni	-10.0	-0.7
S6	Pemba Mnazi-Kigamboni	-0.8	-0.1
S8	Somangila-Kigamboni	-1.4	-0.4
S10	Kurungu-Mkurunga	-1.9	-1.1
S11	Mizani-Mkuranga	0.3	0.4
S12	Kisemvule-Mkuranga	-1.6	-1.0
S13	Mwandege-Mkuranga	0.1	0.1
S14	Mbagala Kizuiani	-15.5	-1.2
S16	Pugu Kajiungeni	0.5	1.3
S17	Kazimzumbwi-Kisarawe	-0.7	-2.0
S18	Pugu-Kinyamwezi	-0.3	-1.2
S19	Chanika-Msumbiji	0.7	2.7
S21	Mkamba-Kigamboni	-1.2	-0.8

**Table 15: Chloro-Alkali Indices for the Singida aquifer**

Sample Number	Place Name	CAI-I	CAI-II
S52	Majengo	-0.28	-0.29
S53	Kindai	-0.79	-1.07
S54	Mwankoko	-1.25	-1.11
S56	Irao	-0.71	-0.50
S57	Puma	-2.54	-0.56
S58	Sepuka	-23.25	-0.70
S59	Singidani	-0.76	-2.69
S60	Ikhanoda	-1.02	-2.39
S61	Kititimo	-0.16	-0.26

The CAIs helped in the interpretation of ion exchange between groundwater and its host environment. While a positive CAI indicates the exchange of  $\text{Na}^+$  and  $\text{K}^+$  from the water with  $\text{Mg}^{2+}$  and  $\text{Ca}^{2+}$  of the rocks, it is negative when there is an exchange of  $\text{Mg}^{2+}$  and  $\text{Ca}^{2+}$  of the water with

$\text{Na}^+$  and  $\text{K}^+$  of the rocks. Dissolution of soluble materials which contribute to mineralization of groundwater in both aquifers. The NaCl dissolution is most likely responsible for the mineralization of groundwater in the Singida aquifer as well as part of the Kimbiji aquifer. This is supported by other previous studies (Lachaal *et al.*, 2016; Re *et al.*, 2017; Kammoun *et al.*, 2018a). The mixed water types are mainly characteristic of the shallow wells (Kammoun *et al.*, 2018a). This is peculiarly characteristic in the Kimbiji aquifer. The Singida aquifer has no many cases of mixed water types due to the nature and depth of the boreholes in that area.

## (ii) Hydrogeochemical Signatures for Determining Geochemical Processes

The geochemical signatures (ratios) were used to assess the origin of groundwater in the Kimbiji and Singida aquifers (Table 16, and Table 17). Where the  $\text{HCO}_3^- : \text{Cl}^-$  was more than 1 (S1, S2, S4, S6, S8, S10, S12, S13, S14, and S21) in the Kimbiji aquifer, it indicates that the groundwater has an interaction with the aquifer materials, and it is related to recharge water. This implies that most of the surveyed shallow wells in the Kimbiji aquifer are locally recharged while the ratio less than 1 implies a low water flow course (S11, S16, S17, S19), possibly of carbonate rocks. Moreover, S18 indicates saline water. This is a water with high levels of TDS and EC around Chanika area. Since it is not proximal to the ocean, human activities have most likely influenced this type of water quality.

On the other hand, some samples exhibited replacement of  $\text{Na}^+$  by  $\text{Ca}^{2+}$  or  $\text{Mg}^{2+}$  (S18), loss of  $\text{Na}^+$  through precipitation of evaporate rocks (S11, S13, S16, S19), and water flowing through crystalline rocks (S1, S2, S4, S6, S8, S10, S12, S13, S14, S21). The  $\text{Na}^+ : \text{Ca}^{2+}$  greater than 1.0 (S1, S4, S8, S10, S12, S14, S17, S18, S19, S21) explains base ion exchange while the ratio less than 1 implies a reverse ion exchange (S2, S6, S11, S13, S16). Moreover, the  $\text{Ca}^{2+} : \text{SO}_4^{2-} + \text{HCO}_3^-$  ratio  $< 1.0$  connotes groundwater flowing through a normal hydrological cycle (S1, S4, S8, S10, S12, S14, S17, S18, S2, S6, S11, S13, S21) and a ratio greater than 1 is an indication of  $\text{Ca}^{2+} - \text{Cl}^-$  brines (S16, S19) (Table 16).

Further to that, the  $\text{HCO}_3^- : \text{Cl}^-$  hydrogeochemical signatures divided the Singida aquifer into upper water flow course, where groundwater recharge occurs (S52, S54, S56, S57, and S58) and the discharge zone (S53, S59, S60, S61) which is a lower groundwater flow course. Nevertheless, the  $\text{Mg}^{2+} + \text{Ca}^{2+} : \text{Na}^+ + \text{K}^+$  ratios (Table 17) as well confirmed that the Singida aquifer is lower groundwater flow course (discharge zone). The greater than 1  $\text{Na}^+ : \text{Ca}^{2+}$  ratios confirm the dominance of base ion exchange in the Singida aquifer as it has been explained by the CAIs and the Piper diagram. Literally, apart from the hydrogeochemical signatures indicating that Singida aquifer has upper and lower groundwater flow courses, the greater information derived here is that

groundwater in the Singida aquifer is from both, regional and local flow systems, where regional flows indicated a high travel and residence times.

The  $\text{Ca}^{2+}$  excess and  $\text{Na}^+$  deficiency scenarios are only characteristic in the Kimbiji aquifer. The Singida aquifer is mainly characterized by  $\text{Na}^+$  excess in all collected samples. The major variation has been on the anions in the Singida aquifer, as it has been in the Kimbiji aquifer as well. This suggests the significance of ion exchange reactions as a key mineralization process, where in the Singida aquifer,  $\text{Na}^+$  of the aquifer materials is exchanged with  $\text{Ca}^{2+}$  in the water. On the contrary, in the Kimbiji aquifer, in the lower parts of the study area (Kimbiji, Mkamba, Kigamboni, Kisarawe 2),  $\text{Na}^+$  of the water is exchanged with  $\text{Ca}^{2+}$  from the aquifer materials, and the reverse reaction also occurs in the middle and upper parts of this Kimbiji aquifer (i.e., Pugu, Chanika and Kisarawe). This is supported by previous studies (Kammoun *et al.*, 2018). While in the Kimbiji aquifer,  $\text{Ca}^{2+}$  and  $\text{Na}^+$  have been the two major competing cations, in the Singida aquifer, only  $\text{Na}^+$  has been the most dominant cation. Just like in other recent studies (Li *et al.*, 2018), ion exchange between  $\text{Ca}^{2+}$  and  $\text{Na}^+$  is a fundamental process controlling groundwater chemistry in the two aquifers.

**Table 16: Hydrogeochemical signatures and ratios for determining geochemical processes in the Kimbiji aquifer**

Sample number	$\text{HCO}_3^- : \text{Cl}^-$	$\text{Na}^+ : \text{Cl}^-$	$\text{Mg}^{2+} : \text{Ca}^{2+}$	$\text{Na}^+ : \text{K}^+$	$\text{Mg}^{2+} + \text{Ca}^{2+} : \text{Na}^+ + \text{K}^+$	$\text{Na}^+ : \text{Ca}^{2+}$	$\text{Ca}^{2+} : \text{SO}_4^{2-} + \text{HCO}_3^-$
S1	2.0	1.4	0.63	10.07	0.29	5.04	0.11
S2	4.2	1.3	0.35	13.24	1.45	0.87	0.32
S4	8.4	7.2	0.10	20.09	0.56	1.87	0.35
S6	13.3	1.2	0.39	12.16	2.55	0.50	0.17
S8	4.2	1.6	1.86	10.86	0.57	4.58	0.07
S10	2.6	1.9	0.41	24.81	0.03	38.73	0.02
S11	0.7	0.5	0.26	11.95	1.46	0.79	0.60
S12	2.4	1.7	0.36	10.31	0.07	17.95	0.04
S13	1.5	0.6	0.19	9.58	1.29	0.83	0.41
S14	9.1	10.7	0.18	12.06	0.11	10.16	0.07
S16	0.3	0.3	0.16	21.36	2.44	0.45	1.53
S17	0.2	1.1	0.14	22.19	0.11	9.68	0.28
S18	0.1	0.8	0.26	23.54	0.31	3.92	0.67
S19	0.2	0.2	0.38	14.48	3.29	0.39	2.00
S21	2.4	1.5	0.18	18.49	0.22	4.99	0.12

Similarities of groundwater and Lake water in the Singida aquifer suggest a high likelihood of groundwater-surface water mixing in the aquifer. Variations of chemical composition and

hydrogeochemical signatures and facies in the two aquifers (Kimbiji and Singida) can be attributed to the geological nature of the groundwater basin as well as the anthropogenic influences on the groundwater systems. This calls for a set of tailored management actions and strategies which take into account the variation in geology and the nature of human activities around the groundwater reservoirs.

Dominance of Sodium in groundwater in the Singida aquifer has been attributed to Cation the exchange mechanism. There is a progressive loss of Ca and Mg ions from the groundwater to the aquifer materials at the expense of  $\text{Na}^+$  and  $\text{K}^+$ , which are constantly being fed into groundwater. This is partly different in the Kimbiji aquifer, where Cation exchange and reverse ion exchange mechanisms have been observed through the CAIs. This justifies the geological contrast between the two aquifers. The enrichment of  $\text{Na}^+$  in the Singida aquifer and part of the Kimbiji aquifer can be explained by the contribution of Na-containing minerals dissolution and/or cation exchange, as opined by other researchers in other study areas (Gao *et al.*, 2020).

**Table 17: Hydrogeochemical signatures and ratios for determining geochemical processes in the Singida aquifer**

Sample Number	$\text{HCO}_3^-$ : $\text{Cl}^-$	$\text{Na}^+$ : $\text{Cl}^-$	$\text{Mg}^{2+}$ : $\text{Ca}^{2+}$	$\text{Na}^+$ : $\text{K}^+$	$\text{Mg}^{2+}$ : $\text{Ca}^{2+}$ : $\text{Na}^+$ + $\text{K}^+$	$\text{Na}^+$ : $\text{Ca}^{2+}$	$\text{Ca}^{2+}$ : $[\text{SO}_4^{2-} + \text{HCO}_3^-]$
S52	1.01	0.78	0.08	9.47	0.77	1.26	0.54
S53	0.99	1.11	0.37	13.96	0.19	6.70	0.15
S54	1.02	1.42	0.12	22.46	0.17	6.14	0.15
S56	1.53	1.08	0.12	22.43	0.63	1.70	0.30
S57	3.25	1.92	0.20	2.88	0.63	1.41	0.33
S58	33.44	15.32	0.15	22.24	0.64	1.73	0.21
S59	0.24	1.13	0.11	90.00	0.05	22.31	0.14
S60	0.29	1.30	0.11	90.34	0.01	113.40	0.02
S61	0.36	0.50	0.20	1.17	0.52	1.23	0.93

The relationship between  $\text{Na}^+$  and  $\text{Cl}^-$  was used to establish the mechanisms which contribute to groundwater salinity as well as establish the atmospheric contribution as it has been carried out by previous studies (Emenike, 2018; Tiwari & Singh 2014). The average  $\text{Na}^+/\text{Cl}^-$  ratio of 1.4 suggests limited contribution from the atmospheric precipitation and reveals that the high levels of these ions are most likely from weathering of rocks and anthropogenic pollution. Five (S11, S13, S16, S18, S19) out of the 15 samples (33%) (Fig. 29) in the coastal Kimbiji showed  $\text{Na}^+/\text{Cl}^- < 1.0$ , indicating limited role of ion exchange from  $\text{Ca}^{2+}$  and  $\text{Mg}^{2+}$ .

However, 67% of the samples which had the  $\text{Na}^+/\text{Cl}^- > 1.0$  underscore the importance of ion exchange as it has been discussed with respect to CAIs. However, this is also an indication that  $\text{Na}^+$  and  $\text{Cl}^-$  are constantly being introduced into groundwater system from such sources as municipal solid waste leachate, septic tank effluent, industrial effluent, and animal and agricultural waste. This takes into account the fact that most shallow wells in the Kimbiji aquifer are dug in the vicinity of residential areas. With regard to the Singida aquifer, only two samples (S52, S61) out of 9 (Fig. 30) had the  $\text{Na}^+/\text{Cl}^- < 1.0$ , indicating a possibility of local recharge from precipitation. However, 71% of the samples indicated the influence of ion exchange and rock weathering as the main mechanisms controlling groundwater chemistry in the Singida aquifer. Nevertheless, there could be a possibility of the influence of anthropogenic activities to groundwater chemistry in the Singida aquifer as well. Sample 58 (S58) from Sepuka demonstrated a dilution behaviour, where, despite having a high Na:Cl ratio, it has relatively low EC. This still indicates that Na is being exchanged from the aquifer materials into the groundwater. This behaviour has also been observed in S4 and S14 in the Kimbiji aquifer.

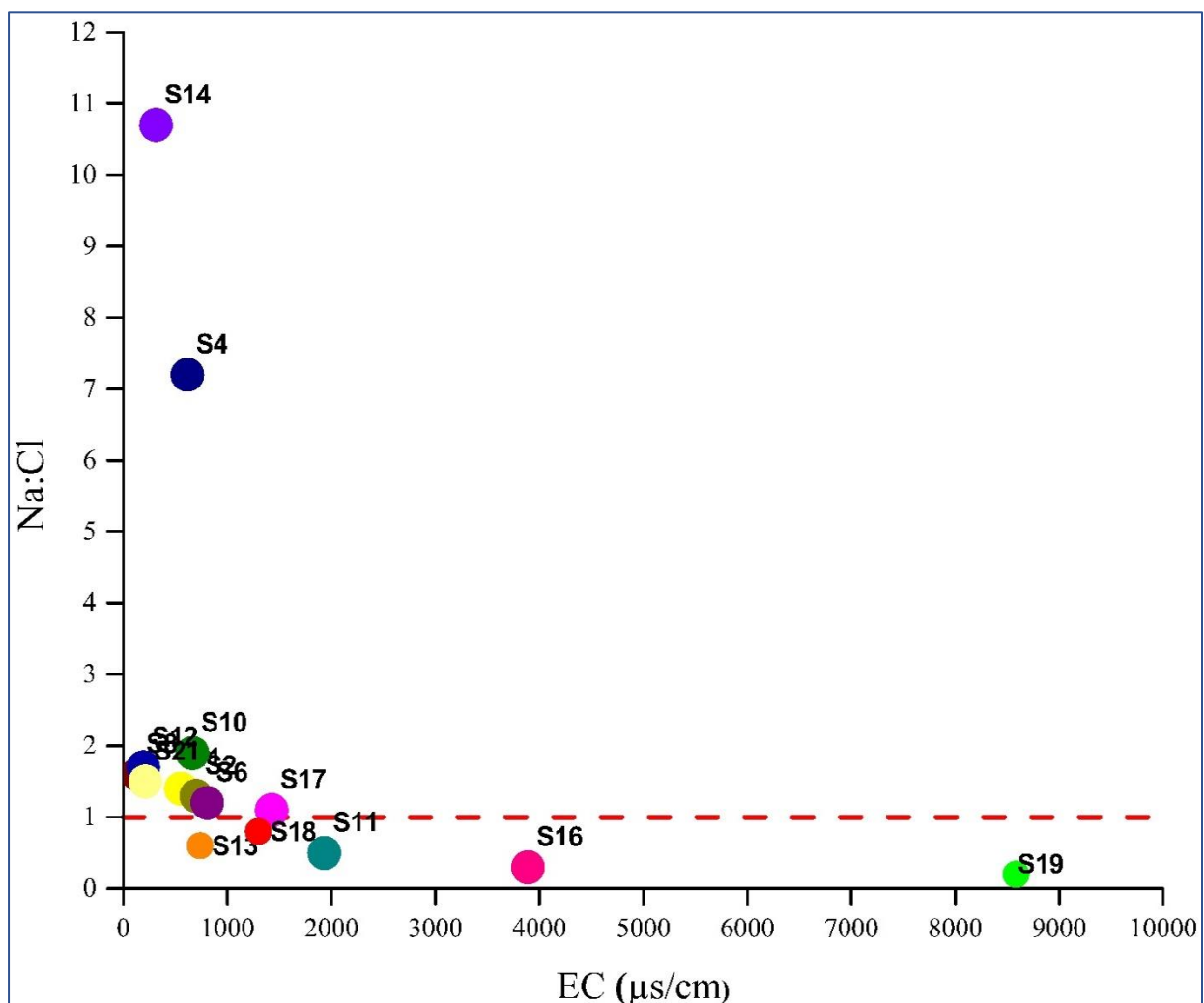


**Figure 29: Na/Cl plot for groundwater samples for the Kimbiji aquifer**

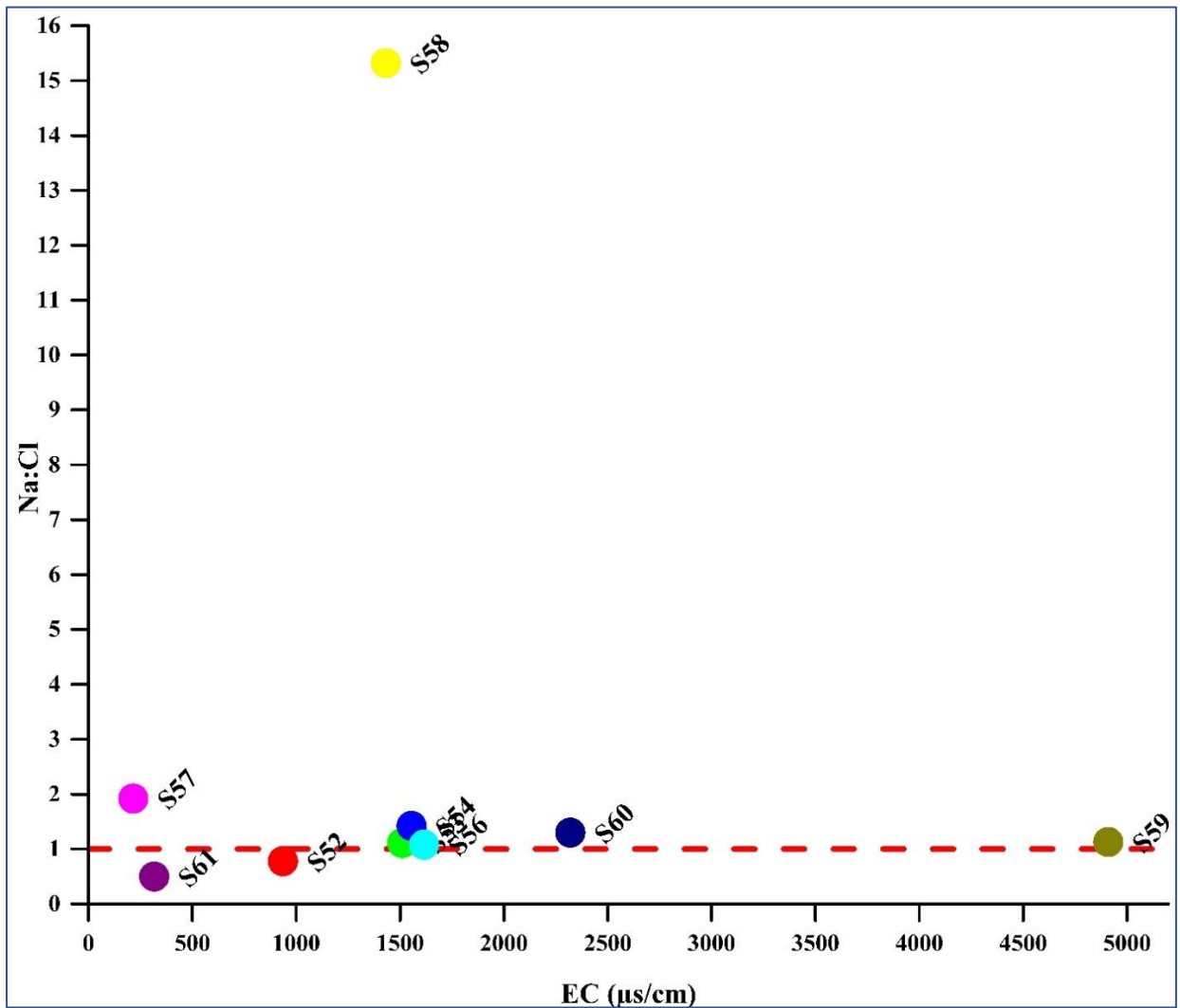


**Figure 30: Na/Cl plot for groundwater samples in the Singida aquifer**

**(iii) Groundwater Residence Time Assessment using Hydrogeochemical Facies**

As per the classification of hydrogeochemical facies in relation to residence time in the Kimbiji aquifer, samples S1, S2, S4, S6, S8, S10, S12, S13, S14, S21 come under type I, relating to recharge water while samples S11, S16, S17, S18, S19 represent discharge water (Type IV) as they exhibit more enrichment of chloride and Sodium, indicating a long residence time and possibly the interference of anthropogenic activities (Table 18). The latter is possibly a representation of regional to sub-regional flows, with the exception of samples drawn from shallow wells that are highly affected by anthropogenic activities in the vicinity of the recharge zones. However, the second group shows a progressive enrichment of minerals along the flow path.

**Table 18: Hydrogeochemical facies of the Kimbiji aquifer in relation to Residence time of groundwater**

Residence time of water	Types	Hydrogeochemical Facies	Water type	Topography	Sample Number
Initial Stage (New and Young Water)	I	$\text{HCO}_3^- + \text{CO}_3^{2-} > \text{SO}_4^{2-} > \text{Cl}^-$	Recharge	High	S1, S2, S4, S6, S8, S10, S12, S13, S14, S21
Duration of Water Stay increases	II	$\text{SO}_4^{2-} > \text{Cl}^- > \text{HCO}_3^-$	-	-	
Still increasing duration of Water Stay	III	$\text{Cl}^- > \text{SO}_4^{2-} > \text{NO}_3^- > \text{HCO}_3^-$	-	-	
Final Stage (Older water)	IV	$\text{Cl}^- > \text{SO}_4^{2-} > \text{HCO}_3^-$	Discharge	Low	S11, S16, S17, S18, S19

**Table 19: Hydrogeochemical facies of the Singida aquifer in relation to Residence time of groundwater**

Residence time of water	Types	Hydrogeochemical Facies	Water type	Topography	Sample Number
Initial Stage (New and Young Water)	I	$\text{HCO}_3^- + \text{CO}_3^{2-} > \text{SO}_4^{2-} > \text{Cl}^-$	Recharge	High	S52, S54, S56, S57, S58
Duration of Water Stay increases	II	$\text{SO}_4^{2-} > \text{Cl}^- > \text{HCO}_3^-$	-	-	
Still increasing duration of Water Stay	III	$\text{Cl}^- > \text{SO}_4^{2-} > \text{NO}_3^- > \text{HCO}_3^-$	-	-	
Final Stage (Older water)	IV	$\text{Cl}^- > \text{SO}_4^{2-} > \text{HCO}_3^-$	Discharge	Low	S53, S59, S60, S61

Identification of groundwater residence time in the Singida aquifer revealed that all the lakes are the discharge zones, located in low topography with groundwater having travelled long distances as depicted in samples (S53, S59, S60, S61). The other samples (S52, S54, S56, S57, S58) depicted the presence of young water, having travelled short distances. However, that is a glimpse of the

groundwater mixing. This also indicates that there is a recharge zone within the vicinity of the wellfields in the Singida aquifer.

However, samples drawn from shallow boreholes (e.g. S57) are highly affected by anthropogenic activities. This is manifested by high level of nitrate concentration in water, followed by bicarbonate ions, indicating that the well is locally recharged. Therefore, the water in the Singida aquifer falls into two groups (i.e. group I and group IV) as depicted in Table 19. Nevertheless, the progressive enrichment of Sodium in surface and groundwater in the Singida aquifer indicates a possibility of long travels as well as a strong base ion exchange between the aquifer materials and the groundwater.

#### 4.1.4 Statistical Analyses of Hydrogeochemical Parameters

The correlation analysis of hydrogeochemical parameters summarized in Table 20 suggests that EC and TDS are positively correlated with  $\text{Cl}^-$  and  $\text{NO}_3^-$ . Moreover,  $\text{NO}_3^-$  occur together with  $\text{Ca}^{2+}$ ,  $\text{Mg}^{2+}$  and  $\text{Cl}^-$ . It is also evident that Na and K occur together ( $r=0.9$ ) while  $\text{Cl}^-$ ,  $\text{SO}_4^{2-}$  are negatively correlated with pH as shown in Table. In addition,  $\text{NO}_3^-$  has not shown any correlation with pH altogether but there is slightly weak correlation ( $r=0.4$ ) between  $\text{HCO}_3^-$  and pH. It can as well be seen that  $\text{Cl}^-$  and  $\text{NO}_3^-$  are correlated, suggesting possible anthropogenic pollution of groundwater in some areas of the Kimbiji aquifer. It was also observed that  $\text{NO}_3^-$ ,  $\text{HCO}_3^-$ ,  $\text{SO}_4^{2-}$  and  $\text{Cl}^-$  are responsible for the salt concentrations observed in the groundwater in the Kimbiji aquifer. That is explained by their relatively strong correlations with TDS (Table 20).

**Table 20: Correlation matrix of hydrogeochemical parameters for the Kimbiji aquifer**

	pH	EC	TDS	$\text{Na}^+$	$\text{K}^+$	$\text{Ca}^{2+}$	$\text{Mg}^{2+}$	$\text{Cl}^-$	$\text{SO}_4^{2-}$	$\text{NO}_3^-$	$\text{HCO}_3^-$
pH	1.0										
EC	-0.1	1.0									
TDS	-0.1	<b>1.0</b>	1.0								
$\text{Na}^+$	-0.4	<b>0.8</b>	<b>0.8</b>	1.0							
$\text{K}^+$	-0.3	<b>0.9</b>	<b>0.9</b>	<b>0.9</b>	1.0						
$\text{Ca}^{2+}$	0.0	<b>1.0</b>	<b>1.0</b>	<b>0.7</b>	<b>0.8</b>	1.0					
$\text{Mg}^{2+}$	-0.1	<b>1.0</b>	<b>1.0</b>	<b>0.7</b>	<b>0.8</b>	<b>1.0</b>	1.0				
$\text{Cl}^-$	-0.2	<b>1.0</b>	<b>1.0</b>	<b>0.8</b>	<b>0.9</b>	<b>1.0</b>	<b>1.0</b>	1.0			
$\text{SO}_4^{2-}$	-0.4	0.5	0.5	<b>0.7</b>	<b>0.7</b>	0.4	0.3	0.5	1.0		
$\text{NO}_3^-$	0.0	<b>0.9</b>	<b>0.9</b>	<b>0.6</b>	<b>0.7</b>	<b>0.9</b>	<b>0.8</b>	<b>0.8</b>	0.4	1.0	
$\text{HCO}_3^-$	0.4	<b>0.6</b>	<b>0.6</b>	0.2	0.4	<b>0.6</b>	<b>0.6</b>	0.5	0.0	0.5	1.0



**Table 21: Correlation matrix of hydrogeochemical parameters for the Singida aquifer**

	pH	EC	TDS	Na <sup>+</sup>	K <sup>+</sup>	Ca <sup>2+</sup>	Mg <sup>2+</sup>	Cl <sup>-</sup>	SO <sub>4</sub> <sup>2-</sup>	NO <sub>3</sub> <sup>-</sup>	HCO <sub>3</sub> <sup>-</sup>	CO <sub>3</sub> <sup>2-</sup>
pH	1.0											
EC	<b>0.8</b>	1.0										
TDS	<b>0.8</b>	<b>1.0</b>	1.0									
Na <sup>+</sup>	<b>0.9</b>	<b>1.0</b>	1.0	1.0								
K <sup>+</sup>	0.0	-0.2	-0.2	-0.1	1.0							
Ca <sup>2+</sup>	0.0	0.0	0.0	-0.2	-0.2	1.0						
Mg <sup>2+</sup>	0.1	-0.1	0.0	-0.2	0.2	<b>0.7</b>	1.0					
Cl <sup>-</sup>	<b>0.8</b>	<b>0.9</b>	<b>0.9</b>	<b>1.0</b>	-0.1	-0.2	-0.3	1.0				
SO <sub>4</sub> <sup>2-</sup>	<b>0.7</b>	<b>0.7</b>	<b>0.7</b>	<b>0.6</b>	-0.5	0.4	0.2	0.5	1.0			
NO <sub>3</sub> <sup>-</sup>	0.1	0.2	0.2	0.2	-0.4	0.3	0.2	0.0	0.4	1.0		
HCO <sub>3</sub> <sup>-</sup>	0.5	0.4	0.4	0.2	-0.1	<b>0.7</b>	<b>0.8</b>	0.1	<b>0.7</b>	0.5	1.0	
CO <sub>3</sub> <sup>2-</sup>	<b>0.7</b>	0.5	0.5	<b>0.6</b>	-0.2	-0.4	-0.5	<b>0.6</b>	0.5	0.0	0.0	1.0

As for the Singida aquifer, Na and Cl are strongly correlated, indicating that the two chemical groundwater constituents occur together (Table 21). The correlation between Cl and pH explains the possible anthropogenic contamination of water in the Singida aquifer. Whenever Mg<sup>2+</sup> occurs in groundwater in the Singida aquifer, it does so in tandem with HCO<sub>3</sub><sup>-</sup>. This has been shown by a strong correlation between the two ions (r=0.8). This trend has also been observed between Ca<sup>2+</sup> and HCO<sub>3</sub><sup>-</sup> (r=0.7). Generally, SO<sub>4</sub><sup>2-</sup> and Cl<sup>-</sup> are responsible for the salt concentrations observed in the groundwater in Singida aquifer. That is explained by their relatively strong correlations with TDS (Table 14) unlike NO<sub>3</sub><sup>-</sup>, HCO<sub>3</sub><sup>-</sup> and CO<sub>3</sub><sup>2-</sup> which have relatively weak correlation with TDS.

The negative correlation between TDS and pH (r=-0.1) explains the fact that the salt concentration in the groundwater in the Kimbiji aquifer is mainly due to dissolution of the most soluble aquifer materials and not necessarily from the acidic environment. Moreover, the strong correlation between TDS and pH (r=0.8) is an indication that salt in the groundwater is not possibly related to dissolution of the aquifer materials, but rather are a result of the acidic environment in the Singida aquifer. The two scenarios are supported by the difference in the aquifer materials constituting the two study areas, one being consolidated, fractures aquifer (Singida) and the other one (Kimbiji) being a porous, unconsolidated sedimentary aquifer.

Four main principal components influence the water chemistry of groundwater within the Kimbiji aquifer, which accounted for 89% of the total variance in the hydrogeochemical data (Table 22). Five principal components influence the water chemistry in the Singida aquifer, and they account for 98% of the total variance (Table 23). For Kimbiji aquifer, PC1 delineates the main natural processes (water-rock interactions) through which groundwater within the basin acquires its chemical characteristics, within some glimpse of anthropogenic activities interfering the groundwater system. Component 3 delineates the inputs of agricultural activities into the

groundwater system (Koh *et al.*, 2007; Al-Ahmadi, 2013) while Component 4 delineates the prevalence of natural recharge as bicarbonates predominates. However, PC1 in the Kimbiji aquifer depicts Ca and Mg as the most important cations as compared to Na and K. It should be noted that for the Kimbiji aquifer PCA, PC3 has a greater explanatory strength than PC2, as explained by the high eigenvalue variance (1.45) as presented in Table 22.

**Table 22: Principal Components Analysis of the Kimbiji aquifer hydrogeochemical parameters**

Parameter	Principal Components					
	PC1	PC3	PC2	PC4	PC5	PC6
pH	-0.04	-0.19	<b>0.96</b>	0.19	-0.1	0.02
EC	<b>0.92</b>	0.22	-0.04	0.21	0.23	0.06
TDS	<b>0.92</b>	0.21	-0.05	0.21	0.23	0.05
Na <sup>+</sup>	<b>0.57</b>	0.39	-0.23	0.04	0.68	0.07
K <sup>+</sup>	<b>0.73</b>	0.43	-0.13	0.12	0.45	-0.13
Ca <sup>2+</sup>	<b>0.93</b>	0.21	0.01	0.24	0.1	0.08
Mg <sup>2+</sup>	<b>0.95</b>	0.07	-0.03	0.24	0.13	-0.03
Cl <sup>-</sup>	<b>0.93</b>	0.19	-0.08	0.16	0.24	0
SO <sub>4</sub> <sup>2-</sup>	0.24	<b>0.93</b>	-0.2	-0.01	0.16	0.04
NO <sub>3</sub> <sup>-</sup>	<b>0.84</b>	0.15	0.1	0.07	0.08	0.49
HCO <sub>3</sub> <sup>-</sup>	0.43	-0.01	0.27	<b>0.86</b>	0.04	0.02
<b><i>Eigenvalue</i></b>	<b>6.16</b>	<b>1.45</b>	<b>1.12</b>	<b>1.03</b>	0.89	0.28
<b><i>Proportion Variance</i></b>	0.56	0.13	0.1	0.09	0.08	0.03
<b><i>Cumulative Variance</i></b>	0.56	0.69	0.79	0.89	0.97	0.99
<b><i>Proportion Explained</i></b>	0.56	0.13	0.1	0.09	0.08	0.03
<b><i>Cumulative Proportion</i></b>	0.56	0.7	0.8	0.89	0.97	1

As for the Singida aquifer PCA PC5 has a higher explanatory strength (1.12 eigenvalue variance) than PC 3 and PC4 (Table 23). The ss loadings reflect the contribution of each component into the variables. It can be shown that, Na and Cl are delineated by PC1, being responsible for groundwater mineralization in the aquifer (Table 16). The PC2 and PC5 delineate natural mechanisms while PC4 portrays the contribution of anthropogenic activities in groundwater mineral constituents.

**Table 23: Principal Components Analysis of the Singida aquifer hydrogeochemical parameters**

Parameter	Principal Components					
	PC1	PC2	PC5	PC3	PC4	PC6
pH	0.8	0.21	0.45	0.05	0.03	0.31
EC	<b>0.98</b>	0.1	0.12	-0.07	0.06	-0.08
TDS	<b>0.98</b>	0.1	0.11	-0.07	0.06	-0.09
Na <sup>+</sup>	<b>0.96</b>	-0.1	0.23	-0.05	0.11	0.04
K <sup>+</sup>	-0.06	-0.01	-0.09	<b>0.97</b>	-0.21	0.01
Ca <sup>2+</sup>	-0.08	<b>0.89</b>	-0.17	-0.26	-0.02	-0.25
Mg <sup>2+</sup>	-0.1	<b>0.91</b>	-0.21	0.26	0.12	0.17
Cl <sup>-</sup>	<b>0.98</b>	-0.15	0.13	-0.01	-0.04	0.04
SO <sub>4</sub> <sup>2-</sup>	<b>0.55</b>	0.47	<b>0.51</b>	-0.35	0.13	-0.25
NO <sub>3</sub> <sup>-</sup>	0.08	0.23	0.02	-0.23	<b>0.94</b>	0
HCO <sub>3</sub> <sup>-</sup>	0.24	<b>0.89</b>	0.18	-0.04	0.33	0.07
CO <sub>3</sub> <sup>2-</sup>	0.42	-0.3	<b>0.85</b>	-0.11	0.01	0.03
<b>Eigenvalue</b>	<b>4.99</b>	<b>2.88</b>	<b>1.38</b>	<b>1.28</b>	<b>1.09</b>	0.27
<b>Proportion variance</b>	0.42	0.24	0.12	0.11	0.09	0.02
<b>Cumulative variance</b>	0.42	0.66	0.77	0.88	0.97	0.99
<b>Proportion Explained</b>	0.42	0.24	0.12	0.11	0.09	0.02
<b>Cumulative Proportion</b>	0.42	0.66	0.78	0.89	0.98	1

#### 4.1.5 Characterization of Groundwater Evolution and Provenance using Stable Isotopes

Oxygen isotopes in boreholes ranged from -2.36 to -6.77‰ with average of -3.47‰ whereas deuterium isotopes ranged from -11.05 to -48.73 with an average value of -17.26 for the Kimbiji aquifer (Table 24). Samples from rivers had oxygen isotopes ranging from -2.36 to -3.21‰ and deuterium isotopes ranged from -17.45 to -11.05‰. Rainfall in the Kimbiji aquifer had -2.85 and -12.52‰ composition of oxygen and deuterium isotopes, respectively. For the Singida aquifer, the Oxygen isotopes in boreholes ranged from -4.67 to -3.21‰ and -28.33 to -15.08‰ for deuterium (Table 25). The lake water had oxygen and deuterium isotopes ranging between -3.23 and -2.45‰, and -18.74 and -16.68‰ respectively. Rainwater sampled from the Singida aquifer had oxygen isotope concentration of -1.5‰ while deuterium was found to be 6.44‰. The rainfall in Singida was found to be more isotopically depleted than the groundwater and surface water samples. This is contrary to the isotopic composition of the rainfall in the Kimbiji aquifer, which is relatively enriched. The position of rainwater above the LMWL in the Singida aquifer is possibly related to

the condensation effect which is controlled by regional air circulation. Reportedly, such a phenomenon happens due to low humidity in the vapor as reported by Praamsma *et al.* (2009) and Abiye (2013).

**Table 24: Stable Isotope Results and Deuterium Excess Analysis for the Kimbiji aquifer**

Sampling Point	Type	$\delta^{18}\text{O} \text{‰}$	$\delta^2\text{H} \text{‰}$	Location (village/Street)	Elevation	d-excess
		(VSMOW)	(VSMOW)			
POINT 1	Borehole	-3.31	-17.56	Mkwajuni	7	8.92
POINT 2	Borehole	-3.12	-15.59	Monduli/Mkwajuni	6	9.37
POINT 3	Rain	-2.85	-12.52	Kifurukwe	26	10.28
POINT 4	Borehole	-3.41	-16.82	Kisarawe II	42	10.46
POINT 5	River	-2.63	-14.97	Vumilia Ukooni	35	6.07
POINT 6	Borehole	-3.63	-15.76	Yaleyale Puna	25	13.28
POINT 7	River	-3.21	-17.45	Kobanya-Kimbiji	5	8.23
POINT 8	Borehole	-3.64	-16.99	Amani Gomvu/Ninondo	49	12.13
POINT 10	Borehole	-3.45	-14.31	Kurungu Mkuranga	67	13.29
POINT 11	Borehole	-3.48	-16.75	Mkuranga Mizani	134	11.09
POINT 12	Borehole	-3.78	-17.52	Kisemvule	84	12.72
POINT 13	Borehole	-3.63	-16.68	Mwandege Nguzo Tatu	70	12.36
POINT 14	Borehole	-3.4	-15.55	Mbagala Kizuiani	64	11.65
POINT 15	River	-2.8	-12.51	Kizinga (Mbagala KTM)	6	9.89
POINT 16	Borehole	-3.48	-15.11	Vasco- Pugu Kajiungeni	153	12.73
POINT 17	Borehole	-3.43	-16.71	Kisarawe- Kazimzumbwi	206	10.73
POINT 18	Borehole	-3.36	-16.33	Pugu- Kinyamwezi	84	10.55
POINT 19	Borehole	-3.14	-15.57	Chanika- Msumbiji	114	9.55
POINT 20	River	-2.36	-11.05	Namanga-Mvuti	75	7.83
POINT 21	Borehole	-3.99	-17.98	Mkamba	49	13.94

**Table 25: Stable Isotope Results and Deuterium Excess Analysis for the Singida aquifer**

Sampling Point	Type	$\delta^{18}\text{O} \text{‰}$	$\delta^2\text{H} \text{‰}$	Location (village/Street)	Elevation	d-excess
		(VSMOW)	(VSMOW)			
POINT 52	Borehole	-3.99	-20.87	Kibaoni-Majengo	1519	11.05
POINT 53	Lake	-3.14	-17.38	Monangi/Kindai	1481	7.74
POINT 54	Borehole	-4.66	-25.34	Mwankoko	1448	11.94
POINT 55	Rain	-1.5	6.49	Singida	1517	18.49
POINT 56	Borehole	-4.67	-28.33	Irao	1503	9.03
POINT 57	Borehole	-4.23	-22.01	Puma	1606	11.83
POINT 58	Borehole	-3.5	-20.46	Sepuka	1486	7.54
POINT 59	Lake	-3.23	-18.74	Singidani	1486	7.1
POINT 60	Lake	-2.45	-16.68	Inkhanoda	1601	2.92
POINT 61	Borehole	-3.21	-15.08	Kititimo	1569	10.6

The isotopic ratios of  $\delta^2\text{H}$  and  $\delta^{18}\text{O}$  from the two aquifers (Kimbiji and Singida) were plotted in Fig. 31 and Fig. 32 in relation to the GMWL, and LMWL derived from the GNIP data from the Dar es Salaam station. In the two study areas, surface water samples plotted below the GMWL as well as the LMWL. In the Kimbiji aquifer, the river water samples plotted below the GMWL and the LMWL, whereas in the Singida aquifer, all the lake water samples plotted below the two reference lines. Moreover, in the Singida and Kimbiji aquifers, a handful of groundwater samples plotted below the GMWL, while many samples in the Singida aquifer plotted along the two reference lines. A comparison of stable isotopes from the study aquifers with GMWL shows local deviations from the world average.

The slopes with values less than 8 (i.e., samples that plotted below the GMWL) indicated greater moisture losses through evaporation while slopes greater than 8 indicate moisture recycling. Evaporation moisture losses occur due to either low rainfall, hot climates or for both reasons simultaneously, which is characteristic of the two study areas. Depending on their affiliation with their geographic areas, individual groups of groundwater and river samples were observed to be located along the LMWL.

Generally, the samples that plotted above the LMWL indicate rapid infiltration of recharge water before evaporation, while samples that plotted below the LMWL are essentially subjected to evaporation prior to recharge. Rapid infiltration therefore occurred in the highly porous vadose zone for the Kimbiji aquifer and the highly weathered regolith of the hard rock Singida aquifer.

Comparison of isotopic composition from borehole, rivers and rainfall showed that generally boreholes in the Kimbiji aquifer had depleted isotopic values and enriched isotopic values were in samples from rivers (Fig. 31). The depletion was prominently so in the deep boreholes, indicating a limited influence of evaporation during groundwater recharge. This is an implication that groundwater in deep boreholes is not locally recharged. This is an important signal of the presence of the subregional to regional flow systems in the Kimbiji aquifer.

All the groundwater samples which draw parallel to the GMWL highlight that there is no strong evidence to prove that they were subjected to evaporation prior to infiltration and later recharging the aquifer. This possibly explains the fact that recharge occurred in a different climatic condition. This is prominently so for the semi-arid Singida aquifer, reports (Carreira *et al.*, 2014). Groundwater and surface water have been observed to have variations in isotopic composition, reflecting enrichment and depletion of stable isotopes. Groundwater was considerably depleted while surface water (lakes, rivers, dam) was enriched, depicting the interplay of moisture recycling and evaporation respectively.

Regarding enriched water samples, evaporation was one of the factors causing enrichment. Normally, evaporation is higher in open water bodies such as rivers compared to groundwater. On the other hand, groundwater samples from shallow boreholes were very close to the Global Meteoric Water Line (GMWL) and the Local Meteoric Water Line (LMWL), reflecting that most of them possibly originate from local rainfall (i.e., Meteoric water). Precipitation originating from higher altitude is more isotopically depleted in  $\delta^2\text{H}$  and  $\delta^{18}\text{O}$  than precipitation at lower altitudes. Therefore, these stable isotopic ratios are useful in evaluating the precipitation source areas of recharge to an aquifer (Kebede & Travi, 2012; Kamtchueng *et al.*, 2015).

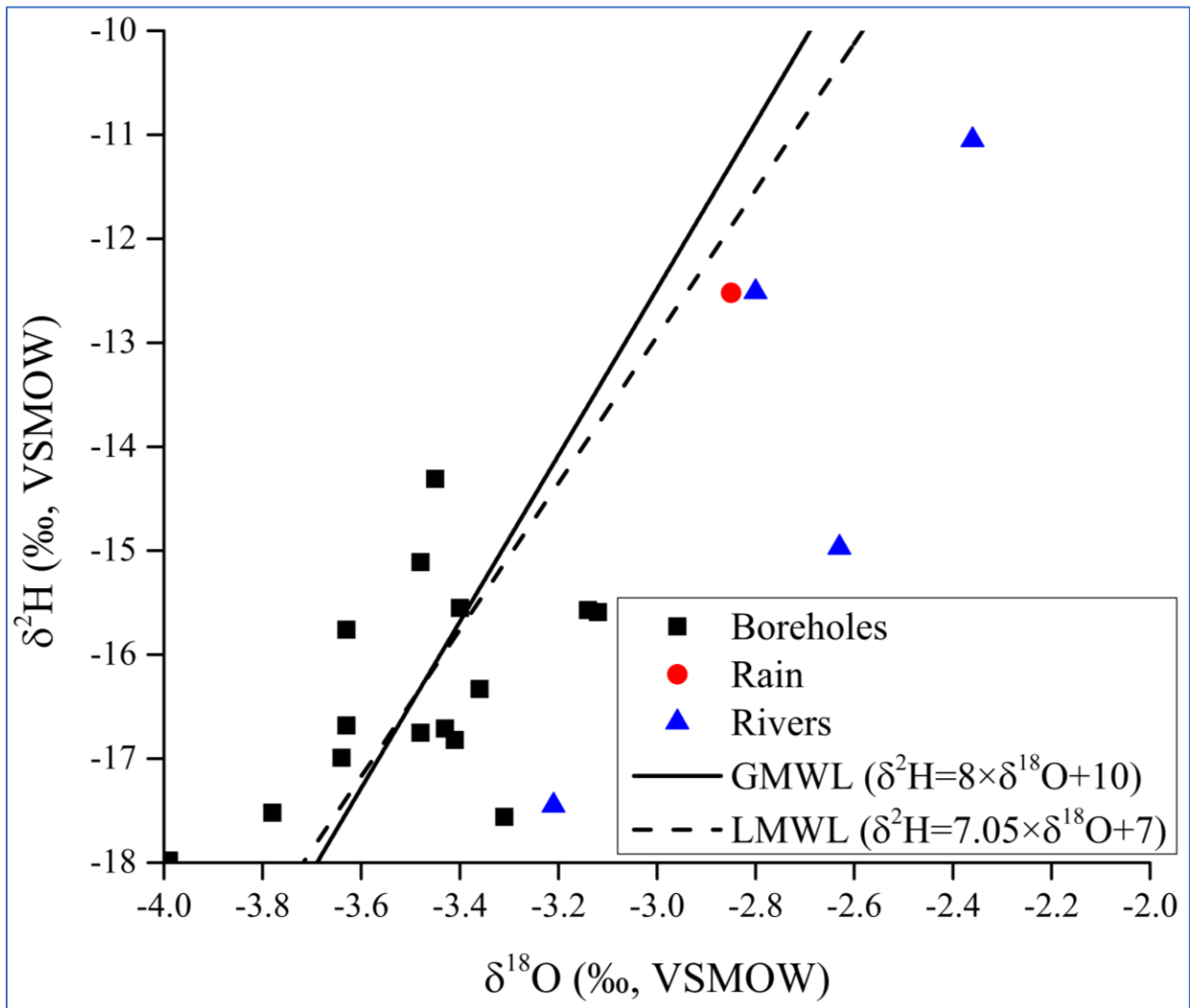
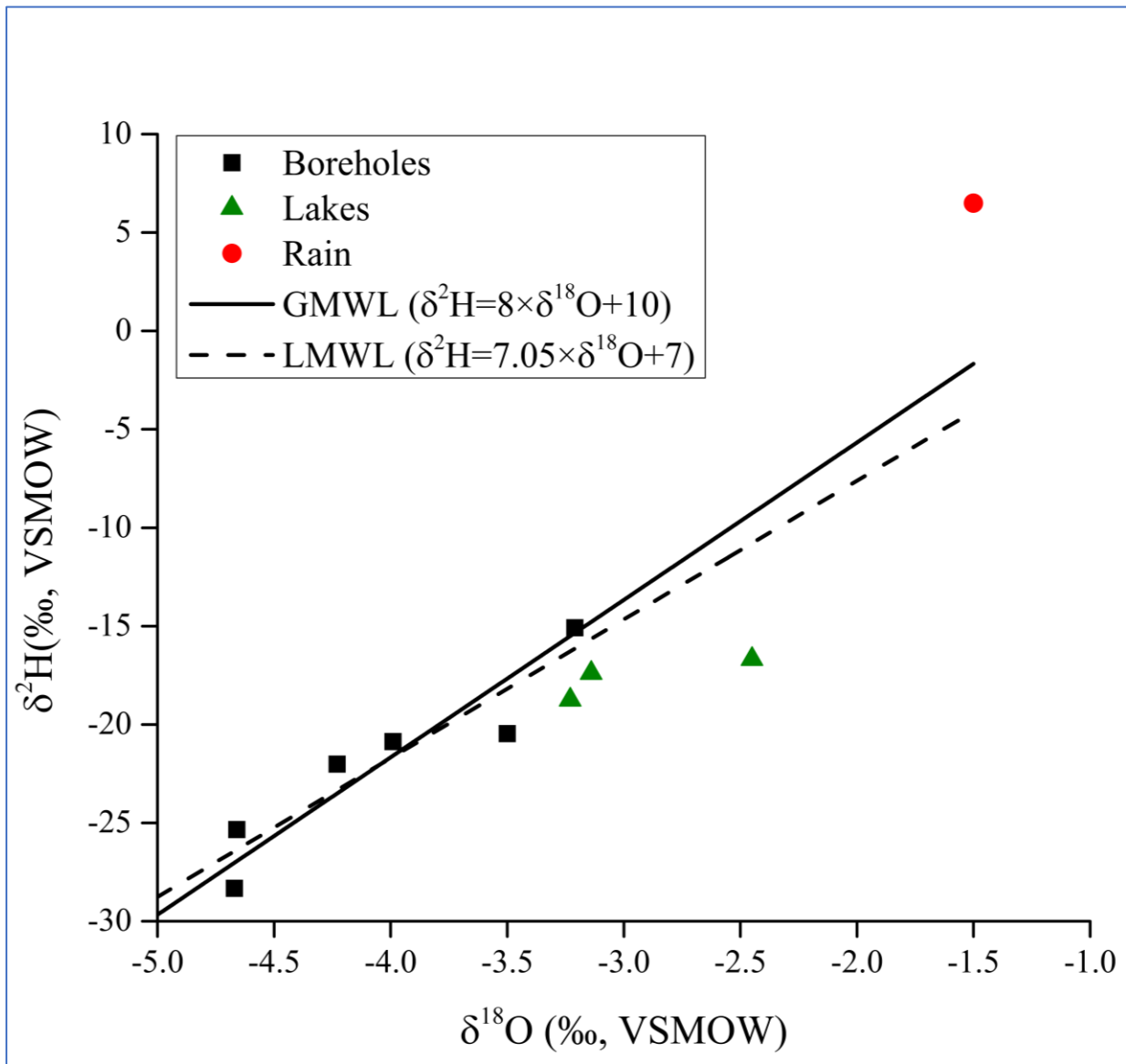


Figure 31: A plot of  $\delta^{2}\text{H}$  versus  $\delta^{18}\text{O}$  for the Kimbiji aquifer



**Figure 32: A plot of  $\delta^2\text{H}$  versus  $\delta^{18}\text{O}$  for the Singida aquifer**

**(i) Deuterium Excess**

The plots in Fig. 33 and Fig. 34 present the results of deuterium excess in the Kimbiji and Singida aquifers, respectively, with letters B, S, R and L representing groundwater, river, rainfall and lake samples in that order. The number beside the letter is a sample number as presented in Tables 24 and 25. Deuterium excess analysis for the Kimbiji and Singida aquifers confirmed that all open water bodies (rivers and lakes) have their deuterium excess less than 10‰, which is below the intercept of the GMWL and below 8‰, which is below the LMWL. This phenomenon signifies the influence of evaporation. This implies that the water in the open water bodies is highly enriched with heavy stable isotopes of water as compared to groundwater in the two study areas. Apart from two river samples in the Kimbiji aquifer which had d-excess values less than 8‰, the other samples (rivers and boreholes) were observed to have d-excess values in the range of 8‰ to around 14‰. This is yet another confirmation that the two sources of water are fed by local rainfall in the Kimbiji



aquifer. In the Singida aquifer, d-excess was in the range of 2.92 to 18.49, with rainwater showing the highest depletion of heavy stable isotopes of water. Using d-excess, the other samples confirmed the presence of mixed water sources, with indications of regional flow systems feeding the aquifer and the lakes. However, the contribution of local rainfall has also been noted through d-excess analysis. All the groundwater samples with high d-excess (>10‰) indicate that local rainfall contributes to recharge the aquifer.

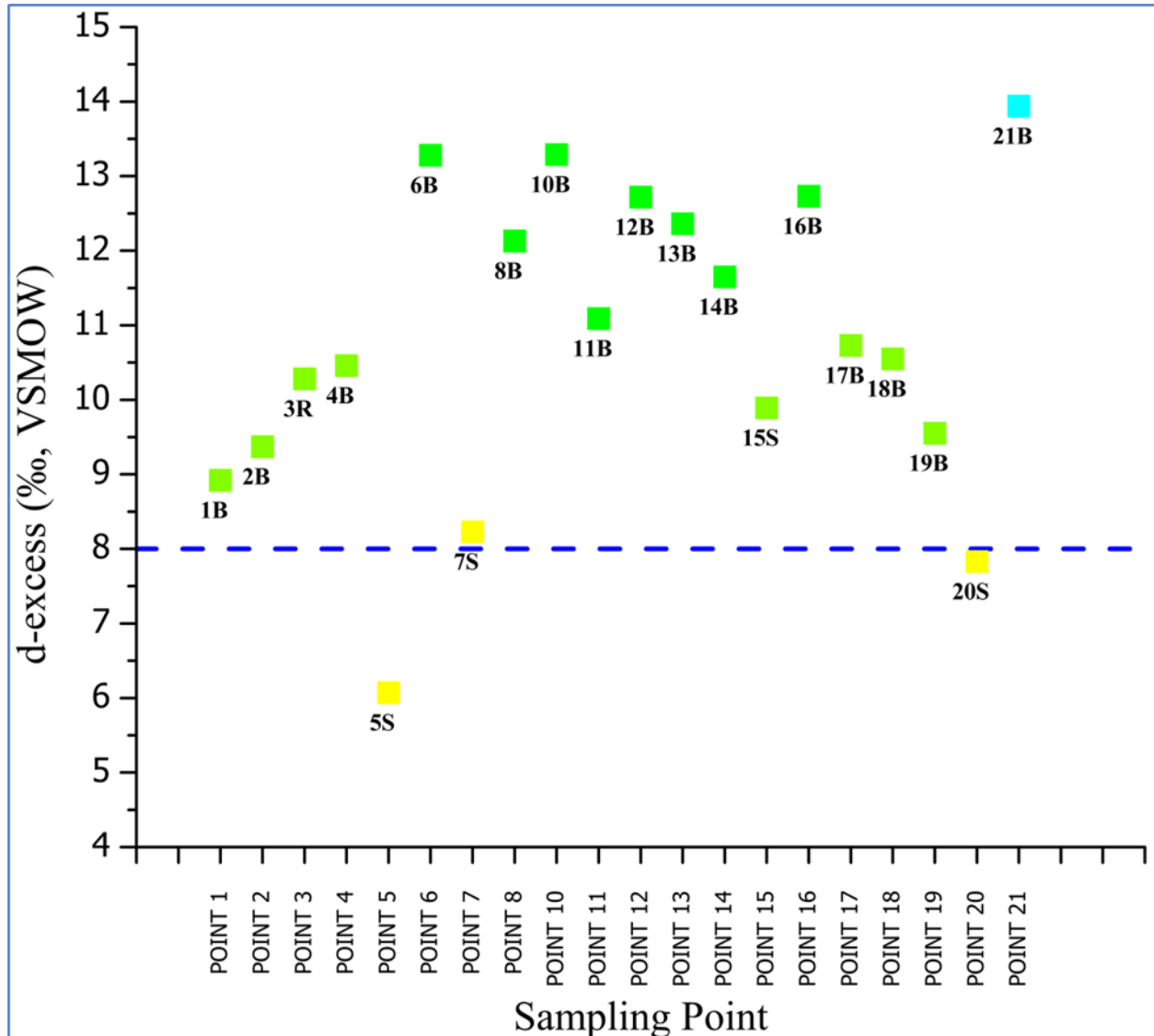
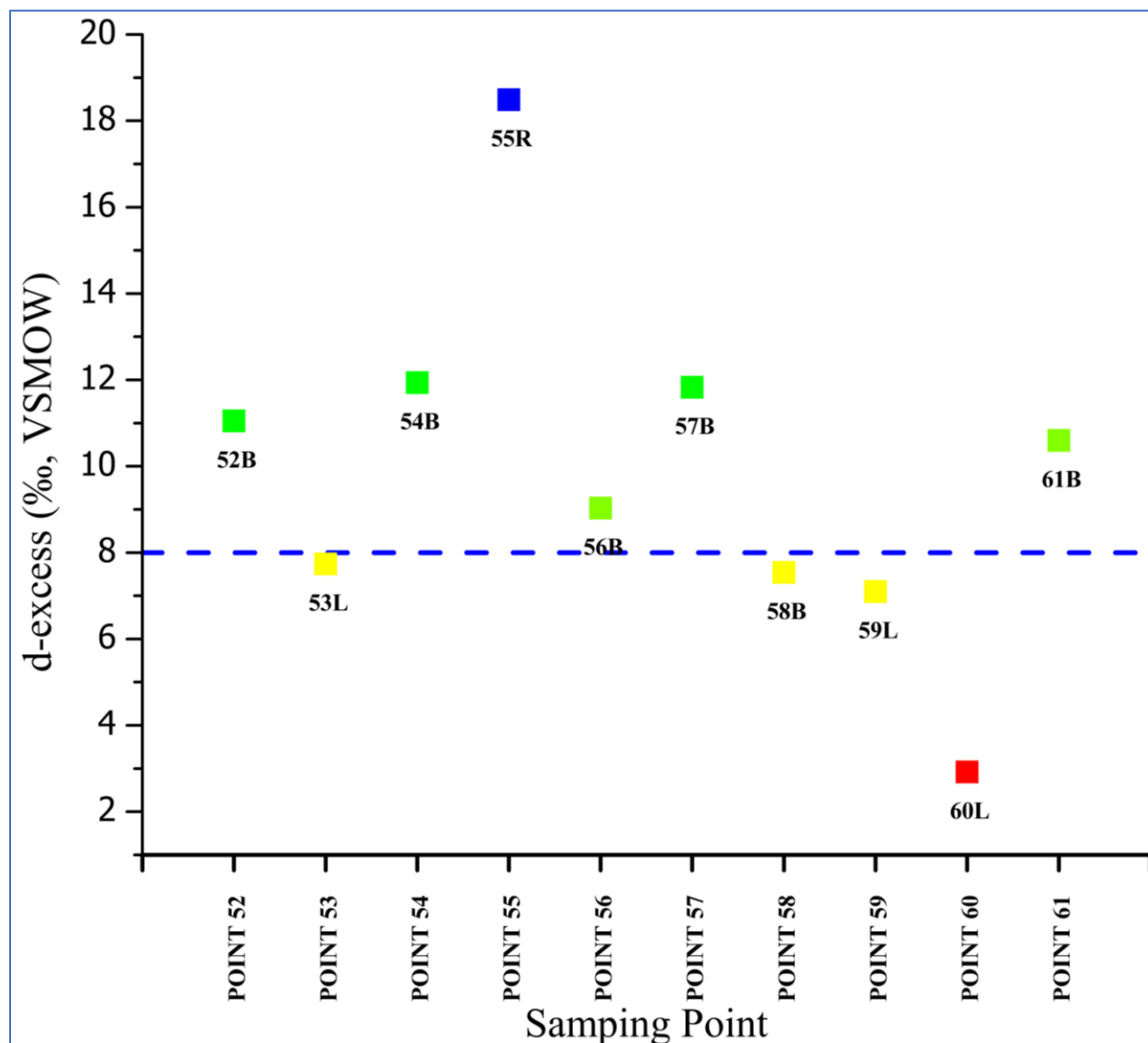


Figure 33: A plot of deuterium excess for the Kimbiji aquifer



**Figure 34:** A plot of deuterium excess for the Singida aquifer

The two plots of deuterium excess versus  $\delta^{18}\text{O}$  for the Kimbiji aquifer (Fig. 35) and Singida aquifer (Fig. 36) present the combination of d-excess with the two plots of deuterium excess versus  $\delta^{18}\text{O}$  to depict climatic influence on groundwater recharge and evolution in the two study areas. The occurrence of lower d-excess values at higher  $\delta^{18}\text{O}$  values for groundwater samples connotes evaporative enrichment from regional circulation, while high d-excess at low  $\delta^{18}\text{O}$  values is an indication of isotopic depletion. This is yet another sign of rapid infiltration of rainfall towards recharging groundwater as well as recharge occurring in areas where evaporation is highly limited, and the rainfall intensity is high. The heavier rainfall is more isotopically depleted in composition than the light intensity rainfall during the dry season as the air moisture is subjected to less condensation process. It can be observed that in both study areas, groundwater samples have attained red colours, signifying that they have high d-excess values and lower  $\delta^{18}\text{O}$  values. All the open water bodies have green to blue colours, indicating that they have low d-excess values but high  $\delta^{18}\text{O}$  values. The rainfall samples have relatively less negative isotopic values. This is an

indication that the moisture source which resulted into the rainfall event had relatively short travel distance. This has been prominently so in the Singida aquifer (Fig. 36).

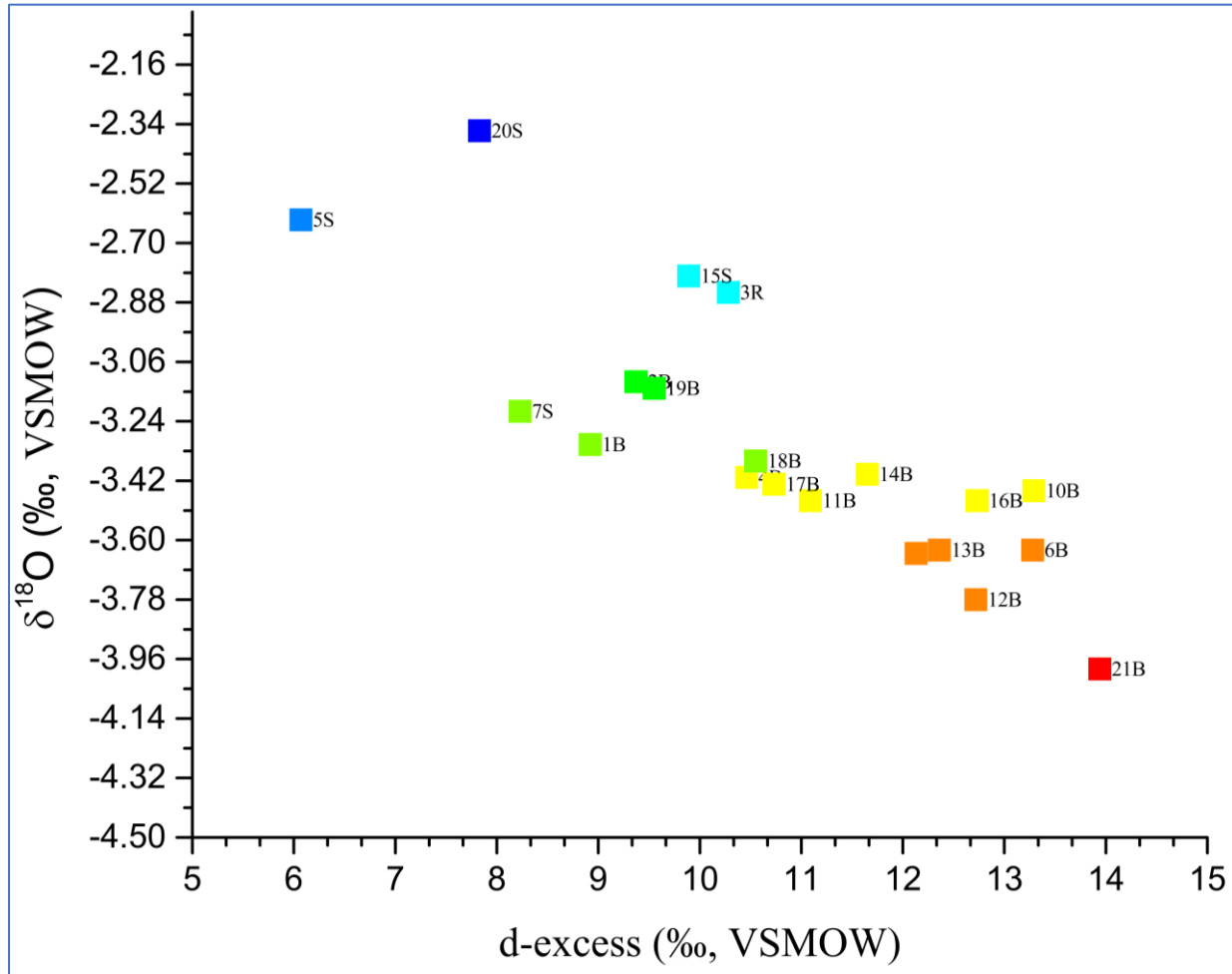
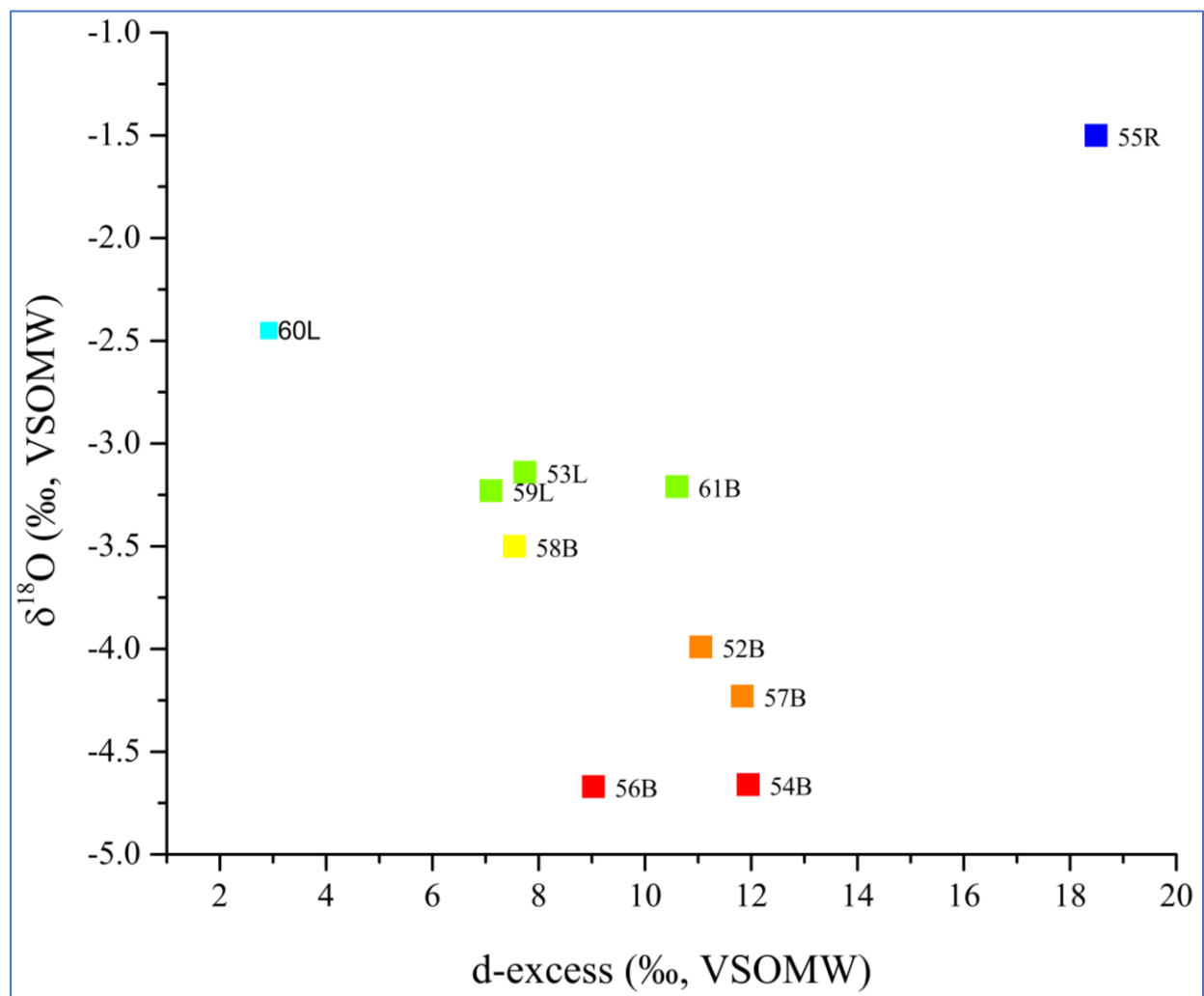


Figure 35: A plot of deuterium excess versus  $\delta^{18}\text{O}$  for the Kimbiji aquifer



**Figure 36: A plot of deuterium excess versus  $\delta^{18}\text{O}$  for the Singida aquifer**

Both evaporative and moisture circulation processes influence groundwater recharge in the two study areas. The former has been indicated by enriched groundwater samples while the latter is demonstrated by depleted groundwater samples. Greater deviations from the meteoric lines are associated with higher evaporation experienced during moisture transfers in air masses and are linked to low humidity conditions, which lead to kinetic fractionation. Accordingly, the higher the humidity, the lower the evaporation rate (Oiro *et al.*, 2018). All the depleted isotope values plotting close to the LMWL indicate the limited influence of evaporation in the recharge process, thus implying that groundwater recharge originated from meteoric waters (Rowley *et al.*, 2001). This has been observed in both study areas.

The possibility of groundwater-surface water interaction is equally evident. In the Kimbiji aquifer, rivers have been observed to have isotopically enriched water samples. Equally so, some groundwater samples have been observed to be isotopically enriched. While this is one of the signs of the interaction between rivers and groundwater in the Kimbiji aquifer, another possibility for the enrichment is the exposure of the infiltrating rainwater to evaporation before percolating to recharge the aquifer. In the Singida aquifer, all lake samples are isotopically enriched, something

which is scientifically accepted and has been proven by other researchers (Rowley *et al.*, 2001; Oiro *et al.*, 2018). However, some boreholes plotted just below the GMWL and LMWL. The interpretation of  $\delta^{18}\text{O}$  and  $\delta^2\text{H}$  shows that groundwater recharge from the meteoric water and evaporative water in the two study areas is evident. This is a sign of the presence of local and regional flow systems in the two aquifers.

Some boreholes in the Singida and Kimbiji aquifers exhibited depleted signatures, signifying the possibility that there could be a regional recharge occurring at high altitudes far away from the aquifer. The elevation of the recharge area is usually evident from increasingly depleted isotope signatures in groundwater with increasing altitude, which in turn reflects altitudinal effects on precipitation (Hemmings *et al.*, 2015). This systematic variation is also affected by lower temperatures and higher relative humidity at high altitude, wind and their lower influence on condensation and evaporation (Rowley *et al.*, 2001).

In general, isotopic values varied from location to location, but there was a small standard deviation in all samples signifying that there was a small variation in isotopic values from one sampling point to another. The LMWL for Tanzania shows low vapor humidity relative to the GMWL resulting from its lower slope value (i.e., 7.05). A slope is a function of humidity, temperature, and other factors of a particular groundwater basin (Kebede & Travi, 2012). The noted variability on the d-excess from the two study areas suggests a variability of the vadose zone in the two aquifers, which is attributed to the evident difference in geology. This has led to variable infiltration rates due to the difference in the materials making up the vadose zone in each study site. This has been reported elsewhere by other researchers (Baskaran *et al.*, 2009; Fynn *et al.*, 2016; Yeh *et al.*, 2009). Arguably, the variable infiltration rates are a result of variable exposures of the infiltrating water to the effects of evaporation as reported previously (Adomako *et al.*, 2010; Fynn *et al.*, 2016; González-Trinidad *et al.*, 2017).

Samples fitting around the local meteoric water line hint on the possibility that local rainfall was responsible for recharging such groundwater. Samples falling on the right-hand side/ below the LMWL show evidence that such water underwent evaporation before it recharged the aquifer. This is a phenomenon in both aquifers. Moreover, samples appearing above the LMWL can deduce the possibility of regional or subregional flow in a sense that the water is isotopically depleted and was possibly recharged in a high elevation area where temperatures are low and humidity is high. The possibility of the presence of different flow systems and their subsequent mixing among them has been noted as reported by other studies (González-Trinidad *et al.*, 2017). This affects the isotopic composition of the groundwater. The mixing probably results from the effect of fracture systems

mainly in the hard rock Singida aquifer (Thivya *et al.*, 2016) as well as surface water and groundwater interaction in the Singida and the Kimbiji aquifers.

Deuterium excess analysis for the two aquifers confirmed that rivers and lakes (open water bodies) have their deuterium excess less than 10‰, signifying the influence of evaporation. This is a sign of enrichment of heavy isotopes of water. To that effect, groundwater samples containing enriched water signifies an interaction between an open water body (a river, a lake, or a dam) and the aquifer system. This also hints on the great possibility of local recharge of the aquifer, particularly from the open water bodies. Groundwater-surface water interaction was very evident from the two aquifers as revealed by stable isotope analyses and supported by the hydrogeochemical signatures. This suggests that conjunctive management of groundwater and surface water is inevitable. That approach will assure a sustainable water resources management in the three aquifers.

The ranges of d-excess values in the Singida and Kimbiji aquifers connote the influence of both local and regional moisture circulation, indicating highly enriched humidity for some samples as well as highly depleted ones in others. Low d-excess values reflect high humidity during formation of vapor mass as it was reported by other researchers (Abiye, 2013; Leketa *et al.*, 2019; Oiro *et al.*, 2018; Yusuf *et al.*, 2018). It is not uncommon therefore to find groundwater samples plotting above the GMWL in the Singida aquifer. Arguably, in low humidity regions like Singida, re-evaporation of precipitation from local surface waters could create vapor masses with isotopic content that plot above the local meteoric water line as it was reported elsewhere (Abbott *et al.*, 2000; Adomako *et al.*, 2010; Hemmings *et al.*, 2015).

Reportedly, groundwater recharge at lower altitude is usually affected by evaporation compared to higher altitude. This is due to the lower percentage of humidity and higher temperature at lower altitudes. A combined effect of lower humidity and high temperature has affected most of the groundwater samples seemed to be locally recharged in the Kimbiji aquifer while the lower percent of humidity has been a prominent factor in the Singida aquifer. Evaporation causes fractionation in water, making them isotopically heavier. The isotopic analyses for local altitudinal effect on recharge have not been evident in the two aquifers. This is because the elevation has not been significantly different in all the study areas.

The scientific explanation of the isotope values above and below the GMWL and the LMWL is either due to: (a) below-cloud evaporation during the dry season causing enriched  $\delta^{18}\text{O}$ , (b) progressive condensation within rainy season weather systems, which can cause the strongly depleted  $\delta^{18}\text{O}$  rain and (c) different water vapour isotopic compositions in the source regions of air masses producing rainfall which recharged the aquifers. The third reason holds true for what has

been observed in the two study areas as the mixture of different isotopic compositions has shown a possibility of varying sources of moisture, with varying travel times.

#### 4.1.6 The Response of Watertable to Local Rainfall Events in the Singida and Kimbiji Aquifers

Groundwater levels showed a quick response to individual precipitation events in the Kimbiji aquifer (Fig. 37 & Fig. 38) which is possibly underlain by a relatively thin vadose zone, and geologically it is made up of the sedimentary (unconsolidated) porous materials.

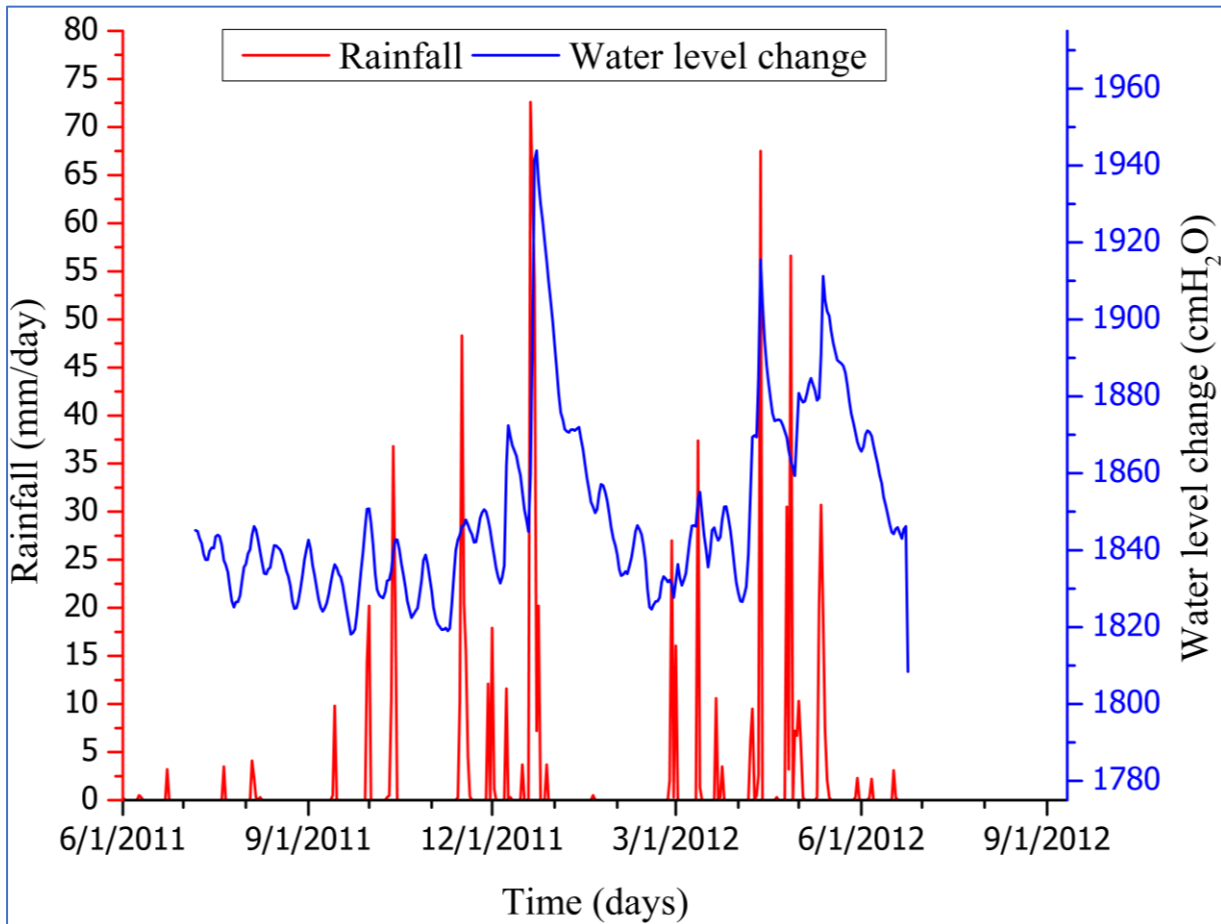
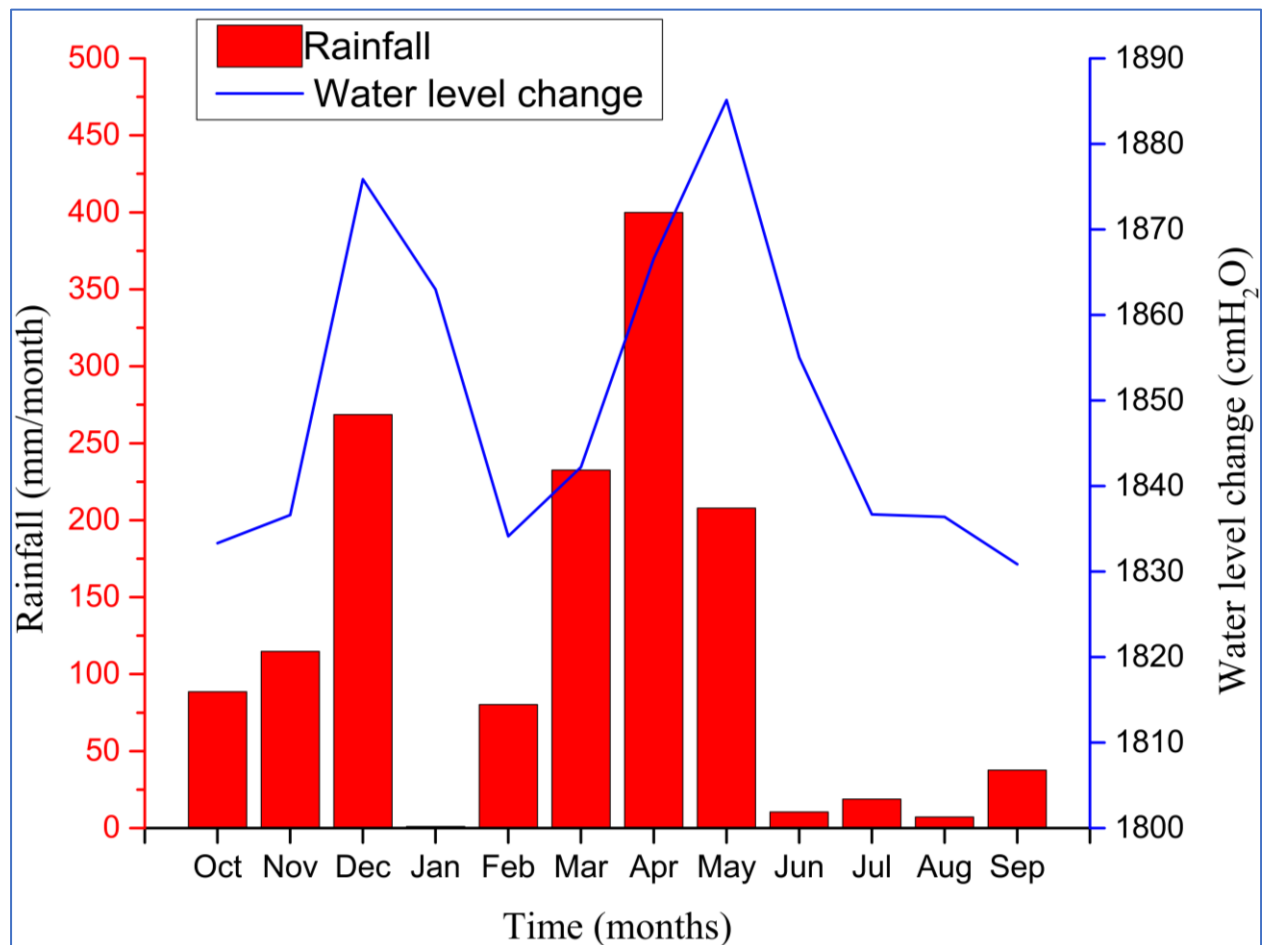


Figure 37: Daily aquifer response to rainfall in the Kimbiji aquifer



**Figure 38: Monthly aquifer response to rainfall in the Kimbiji aquifer**

On the contrary, infiltrated rainwater percolated slowly in the Singida aquifer (Fig. 39 & Fig. 40), causing the water in the aquifer to continue to decline until the infiltrated water reaches the water table. Purportedly, the Singida aquifer has a relatively thick vadose zone as opposed to the Kimbiji aquifer with the weathered hard rock materials making up the lithology of the Singida aquifer. The observed aquifer response to rainfall episodes also reaffirms the difference in geology between the two aquifers.

Water level changes during the two-year monitoring of the Singida aquifer with the diver showed two distinctive water level rise peaks for two different hydrological years. One, relatively small recharge episode in the 2018/2019 hydrological year and the other one, bigger and pronounced was observed in the 2019/2020 hydrological year (Fig. 39). The difference of the two water table fluctuation episodes was estimated using the difference in pressure. The water level change episodes in the Singida aquifer were related to a two-year rainfall time series plotted against water level changes in a hydrological style, and they were found to significantly correlate with rainfall. This was justified using the statistical approach developed by Moon *et al.* (2004) by clustering temporal piezographs as a function of time and relating them to precipitation records of the two hydrological years.



On the other hand, the maximum water level rise in the Kimbiji aquifer is mainly influenced by the March-May rainfall season which produced the highest peak while the October-December season manifests itself through a small water level rise peak (Fig. 38). December and May have shown to attain the maximum water table rises, representing short and long rainfall seasons, respectively as shown in Fig. 38. The daily data for the Kimbiji aquifer show the zigzag water table fluctuation before responding to rainfall events around December. Thereafter, there was a zigzag recession before a rising limb was realized around April. A delayed response from the daily data shows a response of the aquifer to both aquifer recharge and drainage through exploitation. However, using the monthly water level fluctuation data, the response of the Kimbiji aquifer to rainfall is more spontaneous and faster than the Singida aquifer (Fig. 37 & Fig. 38).

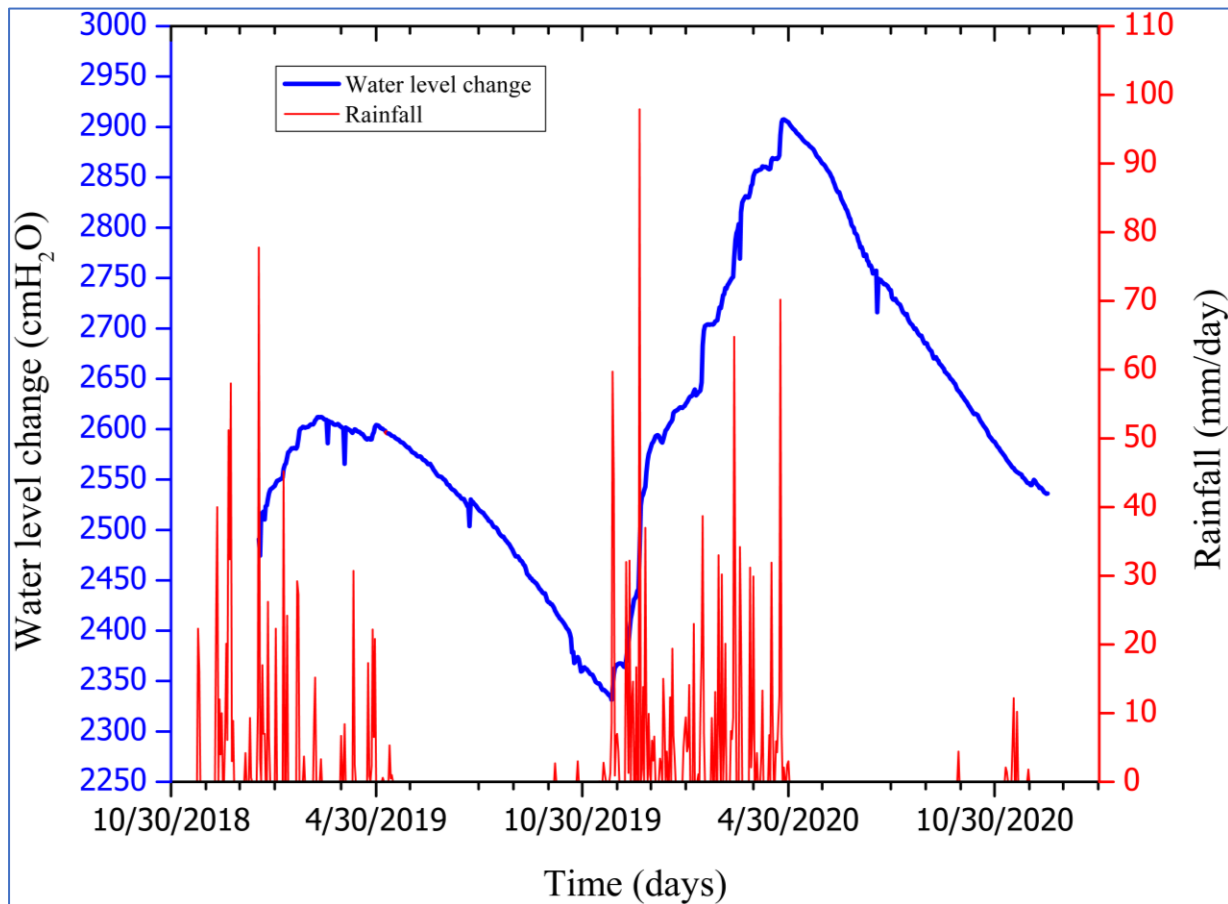


**Figure 39: Daily aquifer response to rainfall in the Singida aquifer**

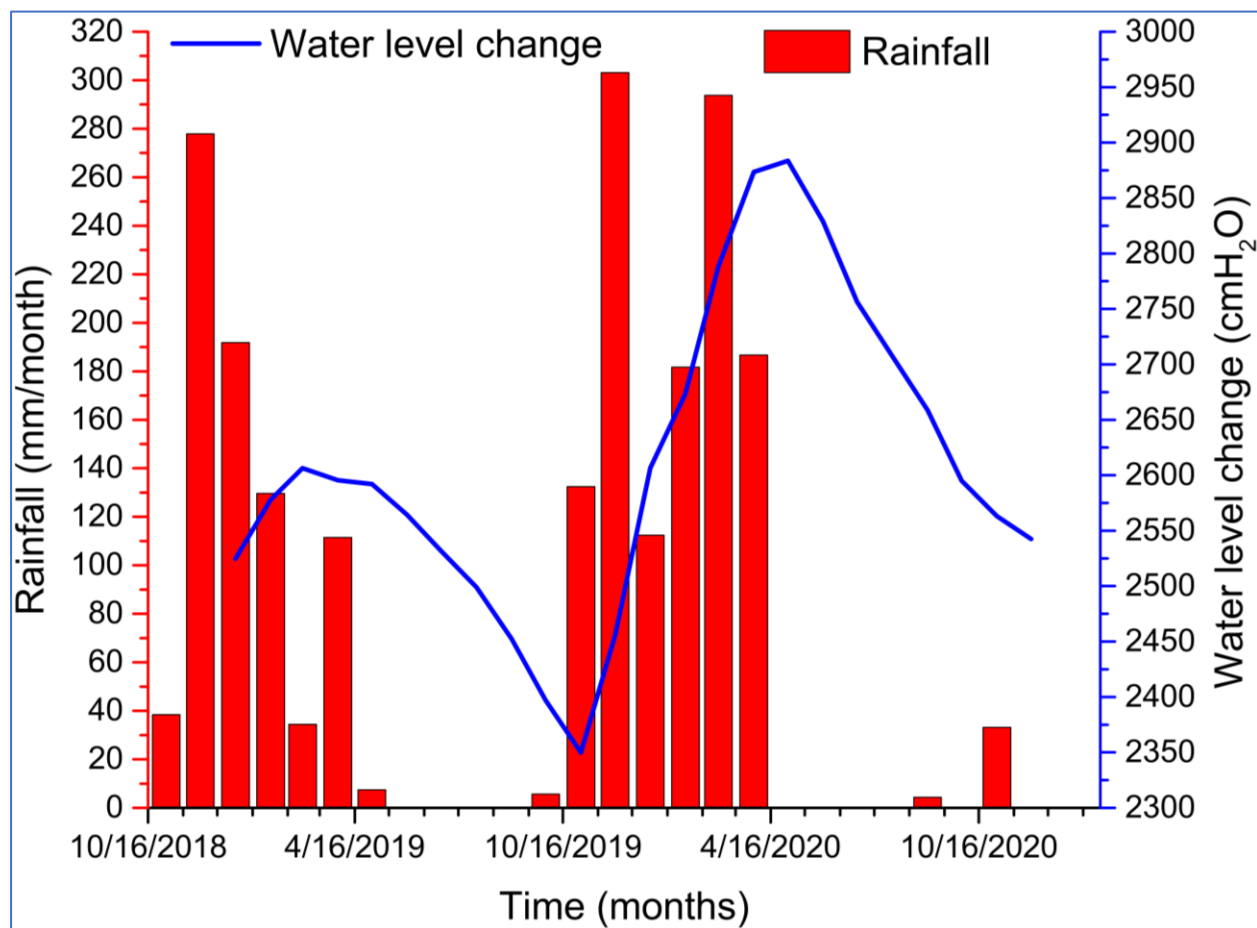


**Figure 40: Monthly aquifer response to rainfall in the Singida aquifer**

The WTF approach used in this study produced results that are commensurate with the hypothesized response of the water table rise to rainfall episodes which is relatively quicker in aquifers with unconsolidated porous materials than it is for the consolidated fractured aquifers (Delin *et al.*, 2007). Moreover, the presence of local flow systems in aquifers with contrasting climate and geology has been revealed by using the water table fluctuation method, informing that the crystalline basement aquifers can as well have a local flow system despite low rainfall, consolidated aquifer materials and possibly a thin vadose zone (Chesnaux, 2013). The degree of weathering and the presence of a weathered zone are some of the factors determining the local recharge in hard rock aquifers like the Singida aquifer.

The response of the upper unconfined aquifers to rainfall in the two study areas has been distinctively different, flaunted through observed time lag. Moreover, the unimodal rainfall pattern, reflected by the unimodal water level changes in the Singida aquifer, as opposed to the bimodal water level changes in response to the bimodal rainfall pattern in the Kimbiji aquifer has as well been depicted by the water level hydrographs. Further, the results show that the fluctuations in the water table level are to a large extent caused by changes in precipitation, camouflaging the influence of other factors, especially groundwater drainage through exploitation.

During the rainfall season, the water table rises, although there is a lag between when precipitation infiltrates the saturated zone and when the water table rises. However, the lag has been profoundly higher in the Singida aquifer than it was observed in the Kimbiji aquifer. The difference in geological settings between the two aquifers explains the observed difference in time lag regarding the response of the water table to a preceding rainfall event. The response is invariably quick in the unconsolidated sedimentary Kimbiji aquifer while there is a delayed response in the consolidated fractured Singida aquifer. This underscores the difference in the geology of the two aquifers, which also calls for differentiated management strategies. Moreover, the response of the water table in the two study areas to rainfall events informs of the presence of the local flow system. This is a groundwater system whose water is recharged and discharged in the same sub-basin.

Apart from finding out the relationship between water table fluctuations and precipitation, the presence of the local flow system has been revealed. This constitutes a succinct approach for groundwater use and management, as opined in other studies (Carretero & Kruse, 2012). Moreover, this approach has enabled the identification of areas with similar geomorphological and climatic characteristics, as well as the presence of a shallow, homogeneous unconfined aquifer in the Singida aquifer, something which was kind of obvious in the Kimbiji aquifer but quite uncertain in the most consolidated fractured aquifers. Some studies (Carretero & Kruse, 2012) assessed and affirmed the relationship between water-table fluctuations and precipitation in a humid climate, considering its seasonal variations. In this study, the relationship of the rainfall and water table fluctuation in a semi-arid climate aquifer in central Tanzania has also been confirmed.

Due to the difference in geology and climate, different groundwater hydrographs have been observed in the two aquifers. This is not uncommon as it was once reported by previous researchers (Moon *et al.*, 2004; Jie *et al.*, 2011). In the Singida aquifer, different hydrographs have been observed in two different hydrological years, being attributed to different intensities of rainfall amounts received in the two seasons, while the Kimbiji aquifer portrayed two different hydrographs in the same hydrological year.

While it is quite obvious that groundwater levels fluctuate depending on the characteristics of precipitation events, which are related to the amount, duration, and intensity, various hydrogeological variables such as topography, the thickness of the unsaturated zone, and matrix composition of saturated and unsaturated materials have contributed to the observed lag difference in water table response to rainfall between the two aquifers. However, the bottom line and a scientific message from the water table fluctuation approach is that the two aquifers have a local

flow system component which is part of the groundwater balance in each of the study areas despite their difference in geology and climate.

## **4.2 Evaluation of the Combined Effect of Climate Variability and Landcover Dynamics on Spatiotemporal Groundwater Recharge Rates across Regional Aquifers**

### **4.2.1 Delineation of Groundwater Recharge Potential Zones**

After various thematic map classes were assigned different numerical values with respect to groundwater recharge potential, they were converted into a scale of 1-5, and each class was categorized into very good to very poor just to depict the influence of each class to groundwater recharge potential. The final map obtained from each thematic factor was regarded as a layer, each with its own weight and special characteristics with respect to contribution to the overall recharge potential for the study areas.

Just like the final output (groundwater recharge) map, the thematic factor classes have a varying effect on groundwater recharge potential. The hydrogeological delineation revealed that the two study areas are each covered by three classes of groundwater recharge potential with respect to the slope as shown in Fig. 41 for the Kimbiji aquifer and Fig. 42 for the Singida aquifer. Flat to gentle slope areas are the areas which are the most suitable for groundwater recharge, while steep slopes are unfavorable for recharge. This is supported by previous researchers (Fenta *et al.*, 2014).

The largest part of the study area is low-lying and thus presents good conditions for water infiltration, and ultimately percolation to the aquifer. Arguably, water usually follows the slope and accumulates in areas with the lowest elevation regardless of the lithological setting of that particular area (Das & Pardeshi, 2018). Therefore, the lower the slope, the higher the potential for groundwater recharge and the higher the slope the lower the suitability of area as a recharge zone (Jaiswal *et al.*, 2003; Rao & Jugran, 2003; Sener *et al.*, 2004; Chowdhury *et al.*, 2008; Hammouri *et al.*, 2012; Fashae *et al.*, 2013). Steep slopes and rocky outcrops (12.1%–20%) presented bad attributes for groundwater recharge potential in the Singida aquifer, while in the Kimbiji aquifer, only steep slopes presented areas with poor groundwater recharge potential. This is further reiterated by previous researchers (Das *et al.*, 2017).

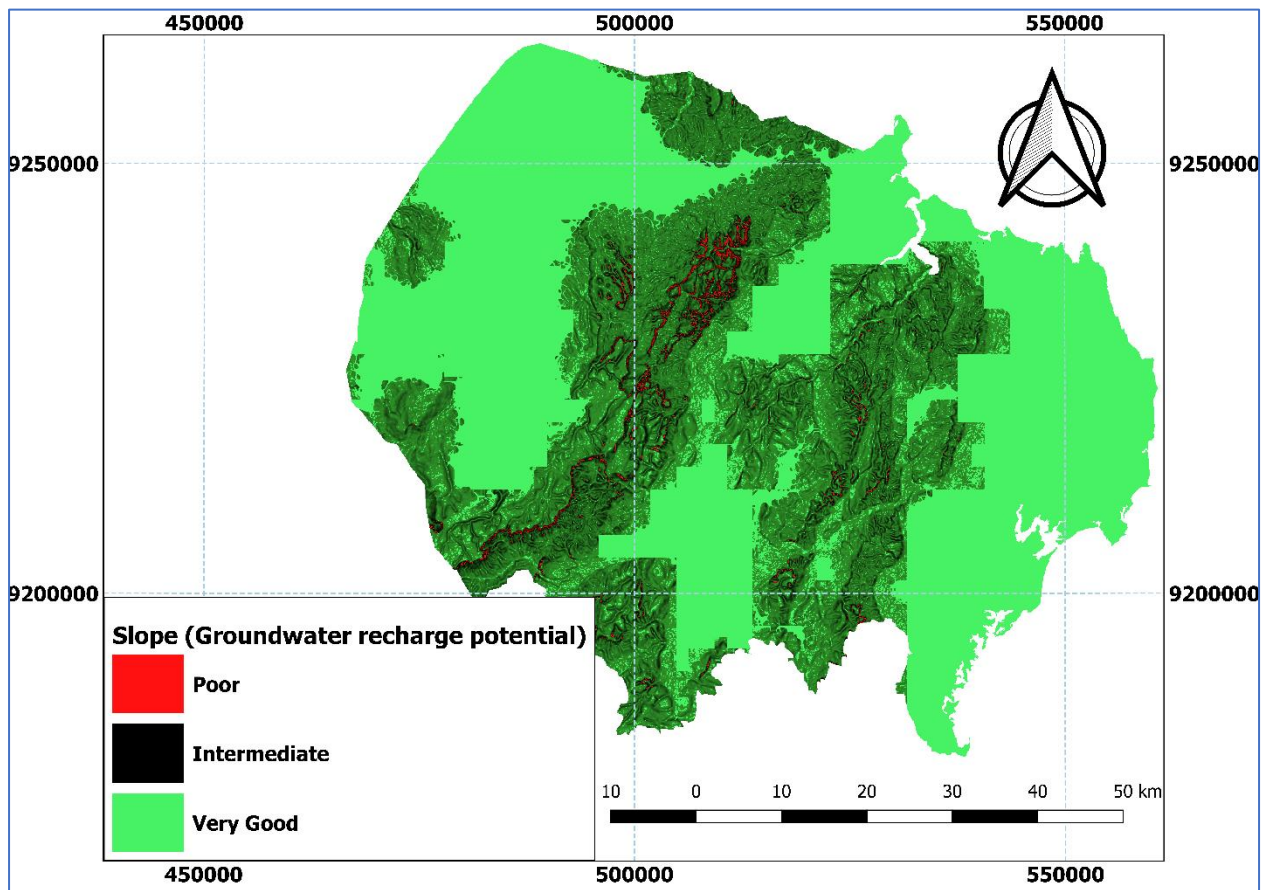


Figure 41: Groundwater recharge potential of slope classes in the Kimbiji aquifer

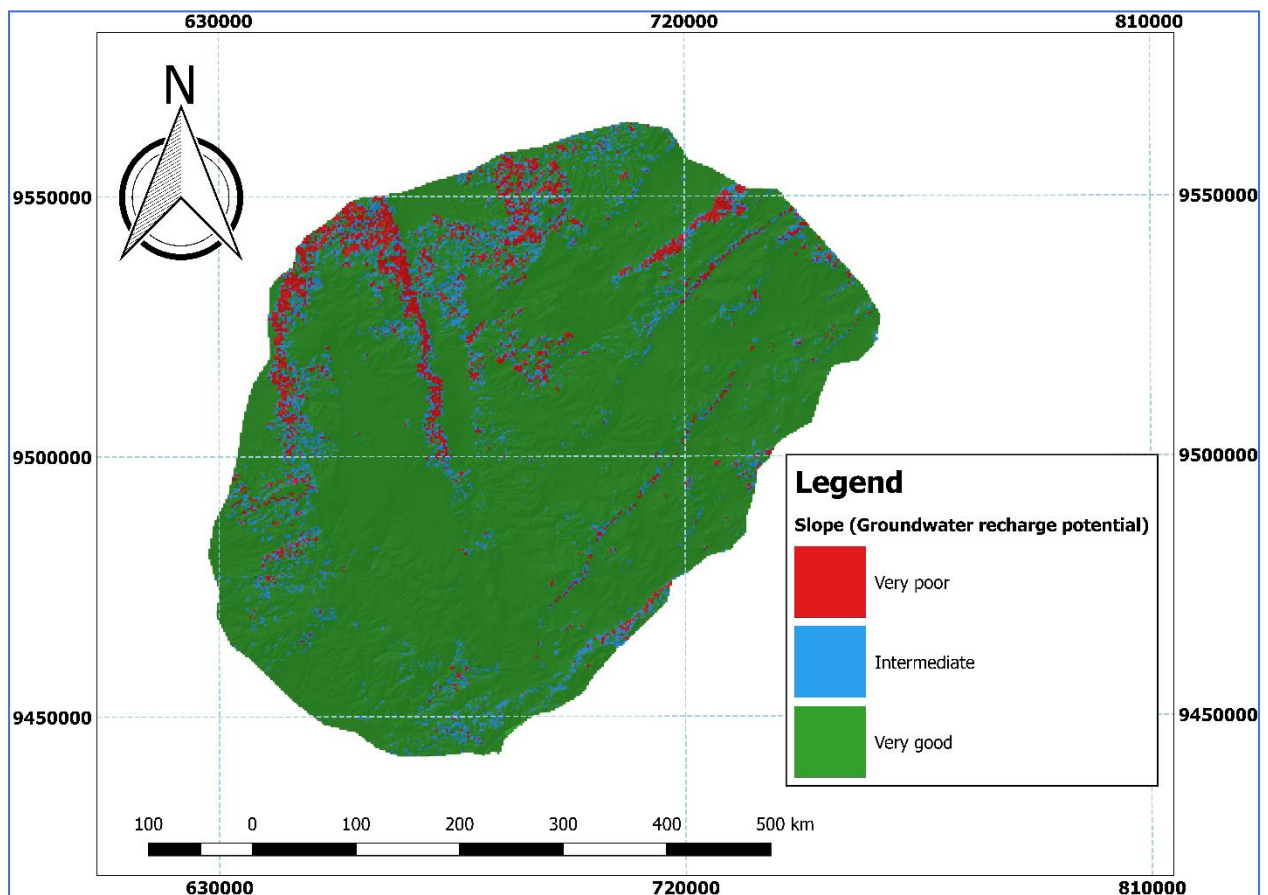
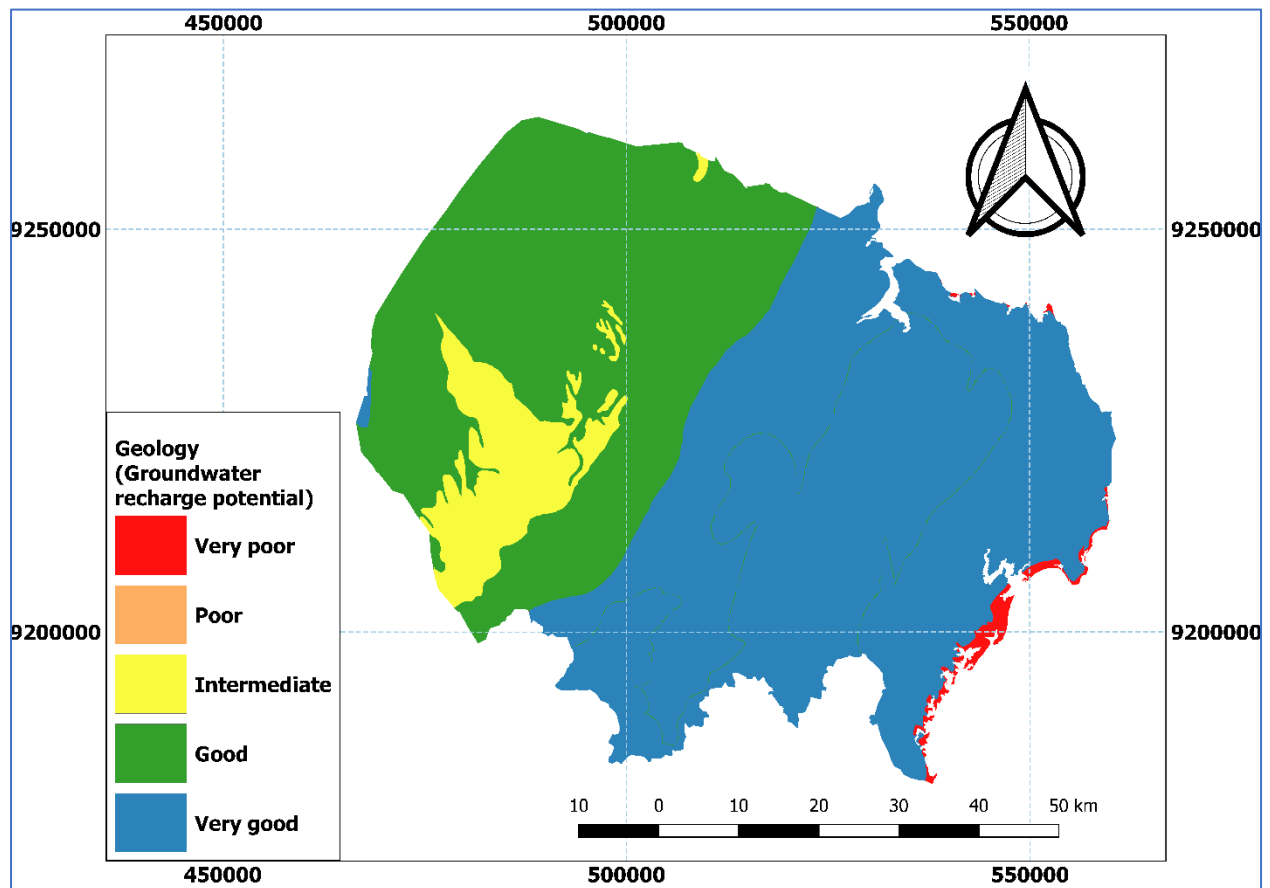
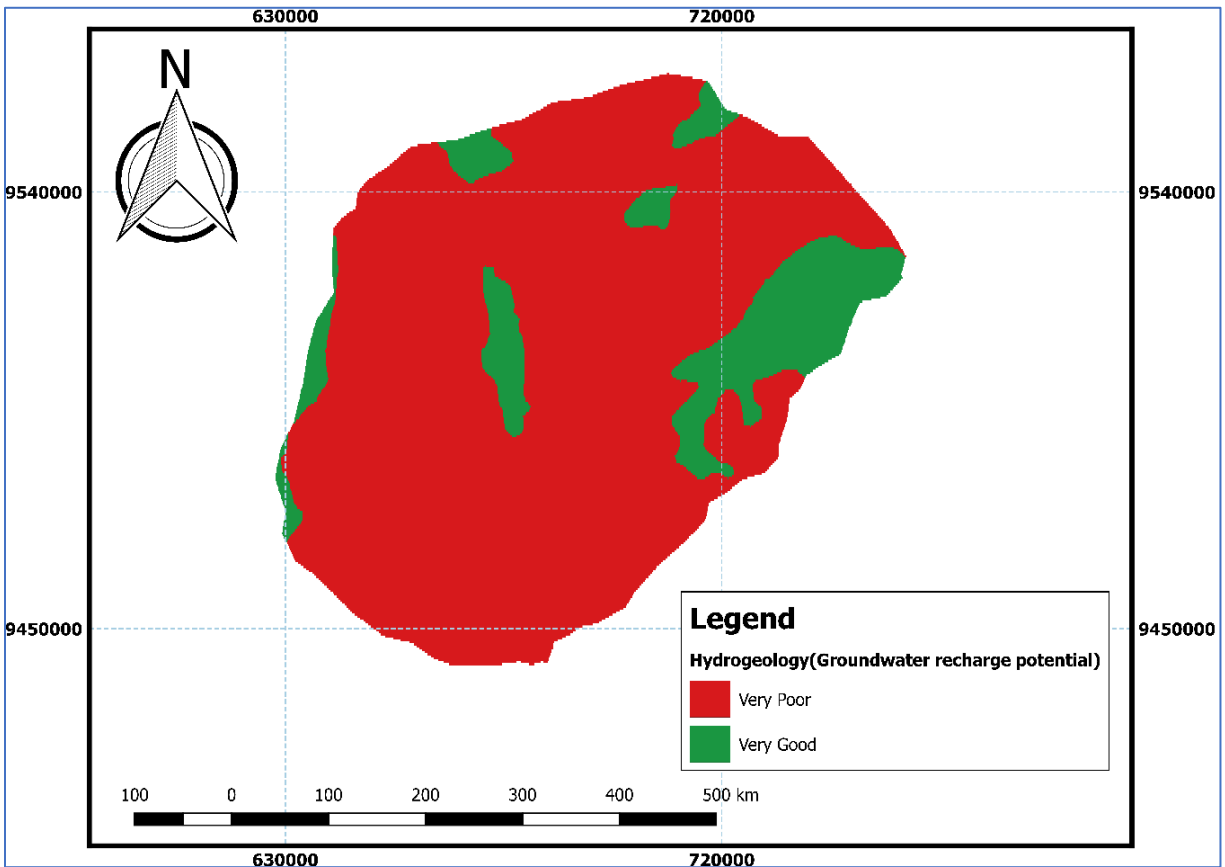


Figure 42: Groundwater recharge potential of slope classes in the Singida aquifer

In another aspect, the distribution of water bearing geological units is one of the most important factors which play significant role in the distribution and occurrence of groundwater in any basin as reported elsewhere (Acharya *et al.*, 2017; Das & Pardeshi, 2018; Ramu & Vinay, 2014). After a thorough lithological assessment, followed by a detailed hydrogeological analysis of the rock formations in the study areas, the hydrogeological units in the Kimbiji aquifer were five (Fig. 43), but they were reduced into two in the Singida aquifer (Fig. 44) with respect to their groundwater recharge potential. In the Singida aquifer, they were classified into very high (unconsolidated materials) to very poor (consolidated, cratonic and kimberlite hard rocks). The later have very poor primary porosity and thus permeability while unconsolidated materials are very good at allowing water passage through their well-connected pores. Most of the Kimbiji coastal aquifer is covered by materials with high to very high recharge potential. The material in the fringes of the Indian ocean have poor recharge potential. The south-western parts (yellow colours) are also covered by geological materials with intermediate groundwater recharge potential (Fig. 43). Arguably, the storage capability of the rock formations depends on the type and porosity of the rock (Grotzinger *et al.*, 2010; Manikandan *et al.*, 2014). In the rock formation, the water moves from areas of recharge to areas of discharge under the influence of hydraulic gradients depending on the permeability and/or hydraulic conductivity of a rock formation (Manikandan *et al.*, 2014).



**Figure 43: Groundwater recharge potential of hydrogeological units in the Kimbiji aquifer**



**Figure 44: Groundwater recharge potential of hydrogeological units in the Singida aquifer**

The potential of groundwater recharge from the rainfall distribution follows an increasing trend. The higher the rainfall amount the higher the potential for groundwater recharge. Groundwater recharge is only possible when rainfall is higher than potential evapotranspiration (PET), after considering the ensuing runoff. This means that recharge is only possible when net rainfall (rainfall minus the runoff) is larger than the PET. Nevertheless, this does not ensure a spontaneous recharge since the amount of water that is left, after subtracting the PET from the net rainfall will first be held by the soil. The Kimbiji aquifer is categorized into 2 groundwater recharge potential zones (Fig. 45), the intermediate and very good. These classes correspond with the amount of rainfall received.

On the other hand, the Singida aquifer is comprised of 3 classes as observed in Fig. 46. The classification is site specific and not generic. Rainfall has a huge bearing on the groundwater potential in arid and semi-arid areas (Das *et al.*, 2017). This is because other sources of water are uncertain and where available are unevenly distributed. Therefore, the more the rainfall received in an area, the higher the likelihood of overcoming potential evapotranspiration and thus surpassing the field capacity of the soil material, towards getting water surplus which usually percolates into the groundwater reservoir. Thus, the area which receives rainfall of 800 mm per year in the Singida

aquifer (Fig. 46) is more apt to influence groundwater recharge than the area receiving rainfall of 600 mm per year or less, given other geological factors are favorable. In the Kimbiji aquifer, the area which receives 1100 mm of rainfall annually has higher groundwater recharge potential than the rest of the study area (Fig. 45). At a certain point the amount of water held by the soil will exceed its maximum threshold called field capacity. The surplus of water after reaching the field capacity will recharge the groundwater reservoir. At this point, the potential evapotranspiration is lower than rainfall.

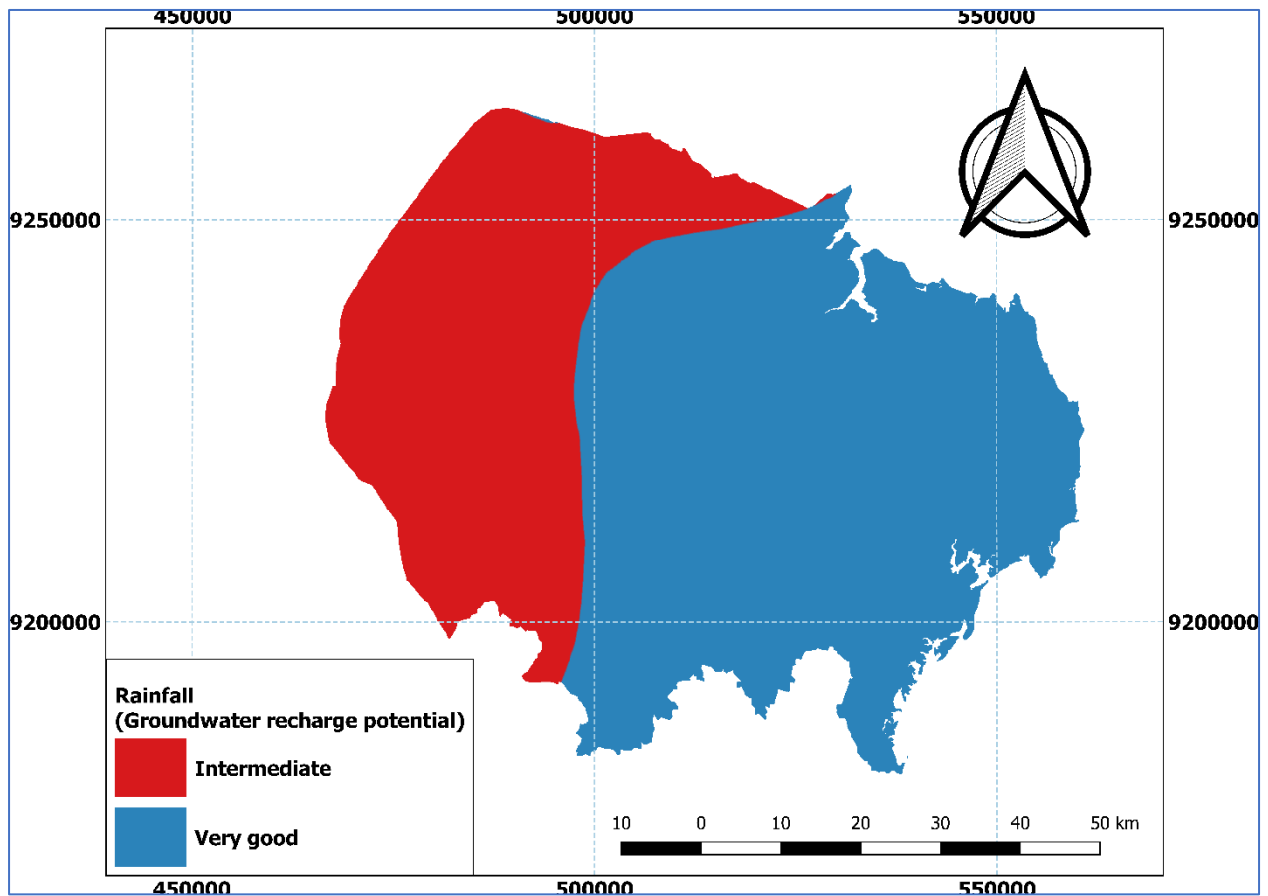


**Figure 45: Groundwater recharge potential of rainfall distribution classes in the Kimbiji aquifer**



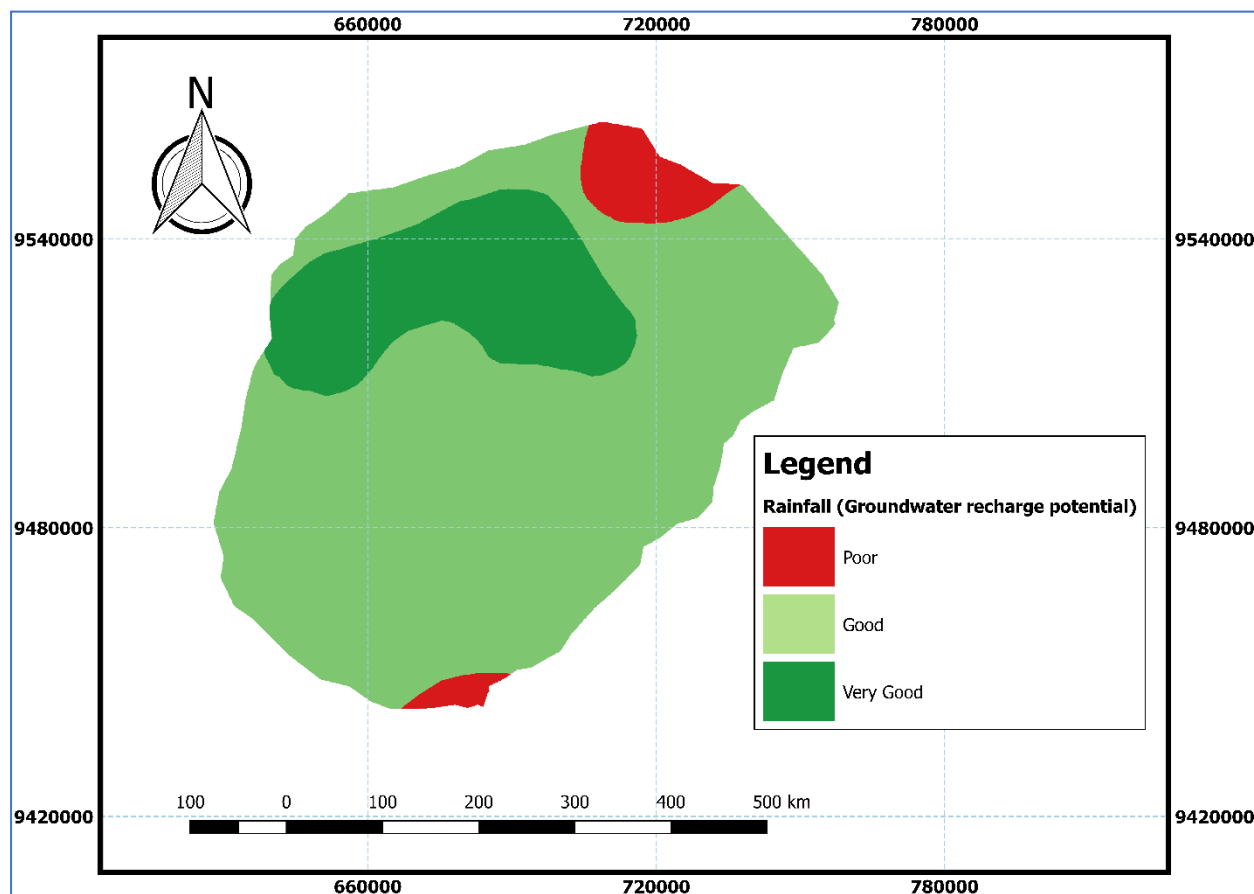


**Figure 46: Groundwater recharge potential of rainfall distribution classes in the Singida aquifer**

Lineaments, peculiar but important geological structures in the Singida aquifer are well distributed in the central to western parts of the aquifer. Thus, areas with high lineament density are classified as very good potential recharge areas as opposed to areas with low lineament density. In consolidated geological structures and highly fractured areas, secondary porosity, which is derived from fractures and lineaments are the most important features for groundwater flow and recharge. Figure 47 categorizes the Singida aquifer into five groups (very good to very poor) with respect to potential for groundwater recharge. Reportedly, areas having high lineament density have very good potential of groundwater recharge (Das *et al.*, 2017). This is well reflected in the findings of this study as shown in Fig. 47. In this study the contribution of lineaments to groundwater recharge potential is very good given the geology and hydrogeology of the area. Lineament density is one of the most prominent influencing factors in consolidated and fractured basement aquifers where they act as secondary porosity through which recharge may occur and groundwater travels (Table 4, Fig. 47).

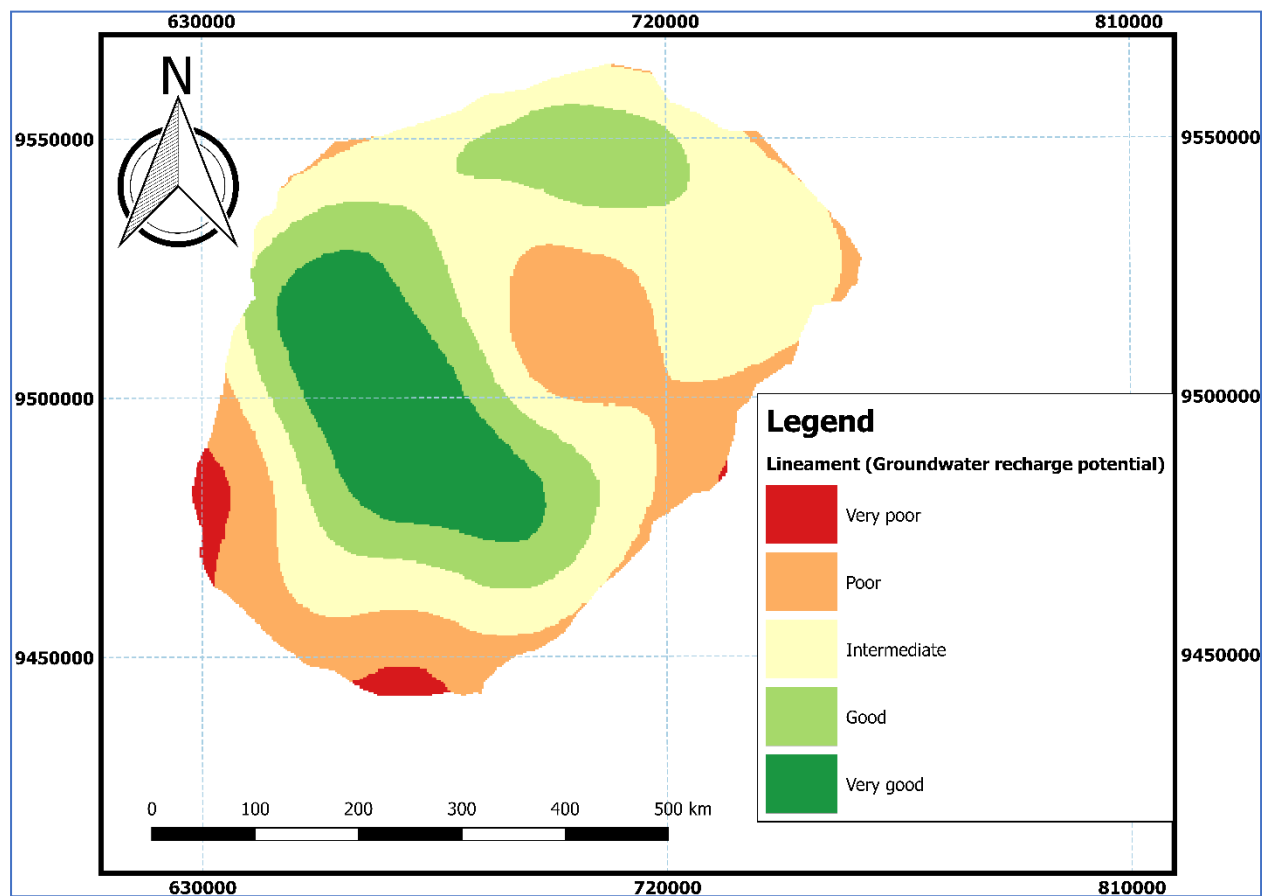


**Figure 47: Groundwater recharge potential of lineament density classes in the Singida aquifer**

With respect to drainage, the chance for water infiltration into the groundwater system is higher in areas where water is drained slower than in areas that have high drainage density. Therefore, areas with lower drainage density have high groundwater recharge potential since runoff is lower. While the peripheries of the Kimbiji aquifer (Fig. 48) seem to have high recharge potential, the central parts of the Singida aquifer are covered by areas with high drainage density (Fig. 49). The drainage density analysis for the two study areas shows that the drainage density in the Kimbiji aquifer is higher than in the Singida aquifer. As reported by previous studies, higher drainage density implies higher run off and therefore little water will find its way through to the aquifer (Bagyaraj *et al.*, 2012; Jenifer & Jha, 2017; Thomas & Duraisamy, 2018).

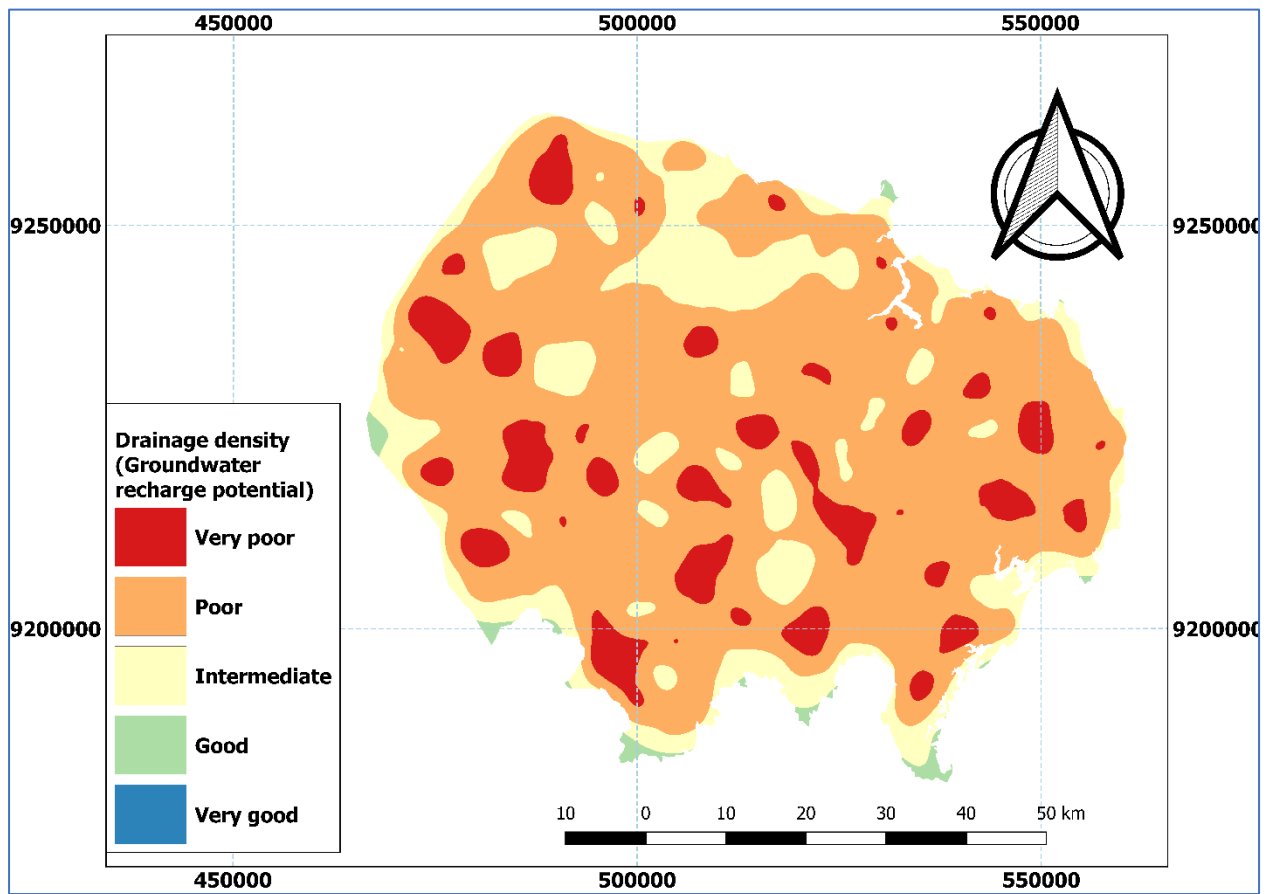


**Figure 48: Groundwater recharge potential of drainage density classes in the Kimbiji aquifer**

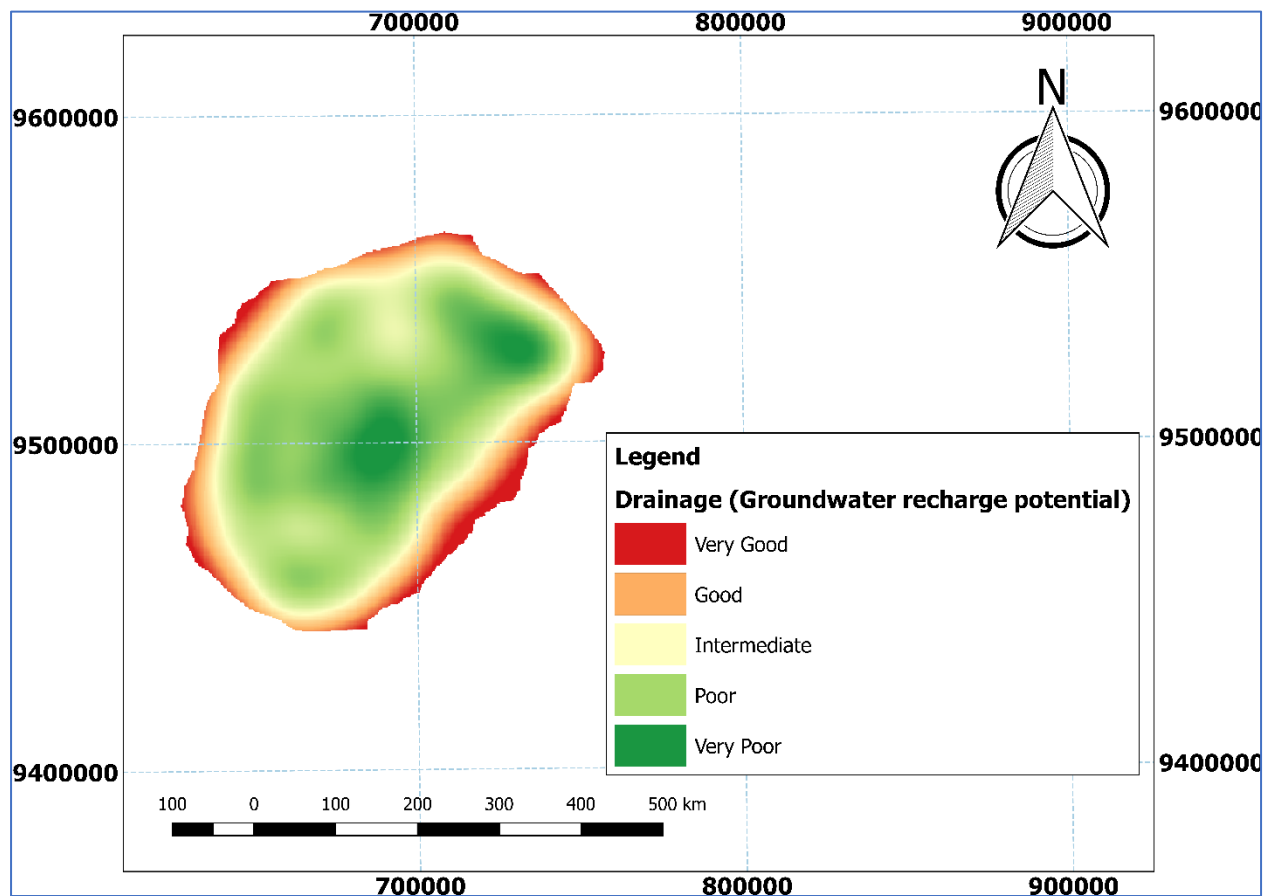


**Figure 49: Groundwater recharge potential of drainage density classes in the Singida aquifer**

The ranking of the soil classes considered soil texture and depth, the factors which have a major impact on groundwater recharge potentiality of an area (Singh *et al.*, 2010; Mehra *et al.*, 2016; Mehra & Singh, 2016). As far as soil is concerned, six groundwater recharge potential classes were obtained in the two study areas (Fig. 50 & Fig. 51), ranging from very good to very poor, with two intermediate classes in the Singida aquifer (Fig. 51). Alluvial soil is potentially very good to good in influencing groundwater recharge while red and brown soils are good to moderate respectively. Black soil is moderate at influencing groundwater recharge as reported by other studies (Manikandan *et al.*, 2014; Samson & Elangovan, 2015). This knowledge has been applied in the ranking of soil classes with respect to groundwater recharge potential. The Kimbiji aquifer shows a high groundwater recharge potential from soil point of view while the Singida aquifer has relatively poor attributes of recharge from the soil perspective. The difference in geology can conceivably be attributed to the observed phenomenon as soil is a result of the underlying geology of an area.

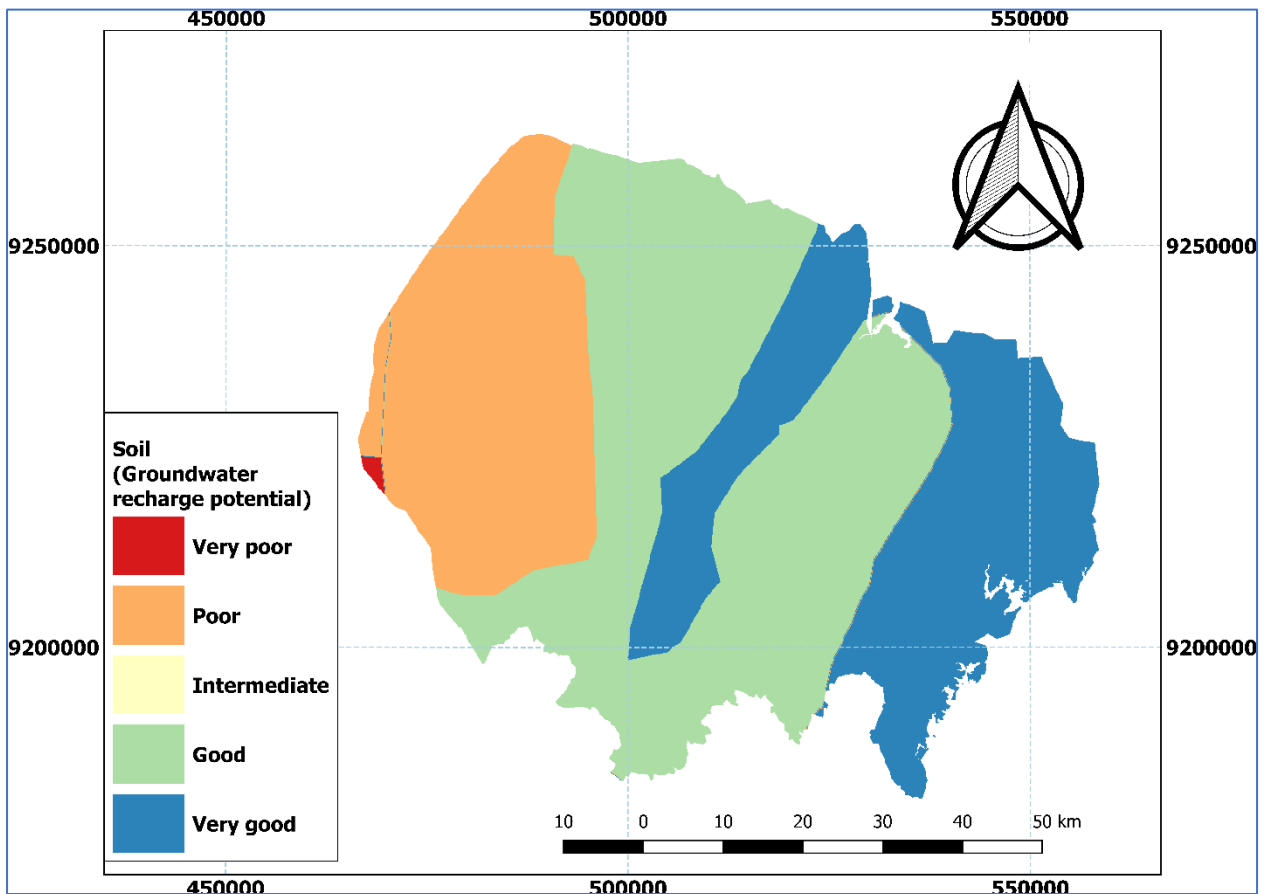


Figure 50: Groundwater recharge potential of soil classes in the Kimbiji aquifer

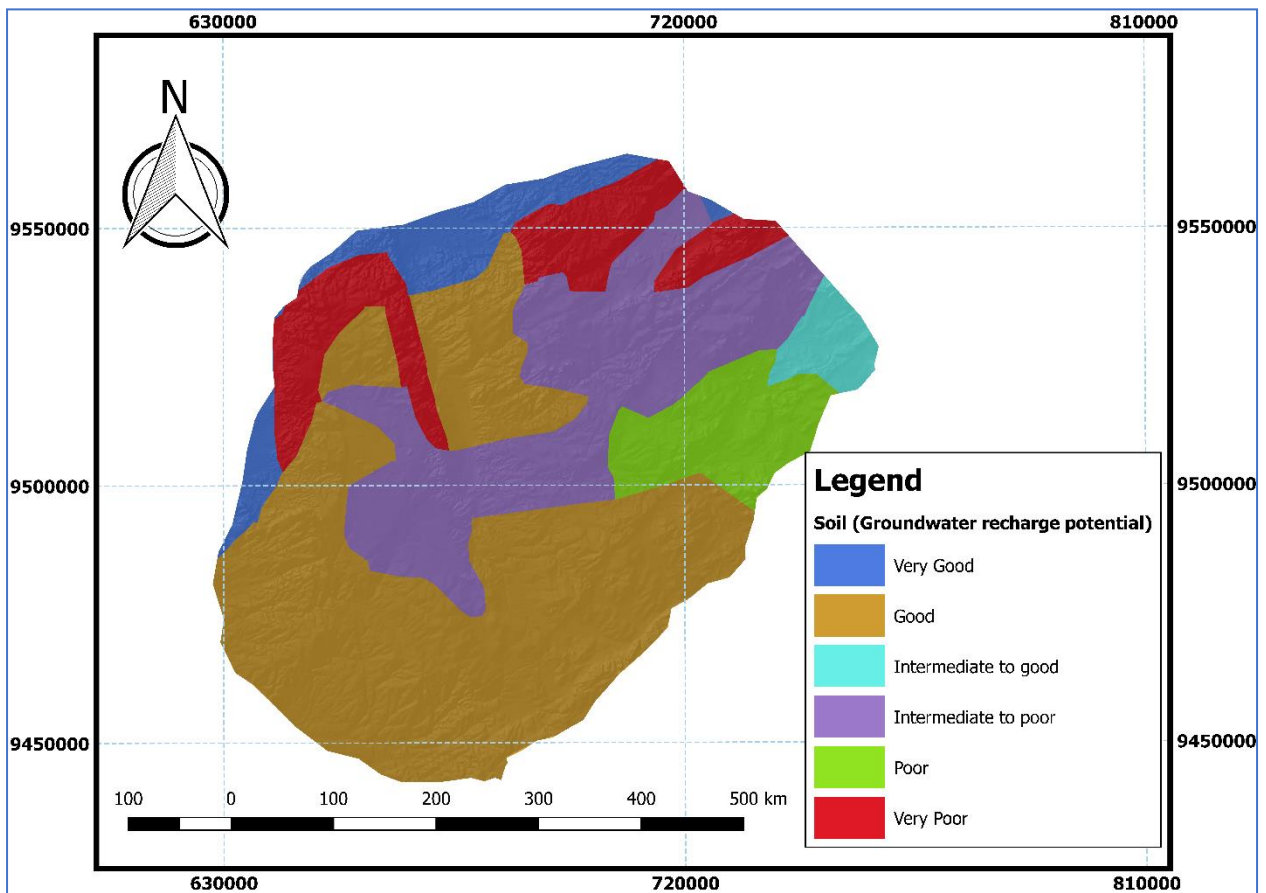
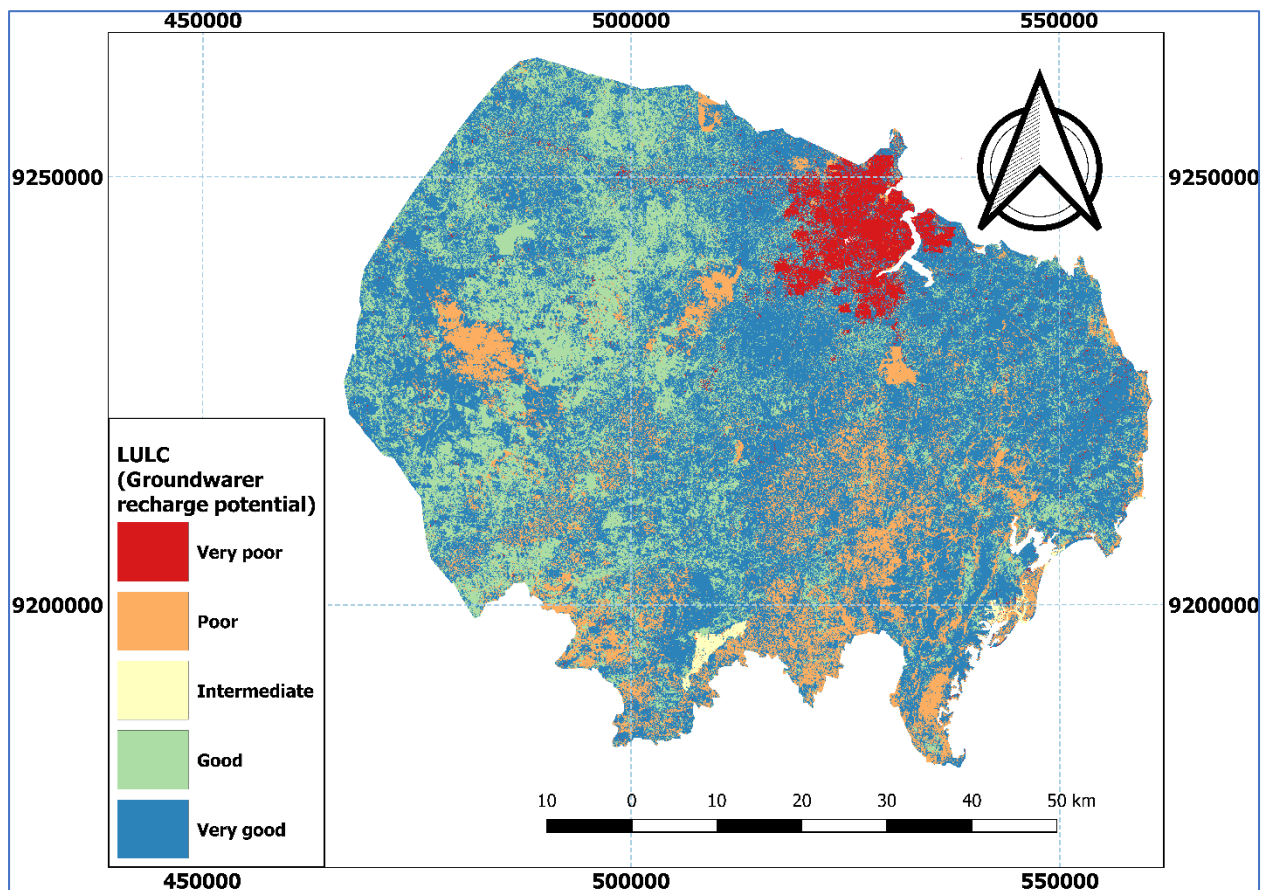


Figure 51: Groundwater recharge potential of soil classes in the Singida aquifer

The classification of land use/cover classes with regard to groundwater recharge potential informs that areas that are highly built-up and paved are least suitable for groundwater recharge. This is because of potentially more surface runoff ensuing from hard surfaces while agricultural and forest lands are good due to the availability of loose soil on the surface as reported elsewhere by Singh *et al.* (2010) and Das *et al.* (2018). As observed from the land use/cover maps, Fig. 52 for the Kimbiji aquifer and Fig. 53 for the Singida aquifer, there are vast grassland and bushes in the two study areas, and together with the cultivated land, they form good to very good recharge potential areas. While forests usually form suitable areas for groundwater recharge in the Kimbiji aquifer as reported in other studies (Singh *et al.*, 2010; Das & Gupta 2017), in the Singida aquifer the potential of forest and woodland in influencing groundwater recharge has been compromised by the fact that they occur in rocky outcrops and highly slopping areas. Therefore, combining the two factors reduces the potential of forested land on groundwater recharge in the Singida aquifer. The aptness of agricultural lands and grasslands for groundwater recharge and the unsuitability of built-up areas have been reported in previous studies (Singh *et al.*, 2010) and the two factors are reflected in the findings of this study in the two study areas.



**Figure 52: Groundwater recharge potential of land cover classes in the Kimbiji aquifer**



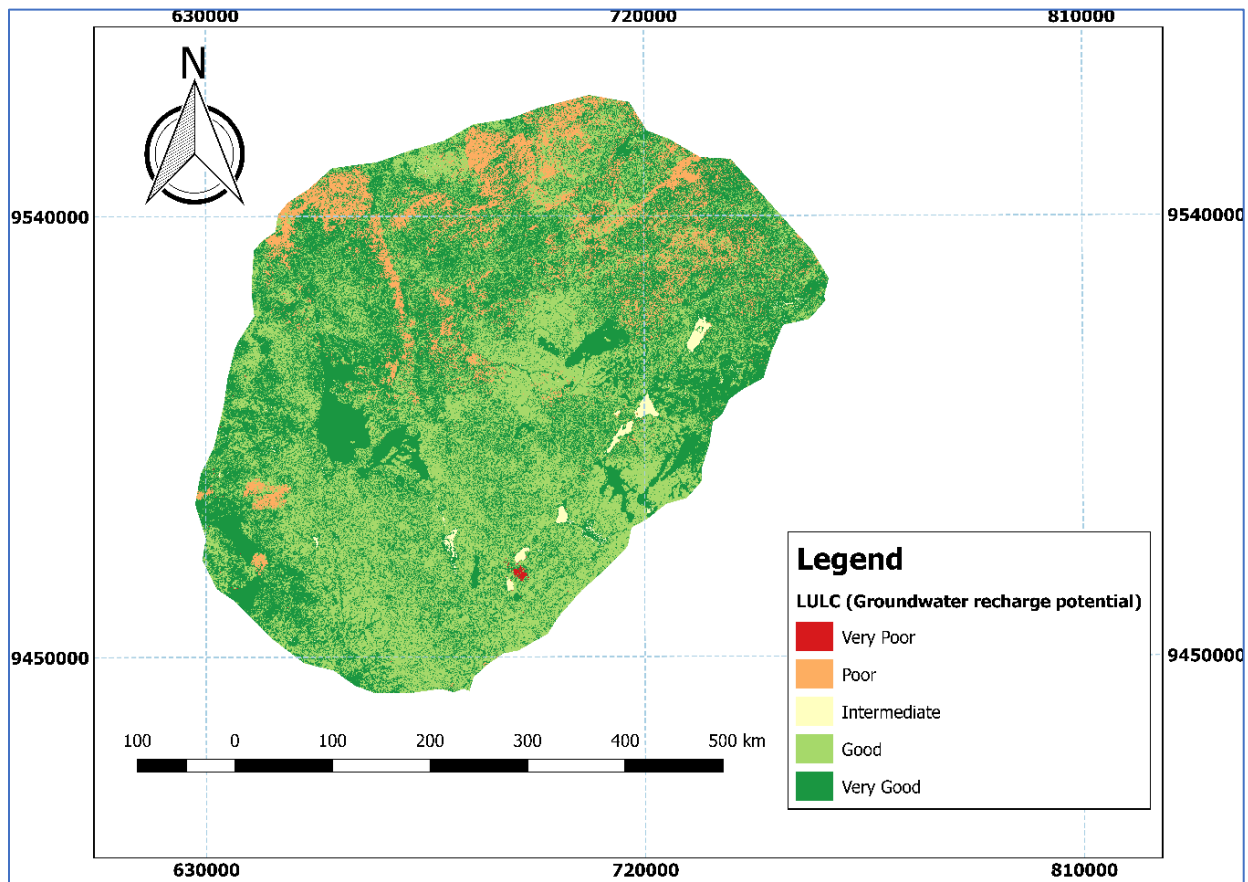


**Figure 53: Groundwater recharge potential of land cover classes in the Singida aquifer**

The study areas have been delineated into five distinct groundwater potential recharge zones with very good, good, intermediate, poor and very poor groundwater recharge potential. A visual interpretation of the groundwater recharge potential maps (Fig. 54 & Fig. 55) for the Kimbiji and Singida aquifers respectively indicates that the area which is suitably good for groundwater recharge is relatively small in the Singida compared to the area which is poor to very poor. In the Kimbiji aquifer, the area with high recharge potential is relatively large, as can be seen from Fig. 54. The coastal areas of the Kimbiji aquifer in the eastern part of the study area (Fig. 54) and a minute part on the western side are highly potential for groundwater recharge. The second most recharge potential area in the Kimbiji aquifer is relatively bigger than in the Singida aquifer due to relatively homogenous soils and unconsolidated geological materials as compared to the relatively more heterogeneous and consolidated geological materials in the Singida aquifer. Therefore, very good to good recharge areas identified in the Singida aquifer correspond to highly fractured zones, with high lineament density, which match with the gentle slope and unconsolidated tertiary to quaternary geological materials. In the Kimbiji aquifer, the homogenous unconsolidated geological materials, soils and rainfall are the main determinants of the groundwater recharge potential. The resulting maps (Fig. 53 & Fig. 55) give an idea of where possibly local recharge occurs.

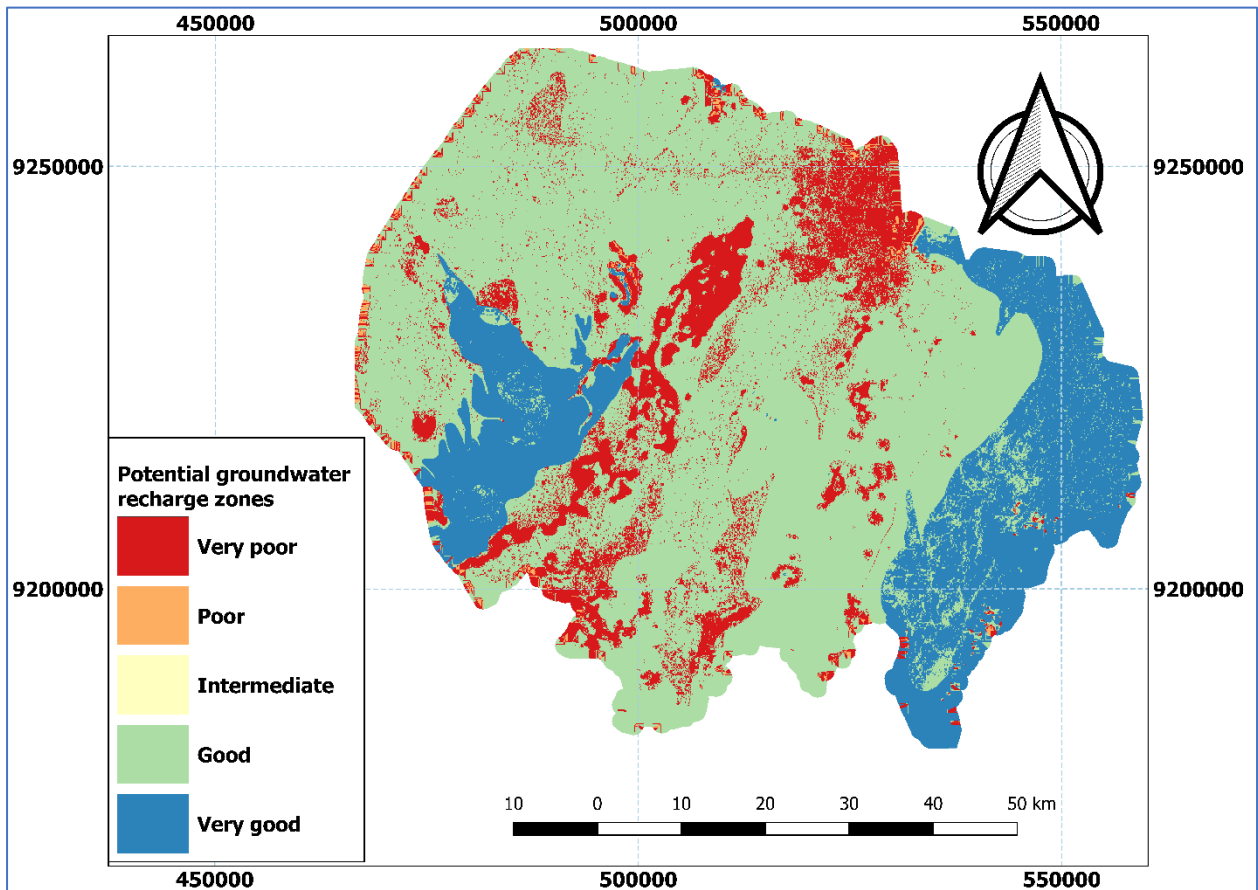


Figure 54: The groundwater recharge potential map of the Kimbiji Neogene humid aquifer

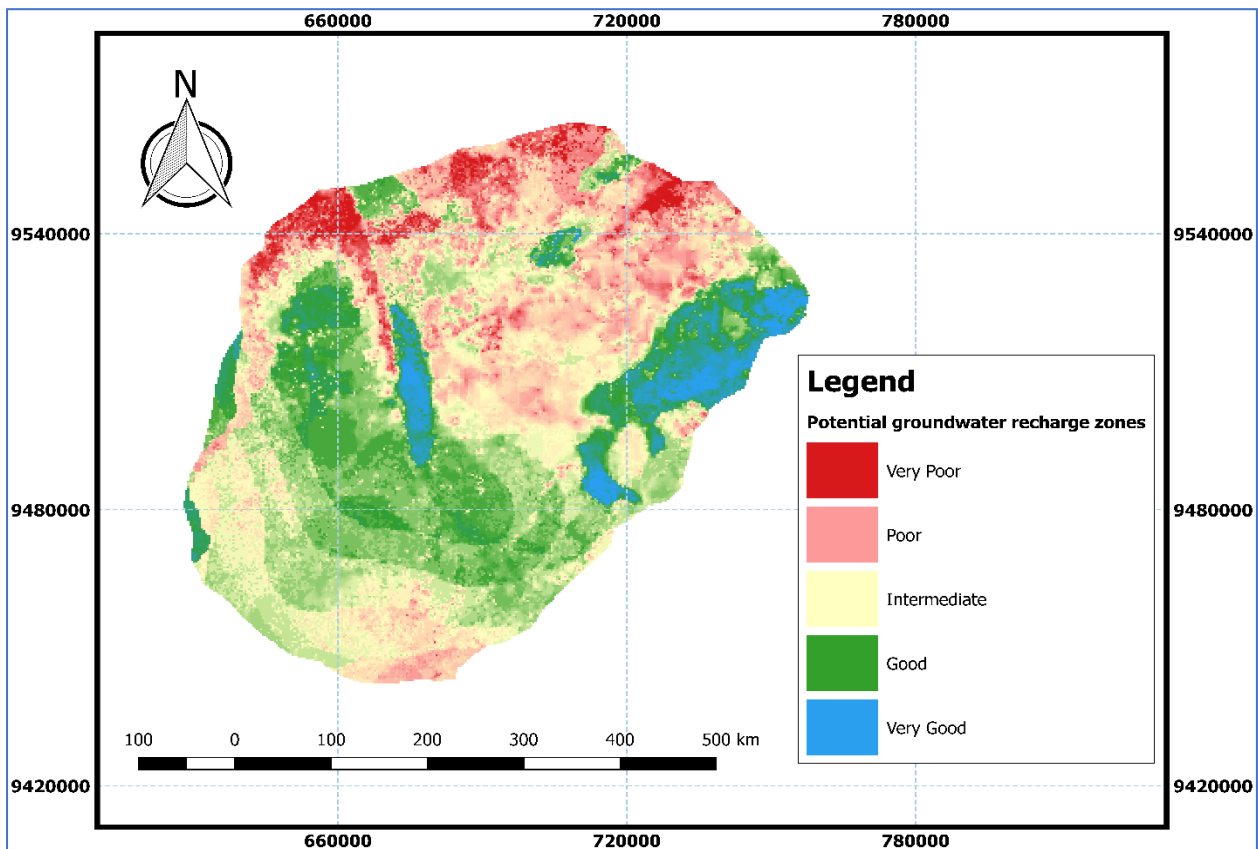


Figure 55: The groundwater recharge potential map of the Singida semi-arid fractured basement aquifer



In addition to the designation of the study areas into groundwater recharge potential areas, this study has also developed equations (Equation 43 and Equation 44) for hydrogeological delineation of potential groundwater recharge areas in humid sedimentary aquifers and semi-arid fractured aquifers, respectively. The Equations are numerical indicators of the relative importance of the factors used in the hydrogeological delineation of groundwater recharge potential. They are also a numerical representation of the factors controlling groundwater recharge in the two study areas.

Notably, the area that is good, which is the second potentially excellent for groundwater recharge is relatively bigger than the area designated very good in the two study areas. However, the two areas (very good and good) are highly influenced by the distribution of lineaments in the Singida aquifer while in the Kimbiji aquifer the lithology, soil type and rainfall distribution are the major controlling factors.

Very good groundwater recharge potential areas have been observed in the coastal areas of the Kimbiji aquifer and the northern-eastern, eastern to central parts of the Singida, while the north-western part is covered by areas with poor groundwater recharge potential in the Singida aquifer. This is due to high slope, poor distribution of lineaments, and high distribution of rock outcrops, especially in the north-western part of the study area. On the other hand, north-eastern, eastern and central parts of the Singida aquifer are covered by high groundwater recharge potential areas due to the presence of high lineament density, and are mostly cultivated areas with patches of unconsolidated geological materials (sandy in the central part and volcanic in the north-eastern part). The combination of unconsolidated geological materials, land use/cover and lineament density influences groundwater recharge zones. In this study, the built-up areas negatively affect recharge, but its impact has been masked by the distribution of lineaments in the Singida aquifer.

Notwithstanding, the built-up area is relatively very small as compared to other land cover types with high influence on groundwater recharge. This is vivid evidence that in consolidated fractured aquifers, secondary porosity dictates recharge to a great extent. Therefore, the movement and occurrence of groundwater in the Singida aquifer very much depends on the secondary porosity and permeability resulting from faulting and fracturing. Thus, the most obvious hydrogeological features that are important from the groundwater and hydrogeology points of view are the lineaments in the Singida aquifer. Generally, the eastern and central parts are very good recharge areas, while the northern and western parts have exhibited very poor characteristics as groundwater recharge zones in the Singida aquifer.

The Equations, in general revealed that land use, lithology and lineament density are the most important factors in fractured consolidated semi-arid areas like Singida while in humid areas,

rainfall, land use and geology are the most important factors. In the Kimbiji aquifer lithology carries 23%, land cover/use (16%), soil (18%), rainfall (20%), slope (14%) and drainage density (9%). Meanwhile, in the Singida aquifer, lineament density carries 21%, lithology (17%), land cover/use (15%), soil (15%), rainfall (13%), slope (11%) and drainage density (8%). Interestingly, drainage density is the least influential factor, while lithology and land use/cover are the most influential factors irrespective of climate and geology.

$$R_e = 0.23L_t + 0.2R_f + 0.18S_o + 0.16L_u + 0.14S_L + 0.09D_d \quad (43)$$

$$R_e = 0.21L_d + 0.17L_t + 0.15L_u + 0.15S_o + 0.13R_f + 0.11S_L + 0.08D_d \quad (44)$$

Where  $L_d$  is lineament density,  $L_t$  is Lithology,  $L_u$  is Land cover/use,  $S_o$  is Soil,  $R_f$  is Rainfall,  $S_L$  is Slope and  $D_d$  is Drainage density.  $R_e$  is the overall groundwater recharge potential.

The developed equations have been benchmarked with other groundwater recharge potential equations developed by other researchers, combining different geological, climatological and topographic factors as shown in Equations 45 to Equation 52. Such Equations are reported in previous studies (Fashae *et al.*, 2013; Fenta *et al.*, 2015; Selvam *et al.*, 2015; Raviraj *et al.*, 2017; Samson & Elangovan, 2017; Das & Pardeshi, 2018; Savita *et al.*, 2018; Etikala *et al.*, 2019) in that order.

Conceivably, the equations emanated from fractured semi-arid groundwater basins to humid, unconsolidated sedimentary aquifers. Notably, from the findings of this study, and the findings of previous studies, rainfall distribution separates semi-arid from humid basins while lineament density is an indicator of hard rock fractured aquifer systems. Therefore, from one equation to the other, it can be observed that they represent different aquifer systems with contrasting climate and geology.

$$R_e = 0.18L_t + 0.17R_f + 0.15S_o + 0.13G_m + 0.13L_u + 0.1S_L + 0.08L_d + 0.04D_d + 0.02D_p \quad (\text{Fashae } et al., 2013) \quad (45)$$

$$R_e = 0.38L_t + 0.24L_d + 0.16G_m + 0.1S_L + 0.06D_d + 0.04R_f + 0.02L_u \quad (\text{Fenta } et al., 2015) \quad (46)$$

$$R_e = 0.29L_u + 0.28L_t + 0.16S_L + 0.13G_m + 0.12L_d + 0.1Dd + 0.03S_o \quad (\text{Selvam } et al., 2015) \quad (47)$$

$$R_e = 0.24L_u + 0.23L_t + 0.15S_L + 0.12L_d + 0.11G_m + 0.09D_d + 0.06S_o \quad (\text{Raviraj } et al., 2017) \quad (48)$$

$$R_e = 0.2G_w + 0.15L_t + 0.12G_m + 0.12L_d + 0.12L_u + 0.1S_L + 0.1S_o + 0.09R_f \quad (\text{Samson \& Elangovan, 2017}) \quad (49)$$

$$R_e = 0.18L_t + 0.16G_m + 0.16L_u + 0.14S_L + 0.11D_d + 0.09L_d + 0.09R_f \quad (\text{Das \& Pardeshi, 2018}) \quad (50)$$

$$R_e = 0.25L_t + 0.25G_m + 0.15S_o + 0.15L_u + 0.1S_L + 0.1D_d \quad (\text{Savita et al., 2018}) \quad (51)$$

$$R_e = 0.22L_t + 0.17L_d + 0.14L_u + 0.14G_m + 0.11D_d + 0.08S_o + 0.08R_f + 0.06S_L \quad (\text{Etikala et al., 2019}) \quad (52)$$

An overall perspective is that lineaments, lithology, land use/cover pattern, slope and the soil type play an important role in influencing groundwater recharge. Recent studies (Das & Gupta, 2017) concluded that lithology is the main controlling factor for groundwater recharge. These findings are supported by the results of this study but with a little improvement. In this study, it was found that lineament density and lithology are the first and second most important controlling factors respectively in the Singida aquifer, while lithology and rainfall are the determining factors in the Kimbiji humid aquifer. The deviation from the findings of a recent study (Das & Gupta, 2017) in the Sngida aquifer is due to the fact that the findings from that study (Das & Gupta, 2017) emanate from a basaltic geological environment while this study was carried out in a consolidated, fractured crystalline basement aquifer with patches of unconsolidated geological materials, covering less than 20% of the Singida aquifer. The Kimbiji aquifer is mostly and probably completely made up of unconsolidated materials. The geological difference between the two study areas can be attributed to the diverging conclusions with regard to the factors that control groundwater recharge. Nevertheless, the findings reported by Das and Gupta (2017) are in agreement with what was found in the Kimbiji aquifer.

The potentially good groundwater recharge areas are predominantly characterized by a good distribution of the lineaments in the Singida aquifer, and the overlying land covers favor low runoff and high-water infiltration, as it is the case in the Kimbiji aquifer. Drainage density, soil texture, slope and rainfall are some of the less important factors in the Singida aquifer but have the opposite influence in the Kimbiji aquifer with the exception of drainage density. This observation has also been supported by other researchers (Nag, 2005; Raviraj *et al.*, 2017). However, some researchers (Selvam *et al.*, 2015) further argued that lineaments and land use are the most influential factors while soil and slope are least influential. In this study, it has been found that cultivated and

grassland areas also favor high groundwater recharge potential. This is in line with the findings of other studies (Das & Gupta, 2017). In addition to that, the built-up areas and forested land with massive rock outcrops in the north-western side of the Singida aquifer have proven to be poor in influencing factors to groundwater recharge. This is contrary to the findings of previous studies (Raviraj *et al.*, 2017), which found out that forested land is good at influencing groundwater recharge. Literally, the findings reported by Raviraj *et al.* (2017) are in line with what has been found in the Kimbiji coastal humid aquifer. It has also been proven that in fractured aquifers, lineaments are hydrogeologically important structures, as supported by previous authors (Solomon & Quiel 2006; Dar *et al.*, 2010; Machiwal *et al.*, 2010; Rajaveni *et al.*, 2015; Savita *et al.*, 2018; Maurice *et al.*, 2018; Hernandez-Marin *et al.*, 2018).

Owing to its semi-arid climatic condition, groundwater recharge potential of rainfall is very low in the Singida aquifer, but it is very high in the Kimbiji humid coastal aquifer. This is because most of the meteoric water in dry areas is discharged through evapotranspiration and runoff, as reported by other studies (Maurice *et al.*, 2018; Hernandez-Marin *et al.*, 2018). On the contrary, in sedimentary humid groundwater basins, rainfall, lithology and land use are the most important factors in determining groundwater recharge potential, while lineament density is the least important parameter (Fashae *et al.*, 2013; Das & Pardeshi, 2018).

#### **4.2.2 Land Cover Change Assessment**

The LULC classification results show a significant decrease in forested land and woodland in the Kimbiji aquifer, while there has been a noticeable increase in grassland and cultivated areas (Table 26), possibly as a result of forest and woodland degradation. Areas covered by water bodies have decreased steadily from almost 1 to 0.2% from 1997 to 2016 in the Kimbiji aquifer. This went hand in hand with the decrease in wetland areas from 2% in 1997 to 0.2% in 2016. This signifies that during that period, 80% of the areas covered by water have been changed to another land cover/use, while 90% of the wetland areas were converted into other land covers as well. The tremendous expansion of agricultural activities from 1997 to 2016 (0.6 to 25%) in the Kimbiji study area, and the growth of urban areas, 1.5% in 1997 to 4% in 2016, can ostensibly be attributed to the observed decrease in other land covers, as shown in Table 26. The bushland maintained its equilibrium level in 2016 after an observed increase in 2008. Cultivated land has increased, as has the built-up area in the Kimbiji aquifer (Table 26).

**Table 26: Temporal land cover change matrix for the Kimbiji aquifer**

Class Type	1997		2008		2016	
	Area (km <sup>2</sup> )	Area (%)	Area (km <sup>2</sup> )	Area (%)	Area (km <sup>2</sup> )	Area (%)
Forest	729	14.71	439	8.86	357	7.20
Woodland	1422	28.71	979	19.77	312	6.29
Bushland	2011	40.60	2440	49.26	2019	40.75
Grassland	530	10.70	527	10.63	809	16.32
Water	49	0.99	35	0.71	11	0.23
Wetland	106	2.13	27	0.55	9	0.18
Cultivated land	31	0.62	354	7.15	1235	24.92
Built-up area	76	1.54	152	3.07	203	4.09
	4954	100	4954	100	4954	100

While woodland, forests, and wetland have been decreasing tremendously in the Singida aquifer, the cultivated land increased by 200% from 1997 to 2018. Purportedly, an increase in sunflower prices due to an increase in the market of sunflower oil, and increased processors are some of the possible reasons for this increase. The growth of the built-up area was almost constant (Table 27), increasing by 0.01% from 1997 to 2018. The decrease in forests and wetlands can be unwittingly attributed to the expansion of agricultural activities. Grasslands and bushlands have experienced some twisting dynamics, increasing from 1997 to 2005, and decreasing by 2018. The bushland was observed to decrease in 2018, but it did not reach the same level as of 1997 as it was the case for the Kimbiji aquifer. In the Singida aquifer, the cultivated land is most likely responsible for the conversion of other land covers such as forests, woodlands, bushes, and grasslands. The most enthralling scenario about the bushland in this study is that there has been an increase and a decrease afterwards in the two study areas. The factors for this observed similarity are most likely the same.

**Table 27: Temporal land cover change matrix for the Singida aquifer**

Class Type	1997		2005		2018	
	Area (km <sup>2</sup> )	Area (%)	Area (km <sup>2</sup> )	Area (%)	Area (km <sup>2</sup> )	Area (%)
Forest	586.40	5.63	463.49	4.45	144.12	1.38
Woodland	3039.31	29.17	1507.71	14.47	830.05	7.96
Bushland	1524.56	14.63	2380.89	22.85	2155.50	20.68
Grassland	2716.01	26.06	2882.39	27.66	2190.98	21.02
Water	26.77	0.26	46.18	0.44	51.48	0.49
Wetland	118.34	1.14	115.30	1.11	31.60	0.30
Cultivated land	2407.82	23.11	3022.95	29.01	4996.04	47.94
Built-up area	2.69	0.02	3.41	0.02	22.41	0.21
	10422	100	10422	100	10422	100

#### 4.2.3 Assessment of the Magnitude and Annual Rate of Land Cover Changes

The assessment of the magnitude and annual rate of land cover changes revealed negative and positive annual rates of land cover changes in both study areas. In the Kimbiji aquifer, for instance, the overall annual rate of change of forest cover was approximately 19 km<sup>2</sup>/year, with the highest annual rate of forest cover change (24.2 km<sup>2</sup>/year) occurring between 1997 and 2008 (Table 28). Forest cover dropped between 2008 and 2016, registering only 9.1 km<sup>2</sup> per year (Table 28). The biggest land cover change in the Kimbiji aquifer between 1997 and 2016 was a gain of cultivated land by almost four times, followed by built-up areas (-170%) and the grassland (-50%). The other land covers in the Kimbiji aquifer had emaciated, with woodland and forests being at the epicenter of land cover losses.

In the Singida aquifer, as it was for the Kimbiji aquifer, cultivated land increased by 2588.2 km<sup>2</sup> per year between 1997 and 2018 (Table 29), while the loss of woodland was the highest of all the land covers in the Singida aquifer (Table 29). Generally, there was a gain in the built-up area (0.9 km<sup>2</sup> per year), area covered by water, and bushes also increased by almost 29 km<sup>2</sup> per year. The other land covers (wetland, forest, woodland, and grassland) declined per year, as shown in Table 29 for the Singida aquifer. The spatiotemporal variation of land covers for the Kimbiji and Singida aquifers is shown in Fig. 56 (A = LULC for 1997 in Singida, B = LULC for 2005 in Singida, C = LULC for 2018 in Singida, D = LULC for 1997 in Kimbiji, E = LULC for 2008 in Kimbiji, F = LULC for 2016 in Kimbiji).

**Table 28: The magnitude of change, percentage of change, and the annual rate of change for land cover classes in the Kimbiji aquifer**

<b>Land Cover Type</b>	<b>MC (km<sup>2</sup>) (1997–2008)</b>	<b>PC (%) (1997–2008)</b>	<b>ARC (km<sup>2</sup>) (1997–2008)</b>	<b>MC (km<sup>2</sup>) (2008–2016)</b>	<b>PC (%) (2008–2016)</b>	<b>ARC (km<sup>2</sup>) (2008–2016)</b>	<b>MC (km<sup>2</sup>) (1997–2016)</b>	<b>PC (%) (1997–2016)</b>	<b>ARC (km<sup>2</sup>) (1997–2016)</b>
Forest	290.0	40	24.2	82.0	20	9.1	372.0	50	18.6
Woodland	443.0	30	36.9	667.0	70	74.1	1110.0	80	55.5
Bushland	-429.0	-20	-35.8	421.0	20	46.8	-8.0	0	-0.4
Grassland	3.0	0	0.3	-282.0	-50	-31.3	-279.0	-50	-14.0
Water	14.0	30	1.2	24.0	70	2.7	38.0	80	1.9
Wetland	79.0	70	6.6	18.0	70	2.0	97.0	90	4.9
Cultivated land	-323.0	-1040	-26.9	-881.0	-250	-97.9	-1204.0	-3880	-60.2
Built-up area	-76.0	-100	-6.3	-51.0	-30	-5.7	-127.0	-170	-6.4

**Table 29: The magnitude of change, percentage of change, and the annual rate of change for land cover classes in the Singida aquifer**

Land Cover Type	MC	PC	ARC	MC	PC	ARC	MC	PC	ARC
	(km <sup>2</sup> ) (1997–2005)	(%) (1997–2005)	(km <sup>2</sup> ) (1997–2005)	(km <sup>2</sup> ) (2005–2018)	(%) (2005–2018)	(km <sup>2</sup> ) (2005–2018)	(km <sup>2</sup> ) (1997–2018)	(%) (1997–2018)	(km <sup>2</sup> ) (1997–2018)
Forest	122.9	0.2	13.7	319.4	68.9	22.8	442.3	75.4	20.1
Woodland	1531.6	0.5	170.2	677.7	44.9	48.4	2209.3	72.7	100.4
Bushland	-856.3	-0.6	-95.1	225.4	9.5	16.1	-630.9	-41.4	-28.7
Grassland	-166.4	-0.1	-18.5	691.4	24.0	49.4	525.0	19.3	23.9
Water	-19.4	-0.7	-2.2	-5.3	-11.5	-0.4	-24.7	-92.3	-1.1
Wetland	3.0	0.0	0.3	83.7	72.6	6.0	86.7	73.3	3.9
Cultivated land	-615.1	-0.3	-68.3	-1973.1	-65.3	-140.9	-2588.2	-107.5	-117.6
Built-up area	-0.7	-0.3	-0.1	-19.0	-557.2	-1.4	-19.7	-733.1	-0.9



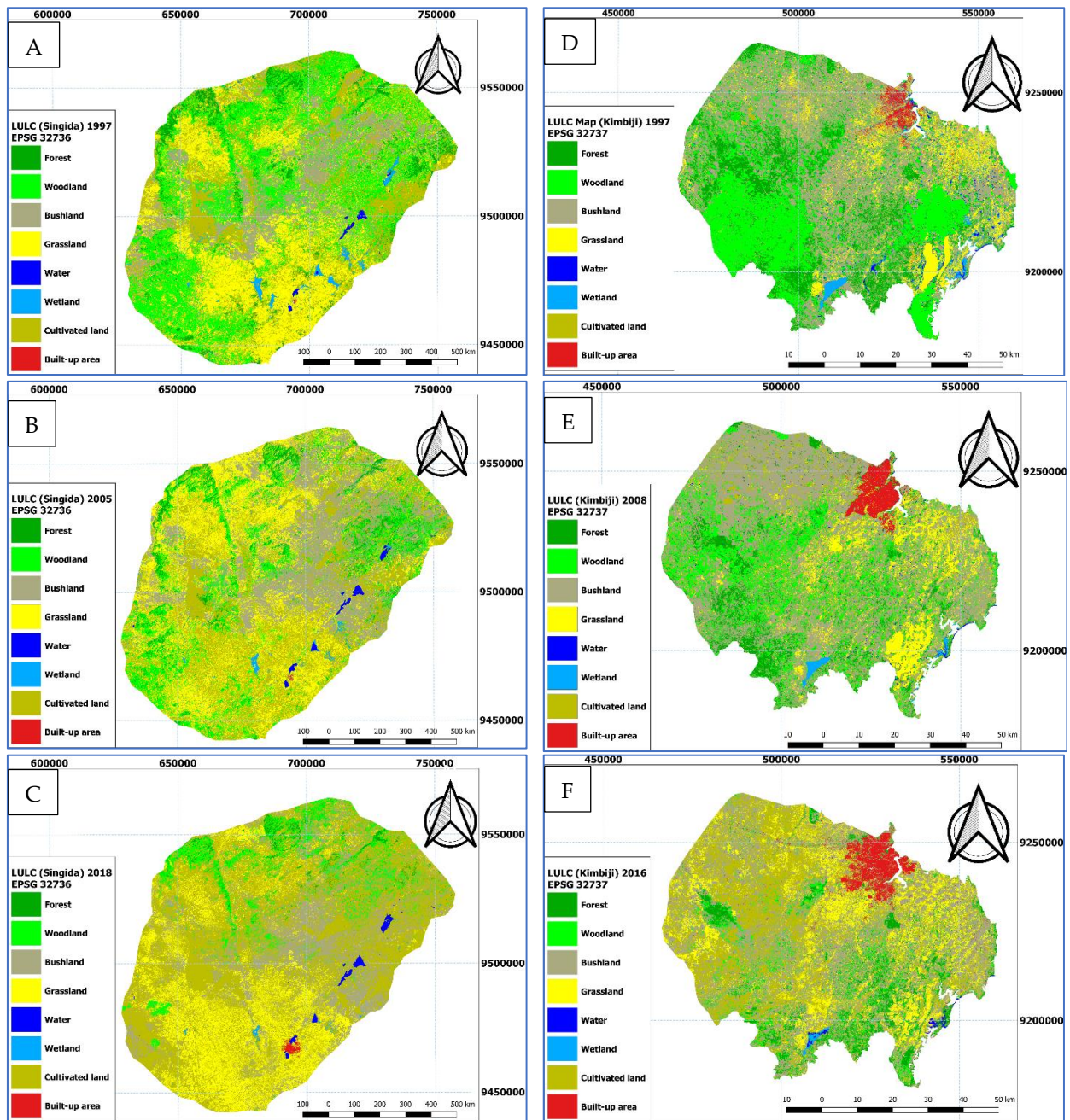


**Figure 56:** Land cover maps for the Kimbiji and Singida aquifers: (A) LULC for 1997 in Singida, (B) LULC for 2005 in Singida, (C) LULC for 2018 in Singida, (D) LULC for 1997 in Kimbiji, (E) LULC for 2008 in Kimbiji, (F) LULC for 2016 in Kimbiji

#### 4.2.4 Land Cover Classification Accuracy Assessment

The overall accuracies for 1997 was 87.3% and 85.7% for Kimbiji and Singida, respectively (Table 30). For the 2008, and 2016 of the Kimbiji aquifer, the overall accuracy was 88.0% and 86.5% respectively, while for 2005 and 2018 in Singida the accuracies were 89.2% and 93.6% respectively (Table 30). The overall accuracy of the 6 different maps represents the percentage of correctly classified pixels as reported in other previous studies (Banko, 1998; Liu *et al.*, 2016). The Kappa coefficients range between 0.81 to 0.89 for the Kimbiji aquifer and 0.79 to 0.86 for the Singida aquifer, indicating a perfect agreement between the classified land covers and the reference sites (ground control points). Reportedly, a minimum kappa threshold of 0.61 is an acceptable agreement threshold (Musa *et al.*, 2019). The land cover classification results in the study areas are in a perfect agreement with the established thresholds.

**Table 30: Accuracy assessment parameters for land cover classification results**

Accuracy Parameters	Kimbiji			Singida		
	1997	2008	2016	1997	2005	2018
Producer's Accuracy (%)	88.9	90.4	96.1	81.4	89.5	92.8
User's Accuracy (%)	82.3	92.3	91.4	78.6	91.1	88.6
Omission Error (%)	11.1	9.6	3.9	18.6	10.5	7.2
Commission Error (%)	16.7	7.7	9.6	21.4	8.9	11.4
Kappa Coefficient	0.81	0.83	0.89	0.79	0.85	0.86
Overall Accuracy	87.3	88.0	86.5	85.7	89.2	93.6

#### 4.2.5 The Weighted Curve Numbers for the Kimbiji and Singida Aquifers

Table 31 presents the weighted curve number results for the two study areas. The curve number for the Kimbiji aquifer is relatively smaller than the Singida aquifer, indicating a higher runoff potential in the Singida aquifer than the Kimbiji aquifer. The curve number in the Singida aquifer was observed to decrease between 1997 and 2005; then it slightly increased in 2018. Comparatively, there has been a quasi-stable CN in the Singida aquifer (74.2 in 1997, 73.64 in 2005, and 73.87 in 2018) but a steadily increasing CN for the Kimbiji aquifer (66.69 in 1997, 69.08 in 2008, and 71.42 in 2016). It was also observed that the forest cover in the Singida aquifer has a

higher curve number than the forest cover in the Kimbiji aquifer. This is due to the difference in the agroclimatological conditions that are considered for choosing a tabulated CN of a particular area. The area covered by water for the Kimbiji aquifer, mainly represented by rivers, has a relatively lower curve number as compared to the same class in the Singida aquifer. This is because the water bodies in the Singida aquifer are mainly lakes, while in the Kimbiji aquifer, the water bodies are mainly represented by rivers. Grassland for the Kimbiji aquifer has a relatively low runoff potential as compared to the same class in the Singida aquifer. This is again attributed to the difference in climate between the two study areas. The drier the area is, the higher the runoff potential is given that other factors remain the same.

The difference in the average curve number between dry and humid environments has been observed, especially for forests, woodlands, and grasslands (Table 31). The contribution of cultivated land to the weighted curve number kept on increasing due to an increase in the size of land under agricultural activities over time in the two study areas. It increased by three folds in the Kimbiji aquifer, while it doubled in the Singida aquifer (Table 31). However, the growth of built-up areas and their contribution to the curve number is fascinatingly exponential, despite the small size of the land under settlement. The contribution of built-up areas in the two aquifers was relatively meager due to the fairly small size of the land as compared to the size of the area under study. However, the runoff potential is higher in the Kimbiji aquifer than it is in the Singida aquifer. An insignificant change in the curve number for the Singida aquifer was observed, although there has been some noticeable land cover dynamics from 1997 to 2018, as depicted in the land cover maps. As for the Kimbiji aquifer, there has been an increase in the curve number (Table 31), which signifies a concurrent change in land covers, which hugely influences runoff in the study area.

**Table 31: Land cover related average and weighted curve number for the Kimbiji and Singida aquifers**

Land Cover Type	Land Cover Related CN II (Kimbiji)	Land Cover Related CN II (Singida)	Kimbiji			Singida		
			1997 CN <sub>i</sub>	2008 CN <sub>i</sub>	2016 CN <sub>i</sub>	1997 CN <sub>i</sub>	2005 CN <sub>i</sub>	2018 CN <sub>i</sub>
Forest	55	73	8.09	4.88	3.96	4.11	3.25	1.01
Woodland	60	77	17.23	11.86	3.77	22.46	11.14	6.13
Bushland	72	72	29.23	35.47	29.34	10.53	16.45	14.89
Grassland	69	71	7.39	7.34	11.26	18.50	19.64	14.93
Water	97	100	0.96	0.69	0.23	0.26	0.44	0.49
Wetland	85	85	1.81	0.47	0.15	0.97	0.94	0.26
Cultivated land	75	75	0.47	5.36	18.69	17.33	21.75	35.95
Built-up area	98	98	1.50	3.01	4.01	0.03	0.03	0.21
Weighted curve number			66.68	69.08	71.41	74.19	73.64	73.87

#### **4.2.6 Potential Evapotranspiration, Rainfall, Runoff, Groundwater Recharge, and Aridity Indices**

In Table 32 and Table 33, the results for rainfall, net rainfall, potential evapotranspiration, runoff, groundwater recharge, and aridity indices are presented for the different hydrological years for Kimbiji and Singida aquifers, respectively. The recharge and aridity indices correspond with the PET values calculated using the two temperature-dependent methods as explained earlier on. For the Kimbiji aquifer (Table 32), the PET values obtained using Penman–Monteith (PM) for the 1996/1997, 2007/2008 and 2015/2016 hydrological years were 1156.5, 1079.5, and 1143.9 mm/year, respectively, while for the Hargreaves–Samani (HS) method, the PET was found to be 1046.1, 1138.3, and 1204.4 mm/year for 1996/1997, 2007/2008, and 2015/2016 hydrological years, respectively. For the Singida aquifer (Table 33), the PM PET method resulted in 2083.3, 2053.6, and 1875.4 mm/year for 1996/1997, 2004/2005 and 2017/2018 hydrological years, respectively. The HS method produced relatively lower PET values for the Singida aquifer, which are 1839.4, 1814.7, and 1710.2 mm/year for 1996/1997, 2004/2005, and 2017/2018 hydrological years, respectively.

It was realized that the HS method overestimated the PET in the Kimbiji humid aquifer except for the 1996/1997 hydrological year (Table 32). This is possibly so due to the excessive rainfall received in that period due to the influence of the ENSO. Excessive rainfall lowers surface temperatures (maximum and minimum), which ultimately lowers the rates of evaporation and transpiration. This explains the high sensitivity of the HS method to changes in the maximum and minimum temperatures as compared to the PM method. In the Singida aquifer, the HS method underestimated the PET, while the PM overestimated it. Nevertheless, the difference in the calculated PET between the two methods is significantly higher in the Singida semi-arid aquifer than the observed difference in the Kimbiji aquifer.

**Table 32: Rainfall, PET, and Recharge for 1996/1997, 2004/2005, and 2017/2018 hydrological years for the Kimbiji Aquifer**

<b>Hydrologic Year (PET Method)</b>	<b>Rainfall (mm/year)</b>	<b>Runoff (mm/year)</b>	<b>PET (mm/year)</b>	<b>Recharge (mm/year)</b>	<b>Aridity Index</b>
1996/1997 (HS)	912.5	23.1	1046.1	258.5	0.9
1996/1997 (PM)	912.5	23.1	1156.5	214.4	0.8
2007/2008 (HS)	907.6	42.2	1138.3	206.8	0.8
2007/2008 (PM)	907.6	42.2	1079.5	190.0	0.8
2015/2016 (HS)	823.1	109.9	1204.3	128.7	0.7
2015/2016 (PM)	823.1	109.9	1143.9	109.6	0.7

**Table 33: Rainfall, PET, and Recharge for 1996/1997, 2004/2005, and 2017/2018 hydrological years for the Singida Aquifer**

Hydrologic Year (PET Method)	Rainfall (mm/year)	Runoff (mm/year)	PET (mm/year)	Recharge (mm/year)	Aridity Index
1996/1997 (HS)	831	46.6	1839.4	132.7	0.45
1996/1997 (PM)	831	46.6	2083.3	107.1	0.40
2004/2005 (HS)	550	12.2	1814.7	40.3	0.30
2004/2005 (PM)	550	12.2	2053.6	20.4	0.27
2017/2018 (HS)	551.9	21.9	1710.2	45.9	0.32
2017/2018 (PM)	551.9	21.9	1875.4	27.5	0.29

#### 4.2.7 Groundwater Recharge Response to Climate and Land Cover Dynamics

The graphing of the PET, rainfall, runoff, recharge, and net rainfall for the Kimbiji aquifer (Fig. 57) revealed that the PET calculated using HS method was more realistic than the PET derived from the PM method. The PM-based PET graph was observed to be above the rainfall and net rainfall graphs throughout the year, even during the rainfall season. This translates into a complete lack of natural recharge due to net rainfall being negative throughout the year. This is quite misleading because during rainfall, the PET values are lowered, and the net rainfall becomes positive, progressively leading to groundwater recharge. This has been demonstrated by the HS PET-based graphs. To that effect and for the sake of consistency, the HS-based PET values were adopted for the two study areas, disregarding the PM-based PET for recharge estimation. The use of the temperature-based Hargreaves–Samani model reaffirms what was reported previously by Allen *et al.* (1998), Romualdo *et al.* (2013) and Shiri (2015) that this model is the best alternative to the FAO56-PM model when only air temperature records are available.

Despite the variability in climate from 1997 to 2018, the aridity indices have confirmed that the Kimbiji aquifer is in a humid area while the Singida aquifer is found in the semi-arid area. The indices in the Kimbiji aquifer were found to range between 0.7 to 0.9 (Table 10) while in the Singida aquifer, they range between 0.3 to 0.45 (Table 11) despite the overestimation of PET by the PM method. According to previous studies (Jain *et al.*, 2010; Gao *et al.*, 2015), these indices are within the humid and semi-arid areas for the Kimbiji and Singida aquifers, respectively.

Figure 57 is a graph for the 1996/1997 hydrological year for the Kimbiji aquifer, which shows a time lag between rainfall and recharge. The response of runoff is spontaneous and directly related

to the observed rainfall event. While peak rainfall was observed in March, the water table fluctuation as a result of the March rainfall was realized in April. In the rainy season, the PET was also seen to decrease because of the reduced surface temperatures. This can also be observed in the short rainfall season between October and December (Fig. 57), where net rainfall, rainfall, and the PET responded to it. There was no discernible response of the aquifer in terms of natural groundwater recharge to the short rainfall season, nor did the runoff change.

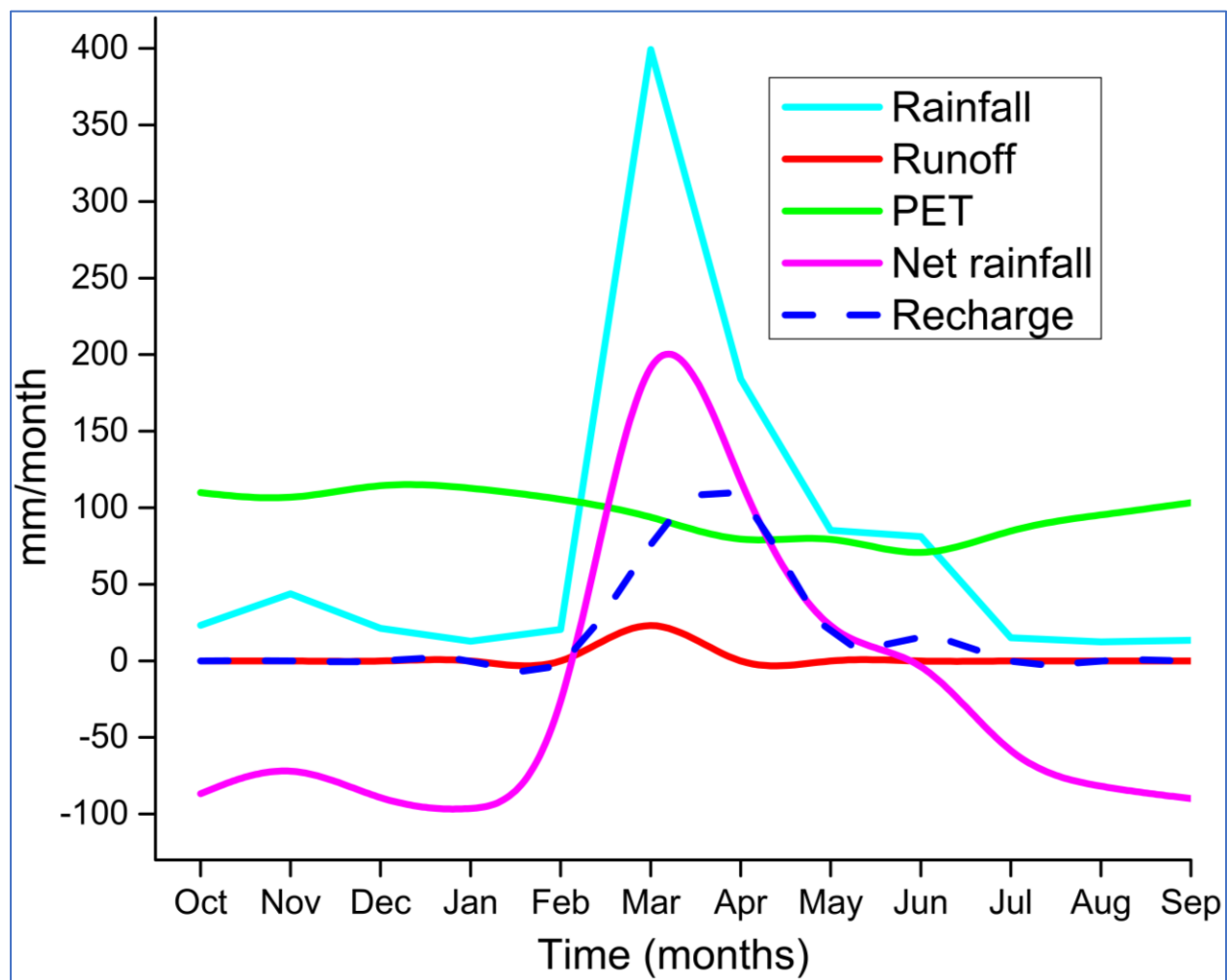
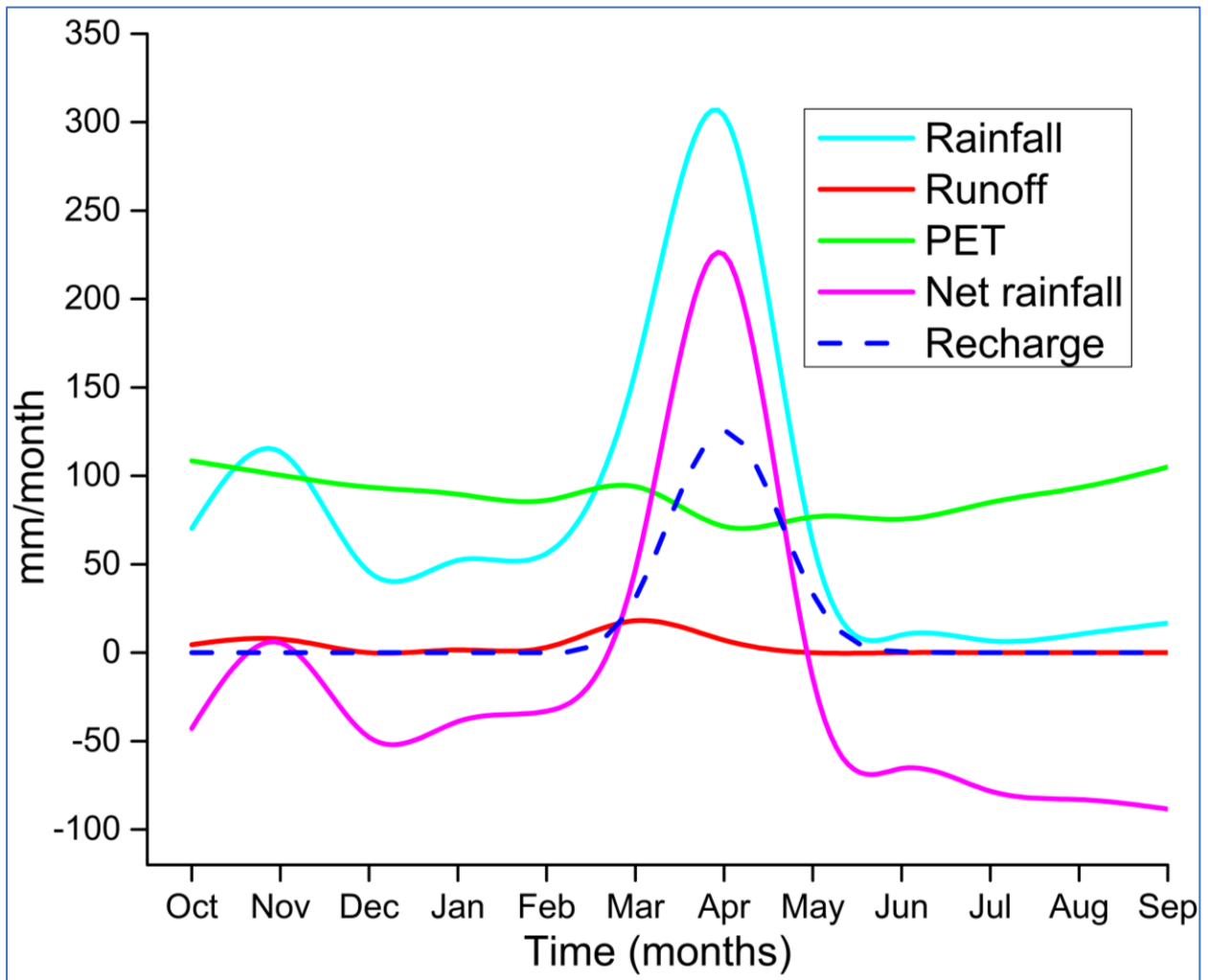


**Figure 57:** A 1996/1997 hydrological year graph of rainfall, runoff, PET, net rainfall, and aridity index in the Kimbiji aquifer

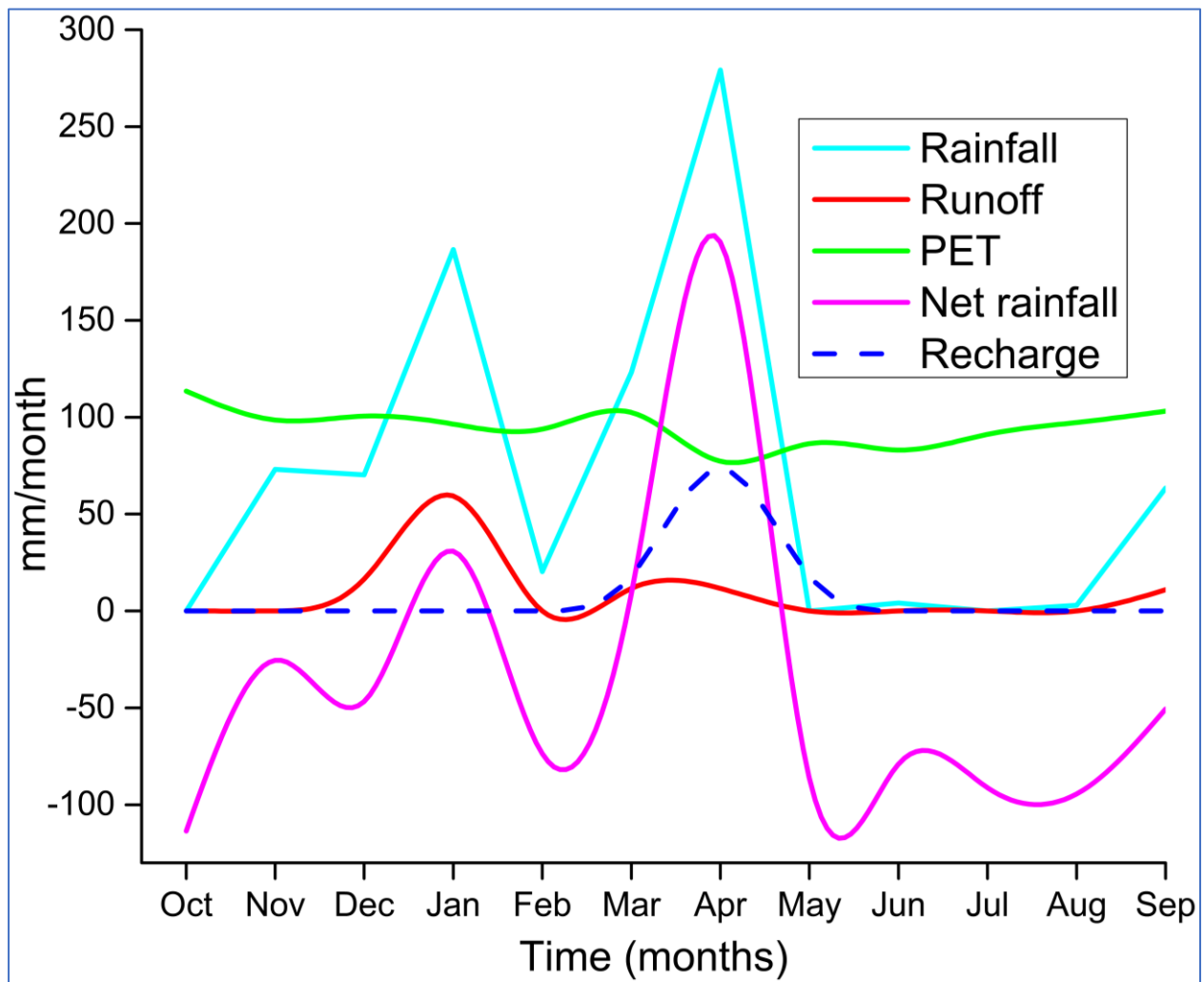
For the 2007/2008 hydrological year in the Kimbiji aquifer (Fig. 58), the time lag diminished as the peaks of rainfall, net rainfall, and recharge are all seen in April. Runoff responded to short rainfall events, unlike in the 1996/1997 hydrological year. Where rainfall exceeded the PET, the PET graph fell below the rainfall graph, while the opposite could be observed when the PET was higher than rainfall. From Fig. 57, it can be seen that in the 2007/2008 hydrological year, there was a prolonged dry spell between December and February, which could be the reason behind the aforesaid soil moisture deficit towards the long rainfall season in the 2007/2008 hydrological year.

The 2015/2016 hydrological year graph (Fig. 59) portrays a discernible response of runoff to the short rainfall event between October and December, with a dwarfed runoff hydrograph in the long rainfall season between March and May. However, recharge was relatively more pronounced than runoff in the long rainfall season, suggesting that in the 2015/2016 hydrological year, soil moisture was relatively higher towards the long rainfall season than in the 2007/2008 hydrological year.



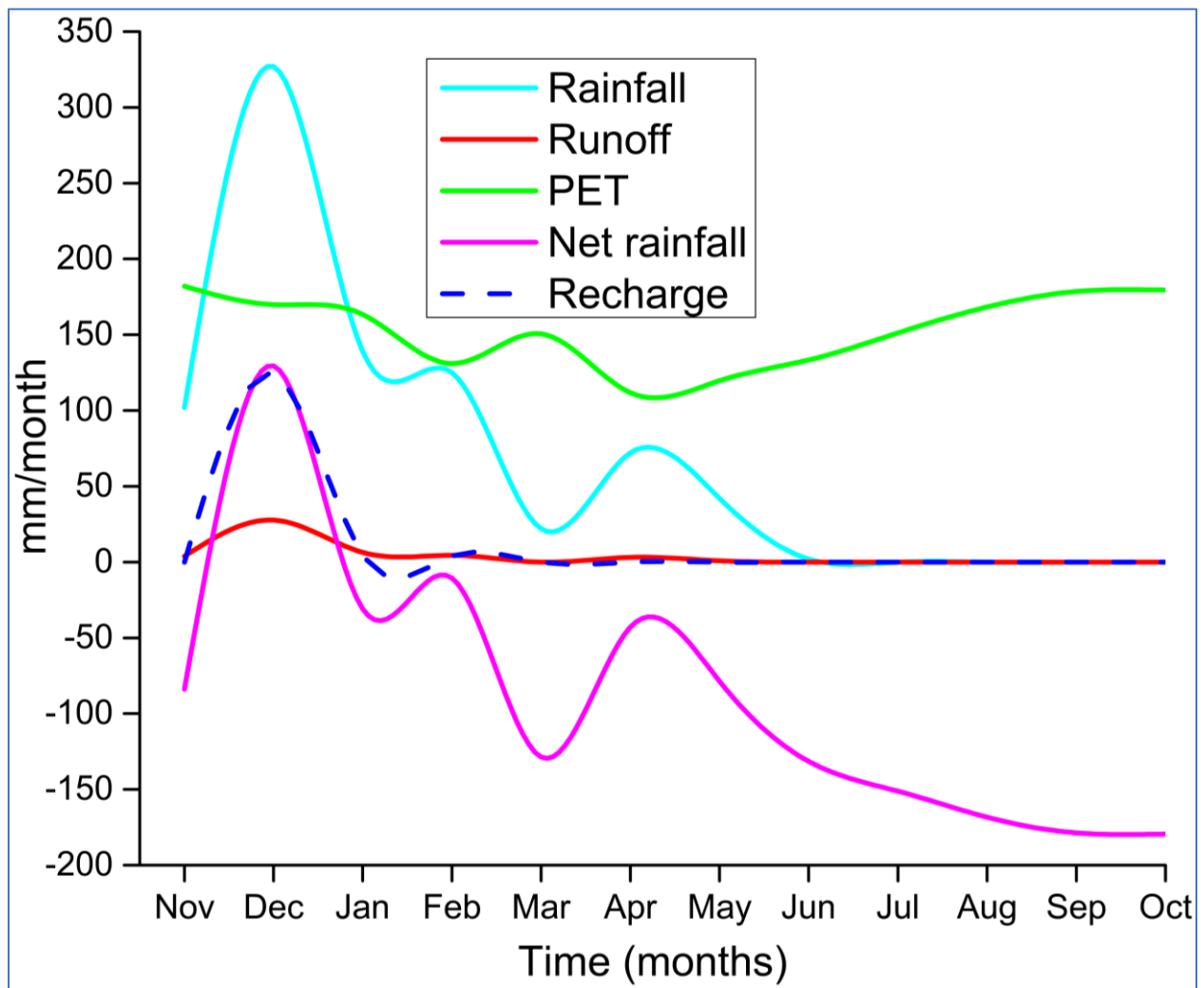


**Figure 58:** A 2007/2008 hydrological year graph of rainfall, runoff, PET, net rainfall, and aridity index in the Kimbiji aquifer



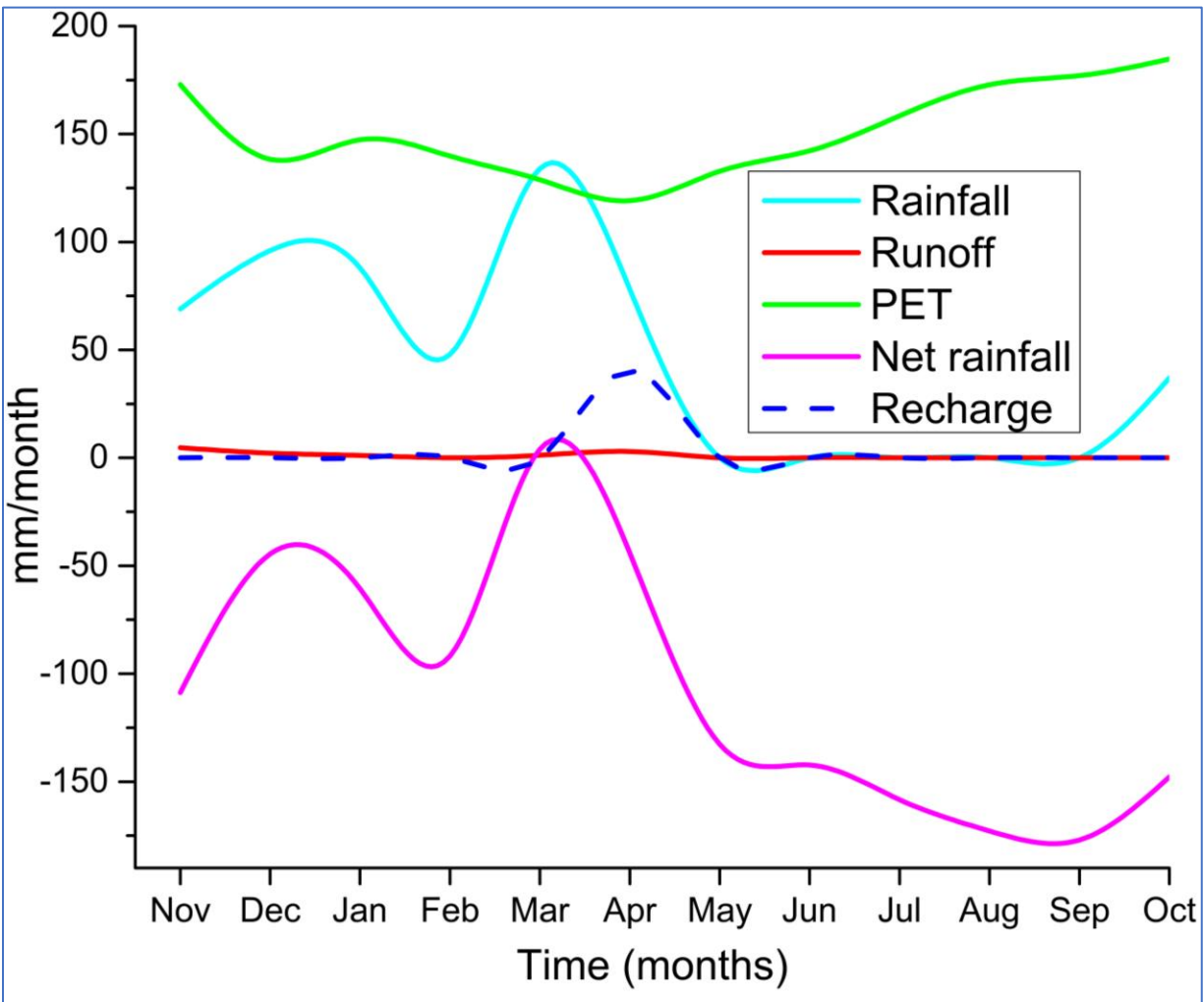
**Figure 59:** A 2015/2016 hydrological year graph of rainfall, runoff, PET, net rainfall, and aridity index in the Kimbiji aquifer

Figure 60 presents the 1996/1997 hydrological year graph for the Singida aquifer. Unlike other hydrological years, the 1996/1997 hydrological year showed a somewhat different trend of the response of recharge to rainfall and net rainfall. The peak rainfall was observed in December, as were the peaks of recharge and net rainfall. This is directly linked to the occurrence of the ENSO, where its major impact in Tanzania is above normal rainfall. This can also be justified from Table 11, where the Singida aquifer received unusually higher rainfall (i.e., 831 mm/year) in the 1996/1997 hydrological year.



**Figure 60:** A 1996/1997 hydrological year graph of rainfall, runoff, PET, net rainfall, and aridity index in the Singida aquifer

A time lag in natural groundwater recharge was quite ostensible in the 2005/2006 hydrological year for the Singida aquifer. A quasi-bimodal season has also been observed in this hydrological year (Fig. 61), suggesting a break in the rainfall season between January and March. This is typical of the areas that receive one long rainfall season (unimodal), where a dry spell in between the rainfall season happens. Due to a pronounced dry spell, soil moisture deficit was high to the extent of suppressing the runoff.



**Figure 61:** A 2005/2006 hydrological year graph of rainfall, runoff, PET, net rainfall, and aridity index in the Singida aquifer

The 2017/2018 hydrological year portrays (Fig. 62) a quasi-bimodal rainfall season in the Singida aquifer. This is because there seemed to be an extended dry spell in February 2017 that resulted in two separate peaks of rainfall events. This is normal for years that receive a relatively low amount of rainfall. The observed scenario is supported by the lack of ENSO teleconnections (Fig. 62). There was no sustained negative SOI, which signals ENSO-related rainfall in the East African region and Tanzania in particular. Runoff is observed to decrease with decreasing rainfall in the Singida aquifer. Despite this trend, recharge was also decreasing.

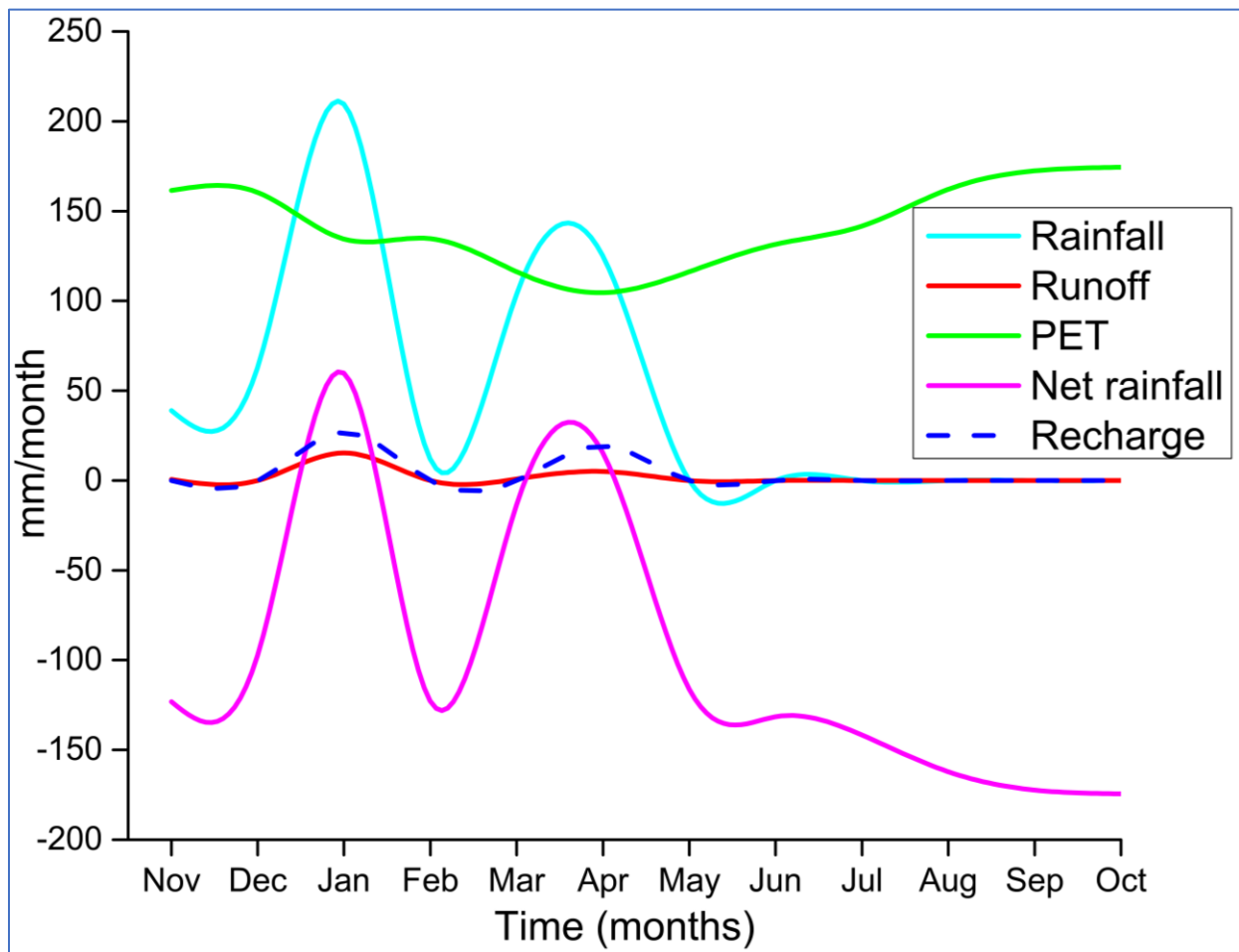


**Figure 62:** A 2017/2018 hydrological year graph of rainfall, runoff, PET, net rainfall, and aridity index in the Singida aquifer

In this study, it has been revealed that climate teleconnection through the Southern Oscillation Index is related to rainfall anomalies observed in the two study areas. During El Niño events, rainfall and groundwater recharge increased. The response of rainfall, and ultimately groundwater recharge, disregard the difference in climate and geology between the Kimbiji, humid, Neogene sedimentary aquifer and the Singida, semi-arid fractured, crystalline basement aquifer. The 1996/1997 and 2015/2016 hydrological years experienced sustained negative SOI values from March to December 1997, October to December 2015, and January to April 2016 (Fig. 63). The 2007/2008 hydrological year had little signs of the ENSO due to more sustained positive SOI values as compared to the rest of the years. The 1996/1997 and 2005/2006 hydrological years were observed to be under the influence of the ENSO more than the other hydrological years. This phenomenon had a noticeable impact on groundwater recharge.

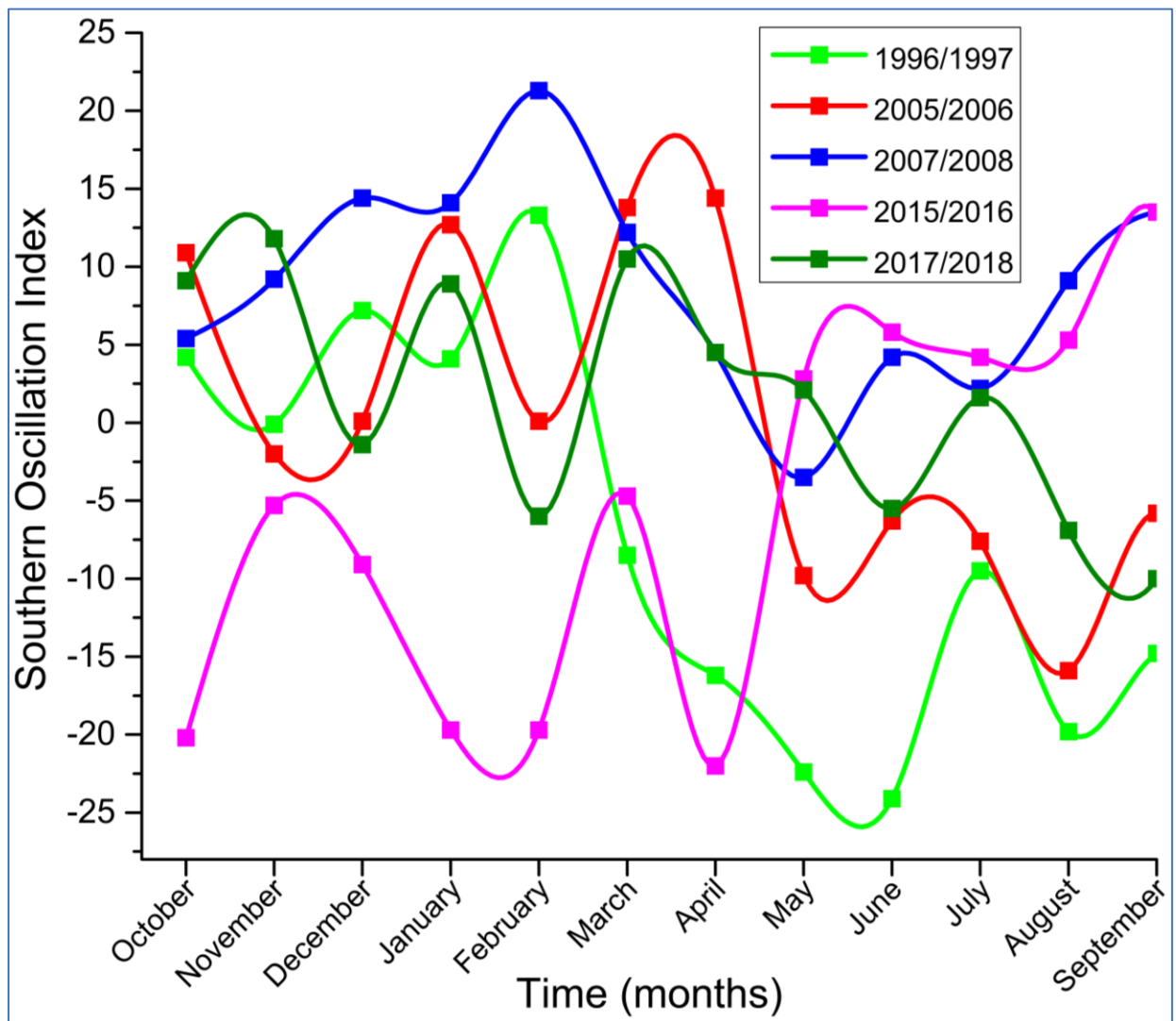


**Figure 63: The graph of Southern Oscillation Index for depicting the influence of El Nino and the Southern oscillation on rainfall**

There is an observed concomitant decrease in forests, woodlands and wetlands, while areas under cultivation and human settlements tend to increase in size over time in the two study areas. The observed trend has also been reported previously (Chilagane *et al.*, 2020). The decrease of forested land in the Kimbiji aquifer can be attributed more to human settlements while in the Singida aquifer, agricultural land has claimed a huge chunk of the forest land and woodlands as explained by the annual rate of change of forests and woodlands in the two study areas. The decrease of wetlands and grassland at the expense of increasing agricultural land has also been reported elsewhere (Majule, 2013). The expansion of urban areas at the expense of agricultural land was also reported in previous studies, highlighting some potential impacts of such land cover changes on water resources (Alawamy *et al.*; 2020; Tena *et al.*; 2019; Waylen *et al.*; 2014; Näschen *et al.*, 2019).

Reportedly, the absence of or the weakness of institutions, including inept accountability are some of the factors which encourage the local people to engage in forest encroachment of forests by

either clearance of vegetation cover for agricultural expansion or by cutting trees for gathering firewood. This was argued by previous researchers (Hibajene & Ellegard, 1994; Eldiabani *et al.*, 2014). Charcoal making for cooking and business can as well be attributed to the loss of forest cover in the two study areas as discussed previously (Alawamy *et al.*, 2020; Waylen *et al.*, 2014). Forests are also affected by forest fires, which cause excessive forest and woodland degradation due to anthropogenic activities (Eldiabani *et al.*, 2014). Other researchers (Alawamy *et al.*, 2020; Tena *et al.*, 2019; Waylen *et al.*, 2014) reported that the decrease of forest and woodland can be associated with the conversion of forest land to built-up areas (in the Kimbiji aquifer) and farmland (in the Singida aquifer).

The study has revealed that Natural groundwater recharge is affected by the dynamics of land covers as well as climate despite the differences in climate and geology. There is a decreasing trend of recharge corresponding with a decreasing trend of rainfall. Moreover, an increasing trend in curve number has been observed in the Kimbiji aquifer, corresponding to the increase in runoff. This is also affecting groundwater recharge negatively. The PET has also been observed to increase in the two aquifers regardless of their difference in climate. Therefore, the increase in PET and curve number justifies the progressive decrease in groundwater recharge with time, representing climate and landcover factors, respectively.

Nevertheless, the effect of climate variability to groundwater recharge is more prominent in the Singida aquifer while in the Kimbiji, a combined effect of climate variability and land cover changes to groundwater recharge has been observed. In the Kimbiji aquifer, runoff is increasing steadily, while other parameters showed a similar trend as those of the Singida aquifer. Recharge kept on decreasing as a result of increasing PET due to an increase in surface temperatures, both maximum and minimum. In the Singida aquifer, the weighted curve number stabilized with time while the recharge was observed to decrease. This enlightens on the influence of rainfall variability on groundwater recharge other than land cover changes in the dry-semi-arid Singida aquifer. This also informs of the presence of local recharge as an important component of groundwater flow systems in the semi-arid Singida aquifer.

The ENSO's contribution to observed groundwater recharge cannot be ignored in the two aquifers despite their contrast in climate and geology. In the Kimbiji aquifer, runoff increased with decreasing rainfall for the 1996/1997, 2007/2008, and 2015/2016 hydrological years. In the Singida aquifer, runoff fluctuated with fluctuating rainfall. The 1996/1997 hydrological year in the Singida aquifer experienced high rainfall, attributable to the observed El Nino and the Southern Oscillation (ENSO) phenomenon. This resulted into almost 47 mm/year of runoff. In the 2004/2005

hydrological year, runoff dropped tremendously to 12.2 mm/year, which reflects a tremendous drop in the annual rainfall in that year to 550 mm/year in the Singida aquifer. The fluctuation of recharge, apart from other factors, followed the fluctuation of PET and rainfall.

Despite the difference in climate and geology, groundwater recharge followed a positive trend as rainfall in the two study areas. This reiterates what was reported earlier on by Oke *et al.* (2014). This study has also proved that decreasing rainfall contributes to decreasing groundwater recharge as pointed out by other researchers (Vazquez-Amábile & Engel, 2015). During the dry season no rainfall surplus was observed and it obeyed this rule of thumb that  $([P - R_o] - PET < 0)$ , and there was no groundwater recharge in all the two basins regardless of the difference in climate and geology. Groundwater recharge occurred whenever rainfall, minus runoff was larger than the PET, obeying the Equation  $([P - R_o] - PET > 0)$  as discussed previously (Bakundukize *et al.*, 2011; Mjemah *et al.*, 2011; Lwimbo *et al.*, 2019), and it usually happened during the rainy season. This is because, during the rainy season, the net rainfall is usually positive. This observation confirms the fact that there is a local flow component in each of the two study areas albeit different in magnitude.

The 1996/1997 and 2005/2006 hydrological years were observed to be under the influence of ENSO more than the other hydrological years. This phenomenon had a noticeable impact on groundwater recharge. It has been noticed that the climate of the two basins, albeit contrasting, is modulated by the El Niño-Southern Oscillation (ENSO) as it has been observed in previous related studies (Chanda *et al.*, 2018). The ENSO has a significant influence on groundwater recharge in both, humid and semi-arid areas as pointed out previously (Ward *et al.*, 2016). The most recent strong El Niño of 1997/1998 was reflected in the magnitude of annual rainfall as well as the annual groundwater recharge in the two study areas. The moderate La Niña which developed slowly during 2007 could possibly be associated with reduced rainfall as well as a decrease in recharge in both study areas. Despite their difference in climate, the response to episodic climate systems (ENSO in particular) has been noticeable.

The ENSO's contribution to observed groundwater recharge cannot be ignored in the two aquifers despite their contrast in climate and geology. In addition, it was revealed that in the Kimbiji aquifer, runoff increased with decreasing rainfall for the 1996/199, 2007/2008 and 2015/2016 hydrological years. In the Singida aquifer, runoff fluctuated with fluctuating rainfall. The 1996/1997 hydrological year in the Singida aquifer experienced high rainfall, attributable to the observed El Niño and the Southern Oscillation (ENSO) phenomenon. This resulted into almost 47 mm/year of run off. In the 2004/2005 hydrological year, runoff dropped tremendously to 12.2 mm/year, which



reflects a tremendous drop in the annual rainfall in that year to 550 mm/year in the Singida aquifer. The fluctuation of recharge, apart from other factors, followed the fluctuation of PET and rainfall.

The effect of urbanization on groundwater recharge has been revealed through urban growth in the Kimbiji aquifer where a growth in built-up area resulted into an increase in curve number. In the Singida aquifer where urban growth was insignificant compared to other land covers showed an insignificant increase in curve number. The findings of this study which relate the response of land cover changes to an increase in surface runoff, which ultimately was found to affect groundwater recharge are in line with what was reported previously (Natkhin *et al.*, 2013; Nobert *et al.*; 2012; Notter *et al.*, 2013; Wambura *et al.*, 2015; Mutayoba *et al.*, 2018; Chilagane *et al.*, 2020; Alawamy *et al.*, 2020; Tena *et al.*, 2019; Waylen *et al.*, 2014). Since surface runoff is linked to changes in land covers through the CN parameter that change in some land covers has had a huge impact on changes of runoff, and groundwater recharge thereof. The implication of land cover changes on water resources is quite discernible, albeit the concentration has been on surface water resources. The findings are also in line with what has been reported by other researchers (Tena *et al.*, 2019 and Näschen *et al.*, 2019), that various ecosystems are persistently being converted into agricultural land to feed the growing populations. Nevertheless, the impacts of such changes on water resources have hugely been ignored. This is likely to threaten the sustainability of water resources and socio-ecological systems at large.

The PM-based PET in the Singida aquifer showed that precipitation can no longer meet the evapotranspiration demand throughout the year. Thus, the unmet amount of water required by the evapotranspiration demand is increasingly taken from the soil moisture storage until it is fully exhausted. This does not represent reality as local recharge is eminently happening in the Singida aquifer. Overestimation of PET by various methods have been highlighted previously and the ensuing risk of generating incorrect recharge estimates thereof has been hinted too (Bakundukize *et al.*, 2011). This study reiterates what has been reported previously on the possibility of underestimation and overestimation of PET, which is an important parameter in groundwater recharge estimation using soil moisture balance methods.

Time lags between rainfall and recharge are so prominent in the 2004/2005 and 2017/2018 hydrological years but less prominent in the 1996/1997 hydrological year in the Singida aquifer. Else, recharge in the other two hydrological years had responded to rainfall in the same month as the peak rainfall (April). For the Kimbiji aquifer, time lags between rainfall and recharge are not so prominent, except for the 1996/1997 hydrological year where rainfall peak was observed in March and the response of the aquifer to rainfall was observed in April. This observed difference

in time lags between recharge and rainfall in the two aquifers explains the influence of geology and soil. The ENSO phenomenon in the 1996/1997 hydrological year offsets the influence in geology in time lag between rainfall and recharge. This study has found that the two aquifers respond to rainfall events differently due to their difference in geology.

### **4.3 Simulation of the Effect of the Difference in Climate and Geology on the Magnitude of (Nested) Local and Regional Groundwater Flow Fluxes and Basin Water Balance in Basins with Contrasting Climate and Geology**

#### **4.3.1 Numerical Modelling of Nested Groundwater Flow Systems**

##### **(i) Groundwater Model Calibration Results**

The standard error between the observed data and the fitted regression line in the Kimbiji aquifer was found to be 0.04 while the root mean square error (RMSE) was 16.3 m. Further, almost 95% of the variation of simulated heads was explained by the fitted model. This is also justified by the high (98%) positive correlation between observed and simulated groundwater heads in the Kimbiji aquifer. As for the Singida aquifer, 82.5% of the variation of the simulated heads is explained by the model, owing to high positive correlation between observed and simulated heads (91%). The root mean square error of the data is 22 m while the standard error stands at 0.07. All the reported regression model parameters are statistically significant at  $p=0.05$ , with levels of significance being  $<0.001$  for the two study areas. The apparently high correlation coefficients and coefficients of determination suggest good model calibration for the two test cases. This reiterates what has been reported previously by Yidana *et al.* (2019).

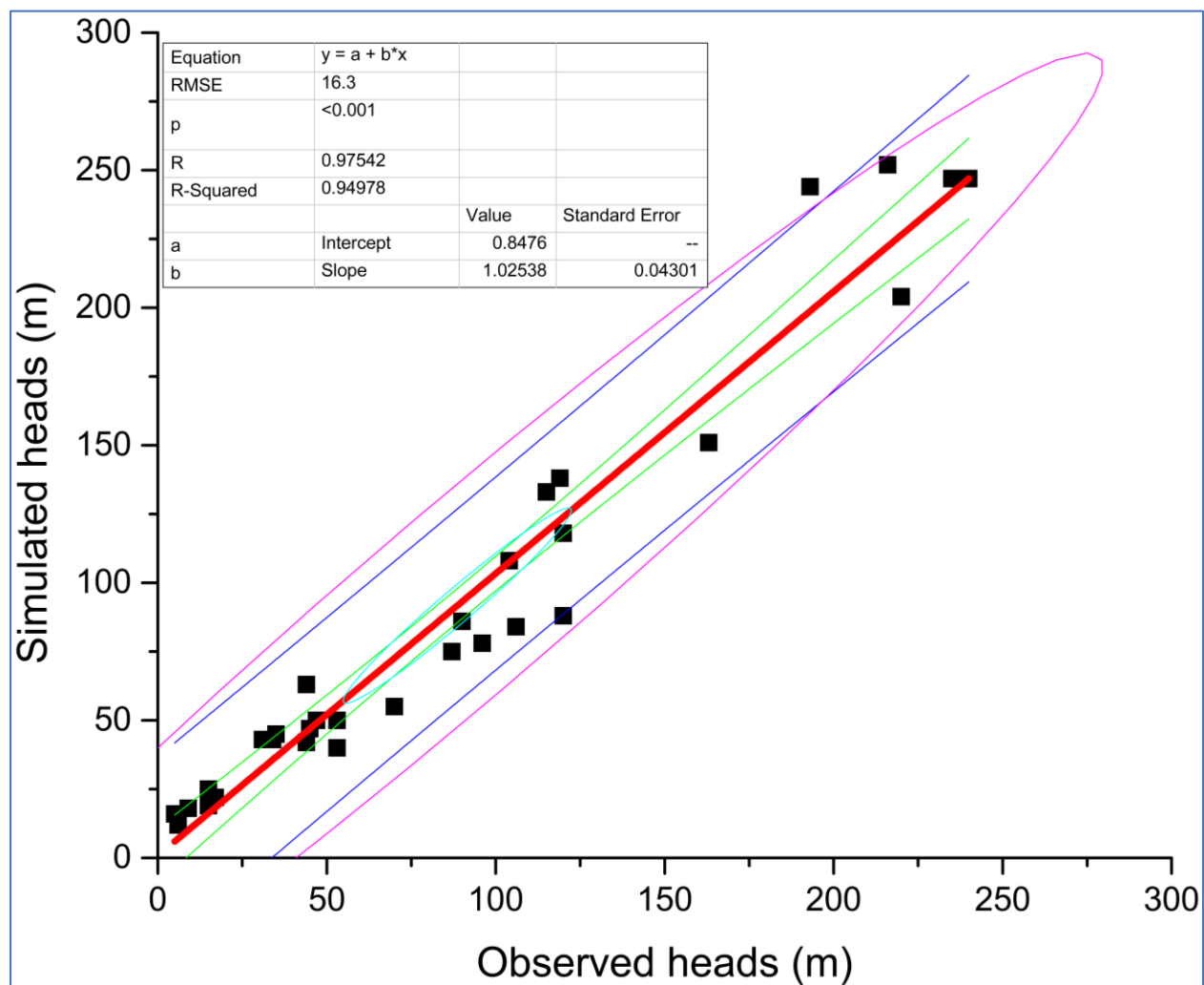


**Figure 64: A calibration plot for the Kimbiji aquifer**

The scatter plots (Fig. 64 & Fig. 65) show a confidence band (green lines), which represent the uncertainty in an estimate of a regression curve. Similarly, a confidence band in the fitted line plot depicts the upper and lower confidence bounds for all groundwater head data on a fitted line within the range of the groundwater head data. The confidence bands can be seen above and below the fitted regression line (red colour), portraying confidence intervals for the mean response of the predictor (observed groundwater head) value. Further, a prediction band (blue line) accounts for the uncertainty in estimating the mean, including the random variation of the individual groundwater head values. Prediction bands give an idea of where you can expect the groundwater head data to lie. Given the 95% confidence level, it is therefore expected that all data points lie within the prediction band limits. In the same scatter plots (Fig. 64 & Fig. 65), there are confidence ellipses (purple coloured line) which serve as visual indicators of correlations. The confidence ellipse approximates a region containing a specified percentage of the population and defines the region that contains 95% of all samples that can be drawn from the underlying distribution.

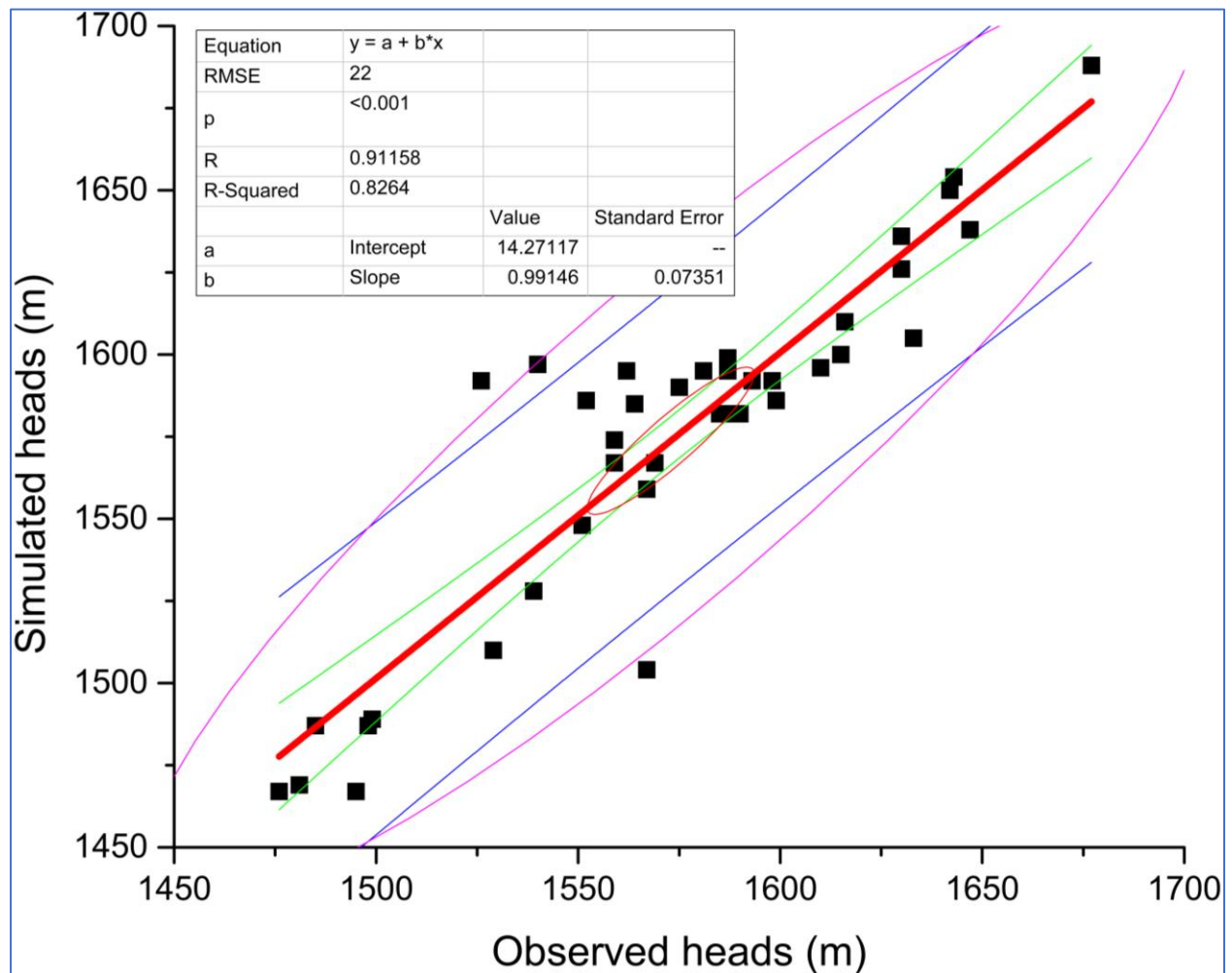


**Figure 65: A calibration plot for the Singida aquifer**

Figure 66 and 67 describe the relationship between observed heads and simulated heads for the Kimbiji aquifer and the Singida aquifers, respectively. It can be observed that there has been slight overestimation of the groundwater heads by models (red graph) as compared to the observed heads (blue graph). Further, there are slight deviations of the simulated heads from the observed ones for both study areas. A notable overestimation of simulated head in the Kimbiji aquifer is seen at borehole number 8 and borehole number 22 (Fig. 66). As for the Singida aquifer, Fig. 67 shows that there is overestimation at borehole number 15, 25, 34 and 35.

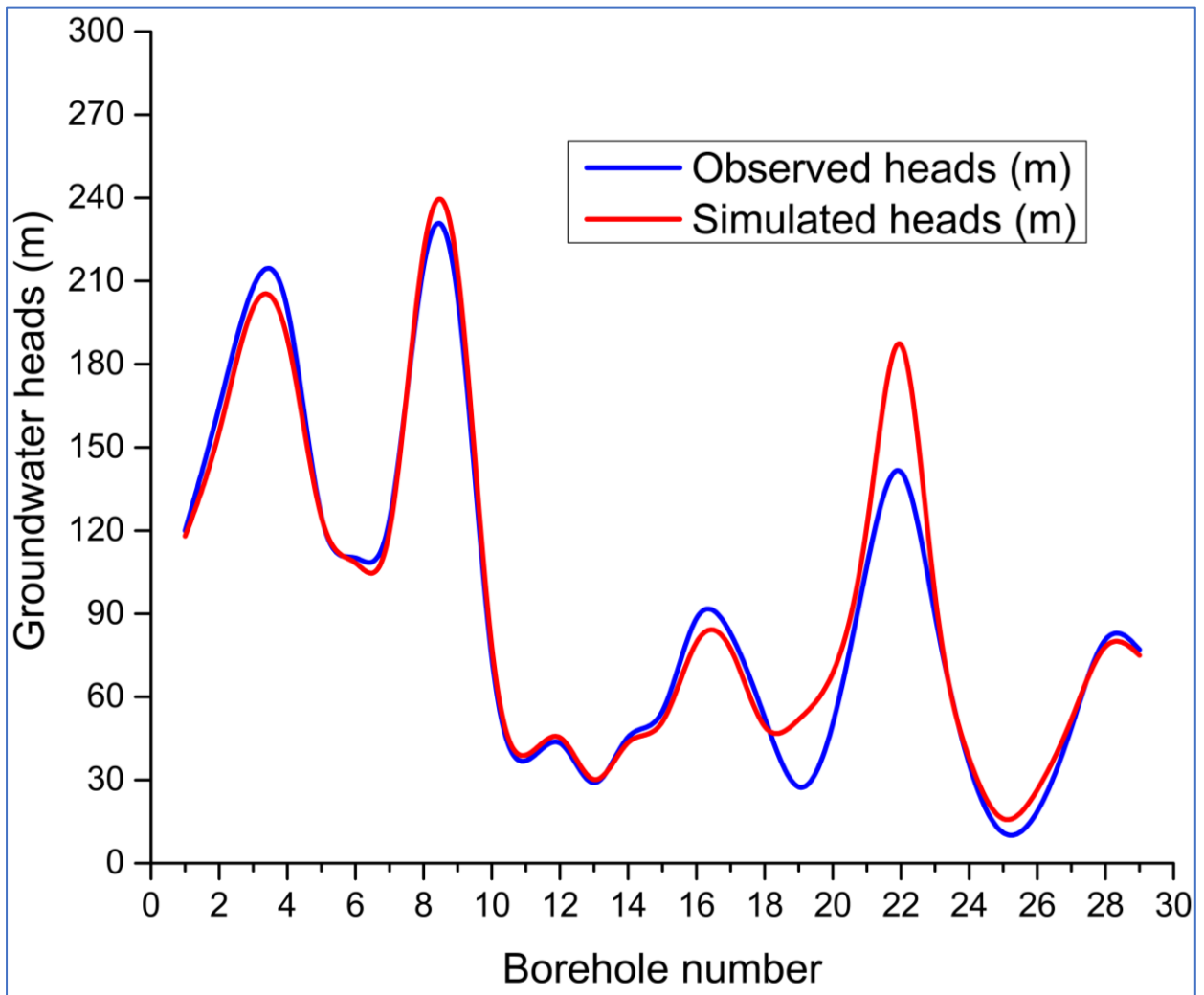


**Figure 66:** A comparison of simulated hydraulic heads and observed hydraulic heads for the Kimbiji aquifer

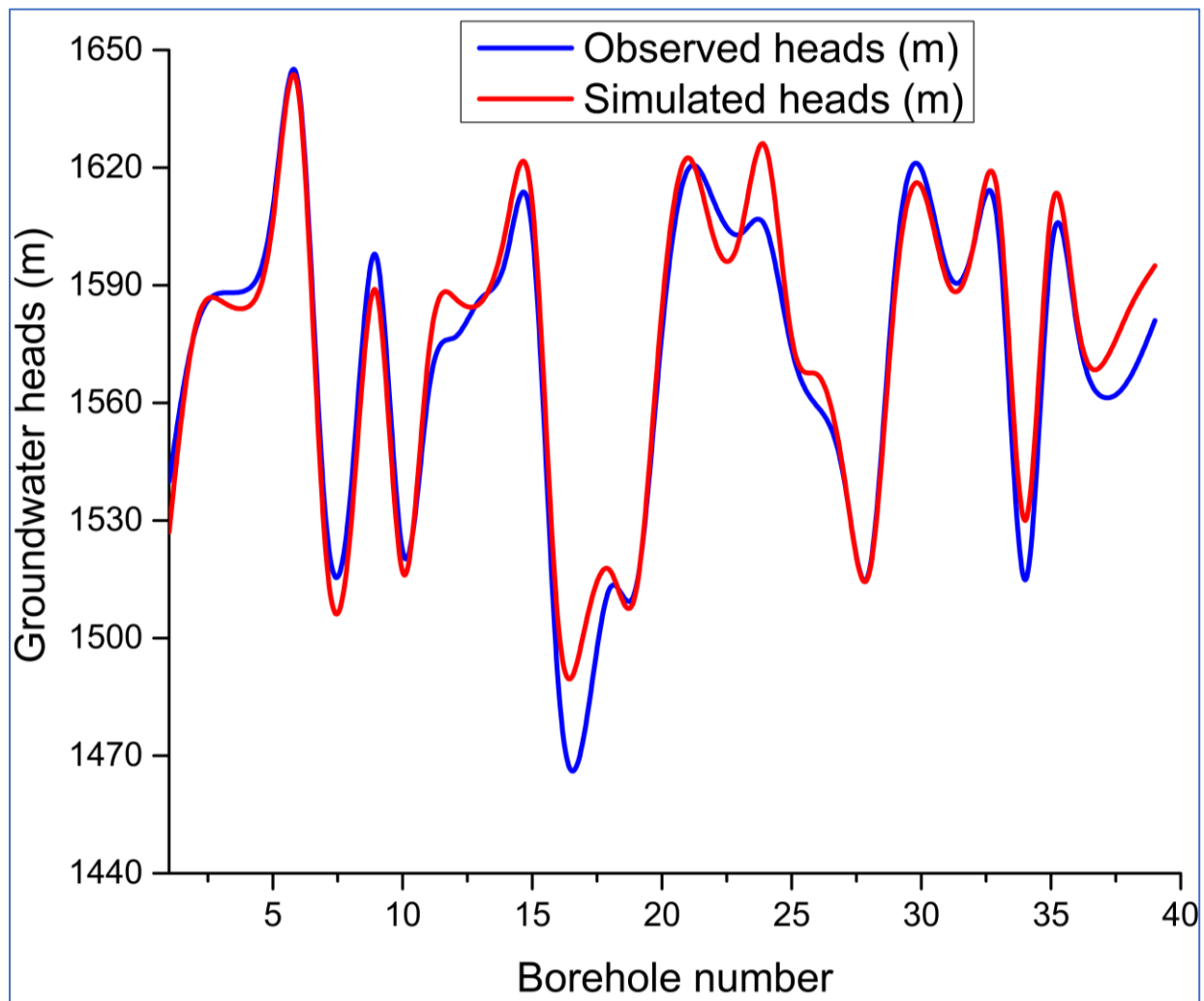


**Figure 67:** A comparison of simulated hydraulic heads and observed hydraulic heads for the Singida aquifer

**(ii) Results of Simulation of Nested Groundwater Flow Systems in the Kimbiji Aquifer**

A steady state groundwater simulation observed a total inflow of  $1.9578 \text{ m}^3/\text{s}$  in the upper layer in the Kimbiji aquifer (Table 34) while the modelled outflow was  $1.9579 \text{ m}^3/\text{s}$ . This makes the difference of  $-9.99 \times 10^{-5} \text{ m}^3/\text{s}$  between inflows and outflows. The discrepancy, which is the groundwater budget performance parameter was  $-1\%$ , indicating slightly more outflow than the inflow. The losing river reaches contribute  $0.64 \text{ m}^3/\text{s}$  to the aquifer while the deep semi-confined aquifer feeds the upper unconfined aquifer at a rate of  $1.32 \text{ m}^3/\text{s}$ . Groundwater recharge into the aquifer is approximately  $0.02 \text{ m}^3/\text{s}$ . The main outflows in the upper aquifer are baseflow to rivers ( $0.82 \text{ m}^3/\text{s}$ ), wells tapped/screened in the upper unconfined aquifer ( $0.48 \text{ m}^3/\text{s}$ ), and an exchange with the deep aquifer, which takes about  $0.66 \text{ m}^3/\text{s}$ . The layout of the inflows and outflows of the upper unconfined layer in the Kimbiji aquifer is schematized in Fig. 68.

**Table 34: The water balance for the upper unconfined layer in the Kimbiji aquifer**

	Well	Recharge	Lower Aquifer	Regional flow	River	Total
	m <sup>3</sup> /s	m <sup>3</sup> /s	m <sup>3</sup> /s	m <sup>3</sup> /s	m <sup>3</sup> /s	m <sup>3</sup> /s
Inflows	0	2.0227 x 10 <sup>-2</sup>	1.3176	0	0.6402	1.9578
Outflows	0.481	0	0.6555	0	0.82	1.9579
Inflows-Outflows						-9.99 X 10 <sup>-5</sup>
Discrepancy (%)						-0.01

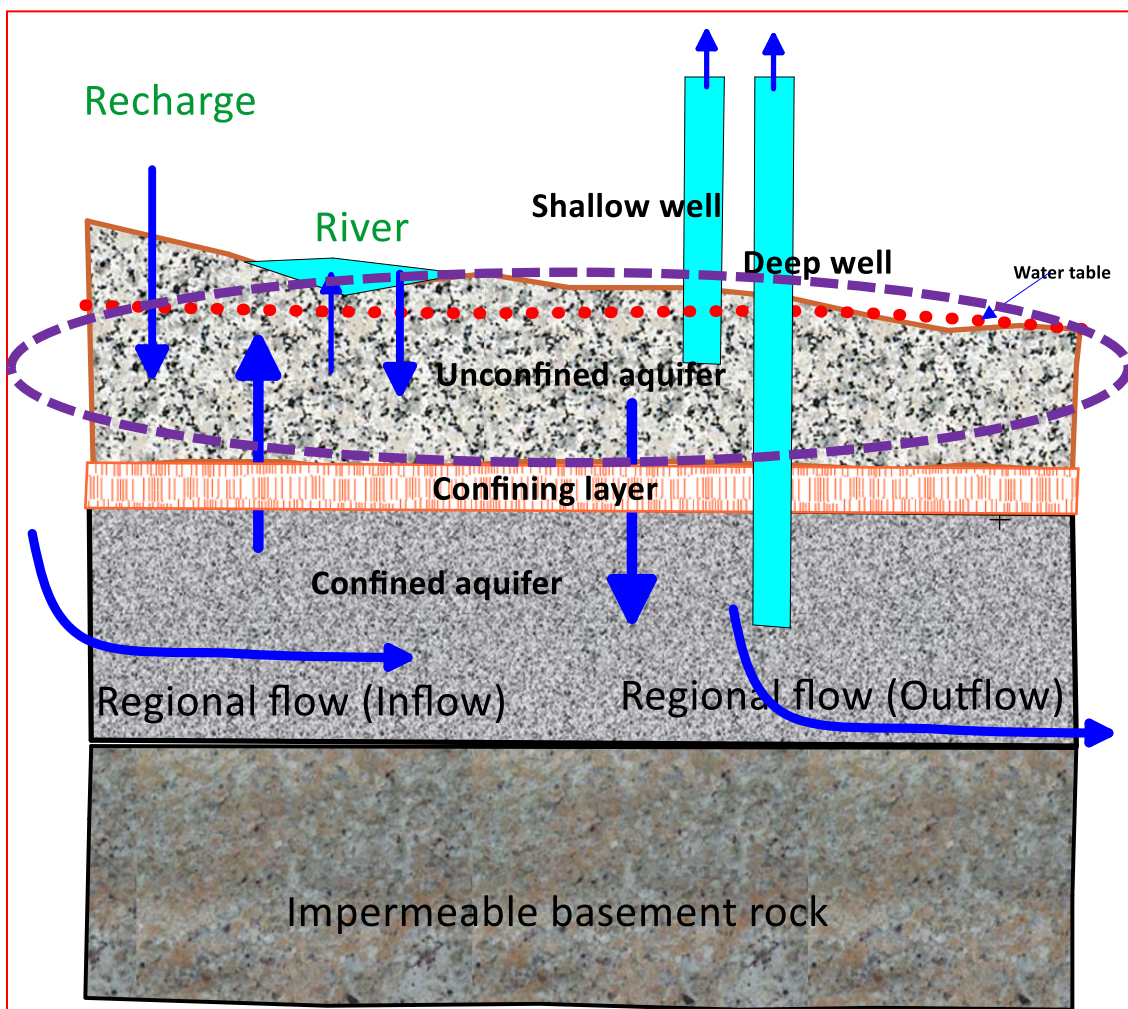


**Figure 68: The layout of the inflows and outflows of the upper unconfined layer in the Kimbiji aquifer (Author's construction)**

There is a regional flow flux of about 1.84 m<sup>3</sup>/s into the lower semi-confined layer of the Kimbiji aquifer (Table 35), as well as 0.66 m<sup>3</sup>/s from the upper unconfined aquifer. These two sources account for a total flux of 2.49 m<sup>3</sup>/s. The main outflows are baseflow to the ocean (0.69 m<sup>3</sup>/s), an exchange with the upper unconfined aquifer (1.3 m<sup>3</sup>/s), and deep aquifer withdrawals by pumping

(0.48 m<sup>3</sup>/s). The difference between inflows (2.4906 m<sup>3</sup>/s) and outflows (2.4913 m<sup>3</sup>/s) in the deep semi-confined layer is -6.46 x 10<sup>-4</sup> m<sup>3</sup>/s, which corresponds to a discrepancy of -0.03. This value is lower than an absolute threshold of 5%. The negative sign connotes a slightly higher amount of outflow fluxes as compared to the inflow fluxes.

There is a noticeable groundwater-surface water interaction in the Kimbiji aquifer as rivers contribute an appreciable amount of water, but also take some water in certain reaches of the three rivers. Moreover, apart from aquifer discharges into rivers, groundwater also discharges into the Indian ocean as baseflow. Nonetheless, regional flow fluxes make up 74% of the total inflows into the Kimbiji coastal Neogene aquifer (Table 35). Therefore, only 26% of the inflows are made up of the local flow systems, comprising of river and rainfall-based local recharge. This is a typical representation of regional flow dominated aquifer system. Figure 69 provides the layout of the inflows and outflows of the lower semi-confined layer in the Kimbiji aquifer.

**Table 35: The water balance for the lower semi-confined layer in the Kimbiji aquifer**

	<b>Well</b>	<b>Recharge</b>	<b>Upper aquifer</b>	<b>Regional flow</b>	<b>River</b>	<b>Total</b>
	<b>m<sup>3</sup>/s</b>	<b>m<sup>3</sup>/s</b>	<b>m<sup>3</sup>/s</b>	<b>m<sup>3</sup>/s</b>	<b>m<sup>3</sup>/s</b>	<b>m<sup>3</sup>/s</b>
Inflows	0	0	0.6555	1.8352	0	2.4906
Outflows	0.481	0	1.3176	0.6927	0	2.4913
Inflows-Outflows						-6.46 X 10 <sup>-4</sup>
Discrepancy (%)						-0.03



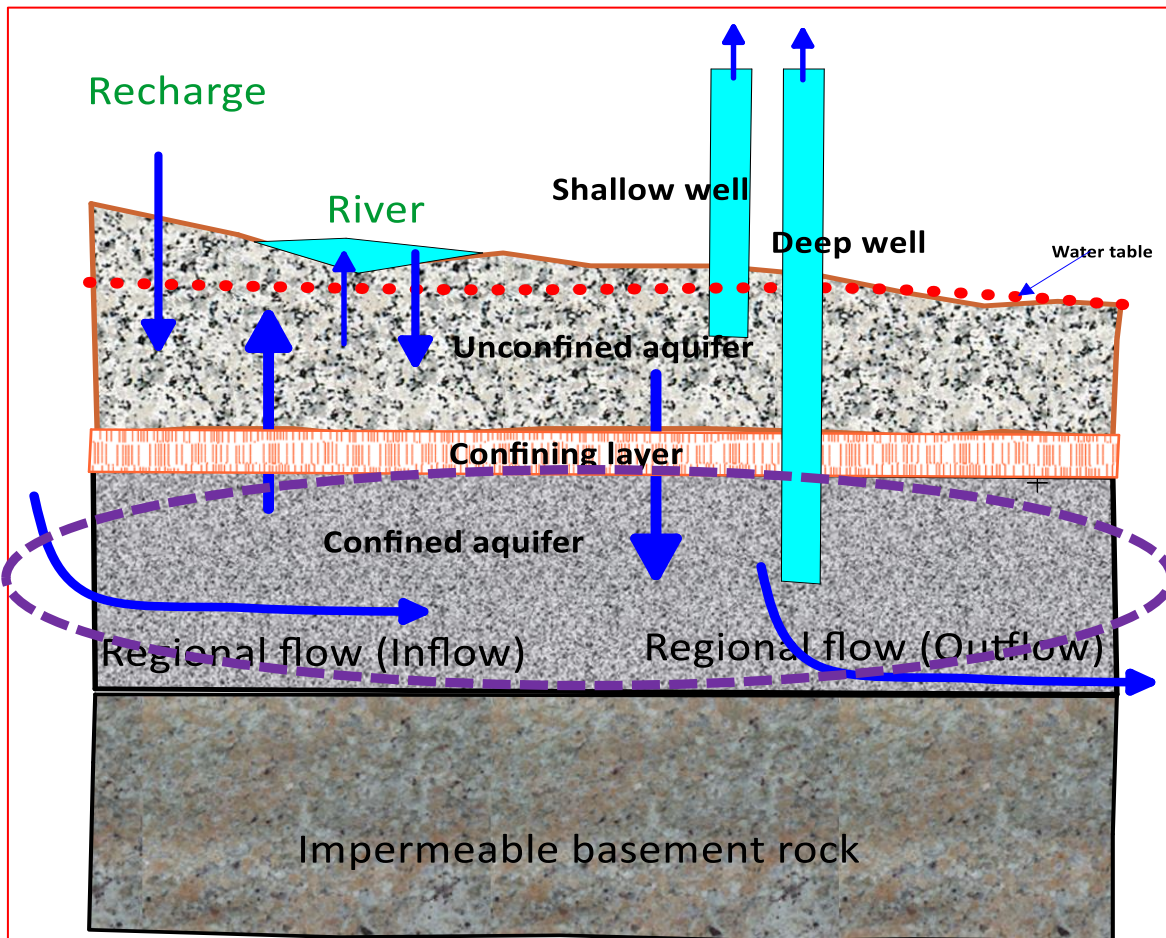


**Figure 69:** The layout of the inflows and outflows of the lower semi-confined layer in the Kimbiji aquifer (Author's construction)

The groundwater heads in the Kimbiji aquifer are observed at 260 m above ground level, and the lower head in the Indian ocean is observed at -20 m below ground level (Fig. 70). Groundwater flows towards the South-east direction where the India ocean, and the only constant head boundary is the Indian ocean. The groundwater flowlines (green-coloured lines in Fig. 70 and blue lines in Fig. 71) show the flow direction of regional groundwater fluxes towards the boreholes and the constant head boundary located on the eastern part of the Kimbiji aquifer.

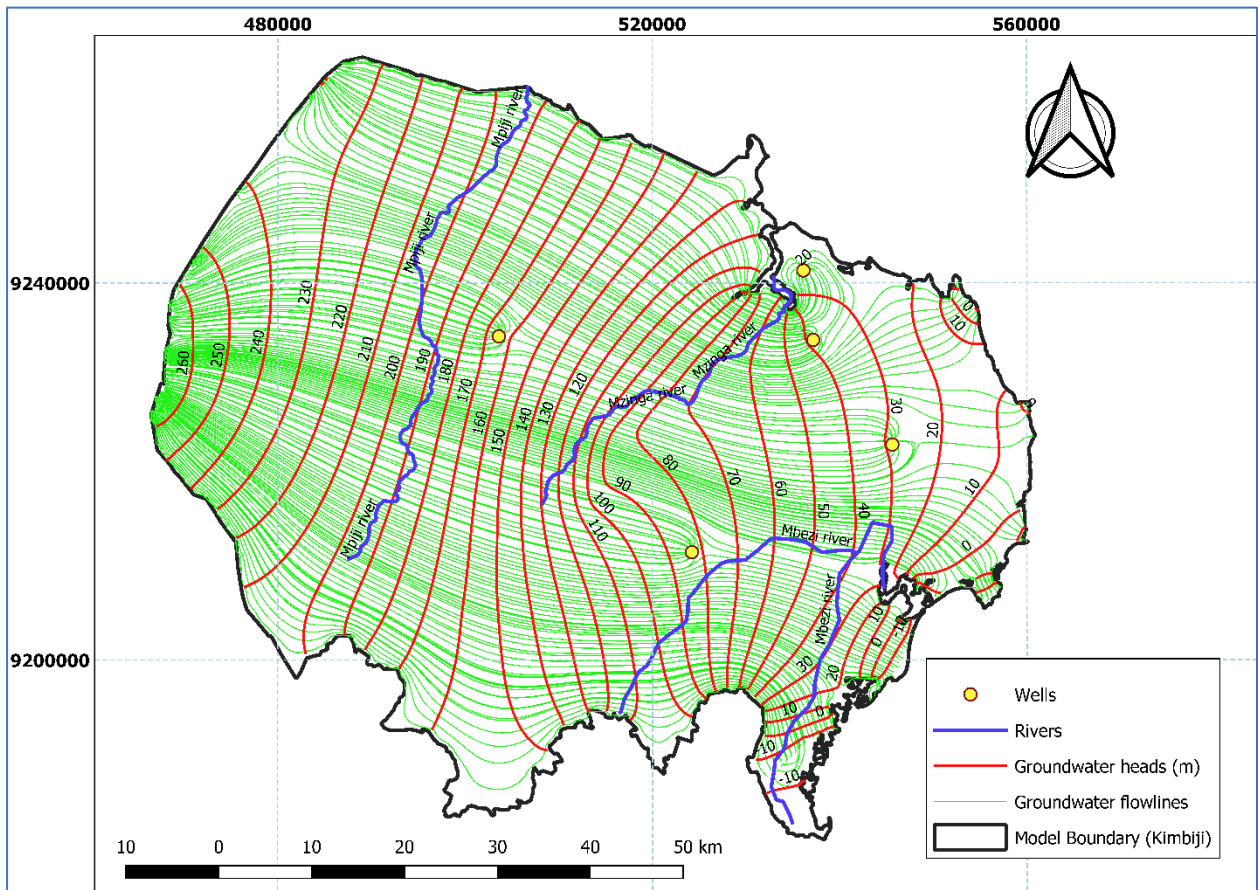


**Figure 70: The map of groundwater heads distribution in the Kimbiji aquifer**

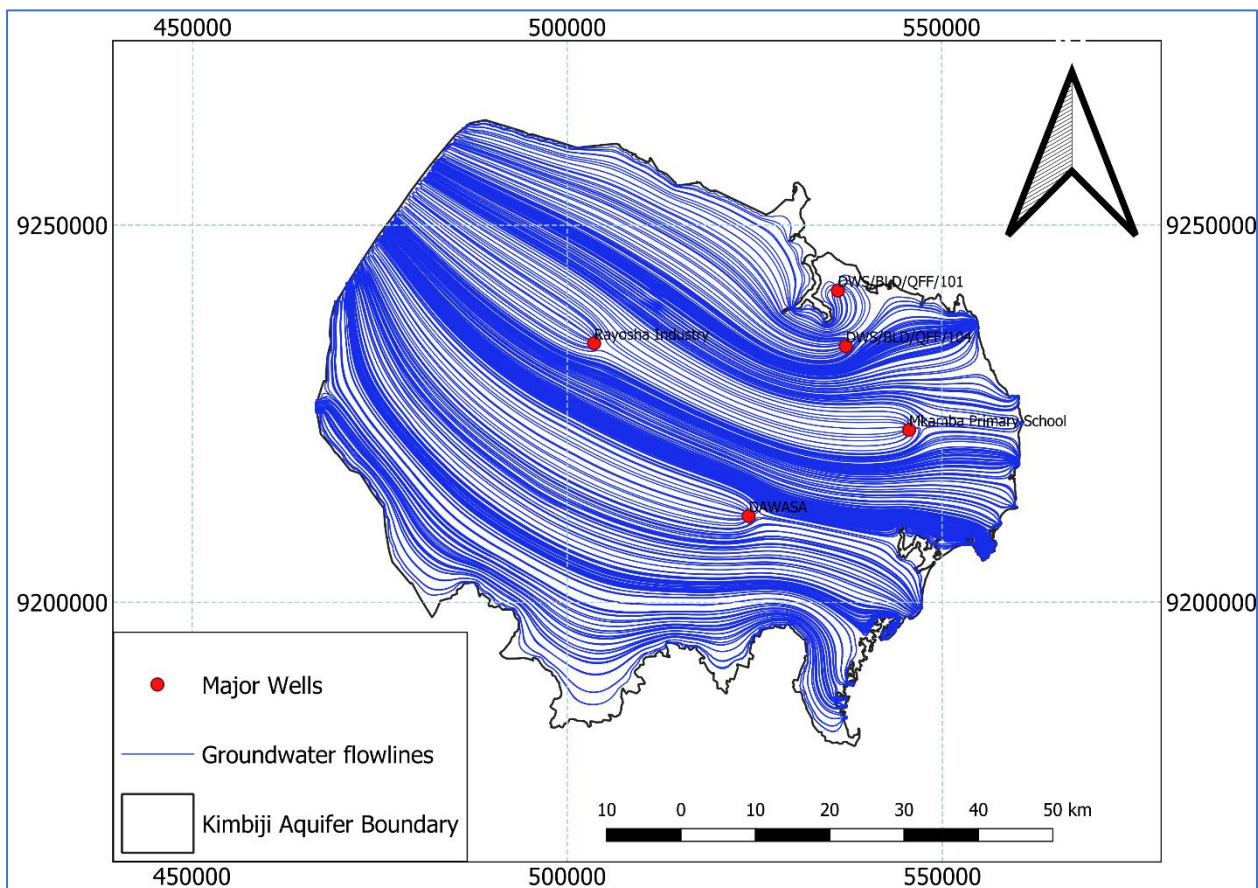


**Figure 71: Groundwater flowlines for the lower semi-confined layer of the Kimbiji aquifer**

Figure 72 shows groundwater flow in the upper unconfined aquifer in the Kimbiji aquifer where the Mpiji river acts as a no flow boundary. It can as well be seen that there is groundwater flow into the boreholes, indicating that the upper unconfined aquifer is also tapped through wells for domestic and other uses. There is also an indication of losing and gaining reaches of the rivers, with gaining mostly happening in the middle to lower sides of the river while losing is mostly expected on the upstream side of the rivers. However, the Mbezi river, unlike the Mzinga river is invariably losing to the aquifer (Fig. 72).

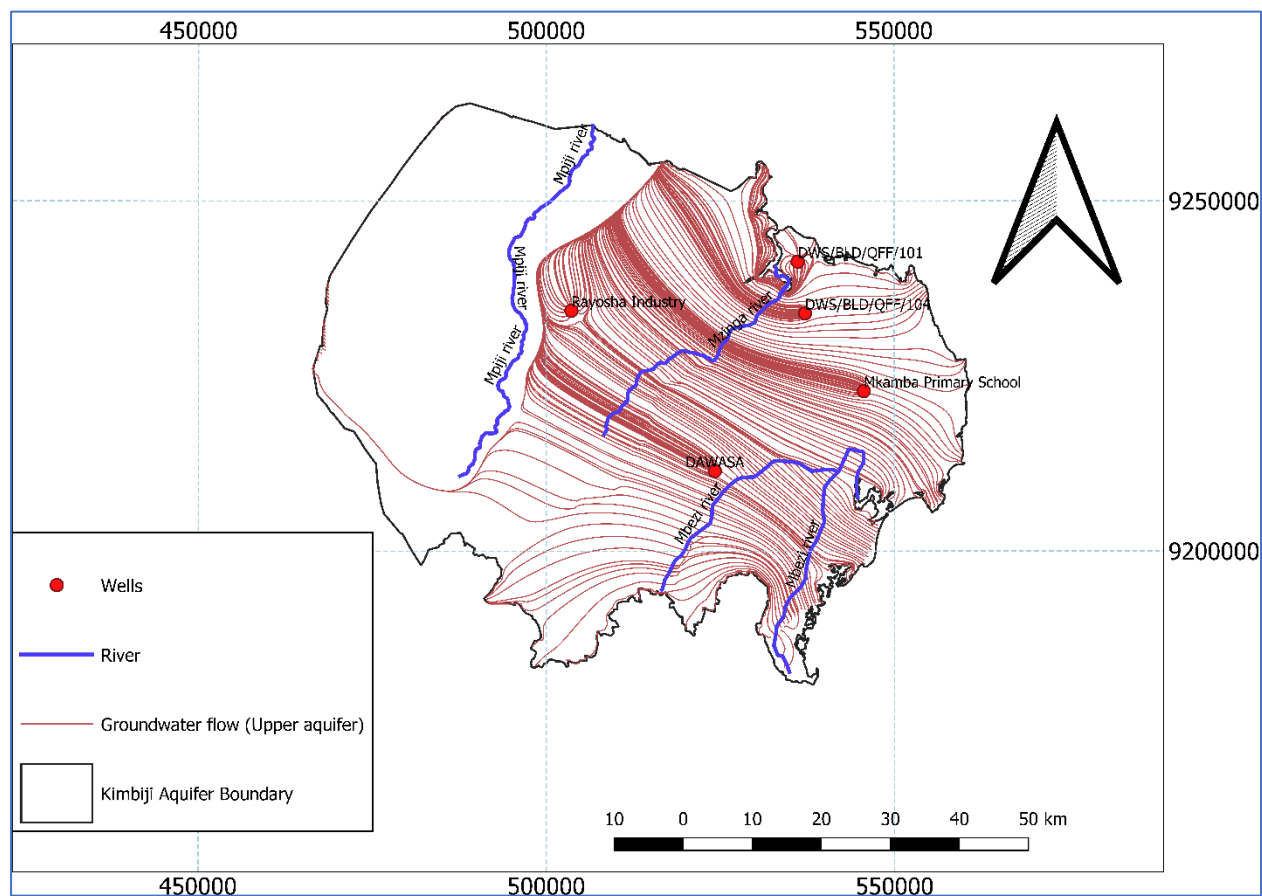


**Figure 72: Groundwater flowlines for the upper unconfined layer of the Kimbiji aquifer**

### (iii) Results of Simulation of Nested Groundwater Flow Systems in the Singida Aquifer

Table 36 and Table 37 contain different budget components at the point of calibration in the Singida aquifer. Groundwater recharge contributes  $1.5 \times 10^{-2} \text{ m}^3/\text{s}$  in the upper aquifer (Table 36) while the lakes and the lower fractured aquifer transmit  $5.25 \times 10^{-3} \text{ m}^3/\text{s}$  and  $0.34 \text{ m}^3/\text{s}$  respectively. There is no direct regional flow flux observed into the upper aquifer as it was also the case for the Kimbiji aquifer. On the other hand, wells extract  $0.14 \text{ m}^3/\text{s}$  from the upper aquifer while the upper aquifer transfers  $0.22 \text{ m}^3/\text{s}$  to the lower fractured aquifer as well as  $2.7651 \times 10^{-3} \text{ m}^3/\text{s}$  to the lakes.

On the other hand, the main inflows into the lower fractured aquifer in the Singida aquifer are regional flow ( $0.2827 \text{ m}^3/\text{s}$ ), vertical movement of water from the upper aquifer ( $0.22 \text{ m}^3/\text{s}$ ) and a contribution from the lakes through vertical structures at the rate of  $5.25 \times 10^{-3} \text{ m}^3/\text{s}$  (Table 37). The lower fractured aquifer is exploited through pumping at the rate of  $8.02 \times 10^{-2} \text{ m}^3/\text{s}$ , the baseflow into the springs takes about  $8.0186 \times 10^{-2} \text{ m}^3/\text{s}$  from the lower fractured aquifer. While lakes are seemed not to be fully penetrating in theory, they receive a momentous contribution from the deep aquifer of about  $2.42 \times 10^{-5} \text{ m}^3/\text{s}$ , slightly lower than the contribution of the upper aquifer to the lakes, indicating that the main source of water in the lakes is the upper weathered aquifer in

the Singida aquifer. This confirms the observed connectivity between the lakes and the groundwater system through hydrogeochemical signatures.

The regional flow accounts for 56% of the total flux in the lower aquifer and makes 94% contribution of the total amount of groundwater inflow in the Singida aquifer. Only 6% of the groundwater storages in the Singida aquifer comes from local recharge and other sources like lakes. Although seemingly the upper weathered zone in the Singida aquifer discharges more water than the lower aquifer, the fact is, the boreholes are fully penetrating and, looking at the exchange rates between the upper and the lower aquifers (Table 36 & Table 37), it was observed that water is invariably and indiscriminately drawn from the two aquifers. Although not fully penetrating, lakes are located in the fault zones, and the faults are fully penetrating. Thus, the exchange of water between the two aquifer layers and lakes is not uncommon. The boreholes are also seen to be located close to the geological structures. This affirms that the high yielding boreholes in the Singida aquifer are drilled in the vicinity of geological structures. The difference between inflows and outflows in the upper weathered layer and lower fractured layer in the Singida aquifer is 0, indicating a 0% discrepancy (Table 36 & Table 37). That is a perfect indicator of a good steady state model, with a reasonably acceptable water balance. In Fig. 73 the layout of inflows and outflows of the upper unconfined layer in the Singida aquifer is provided while Fig. 74 provides the layout of inflows and outflows of the lower semi-confined, fractured layer in the Singida aquifer.



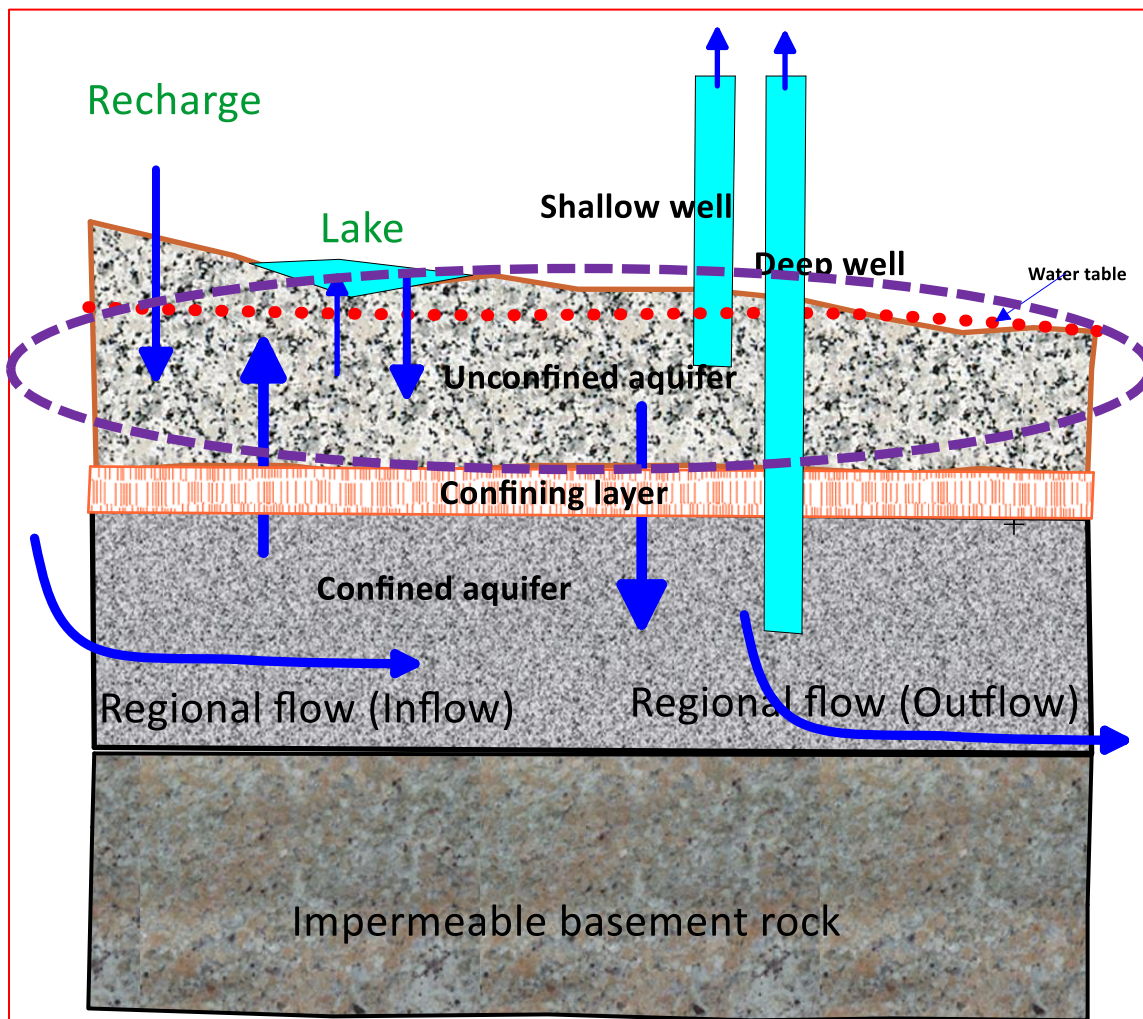


**Figure 73:** The layout of inflows and outflows of the upper unconfined layer in the Singida aquifer (Author's construction)

**Table 36:** The water balance for the upper unconfined weathered layer in the Singida aquifer

	Well	Recharge	Lower Aquifer	Regional flow	Lake	Total
	m <sup>3</sup> /s	m <sup>3</sup> /s	m <sup>3</sup> /s	m <sup>3</sup> /s	m <sup>3</sup> /s	m <sup>3</sup> /s
Inflows	0	1.5153 x 10 <sup>-2</sup>	0.3434	0	5.2539 x 10 <sup>-3</sup>	0.3638
Outflows	0.1400	0	0.221	0	2.7651 x 10 <sup>-3</sup>	0.3638
Inflows-Outflows						0.00
Discrepancy (%)						0.00

**Table 37: The Water balance for the Lower Semi-confined fractured layer in the Singida Aquifer**

	Well	Recharge	Upper Aquifer	Regional flow	Lake	Total
	m <sup>3</sup> /s	m <sup>3</sup> /s	m <sup>3</sup> /s	m <sup>3</sup> /s	m <sup>3</sup> /s	m <sup>3</sup> /s
Inflows	0	0	0.221	0.283	2.14 x 10 <sup>-5</sup>	0.504
Outflows	8.017 x 10 <sup>-2</sup>	0	0.3434	8.0186 x 10 <sup>-2</sup>	2.42 x 10 <sup>-5</sup>	0.504
Inflows-Outflows						0.00
Discrepancy (%)						0.00

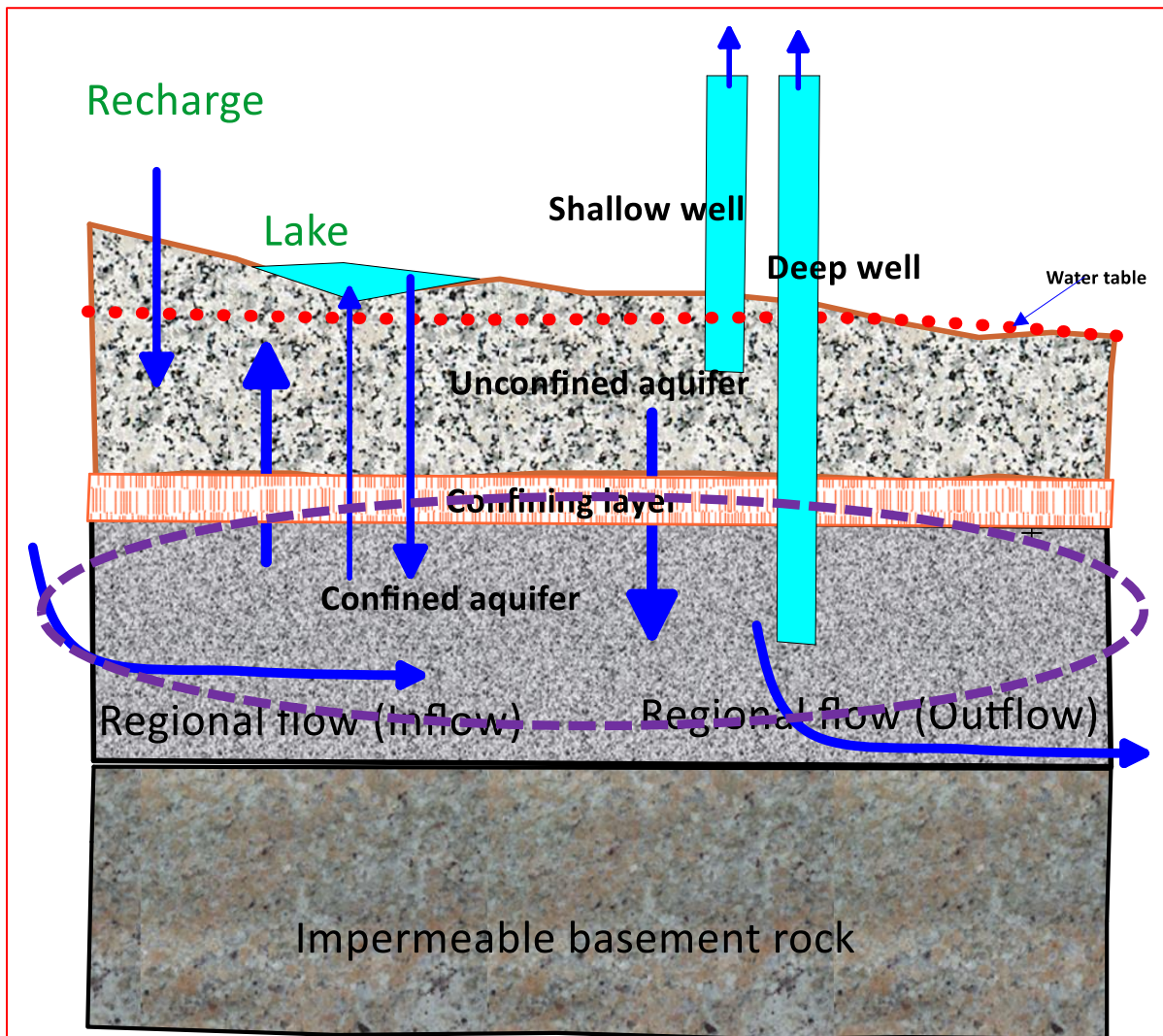


**Figure 74: The layout of inflows and outflows of the lower semi-confined layer in the Singida aquifer (Author’s construction)**

Figure 75 shows groundwater heads in the Singida aquifer. The head difference in the Singida aquifer is 230 m, with the highest simulated head being 1690 m and the lowest simulated head being 1460. Figure 76 shows groundwater flow regime in the upper aquifer while Fig. 77 shows

the groundwater flow regime in the lower fractured aquifer. The flow direction in the two layers conforms with the simulated heads in Fig. 75.

Further, it was observed that groundwater flows from the north eastern part of the aquifer towards the lower south western part, where discharge points are located. Further, in the Singida aquifer, groundwater heads are affected by geological structures (e.g., faults and fractures) and the damage zone where the difference in permeability creates anisotropy, and thus heads are observed to bend, creating tangent angles due to differences in hydraulic conductivities. The weathered zone has undergone a uniform weathering and it thus forms a homogeneous aquifer as it can be observed in Fig. 76. The deep aquifer modeling has revealed that fracturing in the deep aquifer is still the major conduit for groundwater flow in the Singida aquifer (Fig. 77). Therefore, in the Singida aquifer, the faults are not mere geological structures, but are important groundwater resource structures.

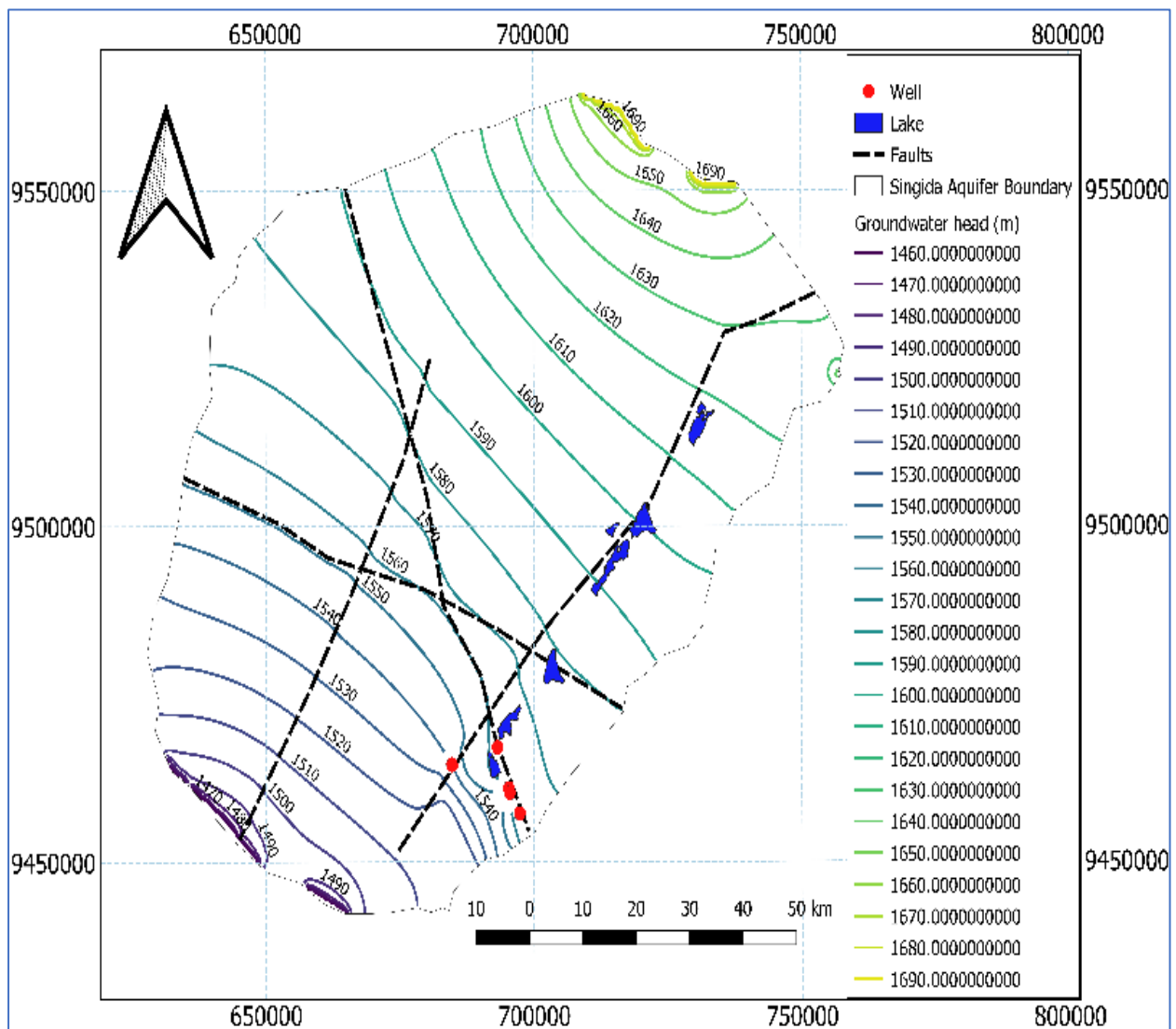


**Figure 75: The map of groundwater heads distribution in the Singida aquifer**



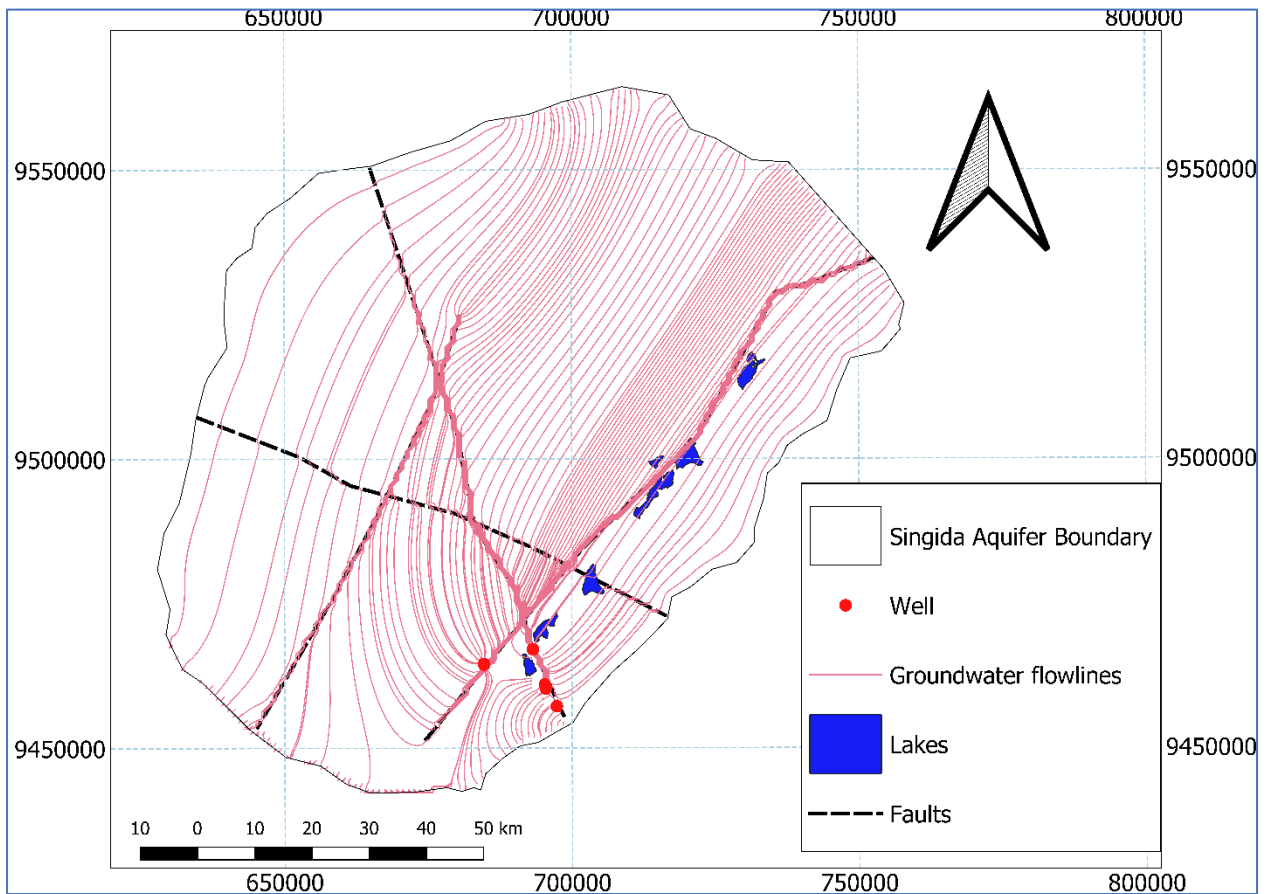


**Figure 76: Groundwater flowline for the upper weathered layer of the Singida aquifer**

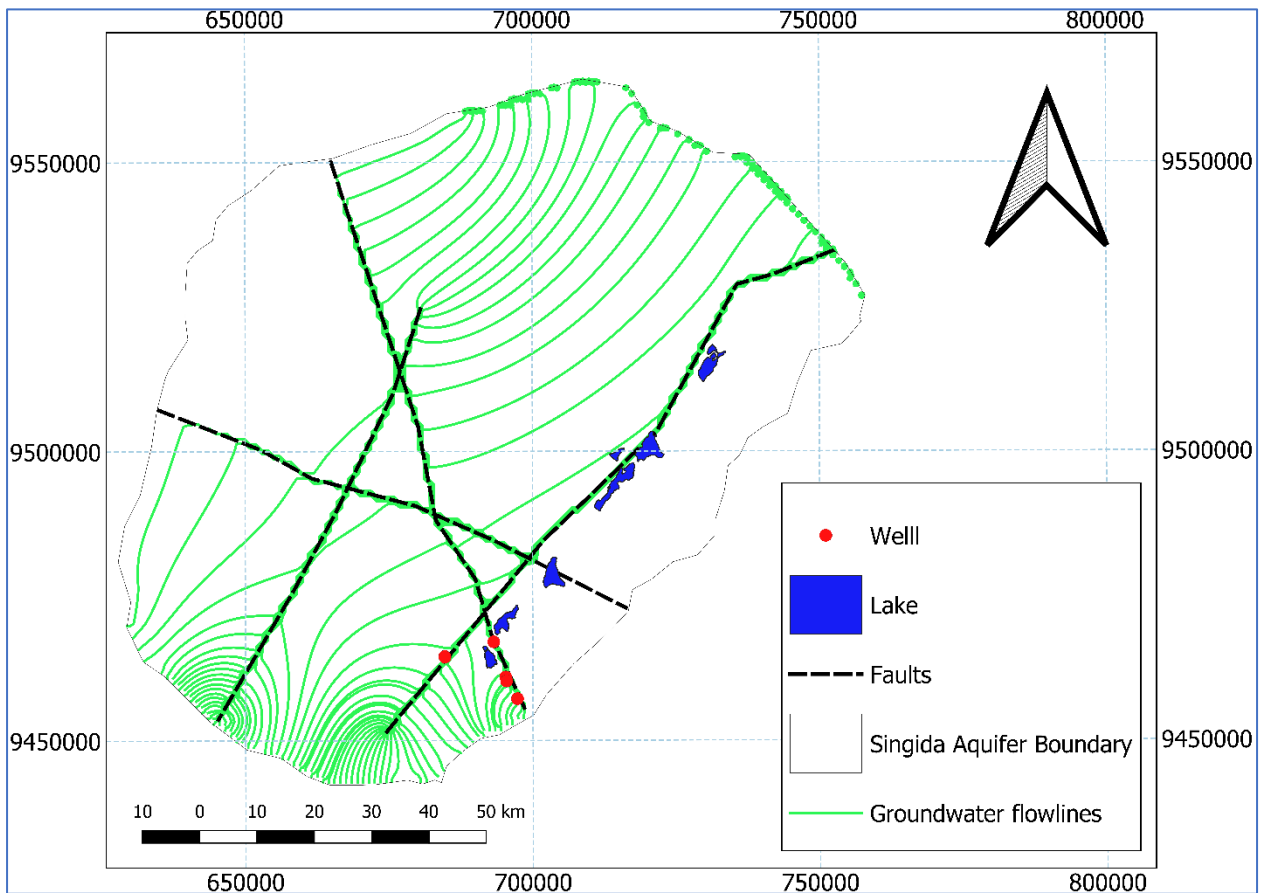


**Figure 77: Groundwater flowline for the lower fractured layer of the Singida aquifer**

The findings of this study are in line with those of previous studies (Gleeson *et al.*, 2008; Haitjema & Mitchel-Brucker, 2005) that in dry regions with high permeability terrains, regional groundwater flow makes up to 60% of the watershed budget. In this study, this implies that more recharge takes place far away from where the aquifers in semi-arid areas are (i.e., there is limited local recharge in the Singida aquifer). This concretizes the argument that there is more regional flow than local flow in semi-arid and arid regions.

Calibrated steady state groundwater flow models for the Kimbiji Neogene coastal aquifer and the Singida fractured crystalline basement aquifer were set to simulate nested (regional and local) groundwater flow systems and understand the contribution of each flux in the basins with contrasting climate and geology. Groundwater occurrence in the Singida semi-arid fractured aquifer exhibits spatial contrasts within very small area. The aquifer is generally of low hydraulic conductivities but high groundwater storages, while the Kimbiji aquifer is of high hydraulic conductivity and high groundwater storages as well. Appreciable regional flow fluxes in the Kimbiji and Singida aquifer and less local influence on groundwater flow fluxes in the two aquifers have been observed, with Singida aquifer predominantly being fed by the regional flow system. This refutes the idea of water table being topography-controlled or recharge-controlled as put forward by Gleeson *et al.* (2008) and Haitjema and Mitchel-Brucker (2005). However, the extent of contribution of each flow system flaunts the varying influence of rainfall-based groundwater recharge, being higher in the Kimbiji humid aquifer and less in the Singida semi-arid aquifer. It therefore suffices reporting that groundwater modeling does not vividly indicate the contrast in water table positions between the Kimbiji and the Singida aquifer.

The steady state model results from the two study areas with contrasting climate and geology indicate that the direct vertical infiltration from rainfall is the main source of groundwater recharge in the upper aquifers but that is not the case for the lower semi-confined aquifers in the two study areas. There are contributions from rivers in the Kimbiji aquifer while there is lake water flow to the aquifer in the Singida aquifer. Nevertheless, the lakes and the rivers do not directly interact with the lower aquifers in the Singida and Kimbiji aquifers respectively. This is because the two hydrological structures are not fully penetrating, unlike the general head boundaries representing regional flow systems.

The weathered zone in the Singida aquifer has undergone a uniform weathering and it thus forms a homogeneous aquifer. The deep aquifer modeling has revealed that fracturing in the deep aquifer is the major conduit for groundwater flow. Interaction with the upper weathered aquifer is through a vertical movement of groundwater. There are both downward and upward movement of

groundwater in the Singida aquifer as shown in the zone budget. There are substantial baseflow amounts to the rivers and the Indian ocean in the Kimbiji aquifer while in the Singida aquifer the observed baseflow feeds the lakes and the wetlands.

The contribution of regional flow systems to groundwater storages in the two aquifers is significantly large. However, the Singida aquifer has shown a more dominant contribution of the regional flow system (94%) as compared to the local flow fluxes. The contrast with the previous studies has been observed in the Kimbiji aquifer where the regional flow system is also dominant, occupying 76% of the total groundwater inflows. This is contrary to the previous postulations put forward by Gleeson *et al.* (2008) and Haitjema and Mitchel-Brucker (2005) that, in humid areas, there are topography-controlled water tables where local flow systems dominate and in the semi-arid areas like Singida regional flow systems are the major water towers to the aquifer storages. The contrast from the previous studies, especially on the status of regional flow systems possibly arises due to the use of zone budget approach in groundwater modeling other than the normal water budget where not separation of aquifers is carried out.

Despite all this, rainfall-based groundwater recharge is still an important process and source of groundwater resources in the two basins which cannot easily be ignored as opined by other researchers (Villeneuve *et al.*, 2015). Moreover, it was revealed that more water is drawn from the lower semi-confined aquifer in the Kimbiji aquifer as opposed to the Singida aquifer where more water was observed to be drawn from the upper weathered unconfined layer. Nonetheless, the reason behind these two scenarios is that the boreholes are fully penetrating, screened from the top to the lower end of the borehole. Thus, water is invariably drawn from the two layers indiscriminately, and thus mixing of regional and local flow fluxes is inevitably obvious.

Previous studies have shown that groundwater recharge in semi-arid areas commonly occurs through leakage from ephemeral streams or ponds (Acworth *et al.*, 2021; Cuthbert *et al.*, 2016; Dahan *et al.*, 2008; Villeneuve *et al.*, 2015). Groundwater modeling for the two aquifers has revealed the same scenario, adding to the niche that groundwater recharge in both semi-arid and humid areas occurs through leakage from both perennial and ephemeral rivers and lakes. Further, contrary to what was found by Acworth *et al.* (2021) and Zarate *et al.* (2021), flood events and high rainfall events control groundwater recharge regimes in the two aquifers, irrespective of their difference in climate and geology. However, there is an agreement with what was reported by Bredehoeft (2002) and Acworth *et al.* (2021) that the deeper aquifers are indirectly separated from the shallow aquifers, but in the aspect of natural groundwater recharge. With regard to river and lake water, this study found an interaction between the two aquifer systems in the two study areas,

and it thus suffices to report that there is connectivity between the deep and the shallow aquifers, owing to their semi-confined nature.

The groundwater simulation has confirmed semi-confined conditions of the two aquifers through observed vertical exchanges of water between the upper and lower aquifers. More water is from the regional flow systems in both aquifers than from the local flow system (mainly recharge). Therefore, regional flow system is as important in the semi-arid fractured consolidated aquifer as it is in the humid, sedimentary Neogene Kimbiji aquifer. As it was reported previously in other fractured crystalline basement aquifers (Seddon *et al.*, 2021), the deep aquifer in the Singida aquifer is structurally controlled while in the Kimbiji aquifer the deep aquifer is quasi homogeneous with appreciable degree of anisotropy.

Further, a flow discontinuity was observed in the upper layer of the Kimbiji aquifer due to heterogeneity and anisotropy. Conceivably, the Mpiji river acts as a no flow boundary for the upper, water-bearing layer in the Kimbiji aquifer, dividing the aquifer into two parts. The division could not be observed in the deep/lower semi-confined layer in the Kimbiji aquifer. As for the Singida aquifer, high permeability in the damaged zone was observed relative to the fractured zone and the rest of the surrounding aquifer materials as reported elsewhere (Mayer *et al.*, 2007). This created anisotropy and heads and flowlines were observed to change direction while changing the aquifer media/structure. The effects of spatial difference in hydraulic conductivity on groundwater flow direction has been reported elsewhere (Anderson and Bakker, 2008), and thus the scenario brought to the limelight by this study is not uncommon.

In the Kimbiji aquifer, the constant head boundary (the Indian ocean) and the head-dependent flux boundaries (the rivers) also affect the structure of the groundwater heads. The rivers in the Kimbiji aquifer have been observed to be both, influent (gaining) in some reaches and effluent (losing) in others. This is explained by the observed inflows to the upper aquifer and the outflows from the upper aquifer. In the Singida aquifer, lakes have also been observed to lose and gain water to and from the aquifer. The same river reaches can be invariably losing and gaining depending on the season (Acworth *et al.*, 2021; Chen *et al.*, 2013).

Groundwater flow in the upper weathered zone in the Singida aquifer has shown similar characteristics as those of the upper unconfined zone in the Kimbiji aquifer. The two aquifers can safely be modelled using the theories governing laminar flow in homogeneous aquifer systems. However, the movement of groundwater in the lower fractured zone in the Singida aquifer is not strictly laminar. Modeling the aquifer using the laws governing laminar flow of liquids in must be considered with great care. With increasing groundwater abstractions, land cover changes and

increasing surface temperatures which go in tandem with a decrease in rainfall, the regional and local flow fluxes are likely to change. In this study, smaller withdrawals for household consumption were ignored in the model due to their infinitesimally small contributions to the overall water withdrawal from the aquifers.

## CHAPTER FIVE

### CONCLUSION AND RECOMMENDATIONS

#### 5.1 Conclusion

This study characterized and simulated nested groundwater flow systems, factoring the contrast in climate and geology using two test cases in Tanzania. Moreover, the study examined the effect of the combined effect of land use/cover dynamics and climate variability on groundwater recharge rates in the two aquifers with contrasting climate and geology. The study demonstrated the ability of a multifaced approaches to characterizing and identification of the occurrence of nested groundwater floor systems. The presence of both, local and regional flow systems through the manifestation of various hydrogeochemical signatures and facies was carried out.

The Kimbiji aquifer has complex and multiple sources of recharge with pockets of local recharge areas, distributed throughout the aquifer owing to its humid climate and porous aquifer media. The aquifer is also characterized by regional groundwater flow system with discharge points located in the upper, middle and lower parts of the aquifer. The Singida aquifer is dominated by regional to sub regional flows as indicated by the hydrogeochemical signatures, especially the dominance of Sodium and Chloride. However, ostensible signs of locally recharged groundwater water were established, more so where bicarbonate dominated the groundwater samples, with progressive  $\text{Ca}^{2+}$  and  $\text{Mg}^{2+}$  enrichment in both study areas.

The study further revealed the extent of rock-water interaction in the two aquifers as the main mechanism controlling groundwater quality and ion concentrations. The hydrogeochemical facies and signatures were instrumental in delineating groundwater recharge and discharge zones and locations. This has been aided by the Gibb's diagrams, which showed that the samples fall in the rock-water interaction as a predominant mechanism controlling groundwater chemistry in the two study areas.

The use of stable isotopes for understanding groundwater provenance and recharge mechanism in the two study areas also revealed details of differentiated atmospheric moisture input. The study also revealed the influence of both, regional and local precipitation. This has a huge implication on the sources of recharge for the two aquifers. Isotopic enrichment is not only attributed to evaporative processes only, but can as well be a result of orographic precipitation, especially in the Kimbiji aquifer. Below cloud fractionation is a very common process in Singida due to relatively lower level of relative humidity (semi-arid climate). In the Kimbiji aquifer, enrichment is mainly attributed to higher air temperatures.

There was a decreasing trend of recharge in both aquifers regardless of their difference in climate and geology. Groundwater recharge is a function of climate and land use/cover dynamics. However, the combination effect of climate and land cover through the curve number parameter was very prominent in the Kimbiji coastal humid aquifer than it was in the Singida semi-arid aquifer. The curve number in the Singida aquifer was nearly constant while there was a steady growth of curve number in the Kimbiji aquifer. This is an indication that, more area with high individual curve numbers is increasing while land use/cover classes with low curve numbers are decreasing in size.

This study further evaluated the effect of the combined effect of land use/cover dynamics and climate variability on groundwater recharge rates in the two aquifers with contrasting climate and geology. There was a decreasing trend of recharge in both aquifers regardless of their difference in climate and geology. Groundwater recharge is a function of climate and land use/cover dynamics. However, the combination effect of climate and land cover through the curve number parameter was very prominent in the Kimbiji coastal humid aquifer than it was in the Singida semi-arid aquifer. The curve number in the Singida aquifer was approximately constant while there was a steady growth of curve number in the Kimbiji aquifer. This is an indication that, more are with high individual curve numbers are growing while land use/cover classes with low curve numbers are decreasing in size.

The Hargreaves and Samani method of estimating potential evapotranspiration seemed suitable, both in the humid Kimbiji aquifer and the semi-arid Singida aquifer because PM-PET method hugely overestimated the potential evapotranspiration in the Singida aquifer. However, this does not staunchly translate into the PM-PET method being less useful in all semi-arid areas because it requires long term studies with succinct longitudinal data collection to establish the empirical evidence on the suitability of the PM-PET based method in semi-arid areas. To that effect, this study uncovered the veiled scientific information on how basins with contrasting climates should be treated with regard to hydrological estimations and the calculation of runoff and groundwater recharge using the curve number as an indicator describing runoff response characteristics. Strenuous attention must be paid to the choice of PET methods. The reported overestimation and underestimation in this study and other previous studies cannot be used as blueprints nonetheless.

The implications of land cover changes and climate variability on natural groundwater recharge in the two aquifers with contrasting climate and geology have unveiled the hovering information with regard to the response to such perturbations. The effect of land cover dynamics on groundwater recharge is more prominent in the Kimbiji aquifer, while the effect of climate (rainfall and

temperature) featured more prominently in the Singida semi-arid aquifer. This study also revealed that the same land cover can have a different runoff potential due to the difference in climate, geology, and soil properties. This study has highlighted the difference in the curve number for similar land cover types owing to their difference in climate and soil properties.

The ENSO phenomenon teleconnection with rainfall and groundwater recharge provided potentially useful information on how the difference in geology and climate cannot significantly feature in the response to El Nino teleconnections. The influence of the ENSO phenomenon on time lags between rainfall and recharge informs that whenever there are ENSO teleconnections, time lags are offset, despite the difference in climate and geology. This is key for water resource development and management in the two basins with contrasting climate and geology.

While this study could not establish the contrast in water table positions due to the difference in geology and climate, dependence of recharge on heavy rainfalls is one of the key features of the Singida semi -arid aquifer while recharge in the Kimbiji humid aquifer is quasi-uniform. Local flow system fluxes were observed to be the main feeders for the upper unconfined aquifers in the two study areas while regional flow systems are for the deep semi-confined aquifers. Nevertheless, the aquifers are constantly exchanging appreciable volumes of water.

Groundwater fluxes of nested (local and regional) groundwater flow systems were established in the two test cases, Kimbiji humid, sedimentary aquifer and the Singida, semi-arid fractured aquifer. The groundwater budget components reflect the 2016 conditions in the Kimbiji aquifer and 2018 in the Singida aquifer. There are both downward and upward movement of groundwater in the two aquifers. This reveals the presence of the interaction between the upper unconfined and the lower semi-confined aquifers through vertical movement of groundwater. Simulation of nested groundwater systems revealed an interaction between the lakes and the aquifer, both in the upper and the lower fractured layers. This indicates that the lakes in the Singida aquifer are situated in a fault zone, and thus they are fully penetrating in all or some parts of the lakes. In the Kimbiji aquifer, simulation of water budgets and individual fluxes of nested groundwater flow systems revealed that rivers are not fully penetrating, and thus they only contribute water budget to the upper unconfined aquifer only.

While both aquifers exhibit local to regional mechanisms of recharge, the Kimbiji aquifer is dominated by local recharge, especially for shallow boreholes while deep aquifers exhibited sub-regional to regional recharge mechanisms. The Singida aquifer has equally exhibited pockets of locally recharged groundwater despite the semi-arid climate and unimodal rainfall pattern.



However, the most dominant mechanism is regional flow. This is supported by the type of climate, especially the amount of annual precipitation received.

The study findings will contribute to various global, regional and local technical and policy-based efforts towards sustainable groundwater development and management, considering climate variability and non-climatic factors. This includes the contribution to Sustainable Development Goals (SDGs), particularly SDG on access to clean water and sanitation. Furthermore, the present study has the following contributions:

- (i) Harnessing the benefits accruing from episodic climate systems such as the ENSO in groundwater management is a foreseeable area of research. Moreover, prediction of the ENSO and its associated rainfall intensity would enable the ensuing natural groundwater recharge to be predicted.
- (ii) Development of two numerical groundwater models, taking into account their difference in climate and geology. The Singida model was developed considering the presence of fractures and damaged zones as water conduits instead of considering the basin as made up of porous media as it has been the case in most models developed this far.
- (iii) The differential influence of climate and land cover changes on the nested groundwater flow systems was studied and well documented in this study through recharge estimation using the modified soil moisture balance method. This paves way for informed and tailored groundwater monitoring and management options depending on the geology, climate, and dominant land cover types.
- (iv) The idea of the presence of usable and non-usable aquifers depending on the amount of water that can be exploited was challenged by this study. It has been ostensibly established that, considering a multilayered aquifer system, not distinctive features of water table differences in the two aquifers.
- (v) Characterization and simulation of nested groundwater flow systems in basins with contrasting climate and geology has been successfully carried out. A combination of tools and methods has been deployed and yielded into congruent results about how the nested flow systems behave in different aquifers.
- (vi) This study has afforded to evaluate the capabilities of QGIS and its inherent tools and algorithms in, not only carrying out weighted overlay analysis, but a comprehensive understanding of the potential groundwater recharge zones in a crystalline basement and

highly fractured semi-arid area and a sedimentary humid area as well. Therefore, this study serves as a methodological breakthrough in terms of weighted overlay methodological approach and the use of open-source remote sensing and GIS software.

- (vii) In addition to the designation of the study areas into groundwater recharge potential areas, this study has also developed Equations (Equation 43 and Equation 44) for hydrogeological delineation of potential groundwater recharge areas in humid sedimentary aquifers and semi-arid fractured aquifers, respectively. These are numerical indicators of the relative importance of the factors used in the hydrogeological delineation of groundwater recharge potential.
- (viii) The development of equations which can be used for mapping groundwater recharge potential in basins with contrasting climate and geology. The equations can serve as startup packages for developing groundwater potential maps combining a multitude of hydrogeological and climatic parameters in Tanzania and elsewhere in the world.
- (ix) This PhD study published three (3) journal papers in various peer-reviewed journals. One of the published journal articles is a review article, covering a review of scientific and theoretical contentions in numerical groundwater modeling. The other two papers are research articles, one covering issues of natural groundwater response to varying climate and the other one focused on delineation of groundwater potential zones in the Singida fractures semi-arid aquifer. The published papers serve as a contribution to the scientific community in this niche, and outside the hydrology and hydrogeology niches.

## **5.2 Recommendations**

In addition to the results and discussions, this study proposes the following recommendations for improved groundwater resources management in basins with contrasting climate and geology:

- (i) Open-source remote-sensing and GIS techniques used in this study have proven effective tools in delineating groundwater recharge zones and locations. Thus, this approach is recommended to complement geophysical and other groundwater exploration surveys, including geochemical and isotopic approaches. Researchers, especially those familiar with QGIS software can utilize this blended approach for carrying out suitability analysis using the weighted overlay analysis approach. To that effect, artificial groundwater recharge initiatives should practically target the identified potential groundwater recharge zones. This effort will enhance the contribution of local flow systems to groundwater availability in all basins regardless of the difference in climate and geology.

- (ii) Potential Evapotranspiration is an integral part of groundwater assessment processes, including groundwater modeling. However, most PET estimation methods cannot truly reflect the real field conditions. Nevertheless, this study recommends the use of HS method as it suitably estimated PET for the two study areas, utilizing minimally available climate data.
- (iii) The observed surface water groundwater interaction calls for improved monitoring of the groundwater sources to track any changes in quality since there is a potential evolution to an undesirable state for domestic uses.
- (iv) Pressure transducers have proven useful at tracking the response of shallow aquifers to rainfall events. Nevertheless, water basins are struggling with monitoring their aquifers using this state-of-the-art technique. This study recommends an increased effort to install pressure transducers (divers) so as to monitor water table fluctuations as a result of groundwater withdrawal and recharge of the shallow aquifers from local rainfall. This is very useful in understanding the association between local rainfall and local groundwater recharge.
- (v) Although general conclusions are drawn that groundwater recharge follows as positive a trend as rainfall, a more quantitative evaluation of the temporal variation of groundwater recharge due to the changing land covers and the implication of episodic weather events such as the ENSO is imperative to establish a more robust trend, which takes into account a number of variables other than rainfall alone. This is important for the management of groundwater resources in an optimal manner.
- (vi) Future works which seek to assess the hierarchy, organization and proportional contribution of nested groundwater flow systems in basin water budgets require concerted considerations of multi-layered aquifer systems instead of single-layered aquifers. The latter tend to ignore or underestimate the contributions of regional flow systems in basin water budgets as revealed by the findings of this study.

## REFERENCES

- Abbott, M. D., Lini, A., & Bierman, P. R. (2000).  $\delta^{18}\text{O}$ ,  $\delta\text{D}$  and  $^3\text{H}$  measurements constrain groundwater recharge patterns in an upland fractured bedrock aquifer, Vermont, USA. *Journal of Hydrology*, 228(1–2), 101–112. [https://doi.org/10.1016/S0022-1694\(00\)00149-9](https://doi.org/10.1016/S0022-1694(00)00149-9)
- Abid, K., Dulinski, M., Ammar, F. H., Rozanski, K., & Zouari, K. (2012). Deciphering interaction of regional aquifers in Southern Tunisia using hydrochemistry and isotopic tools. *Applied Geochemistry*, 27(1), 44–55. doi:10.1016/j.apgeochem.2011.08.015
- Abiye, T. A., (2013). *The use of Isotope Hydrology to Characterize and Assess Water Resources in South (Ern) Africa*. WRC Report No. TT570/13, Pretoria. 211pp.
- Abou-Zakhem, B., Al-Charideh, A., & Kattaa, B. (2017). Using principal component analysis in the investigation of groundwater hydrochemistry of Upper Jezireh Basin, Syria. *Hydrological Sciences Journal*, 62(14), 2266–2279.
- Acharya, T., Kumbhakar, S., Prasad, R., Mondal, S., & Biswas, A. (2017). Delineation of potential groundwater recharge zones in the coastal area of north-eastern India using geoinformatics. *Sustainable Water Resources Management*, 5, 533–540, doi:10.1007/s40899-017-0206-4.
- Acworth, R. I., Rau, G. C., Cuthbert, M. O., Leggett, K., & Andersen, M. S. (2021). Runoff and focused groundwater-recharge response to flooding rains in the arid zone of Australia. *Hydrogeology Journal*, 2021, 1–28. <https://doi.org/10.1007/s10040-020-02284-x>
- Adams, S., Titus, R., Pietersen, K., Tredoux, G., & Harris, C. (2001). Hydrochemical characteristics of aquifers near Sutherland in the Western Karoo, South Africa. *Journal of hydrology*, 241(1-2), 91-103.
- Adomako, D., Maloszewski, P., Stumpp, C., Osae, S., & Akiti, T. T. (2010). Estimation de la recharge des eaux souterraines à partir des profils en profondeur des isotopes de l'eau ( $\text{d}^2\text{H}$ ,  $\text{d}^{18}\text{O}$ ) dans le bassin de la Rivière Densu, Ghana. *Hydrological Sciences Journal*, 55(8), 1405–1416. <https://doi.org/10.1080/02626667.2010.527847>
- Aggarwal, P. K., hlich, K., Kulkarni, K. M., & Laurence, L. (2004). Stable isotope evidence for moisture sources in the Asian summer monsoon under present and past climate regimes. *Geophysical Research Letters*, 31, L08203.

- Ahmad, I., Verma, V., & Verma, M. K. (2012). *Application of Curve Number Method for Estimation of Runoff Potential in GIS Environment*. In *2<sup>nd</sup> International Conference on Geological and Civil Engineering*. <https://scholar.google.com>
- Al-Ahmadi, M. E. (2013). Hydrochemical characterization of groundwater in wadi Sayyah, Western Saudi Arabia. *Applied Water Science*, 3(4), 721–732.
- Alawamy, J. S., Balasundram, S. K., Mohd-Hanif, A. H., & Boon-Sung, C. T. (2020). Detecting and analyzing land use and land cover changes in the region of Al-Jabal Al-Akhdar, Libya using time-series landsat data from 1985 to 2017. *Sustainability*, 12(11), 4490.
- Allen, R. G., Pereira, L. S., Raes, D., & Smith, M. (1998). *Crop Evapotranspiration-Guidelines for Computing Crop Water Requirements-FAO Irrigation and Drainage Paper 56*. Fao, Rome. <https://scholar.google.com>
- Al-Tamir, M. A. (2008). Interpretation of ground water quality data variation in Erbil city, Northern Iraq. *Al-Rafidain Engineering*, 16 (2), 24–30.
- Arora, K. M., & Mathur, S. (2001). Multi-source classification using artificial neural network in a rugged terrain. *Geocarto International*, 16(3), 37-44.
- Bagyaraj, M., Ramkumar, T., Venkatramanan, S., & Gurugnanam, B. (2013). Application of remote sensing and GIS analysis for identifying groundwater potential zone in parts of Kodaikanal Taluk, South India. *Frontiers of Earth Science*, 7(1), 65-75.
- Bakari, S. S., Aagaard, P., Vogt, R. D., Ruden, F., Johansen, I., & Vuai, S. A. (2012). Delineation of groundwater provenance in a coastal aquifer using statistical and isotopic methods, Southeast Tanzania. *Environmental Earth Sciences*, 66(3), 889-902.
- Bakundukize, C. (2012). *Hydrogeological and Hydrogeochemical Investigation of a Precambrian Basement Aquifer in Bugesera Region (Burundi)* [Doctoral dissertation]. Ghent University. <https://scholar.google.com>
- Bakundukize, C., van Camp, M., & Walraevens, K. (2011). Estimation of Groundwater Recharge in Bugesera Region (Burundi) using Soil Moisture Budget Approach. *Geologica Belgica*, 14(1–2), 85–102.

- Banko, G. (1998). A review of assessing the accuracy of classifications of remotely sensed data and of methods including remote sensing data in forest inventory. *International Institute for Applied Systems Analysis, 1998, 1-43.*
- Baskaran, S., Ransley, T., Brodie, R. S., & Baker, P. (2009). Investigating groundwater-river interactions using environmental tracers. *Australian Journal of Earth Sciences, 56*(1), 13–19. <https://doi.org/10.1080/08120090802541887>
- Bertrand, G., Siergieiev, D., Ala-Aho, P., & Rossi, P. M. (2014). Environmental tracers and indicators bringing together groundwater, surface water and groundwater-dependent ecosystems: Importance of scale in choosing relevant tools. *Environmental Earth Sciences, 72*(3), 813-827.
- Bonan, G. B. (1997). Effects of land use on the climate of the United States. *Climatic Change, 37*(3), 449-486.
- Bonzanigo, L., Eberhardt, E., & Loew, S. (2001). Hydromechanical factors controlling the creeping Campo Vallemaggia landslide. *International Conference on Landslides-Causes, Impacts and Countermeasures, 2001, 13-22.*
- Bresciani, E., Gleeson, T., Goderniaux, P., De Dreuzy, J. R., Werner, A. D., Wörman, A., Zijl, W. & Batelaan, O. (2016). Groundwater flow systems theory: research challenges beyond the specified-head top boundary condition. *Hydrogeology Journal, 24*(5), 1087-1090.
- Bray, R. H., & Kurtz, L. T. (1945). Determination of total, organic, and available forms of phosphorus in soils. *Soil Science, 59*(1), 39-46.
- Calmels, D., Galy, A., Hovius, N., Bickle, M., West, A. J., Chen, M. C., & Chapman, H. (2011). Contribution of deep groundwater to the weathering budget in a rapidly eroding mountain belt, Taiwan. *Earth and Planetary Science Letters, 303*, 48–58.
- Cardenas, M. B., Slotke, D. T., Ketcham, R. A., & Sharp, J. M. (2007). Navier-Stokes flow and transport simulations using real fractures shows heavy tailing due to eddies. *Geophysical Research Letters, 34*(14), 34, 1–5. [https://doi.org/10.1029/2006GL029126.](https://doi.org/10.1029/2006GL029126)
- Cervi, F., Ronchetti, F., Martinelli, G., Bogaard, T. A., & Corsini, A. (2012). Origin and assessment of deep groundwater inflow in the Ca'Lita landslide using hydrochemistry and in situ monitoring. *Hydrology and Earth System Sciences, 16*(11), 4205-4221.

- Chanda, A., Das, S., Mukhopadhyay, A., Ghosh, A., Akhand, A., Ghosh, P., Ghosh, T., Mitra, D., & Hazra, S. (2018). Sea surface temperature and rainfall anomaly over the Bay of Bengal during the El Niño-Southern Oscillation and the extreme Indian Ocean Dipole events between 2002 and 2016. *Remote Sensing Applications: Society and Environment*, 12, 10-22.
- Chebotarev, I. I. (1955). Metamorphism of natural waters in the crust of weathering. *Geochimica et Cosmochimica Acta*, 8(3), 137-170.
- Chesnaux, R. (2013). Regional recharge assessment in the crystalline bedrock aquifer of the Kenogami Uplands, Canada. *Hydrological sciences journal*, 58(2), 421-436.
- Chilagane, N. A., Kashaigili, J. J., & Mutayoba, E. (2020). Historical and Future Spatial and Temporal Changes in Land Use and Land Cover in the Little Ruaha River Catchment, Tanzania. *Journal of Geoscience and Environment Protection*, 08(02), 76–96. <https://doi.org/10.4236/gep.2020.82006>.
- Chowdhury, A., Jha, M. K., Chowdary, V. M., & Mal, B. C. (2009). Integrated remote sensing and GIS-based approach for assessing groundwater potential in West Medinipur district, West Bengal, India. *International Journal of Remote Sensing*, 30(1), 231-250.
- Clark, I. D., & Fritz, P. (1997). *Environmental Isotopes in Hydrogeology*. Lewis, New York, p. 328.
- Cloutier, V., Lefebvre, R., Therrien, R., & Savard, M. M. (2008). Multivariate statistical analysis of geochemical data as indicative of the hydrogeochemical evolution of groundwater in a sedimentary rock aquifer system. *Journal of Hydrology*, 353(3-4), 294-313.
- Cobaner, M., Citakoğlu, H., Haktanir, T., & Kisi, O. (2017). Modifying Hargreaves: Samani equation with meteorological variables for estimation of reference evapotranspiration in Turkey. *Hydrology Research*, 48(2), 480-497.
- Craig, H. (1961). Isotopic variations in meteoric waters. *Science*, 133(3465), 1702–1703. [doi:10.1126/](https://doi.org/10.1126/)
- Christy, A. C., Brain, G. K., & Joshua, J. H. (1999). Hydrochemical evidence for mixing of river water and groundwater during high-flow condition, lower Suwannee river basin, Florida, USA. *Hydrogeol Journal*, 7, 454-467.

- Crosbie, R. S., McCallum, J. L., Walker, G. R., & Chiew, F. H. (2012). Episodic recharge and climate change in the Murray-Darling Basin, Australia. *Hydrogeology Journal*, 20(2), 245-261.
- Cuthbert, M. O. (2010). An improved time series approach for estimating groundwater recharge from groundwater level fluctuations. *Water Resources Research*, 46(9), 1-11.
- Cuthbert, M. O., Acworth, R. I., Andersen, M. S., Larsen, J. R., McCallum, A. M., Rau, G. C., & Tellam, J. H. (2016). Understanding and quantifying focused, indirect groundwater recharge from ephemeral streams using water table fluctuations. *Water Resources Research*, 52(2), 827-840.
- Dahan, O., Tatarsky, B., Enzel, Y., Kullis, C., Seely, M., & Benito, G. (2008). Dynamics of flood water infiltration and ground water recharge in Hyperarid Desert. *Ground Water*, 46, 450–461. <https://doi.org/10.1111/j.1745-6584.2007.00414.x>.
- Dakhlalla, A. O., Parajuli, P. B., Ouyang, Y., & Schmitz, D. W. (2016). Evaluating the impacts of crop rotations on groundwater storage and recharge in an agricultural watershed. *Agricultural Water Management*, 163, 332-343.
- Dar, I. A., Sankar, K., & Dar, M. A. (2010). Remote sensing technology and geographic information system modeling: an integrated approach towards the mapping of groundwater potential zones in Hardrock terrain, Mamundiyar basin. *Journal of Hydrology*, 394(3-4), 285-295.
- Prakash, K., Mohanty, T., Pati, J. K., Singh, S., & Chaubey, K. (2017). Morphotectonics of the Jamini River basin, Bundelkhand Craton, Central India; using remote sensing and GIS technique. *Applied Water Science*, 7(7), 3767-3782.
- Das, S., Gupta, A., & Ghosh, S. (2017). Exploring groundwater potential zones using MIF technique in semi-arid region: A case study of Hingoli district, Maharashtra. *Spatial Information Research*, 25(6), 749-756.
- Davis, J. C. (1973). *Statistics and Data Analysis in Geology*. New York: John Wiley and Sons.
- Davis, J. C. (1986). *Statistics and Data Analysis in Geology*. New York: Wiley.



- Delin, G. N., Healy, R. W., Lorenz, D. L., & Nimmo, J. R. (2007). Comparison of local-to regional-scale estimates of ground-water recharge in Minnesota, USA. *Journal of Hydrology*, 334(1-2), 231-249.
- Desbarats, A. J., Logan, C. E., Hinton, M. J., & Sharpe, D. R. (2002). On the Kriging of water table elevations using collateral information from a digital elevation model. *Journal of Hydrology*, 255, (1), 25–39.
- Doble, R. C., & Crosbie, R. S. (2017). Current and emerging methods for catchment-scale modelling of recharge and evapotranspiration from shallow groundwater. *Hydrogeology journal*, 25(1), 3-23.
- Dowlatabadi, S., & Zomorodian, S. M. A. (2016). Conjunctive simulation of surface water and groundwater using SWAT and MODFLOW in Firoozabad watershed. *Journal of Civil Engineering*, 20(1), 485–496. DOI. 10.1007/s12205-015-0354-8
- Eldiabani, G. S., Hale, W. H. G., & Heron, C. P. (2014). The Effect of Forest Fires on Physical Properties and Magnetic Susceptibility of Semi-Arid Soils in North-Eastern, Libya. *International Journal of Environmental, Ecological, Geological and Mining Engineering*, 8(1), 54–60. doi.org/10.5281/zenodo.1091048
- Emenike, P. C., Nnaji, C. C., & Tenebe, I. T. (2018). Assessment of geospatial and hydrochemical interactions of groundwater quality, southwestern Nigeria. *Environmental monitoring and assessment*, 190(7), 1-17.
- Etikala, B., Golla, V., Li, P., & Renati, S. (2019). Deciphering groundwater potential zones using MIF technique and GIS: A study from Tirupati area, Chittoor District, Andhra Pradesh, India. *HydroResearch*, 1, 1–7. <https://doi.org/10.1016/j.hydres.2019.04.001>.
- Prakash, K., Mohanty, T., Pati, J. K., Singh, S., & Chaubey, K. (2017). Morphotectonics of the Jamini River basin, Bundelkhand Craton, Central India; using remote sensing and GIS technique. *Applied Water Science*, 7(7), 3767-3782.
- Fenta, A. A., Kifle, A., Gebreyohannes, T., & Hailu, G. (2015). Spatial analysis of groundwater potential using remote sensing and GIS-based multi-criteria evaluation in Raya Valley, northern Ethiopia. *Hydrogeology Journal*, 23(1), 195-206.
- Foody, G. M. (2002). Status of land cover classification accuracy assessment. *Remote Sensing of Environment*, 80(1), 185–201. [https://doi.org/10.1016/S0034-4257\(01\)00295-4](https://doi.org/10.1016/S0034-4257(01)00295-4).

- Freeze, R. A., & Witherspoon, P. A. (1966). Theoretical analysis of regional groundwater flow: Analytical and numerical solutions to the mathematical model. *Water Resources Research*, 2(4), 641-656.
- Freeze, R. A., & Witherspoon, P. A. (1967). Theoretical analysis of regional groundwater flow: Effect of water table configuration and subsurface permeability variation. *Water Resources Research*, 4(3), 581-590.
- Fynn, O. F., Yidana, S. M., Chegbeleh, L. P., & Yiran, G. B. (2016). Evaluating groundwater recharge processes using stable isotope signatures: The Nabogo catchment of the White Volta, Ghana. *Arabian Journal of Geosciences*, 9(4), 1–15. <https://doi.org/10.1007/s12517-015-2299-0>
- Gao, H. (2011). Groundwater Modeling for Flow Systems with Complex Geological and Hydrogeological Conditions. *Procedia Earth and Planetary Science*, 3, 23 – 28. doi: 10.1016/j.proeps.2011.09.061.
- Gao, X., Li, X., Wang, W., & Li, C. (2020). Human Activity and Hydrogeochemical Processes Relating to Groundwater Quality Degradation in the Yuncheng Basin, Northern China. *International Journal of Environmental Research and Public Health*, 17(3), 867 DOI: 10.3390/ijerph17030867
- Gao, Y., Li, X., Ruby-Leung, L., Chen, D., & Xu, J. (2015). Aridity changes in the Tibetan Plateau in a warming climate. *Environmental Research Letters*, 10(3), 1-13.
- Gassiat, C., Gleeson, T., Lefebvre, R., & McKenzie, J. (2013). Hydraulic fracturing in faulted sedimentary basins: Numerical simulation of potential contamination of shallow aquifers over long time scales. *Water Resources Research*, 49(12), 8310-8327.
- Gassiat, C., Gleeson, T., & Luijendijk, E. (2013). The location of old groundwater in hydrogeologic basins and layered aquifer systems. *Geophysical Research Letters*, 40(12), 3042–3047. <https://doi.org/10.1002/grl.50599>.
- Gibbs, R. J. (1970) Mechanisms controlling world water chemistry. *Science*, 170, 3962, 1088-1090, DOI:10.1126/science.170.3962.1088.
- Gitika, T., & Ranjan, S. (2014). Estimation of Surface Runoff using NRCS Curve number procedure in Buriganga Watershed, Assam, India: A Geospatial Approach. *International Research Journal of Earth Sciences*, 2(5), 2321–2527.

- Gleeson, T., & Manning, A. H. (2008). Regional groundwater flow in mountainous terrain: Three-dimensional simulations of topographic and hydrogeologic controls. *Water Resources Research*, 44(10), 1-16.
- Gleeson, T., Befus, K. M., Jasechko, S., Luijendijk, E., & Cardenas, M. B. (2016). The global volume and distribution of modern groundwater. *Nature Geoscience*, 9(2), 161–164. <https://doi.org/10.1038/ngeo2590>.
- Gleeson, T., Marklund, L., Smith, L., & Manning, A. H. (2011). Classifying the water table at regional to continental scales. *Geophysical Research Letters*, 38(5), 1–6,
- Goderniaux, P., Davy, P., Bresciani, E., de Dreuzy, J. R., & Le Borgne, T. (2013). Partitioning a regional groundwater flow system into shallow local and deep regional flow compartments. *Water Resources Research*, 49(4), 2274-2286.
- González-Trinidad, J., Pacheco-Guerrero, A., Júnez-Ferreira, H., Bautista-Capetillo, C., & Hernández-Antonio, A. (2017). Identifying groundwater recharge sites through environmental stable isotopes in an alluvial aquifer. *Water*, 9(8), 569.
- Grotzinger, J. P., & Jordan, T. H. (2010). *Understanding Earth*, 6<sup>th</sup> (Ed). New York, NY, USA. ISBN 978-1429219518. <https://scholar.google.com>
- Guglielmi, Y., Bertrand, C., Compagnon, F., Follacci, J. P., & Mudry, J. (2000). Acquisition of water chemistry in a mobile fissured basement massif: Its role in the hydrogeological knowledge of the La Clapiere landslide (Mercantour massif, southern Alps, France). *Journal of Hydrology*, 229(3-4), 138-148.
- Guglielmi, Y., Vengeon, J., Bertrand, C., Mudry, J., Follacci, J., & Giraud, A. (2002). Hydrogeochemistry: An investigation tool to evaluate infiltration into large moving rock masses (case study of La Clapière and Séchilienne alpine landslides). *Bulletin of Engineering Geology and the Environment*, 61(4), 311-324.
- Gusyev, M. A., Abrams, D., Toews, M. W., Morgenstern, U., & Stewart, M. K. (2014). A comparison of particle-tracking and solute transport methods for simulation of tritium concentrations and groundwater transit times in river water. *Hydrology and Earth System Sciences*, 18(8), 3109–3119. <https://doi.org/10.5194/hess-18-3109-2014>

- Guzha, A. C., Rufino, M. C., Okoth, S., Jacobs, S., & Nóbrega, R. L. B. (2017). Impacts of land use and land cover change on surface runoff, discharge and low flows: Evidence from East Africa. *Journal of Hydrology: Regional Studies*, (15), 49–67.
- Haitjema, H., & Mitchell-Bruker, S. (2005). Are Water Tables a Subdued Replica of the Topography? *Ground Water*, 43, 781–786.
- Hamilton, W. B. (1998). Archean magmatism and deformation were not products of plate tectonics. *Precambrian Research*, 91(1-2), 143-179.
- Hammouri, N., El-Naqa, A., & Barakat, M. (2012). An integrated approach to groundwater exploration using remote sensing and geographic information system. *Journal of Water Resource and Protection*, 4, 717–724. doi:10.4236/jwarp.2012.49081.
- Hamzaoui-Azaza, F., Bouhlila, R., & Gueddari, M. (2009). Geochemistry of fluoride and major ion in the groundwater samples of triassic aquifer (South Eastern Tunisia), Through multivariate and hydrochemical techniques. *Journal of Applied Scientific Research*, 5 (11), 1941–1951.
- Harbaugh, A. W. (2005). *MODFLOW-2005, the US Geological Survey Modular Ground-Water Model: The Ground-Water Flow Process (Vol. 6)*. Reston, VA, USA: US Department of the Interior, US Geological Survey. <https://scholar.google.com>
- Harrington, G. A., Cook, P. G., & Herczeg, A. L. (2002). Spatial and temporal variability of ground water recharge in central Australia: A tracer approach. *Groundwater*, 40(5), 518-527.
- Havril, T., Tóth, Á., Molson, J. W., Galsa, A., & Mádl-Szonyi, J. (2017). Impacts of predicted climate change on groundwater flow systems: Can wetlands disappear due to recharge reduction? *Journal of Hydrology*. <https://doi.org/10.1016/j.jhydrol.2017.09.020>
- Healy, R. W., & Cook, P. G. (2002). Using groundwater levels to estimate recharge. *Hydrogeology journal*, 10(1), 91-109.
- Helena, B., Pardo, R., Vega, M., Barrado, E., Fernandez, J. M., & Fernandez, L. (2000). Temporal Evolution of Groundwater Composition in an Alluvial Aquifer (Pisuerga River, Spain) by Principal Component Analysis. *Water Research*, 34, 807-816.

- Hemmings, B., Goody, D., Whitaker, F., George, D. W., Jasim, A., & Gottsmann, J. (2015). Groundwater recharge and flow on Montserrat, West Indies: Insights from groundwater dating. *Journal of Hydrology: Regional Studies*, 4, 611–622.
- Hernández-Marín, M., Guerrero-Martínez, L., Zermeño-Villalobos, A., Rodríguez-González, L., Burbey, T. J., Pacheco-Martínez, J., Martínez-Martínez, S. I., & González-Cervantes, N. (2018). Spatial and temporal variation of natural recharge in the semi-arid valley of Aguascalientes, Mexico. *Hydrogeology Journal*, 26(8), 2811-2826.
- Hibajene, S. H., & Ellegard, A. (1994). *Charcoal Transportation and Distribution: A study of the Lusaka Market; Energy, Environment and Development Series: Stockholm Environment Institute*. Stockholm, Sweden. <https://scholar.google.com>
- Huang, M., Jacques, G., Wang, Z., & Monique, G. (2006). A modification to the soil conservation service curve number method for steep slopes in the Loess Plateau of China. *Hydrological Processes*, 20(3), 579-589. <https://doi.org/10.1002/hyp.5925>
- Huet, M., Chesnaux, R., Boucher, M. A., & Poirier, C. (2016). Comparing various approaches for assessing groundwater recharge at a regional scale in the Canadian Shield. *Hydrological Sciences Journal*, 61(12), 2267-2283.
- Huizar-Alvarez, R., Ouyse, S., Espinoza-Jaramillo, M. M., Carrillo-Rivera, J. J., & Mendoza-Archundia, E. (2016). The effects of water use on Tothian flow systems in the Mexico City conurbation determined from the geochemical and isotopic characteristics of groundwater. *Environmental Earth Sciences*, 75(13), 1-17.
- Jackson, J. E. (1991). *A User's Guide to Principal Components*. New York: Wiley. <https://scholar.google.com>
- Jain, S. K., Keshri, R., Goswami, A., & Sarkar, A. (2010). Application of meteorological and vegetation indices for evaluation of drought impact: A case study for Rajasthan, India. *Natural hazards*, 54(3), 643-656.
- Hall-Beyer, M. (2017). Practical guidelines for choosing GLCM textures to use in landscape classification tasks over a range of moderate spatial scales. *International Journal of Remote Sensing*, 38(5), 1312-1338.
- Jassas, H., & Merkel, B. (2014). Estimating Groundwater Recharge in the Semiarid Al-Khazir Gomal Basin, North Iraq. *Water*, 6(8), 2467-2481.

- Jenifer, M. A., & Jha, M. K. (2017). Comparison of analytic hierarchy process, catastrophe and entropy techniques for evaluating groundwater prospect of hard-rock aquifer systems. *Journal of Hydrology*, 548, 605-624.
- Jie, Z., van Heyden, J., Bendel, D., & Barthel, R. (2011). Combination of soil-water balance models and water-table fluctuation methods for evaluation and improvement of groundwater recharge calculations. *Hydrogeology Journal*, 19(8), 1487-1502.
- Kammoun, S., Trabelsi, R., Re, V., Zouari, K., & Henchiri, J. (2018). Groundwater quality assessment in semi-arid regions using integrated approaches: The case of Grombalia aquifer (NE Tunisia). *Environmental Monitoring and Assessment*, 190(2), 1-22.
- Kammoun, S., Re, V., Trabelsi, R., Zouari, K., & Daniele, S. (2018). Assessing seasonal variations and aquifer vulnerability in coastal aquifers of semi-arid regions using a multi-tracer isotopic approach: The case of Grombalia (Tunisia). *Hydrogeology Journal*, 26(8), 2575-2594.
- Kammoun, S., Re, V., Trabelsi, R., Zouari, K., & Daniele, S. (2018). Assessing seasonal variations and aquifer vulnerability in coastal aquifers of semi-arid regions using a multi-tracer isotopic approach: the case of Grombalia (Tunisia). *Hydrogeology Journal*, 26(8), 2575-2594.
- Kashaigili, J. J. (2011). *Rapid Environmental Flow Assessment for the Ruvu River*. iWASH. <https://scholar.google.com>
- Kebede, S., & Travi, Y. (2012). Origin of the  $\delta^{18}\text{O}$  and  $\delta^2\text{H}$  composition of meteoric waters in Ethiopia. *Quaternary International*, 257, 4-12.
- Kendall, C. (1995). Isotope tracers of water and solute sources in catchments. *Solute Modeling in Catchment Systems*, 1995, 261-303.
- Kent, P. E. (1971). The geology and geophysics of coastal Tanzania. *Institute of Geological Sciences, Geophysical Papers*, 6, 1-101.
- Kim, H., Bishop, J. K., Dietrich, W. E., & Fung, I. Y. (2014). Process dominance shift in solute chemistry as revealed by long-term high-frequency water chemistry observations of groundwater flowing through weathered argillite underlying a steep forested hillslope. *Geochimica et Cosmochimica Acta*, 140, 1-19.

- Kingston, D. G., Todd, M. C., Taylor, R. G., Thompson, J. R., & Arnell, N. W. (2009). Uncertainty in the estimation of potential evapotranspiration under climate change. *Geophysical Research Letters*, 36(20), 1-6.
- Koh, D. C., Chang, H. W., Lee, K. S., Ko, K. S., Kim, Y., & Park, W. B. (2005). Hydrogeochemistry and environmental isotopes of ground water in Jeju volcanic island, Korea: Implications for nitrate contamination. *Hydrological Processes: An International Journal*, 19(11), 2225-2245.
- Koh, D. C., Ko, K. S., Kim, Y., Lee, S. G., & Chang, H. W. (2007). Effect of agricultural land use on the chemistry of groundwater from basaltic aquifers, Jeju Island, South Korea. *Hydrogeology Journal*, 15(4), 727-743.
- Konikow, L. F. (2013). *Groundwater Depletion in the United States (1900– 2008): US Geological Survey Scientific Investigations Report 2013– 5079*. Washington, DC: US Geological Survey. <https://scholar.google.com>
- Kralik, M. (2015). How to estimate mean residence times of groundwater. *Procedia Earth and Planetary Science*, 13, 301-306.
- Kurylyk, B. L., MacQuarrie, K. T. B., Caissie, D., & McKenzie, J. M. (2015). Shallow groundwater thermal sensitivity to climate change and land cover disturbances: Derivation of analytical expressions and implications for stream temperature modeling. *Hydrology and Earth System Sciences*, 19(5), 2469–2489. <https://doi.org/10.5194/hess-19-2469-2015>
- Lachaal, F., Chekirbane, A., Chargui, S., Sellami, H., Tsujimura, M., Hezzi, H., Faycel, J., & Mlayah, A. (2016). Water resources management strategies and its implications on hydrodynamic and hydrochemical changes of costal groundwater: Case of Grombalia shallow aquifer, NE Tunisia. *Journal of African Earth Sciences*, 124, 171-188.
- Leketa, K., Abiye, T., Zondi, S., & Butler, M. (2019). Assessing groundwater recharge in crystalline and karstic aquifers of the Upper Crocodile River Basin, Johannesburg, South Africa. *Groundwater for Sustainable Development*, 8, 31-40.
- Liang, X., Quan, D., Jin, M., Liu, Y., & Zhang, R. (2013). Numerical simulation of groundwater flow patterns using flux as upper boundary. *Hydrological Processes*, 27(24), 3475-3483.
- Liu, F., Song, X. F., Yang, L., Zhang, Y., Han, D., Ma, Y., & Bu, H. (2015). Identifying the origin and geochemical evolution of groundwater using hydrochemistry and stable isotopes in the

- Subei Lake basin, Ordos energy base, Northwestern China. *Hydrology and Earth System Sciences*, 19(1), 551-565.
- Liu, M., Cao, X., Li, Y., Chen, J., & Chen, X. (2016). Method for land cover classification accuracy assessment considering edges. *Science China Earth Sciences*, 59(12), 2318-2327.
- Lwimbo, Z. D., Komakech, H. C., & Muzuka, A. N. (2019). Estimating groundwater recharge on the southern slope of Mount Kilimanjaro, Tanzania. *Environmental Earth Sciences*, 78(24), 1-22.
- Chowdhury, A., Jha, M. K., & Chowdary, V. M. (2010). Delineation of groundwater recharge zones and identification of artificial recharge sites in West Medinipur district, West Bengal, using RS, GIS and MCDM techniques. *Environmental Earth Sciences*, 59(6), 1209-1222.
- Madhav, S., Ahamad, A., Kumar, A., Kushawaha, J., Singh, P., & Mishra, P. K. (2018). Geochemical assessment of groundwater quality for its suitability for drinking and irrigation purpose in rural areas of Sant Ravidas Nagar (Bhadohi), Uttar Pradesh. *Geology, Ecology, and Landscapes*, 2(2), 127-136.
- Majule, A. E. (2013). Establishing landuse/cover change patterns over the last two decades and associated factors for change in semi-arid and sub humid zones of Tanzania. *Open Journal of Ecology*, 03(06), 445–453. <https://doi.org/10.4236/oje.2013.36051>.
- Manikandan, J., Kiruthika, A. M., & Sureshababu, S. (2014). Evaluation of groundwater potential zones in Krishnagiri District, Tamil Nadu using MIF Technique. *International Journal of Innovative Research in Science, Engineering and Technology*, 3(3), 10524-10534.
- Marandi, A., & Shand, P. (2018). Groundwater chemistry and the Gibbs Diagram. *Applied Geochemistry*, 97, 209-212.
- Marc, V., Bertrand, C., Malet, J. P., Carry, N., Simler, R., & Cervi, F. (2017). Groundwater: Surface waters interactions at slope and catchment scales: Implications for landsliding in clay-rich slopes. *Hydrological Processes*, 31(2), 364-381.
- Martinez-Cob, A., & Tejero-Juste, M. (2004). A wind-based qualitative calibration of the Hargreaves ET<sub>0</sub> estimation equation in semiarid regions. *Agricultural Water Management*, 64(3), 251-264.



- Maurice, L., Taylor, R.G., Tindimugaya, C., MacDonald, A. M., Johnson, P., Kaponda, A., Owor, M., Sanga, H., Bonsor, H. C., Darling, W. G., & Goody, D. (2019). Characteristics of high-intensity groundwater abstractions from weathered crystalline bedrock aquifers in East Africa. *Hydrogeology Journal*, 27(2), 459-474.
- Mbungu, W. B., & Kashaigili, J. J. (2017). Assessing the Hydrology of a Data-Scarce Tropical Watershed Using the Soil and Water Assessment Tool: Case of the Little Ruaha River Watershed in Iringa, Tanzania. *Open Journal of Modern Hydrology*, 7, 65-89. DOI: 10.4236/ojmh.2017.72004.
- McCabe, G. J., & Markstrom, S. L. (2007). *A Monthly Water-Balance Model Driven by a Graphical User Interface (Vol. 1088)*. Reston, VA, USA: US Geological Survey. <https://scholar.google.com>
- McGuire, K. J., McDonnell, J. J., Weiler, M., Kendall, C., McGlynn, B. L., Welker, J. M., & Seibert, J. (2005). The role of topography on catchment-scale water residence time. *Water Resources Research*, 41(5), W05002, doi:10.1029/2004WR003657.
- McKenna, O. P., & Sala, O. E. (2018). Groundwater recharge in desert playas: Current rates and future effects of climate change. *Environmental Research Letters*, 13(1), 014025.
- Mehra, M., & Singh, C. K. (2018). Spatial analysis of soil resources in the Mewat district in the semiarid regions of Haryana, India. *Environment, Development and Sustainability*, 20(2), 661-680.
- Mehra, M., Oinam, B., & Singh, C. K. (2016). Integrated assessment of groundwater for agricultural use in Mewat district of Haryana, India using geographical information system. *Journal of the Indian Society of Remote Sensing*, 44(5), 747-758.
- Mishra, S. K., Jain, M. K., & Singh, V. P. (2004). Evaluation of the SCS-CN-based model incorporating antecedent moisture. *Water Resources Management*, 18(6), 567-589. <https://doi.org/10.1007/s11269-004-8765-1>
- Mitchell-Bruker, S. (1993). *Modeling Steady State Groundwater Flow and Surface Water Interactions* [Doctoral dissertation]. School of Public and Environmental Affairs, Indiana University. <https://scholar.google.com>

- Mjemah, I. C., Van Camp, M., Martens, K., & Walraevens, K. (2011). Groundwater exploitation and recharge rate estimation of a quaternary sand aquifer in Dar-es-Salaam area, Tanzania. *Environmental Earth Sciences*, 63(3), 559-569.
- Moon, S. K., Woo, N. C., & Lee, K. S. (2004). Statistical analysis of hydrographs and water-table fluctuation to estimate groundwater recharge. *Journal of Hydrology*, 292(1-4), 198-209.
- Msindai, K. (1988). *Engineering Geological Aspects of Soils and Rocks in the Dar Es Salaam Region*. Turun yliopiston julkaisu. Sarja A 2. Biologica. Geographica. Geologica. <https://scholar.google.com/>
- Musa, S. I., Hashim, M., & Reba, M. N. M. (2019). Geospatial modelling of urban growth for sustainable development in the Niger Delta Region, Nigeria. *International Journal of Remote Sensing*, 40(8), 3076-3104.
- Mussa, K. R., Mjemah, I. C., & Machunda, R. L. (2020). Open-source software application for hydrogeological delineation of potential groundwater recharge zones in the singida semi-arid, fractured aquifer, Central Tanzania. *Hydrology*, 7(2), 28.
- Mussa, K. R., Mjemah, I. C., & Muzuka, A. N. N. (2020). A review on the state of knowledge, conceptual and theoretical contentions of major theories and principles governing groundwater flow modeling. *Applied Water Science*, 10(6), 1-10.
- Mussa, K. R., Mjemah, I. C., & Walraevens, K. (2019). Quantification of Groundwater Exploitation and Assessment of Water Quality Risk Perception in the Dar Es Salaam Quaternary Aquifer, Tanzania. *Water*, 11(12), 2552.
- Mutayoba, E., Kashaigili, J. J., Kahimba, F. C., Mbungu, W., & Chilagane, N. A. (2018). Assessment of the Impacts of Climate Change on Hydrological Characteristics of the Mbarali River Sub Catchment Using High Resolution Climate Simulations from CORDEX Regional Climate Models. *Applied Physics Research*, 10(5), 61.
- Nag, S. K. (2005). Application of lineament density and hydrogeomorphology to delineate groundwater potential zones of Baghmundi block in Purulia district, West Bengal. *Journal of the Indian Society of Remote Sensing*, 33(4), 521-529.
- Näschen, K., Diekkrüger, B., Evers, M., Höllermann, B., Steinbach, S., & Thonfeld, F. (2019). The impact of land use/land cover change on water resources in a tropical catchment in Tanzania under different climate change scenarios. *Sustainability*, 11(24), 7083.

- Natkhin, M., Dietrich, O., Schäfer, M. P., & Lischeid, G. (2015). The effects of climate and changing land use on the discharge regime of a small catchment in Tanzania. *Regional Environmental Change*, 15(7), 1269-1280.
- Nobert, J., & Jeremiah, J. (2012). Hydrological Response of Watershed Systems to Land Use/Cover Change. A Case of Wami River Basin. *The Open Hydrology Journal*, 6, 78–87. DOI: 10.2174/1874378101206010078
- Notter, B., Hurni, H., Wiesmann, U., & Ngana, J. O. (2013). Evaluating watershed service availability under future management and climate change scenarios in the Pangani Basin. *Physics and Chemistry of the Earth, Parts A/B/C*, 61, 1-11.
- Nugroho, A. R., Tamagawa, I., Riandraswari, A., & Febrianti, T. (2019). Thornthwaite-Mather water balance analysis in Tambakbayan watershed, Yogyakarta, Indonesia. *MATEC Web of Conferences*, 280, 05007. <https://doi.org/10.1051/mateconf/201928005007>
- Oiro, S., Comte, J. C., Soulsby, C., & Walraevens, K. (2018). Using stable water isotopes to identify spatio-temporal controls on groundwater recharge in two contrasting East African aquifer systems. *Hydrological Sciences Journal*, 63(6), 862–877.
- Oke, M. O., Martins, O., & Idowu, O. A. (2014). Determination of rainfall-recharge relationship in River Ona basin using soil moisture balance and water fluctuation methods. *International Journal of Water Resources and Environmental Engineering*, 6(1), 1–11.
- Oki, T., & Kanae, S. (2006). Global hydrological cycles and world water resources. *Science*, 313(5790), 1068–1072. doi:10.1126/science.1128845
- Olarinoye, T., Foppen, J. W., Veerbeek, W., Morienyane, T., & Komakech, H. (2020). Exploring the future impacts of urbanization and climate change on groundwater in Arusha, Tanzania. *Water International*, 45(5), 497–511. <https://doi.org/10.1080/02508060.2020.1768724>.
- Otte, I., Detsch, F., Gütlein, A., Scholl, M., Kiese, R., Appelhans, T., & Nauss, T. (2017). Seasonality of stable isotope composition of atmospheric water input at the southern slopes of Mt. Kilimanjaro, Tanzania. *Hydrological Processes*, 31(22), 3932-3947.
- Oudin, L., Hervieu, F., Michel, C., Perrin, C., Andréassian, V., Anctil, F., & Loumagne, C. (2005). Which potential evapotranspiration input for a lumped rainfall-runoff model? Part 2- Towards a simple and efficient potential evapotranspiration model for rainfall-runoff modelling. *Journal of Hydrology*, 303(1–4), 290–306.

- Oyem, H. H., Oyem, I. M., & Ezeweali, D. (2014). Temperature, pH, electrical conductivity, total dissolved solids and chemical oxygen demand of groundwater in Boji-BojiAgbor/Owa area and immediate suburbs. *Research Journal of Environmental Sciences*, 8(8), 444.
- Palmer, P. C., Gannett, M. W., & Hinkle, S. R. (2007). Isotopic characterization of three groundwater recharge sources and inferences for selected aquifers in the upper Klamath Basin of Oregon and California, USA. *Journal of Hydrology*, 336(1-2), 17-29.
- Patil, J. P., Sarangi, A., Singh, O. P., Singh, A. K., & Ahmad, T. (2008). Development of a GIS interface for estimation of runoff from watersheds. *Water Resources Management*, 22(9), 1221-1239.
- Peng, H., Jia, Y., Qiu, Y., Niu, C., & Ding, X. (2013). Assessing climate change impacts on the ecohydrology of the Jinghe River basin in the Loess Plateau, China. *Hydrological Sciences Journal*, 58(3), 651-670.
- Petit, C. (2010). Continental hearts: Ancient expanses called cratons pose a geological puzzle. *Science News*, 178(13), 22-26.
- Pielke, R. A., Avissar, R., Raupach, M., Dolman, A. J., Zeng, X., & Denning, A. S. (1998). Interactions between the atmosphere and terrestrial ecosystems: influence on weather and climate. *Global Change Biology*, 4(5), 461-475.
- Piper, A.M. (1953) A graphic procedure in the geochemical interpretation of water analysis. *American Geophysical Union Transactions*, 25, 105, 914-923.
- Piper, A.M., (1944). A graphic procedure in the geochemical interpretation of water analyses. *Eos Transactions American Geophysical Union*, 25, 914-928.
- Poeter, E. E., Hill, M. C., Banta, E. R., Mehl, S., & Christensen, S. (2005). *UCODE\_2005 and Six Other Computer Codes for Universal Sensitivity Analysis, Calibration, And Uncertainty Evaluation Constructed using the JUPITER API (No. 6-A11)*. US Geological Survey. <https://scholar.google.com>
- Polemio, M. (2016). Monitoring and management of karstic coastal groundwater in a changing environment (Southern Italy): A review of a regional experience. *Water*, 8(4), 148.

- Praamsma, T., Novakowski, K., Kyser, K., & Hall, K. (2009). Using stable isotopes and hydraulic head data to investigate groundwater recharge and discharge in a fractured rock aquifer. *Journal of Hydrology*, 366(1–4), 35–45. <https://doi.org/10.1016/j.jhydrol.2008.12.011>
- Qin, D., Zhao, Z., Guo, Y., Liu, W., Haji, M., Wang, X., Xin, B., Li, Y., & Yang, Y. (2017). Using hydrochemical, stable isotope and river water recharge data to identify groundwater flow paths in a deeply buried karst system. *Hydrological Processes*, 31(24), 4297-4314.
- Raes, D., Steduto, P., Hsiao, C. T., Fereres, E. (2016). *Reference Manual*. [https:// scholar. google. com](https://scholar.google.com)
- Rajaveni, S. P., Brindha, K., & Elango, L. (2017). Geological and geomorphological controls on groundwater occurrence in a hard rock region. *Applied Water Science*, 7(3), 1377-1389.
- Ramu, M. B., & Vinay, M. (2014). Identification of groundwater potential zones using GIS and Remote Sensing Techniques: A case study of Mysore Taluk–Karnataka. *International Journal of Geomatics and Geosciences*, 2014, 5, 393–403.
- Rao, S. Y., & Jugran, D. K. (2003). Delineation of groundwater potential zones and zones of groundwater quality suitable for domestic purposes using remote sensing and GIS. *Hydrological Sciences Journal*, 48(5), 821-833.
- Raviraj, A., Kuruppath, N., & Kannan, B. (2017). Identification of potential groundwater recharge zones using remote sensing and geographical information system in Amaravathy basin. *Journal of Remote Sensing and GIS*, 6(4), 1-10.
- Re, V., Sacchi, E., Kammoun, S., Tringali, C., Trabelsi, R., Zouari, K., & Daniele, S. (2017). Integrated socio-hydrogeological approach to tackle nitrate contamination in groundwater resources: The case of Grombalia Basin (Tunisia). *Science of the Total Environment*, 593, 664-676.
- Rezaei-Sadr, H., & Sharifi, G. (2018). Variation of runoff source areas under different soil wetness conditions in a semi-arid mountain region, Iran. *Water SA*, 44(2), 290-296.
- Rhoades, J. D., Kandiah, A., & Mashali, A. M. (1992). *The Use of Saline Waters for Crop Production-FAO Irrigation and Drainage Paper 48*. FAO, Rome, 133. <https://scholar.google.com>

- Romualdo, J., Lima, D. S., Celso, A., Antonino, D., Souza, E. S. De, Hammecker, C., Maria, S., Lima, G., Alberto, C., & Oliveira, B. D. (2013). Calibration of Hargreaves-Samani Equation for Estimating Reference Evapotranspiration in Sub-Humid Region of Brazil. *Journal of Water Resource and Protection*, 2013, 1–5.
- Rowley, D. B., Pierrehumbert, R. T., & Currie, B. S. (2001). A new approach to stable isotope-based paleoaltimetry: Implications for paleoaltimetry and paleohypsometry of the High Himalaya since the Late Miocene. *Earth and Planetary Science Letters*, 188(1-2), 253-268.
- Ruden, F. (2007). The discovery of a regional Neogene aquifer in coastal Tanzania. *Coastal Aquifers: Challenges and Solutions*, 1, 363-372.
- Rusydi, A. F. (2018, February). Correlation between Conductivity and Total Dissolved Solid in Various Type of Water: A Review. *In IOP Conference Series: Earth And Environmental Science*, 118, 1, 012019.
- Saghravani, S. R., Yusoff, I., Wanmd-Tahir, W. Z., & Othman, Z. (2015). Estimating recharge based on long-term groundwater table fluctuation monitoring in a shallow aquifer of Malaysian tropical rainforest catchment. *Environmental Earth Sciences*, 74(6), 4577-4587.
- Saha, A. K., Arora, M. K., Csaplovics, E., & Gupta, R. P. (2005). Land cover classification using IRS LISS III image and DEM in a rugged terrain: A case study in Himalayas. *Geocarto International*, 20(2), 33-40.
- Samson, S., & Elangovan, K. (2015). Delineation of groundwater recharge potential zones in Namakkal District, Tamilnadu, India using remote sensing and GIS. *Journal of the Indian Society of Remote Sensing*, 43(4), 769-778.
- Sanford, W. (2002). Recharge and groundwater models: An overview. *Hydrogeology Journal*, 10(1), 110-120.
- Saraf, A. K., & Choudhury, P. R. (1998). Integrated remote sensing and GIS for groundwater exploration and identification of artificial recharge sites. *International journal of Remote sensing*, 19(10), 1825-1841.
- Satheeshkumar, S., Venkateswaran, S., & Kannan, R. (2017). Rainfall–runoff estimation using SCS–CN and GIS approach in the Pappiredipatti watershed of the Vaniyar sub basin, South India. *Modeling Earth Systems and Environment*, 3(1), 1–8.

- Savita, R., Mittal, H.; Satishkumar, U., Singh, P., Yadav, K. K., Jain, H., Mathur, S., & Davande, S. (2018). Delineation of Groundwater Potential Zones using Remote Sensing and GIS Techniques in Kanakanala Reservoir Subwatershed, Karnataka. *International Journal of Current Microbiology and Applied Sciences*, 7, 273–288,
- Schaller, M. F., & Fan, Y. (2009). River basins as groundwater exporters and importers: Implications for water cycle and climate modeling. *Journal of Geophysical Research: Atmospheres*, 114(D4), 1-21.
- Schoeller, H. (1965). *Qualitative Evaluation of Groundwater Resources. Methods and Techniques of Groundwater Investigations and Development*. UNESCO, 5483. <https://scholar.google.com>
- Schoeller H (1967). *Geochemistry of Groundwater. An International Guide for Research and Practice*. UNESCO. <https://scholar.google.com>
- Schoeller, H. (1977). *Geochemistry of Groundwater. Groundwater Studies: An International Guide for Research and Practice*. UNESCO. <https://scholar.google.com>
- Selvam, S., Dar, F. A., Magesh, N. S., Venkatramanan, S., & Chung, S. Y. (2016). Application of remote sensing and GIS for delineating groundwater recharge potential zones of Kovilpatti Municipality, Tamil Nadu using IF technique. *Earth Science Informatics*, 9(2), 137-150.
- Sener, E., Davraz, A., & Ozcelik, M. (2005). An integration of GIS and remote sensing in groundwater investigations: a case study in Burdur, Turkey. *Hydrogeology Journal*, 13(5), 826-834.
- Sharma, M. L. (1986). Measurement and prediction of natural groundwater recharge: An overview. *Journal of Hydrology*, 1986, 49-56.
- Sheikhy Narany, T., Ramli, M. F., Aris, A. Z., Sulaiman, W. N. A., Juahir, H., & Fakharian, K. (2014). Identification of the hydrogeochemical processes in groundwater using classic integrated geochemical methods and geostatistical techniques, in Amol-Babol Plain, Iran. *The Scientific World Journal*, 2014, 1-16.
- Shiri, J., Sadraddini, A. A., Nazemi, A. H., Marti, P., Fard, A. F., Kisi, O., & Landeras, G. (2015). Independent testing for assessing the calibration of the Hargreaves–Samani equation: New heuristic alternatives for Iran. *Computers and Electronics in Agriculture*, 117, 70-80.

- Siebert, S., Burke, J., Faures, J. M., Frenken, K., Hoogeveen, J., Döll, P., & Portmann, F. T. (2010). Groundwater use for irrigation—a global inventory. *Hydrology and Earth System Sciences*, 14(10), 1863-1880.
- Singh, C. K., Shashtri, S., Singh, A., & Mukherjee, S. (2011). Quantitative modeling of groundwater in Satluj River basin of Rupnagar district of Punjab using remote sensing and geographic information system. *Environmental Earth Sciences*, 62(4), 871-881.
- Solomon, S., & Quiel, F. (2006). Groundwater study using remote sensing and geographic information systems (GIS) in the central highlands of Eritrea. *Hydrogeology Journal*, 14(6), 1029-1041.
- Somaratne, N., Mustafa, S., & Lawson, J. (2016). Use of hydrochemistry, stable isotope, radiocarbon,  $^{222}\text{Rn}$  and terrigenic  $^4\text{He}$  to study the geochemical processes and the mode of vertical leakage to the Gambier Basin tertiary confined sand aquifer, South Australia. *Water*, 8(5), 180.
- Srinivas, Y., Aghil, T. B., Hudson Oliver, D., Nithya Nair, C., & Chandrasekar, N. (2017). Hydrochemical characteristics and quality assessment of groundwater along the Manavalakurichi coast, Tamil Nadu, India. *Applied Water Science*, 7(3), 1429-1438.
- Stamatis, G., Parpodis, K., Filintas, A., & Zagana, E. (2011). Groundwater quality, nitrate pollution and irrigation environmental management in the Neogene sediments of an agricultural region in central Thessaly (Greece). *Environmental Earth Sciences*, 64(4), 1081-1105.
- Mussa, K. R., Mjemah, I. C., & Machunda, R. L. (2020). Open-source software application for hydrogeological delineation of potential groundwater recharge zones in the singida semi-arid, fractured aquifer, Central Tanzania. *Hydrology*, 7(2), 28.
- Sterling, S. M., Ducharne, A., & Polcher, J. (2013). The impact of global land-cover change on the terrestrial water cycle. *Nature Climate Change*, 3(4), 385-390.
- Szocs, T., Frape, S., & Gwynne, R. (2015). Integrating hydrogeochemical and isotope data in studying regional groundwater flow systems in the Great Hungarian Plain. *Procedia Earth and Planetary Science*, 13, 177-180.
- Tay, C. K., Hayford, E. K., & Hodgson, I. O. A. (2017). Application of multivariate statistical technique for hydrogeochemical assessment of groundwater within the Lower Pra Basin, Ghana. *Applied Water Science*, 7(3), 1131-1150.



- Tena, T. M., Mwaanga, P., & Nguvulu, A. (2019). Impact of land use/land cover change on hydrological components in Chongwe River Catchment. *Sustainability*, 11(22), 6415.
- Terzoudi, C. B., Gemtos, T. A., Danalatos, N. G., & Argyrokastritis, I. (2007). Applicability of an empirical runoff estimation method in central Greece. *Soil and Tillage Research*, 92(1-2), 198-212.
- Thivya, C., Chidambaram, S., Rao, M. S., Gopalakrishnan, M., Thilagavathi, R., Prasanna, M. V., & Nepolian, M. (2016). Identification of recharge processes in groundwater in hard rock aquifers of Madurai District using stable isotopes. *Environmental Processes*, 3(2), 463-477.
- Thomas, R., & Duraisamy, V. (2018). Hydrogeological delineation of groundwater vulnerability to droughts in semi-arid areas of western Ahmednagar district. *The Egyptian Journal of Remote Sensing and Space Science*, 21(2), 121-137.
- Thornthwaite, C. W. (1948). An approach toward a rational classification of climate. *Geographical Review*, 38(1), 55-94.
- Thornthwaite, C. W., & Mather, J. R. (1957). Instructions and tables for computing potential evapotranspiration and the water balance. *Climatology*, 1957, 10(3), 183 – 311.
- Tiwari, A. K., & Singh, A. K. (2014). Hydrogeochemical Investigation and Groundwater Quality Assessment of Pratapgarh District, Uttar Pradesh. *Journal of the Geological Society of India*, 83, 329-343. <https://doi.org/10.1007/s12594-014-0045-y>
- Tóth, J. (1962). A theory of groundwater motion in small drainage basins in Central Alberta. *Journal of Geophysical Research*, 67(11), 4375-4387
- Toth, J. (1963). A theoretical analysis of groundwater flow in small drainage basins. *Journal of Geophysical Research*, 68(16), 4795-4812.
- Twisa, S., Kazumba, S., Kurian, M., & Buchroithner, M. F. (2020). Evaluating and predicting the effects of land use changes on hydrology in Wami River Basin, Tanzania. *Hydrology*, 7(1), 17.
- USDA-NRCS. (1986). *Urban Hydrology for Small Watersheds. Technical Release.* <https://scholar.google.com>
- USDA-SCS. (1972). U.S. Government Printing Office. Washington, D.C. [https:// scholar. google. com](https://scholar.google.com)

- Uwizeyimana, D., Mureithi, S. M., Mvuyekure, S. M., Karuku, G., & Kironchi, G. (2019). Modelling surface runoff using the soil conservation service-curve number method in a drought prone agro-ecological zone in Rwanda. *International Soil and Water Conservation Research*, 7(1), 9-17.
- Vallet, A., Bertrand, C., Mudry, J., Bogaard, T., Fabbri, O., Baudement, C., & Régent, B. (2015). Contribution of time-related environmental tracing combined with tracer tests for characterization of a groundwater conceptual model: a case study at the Séchilienne landslide, western Alps (France). *Hydrogeology Journal*, 23(8), 1761-1779.
- Vandenberg, A. (1980). Regional groundwater motion in response to an oscillating water table. *Journal of Hydrology*, 47(3-4), 333-348.
- Varol, S., & Köse, İ. (2018). Effect on human health of the arsenic pollution and hydrogeochemistry of the Yazır Lake wetland (Çavdır-Burdur/Turkey). *Environmental Science and Pollution Research*, 25(16), 16217-16235.
- Vazquez-Amábile, G. G., & Engel, B. A. (2005). Use of SWAT to compute groundwater table depth and streamflow in the Muscatatuck River watershed. *Transactions of the ASAE*, 48(3), 991-1003.
- Villeneuve, S., Cook, P. G., Shanafield, M., Wood, C., & White, N. (2015). Groundwater recharge via infiltration through an ephemeral riverbed, central Australia. *Journal of Arid Environments*, 117, 47-58.
- Venkatesan, M. I. (1988). Occurrence and possible sources of perylene in marine sediments: A review. *Marine Chemistry*, 25(1), 1-27.
- Vinithra, R., & Yeshodha, L. (2016). Rainfall-Runoff Modelling Using SCS-CN Method: A Case Study of Krishnagiri District, Tamilnadu. *International Journal of Science and Research*, 5(3), 2080–2084. <https://doi.org/10.21275/v5i3.nov162365>.
- Wambura, F. J., Ndomba, P. M., Kongo, V., & Tumbo, S. D. (2015). Uncertainty of runoff projections under changing climate in Wami River sub-basin. *Journal of Hydrology: Regional Studies*, 4, 333-348.
- Wang, J., Wörman, A., Bresciani, E., Wan, L., Wang, X., & Jiang, X. (2016). On the use of late-time peaks of residence time distributions for the characterization of hierarchically nested groundwater flow systems. *Journal of Hydrology*, 543, 47–58.

- Wang, X. S., Wan, L., Jiang, X. W., Li, H., Zhou, Y., Wang, J., & Ji, X. (2017). Identifying three-dimensional nested groundwater flow systems in a Tóthian basin. *Advances in Water Resources*, 108, 139–156. <https://doi.org/10.1016/j.advwatres.2017.07.016>.
- Ward, P. J., Kummu, M., & Lall, U. (2016). Flood frequencies and durations and their response to El Niño Southern Oscillation: Global analysis. *Journal of Hydrology*, 539, 358-378.
- Waylen, P., Southworth, J., Gibbes, C., & Tsai, H. (2014). Time series analysis of land cover change: Developing statistical tools to determine significance of land cover changes in persistence analyses. *Remote Sensing*, 6(5), 4473-4497.
- Welch, L. A., & Allen, D. M. (2012). Consistency of groundwater flow patterns in mountainous topography: Implications for valley bottom water replenishment and for defining groundwater flow boundaries. *Water Resources Research*, 48(5), W05526.
- Wörman, A., Packman, A. I., Marklund, L., Harvey, J. W., & Stone, S. H. (2006). Exact three-dimensional spectral solution to surface-groundwater interactions with arbitrary surface topography. *Geophysical Research Letters*, 33(7), 2–5. <https://doi.org/10.1029/2006GL025747>.
- Wu, J., Li, P., & Qian, H. (2015). Hydrochemical characterization of drinking groundwater with special reference to fluoride in an arid area of China and the control of aquifer leakage on its concentrations. *Environmental Earth Sciences*, 73(12), 8575-8588.
- Wu, J., Li, P., Qian, H., Duan, Z., & Zhang, X. (2014). Using correlation and multivariate statistical analysis to identify hydrogeochemical processes affecting the major ion chemistry of waters: a case study in Laoheba phosphorite mine in Sichuan, China. *Arabian Journal of Geosciences*, 7(10), 3973-3982.
- Yeh, H. F., Lee, C. H., Hsu, K. C., Chang, P. H., & Wang, C. H. (2009). Using stable isotopes for assessing the hydrologic characteristics and sources of groundwater recharge. *Environmental Engineering and Management Journal*, 19(4), 185-191.
- Yusuf, M. A., Abiye, T. A., Butler, M. J., & Ibrahim, K. O. (2018). Origin and residence time of shallow groundwater resources in Lagos coastal basin, south-west Nigeria: An isotopic approach. *Heliyon*, 4(11), e00932. <https://doi.org/10.1016/j.heliyon.2018.e00932>
- Zarate, E., Hopley, D., Macdonald, A. M., Swift, R. T., Chambers, J., Kashaigili, J. J., Mutayoba, E., Taylor, R. G., & Cuthbert, M. O. (2021). The role of superficial geology in controlling

groundwater recharge in the weathered crystalline basement of semi-arid Tanzania. *Journal of Hydrology: Regional Studies*, 36, 100833. <https://doi.org/10.1016/j.ejrh.2021.100833>.

Zhang, H., Chen, Z. Y., & Tang, C. Y. (2021). Quantifying groundwater recharge and discharge for the middle reach of Heihe River of China using isotope mass balance method. *Journal of Groundwater Science and Engineering*, 9(3), 225-232.

Zhao, K. Y., Jiang, X. W., Wang, X. S., Wan, L., Wang, J. Z., Wang, H., & Li, H. (2018). An analytical study on nested flow systems in a Tóthian basin with a periodically changing water table. *Journal of Hydrology*, 556(2016), 813–823.

## RESEARCH OUTPUTS

### (i) Publications

Mussa, K. R., Mjemah, I. C., & Muzuka, A. N. N. (2020). A review on the state of knowledge, conceptual and theoretical contentions of major theories and principles governing groundwater flow modeling. *Applied Water Science*, 10(6), 1-10.

Mussa, K. R., Mjemah, I. C., & Machunda, R. L. (2021). Natural Groundwater Recharge Response to Climate Variability and Land Cover Change Perturbations in Basins with Contrasting Climate and Geology in Tanzania. *Earth*, 2(3), 556-585.

Mussa, K. R., Mjemah, I. C., & Machunda, R. L. (2020). Open-source software application for hydrogeological delineation of potential groundwater recharge zones in the singida semi-arid, fractured aquifer, Central Tanzania. *Hydrology*, 7(2), 28.